Fakultät für Medizin

III. Medizinische Klinik und Poliklinik

Functional characterization of Cereblon, the molecular target of immunomodulatory drugs

Ruth Eichner

Vollständiger Abdruck der von der Fakultät für Medizin der Technischen Universität München zur Erlangung des akademischen Grades eines

Doctor of Philosophy (Ph.D.)

genehmigten Dissertation.

Vorsitzender: Prof. Dr. Roland Schmid

Betreuer: Prof. Dr. Florian Bassermann

Prüfer der Dissertation:

1. Prof. Dr. Bernhard Küster
2. Prof. Dr. Ulrich Keller
3. Prof. Dr. Helmut Ostermann

Die Dissertation wurde am 22.06.2016 bei der Fakultät für Medizin der Technischen Universität München eingereicht und durch die Fakultät für Medizin am 06.09.2016 angenommen.

Contents

Abbreviations

µg	10-6 gram
µl	10-6 liter
µmol	10-6 mol
µM (µmol/l)	10-6 mol/liter
AA	amino acid
AML	acute myeloid leukemia
Amp	Ampicillin
APS	ammonium persulfate
ARPP P0	acidic ribosomal phosphoprotein P0
ATCC	American Type Culture Collection
ATP	adenosin-5'-triphosphate
BES	N,N-Bis(2-hydroxyethyl)-2-aminoethanesulfonic acid
BM	bone marrow
bp	base pairs
BSA	bovine serum albumin
°C	degree Celsius
CHX	cycloheximide
CMML	chronic myelomonocytic leukemia
CRBN	Cereblon
CRL	cullin ring ligase
CUL1/CUL4	cullin 1/cullin 4
CK1-α	casein kinase 1 α
C-terminal	carboxy terminal
ctrl	control
DCAF	DDB1-CUL4-associated factor
DDB1	DNA damage-binding protein 1
del(5q) MDS	myelodysplastic syndrome with deletion of chromosome 5q
dest.	destillata
DMEM	Dulbecco's Modified Eagle Medium
DMSO	dimethylsulfoxide
DNA	desoxyribonucleic acid
dNTP	2'-desoxynukleosid-5'-triphosphat
DSMZ	Deutsche Sammlung von Mikroorganismen und Zellkulturen
DSS	disuccinimidyl suberate
DTT	dithiothreitol
E. coli	escherichia coli
EDTA	ethylenediaminetetraacetic acid
ELISA	Enzyme Linked Immunosorbent Assay

ENL	erythema nodosum leprosum
EV	empty vector
FAB	French-American-British
FACS	fluorescence activated cell scanning/sorting
FBS	fetal bovine serum
FGF	fibroblast growth factor
FGFR	fibroblast growth factor receptor
Fig.	figure
FITC	fluorescein isothiocyanate
fw	forward
Gag	group specific antigen
G2P	glycerol 2-phosphate disodium salt hydrate
GFP	green fluorescent protein
GST	glutathione S-transferase
h/hrs	hour, hours
HBSS	Hank’s Balanced Salt Solution
HCC	hepatocellular carcinoma
HD	high-dose
HEPES	4-(2-hydroxyethyl)-1-piperazineethanesulfonic acid
HRP	horseraddish peroxidase
IF	immunofluorescence
IFN-γ	interferon gamma
IMDM	Iscove's Modified Dulbecco's Medium
IMiD	immunomodulatory drug
ISS	International Staging System
incl.	including/inclusive
IP	immunoprecipitation
ISS	International Staging System
IPTG	Isopropyl β-D-1-thiogalactopyranoside
IRES	internal ribosomal entry site
kD	kilodalton
Ko	Kozak sequence
LB	Luria-Bertani
LDH	lactate dehydrogenase
LE	long exposure
Len	lenalidomide
MAF	musculoaponeurotic fibrosarcoma
MCT1	monocarboxylate transporter 1
MDS	myelodysplastic syndrome
MFI	median fluorescence intensity

MGUS	monoclonal gammopathy of unclear significance
MM	multiple myeloma
mM (mmol/l)	10^{-3} mol/liter
MMP	matrix metalloproteinase
MO	morpholino
MS	mass spectrometry / spectrometric
NaVa	Sodium orthovanadate (Na_3VO_4)
nM (nmol/l)	10^{-9} mol/liter
N-terminal	amino-terminal
ORR	overall response rates
OS	overall survival
PAGE	polyacrylamide gel electrophoresis
PBS	phosphate buffered saline
PCR	polymerase chain reaction
PD	pull-down
PET	positron emission tomography
PFS	progression-free survial
PI	propidium iodide // proteasome inhibitor
PMSF	phenylmethylsulfonyl fluoride
Pol	polymerase
Pom	pomalidomide
PP	polypropylene
P/S	penicillin / streptomycin
PSM	peptide spectrum match
PVDF	polyvinylidene fluoride
qPCR	quantitative PCR
RA	refractory anemia
RARS	refractory anemia with ring sideroblasts
RING	really interesting new gene
RNA	ribonucleic acid
RPL13A	ribosomal protein L13a
RPMI	Roswell Park Memorial Institute
RR	response rate
RT	reverse transcription // room temperature
rv	reverse
SCT	stem cell transplantation
S.D.	standard deviation
SDS	sodium dodecyl sulfate
SE	short exposure
S.E.M.	standard error of the mean

sec	second
shRNA	short hairpin RNA
TAP	tandem affinity purification
TBE	TRIS-Borat-EDTA
TCA	Trichloroacetic acid
TCR	T-cell receptor
TEMED	N,N,N',N'-Tetramethylethylendiamine
Thal	thalidomide
TLCK	Tosyl-L-lysyl-chloromethyl ketone
TNFα	tumor-necrosis-factor alpha
TPCK	Tosyl-phenylalanyl-chloromethyl ketone
TRIS	tris(hydroxymethyl)aminomethane
TPO	thrombopoietin
U	unit
UPS	ubiquitin proteasome system
UPR	unfolded protein response
VEGF	vascular endothelial growth factor
VSV-G	vesicular stomatitis virus G glycoprotein
WCE	whole cell extracts
WD40 domain	domain of 40 amino acids terminating in the amino acids W and D
wt	wildtype
w/v	weight per volume
zf	zebrafish

1 Summary

Thalidomide and the related immunomodulatory drugs (IMiDs) lenalidomide and pomalidomide are characterized by anti-proliferative, anti-angiogenic and immunomodulatory properties (Shortt et al., 2013). Although thalidomide became infamous for its severe teratotoxic effects when prescribed as sedative under the name of “Contergan” in the 1950s (Mellin and Katzenstein, 1962), IMiDs have established as key therapeutics for multiple myeloma (MM) and del(5q) myelodysplastic syndrome (MDS) over the last years, and show promising activity in further hematological and non-hematological malignancies (Shortt et al., 2013). Their molecular mechanism of action has long remained elusive, until Cereblon (CRBN) was discovered to be the primary target by which IMiDs mediate their anti-tumor and teratotoxic effects (Ito et al., 2010; Lopez-Girona et al., 2012; Zhu et al., 2011). CRBN is characterized by a large LON–domain, which is shared by some proteases and chaperones, and is described to be a substrate receptor of the CRL4 (cullin ring ligase 4) ubiquitin ligase complex.

Recent studies unveiled that lenalidomide enables CRBN to target the lymphoid transcription factors IKZF1 and IKZF3 for proteasomal degradation in MM (Kronke et al., 2014; Lu et al., 2014), while in MDS, lenalidomide induces CRBN-mediated degradation of the kinase CK1-α (Kronke et al., 2015). Although these mechanisms certainly contribute to the IMiD-induced effects in MM and MDS; many open questions remain.

In order to elucidate further means by which IMiDs exert their pleiotropic effects and to better understand the cellular function of CRBN, an affinity-based screen for CRBN interactors was performed in this study. Mass spectrometric analyses revealed CD147 and MCT1 (monocarboxylate transporter 1), two membrane proteins frequently overexpressed in MM and further hematologic and non-hematologic malignancies, as novel CRBN interactors. While CD147 is known to regulate angiogenesis via VEGF, promote proliferation of MM and further cancer cells, and enhance invasion via activation of matrix metalloproteinases (MMPs), MCT1 has metabolic functions transporting lactate and other carboxylates across the plasma membrane. Importantly, MCT1 forms a complex with CD147 and essentially needs this interaction for proper maturation and expression at the plasma membrane.

This study reveals a previously unknown physiological chaperone-like function of CRBN, which promotes maturation of CD147 and MCT1. Via binding to immature CD147 and MCT1, CRBN enhances formation and membrane expression of the CD147/MCT1 transmembrane complex, which proved of vital importance for survival and proliferation of MM and del(5q)MDS cells.

Co-immunprecipitations and GST-pulldown experiments found IMiDs to compete with CD147 and MCT1 for binding to CRBN. Accordingly, both CRBN silencing as well as treatment with any of the three established IMIDs led to CD147/MCT1 destabilization and concomitant

reduction in proliferation and survival, while induced expression of CD147/MCT1 counteracted these effects.

Moreover, both reduction of VEGF and MMP7 secretion and increase of intracellular lactate were observed under IMiD treatment. These effects only occurred in IMiD-sensitive MM cells, while IMiDs did not affect CD147/MCT1 and their downstream targets in resistant MM cell lines. Analyses of primary MM cells from patients with lenalidomide-sensitive or –resistant disease proved this mechanism to be true also in the primary setting.

Murine xenograft models with human MM cell lines with induced expression or silencing of CD147 and MCT1 further confirmed the vital importance of CD147/MCT1 for MM tumor growth as well as for mediation of IMiD induced anti-tumor effects.

Additionally, the compariscon of del(5q)MDS to non-del(5q)MDS patient samples and cell lines revealed CD147 and MCT1 to be overexpressed in del(5q)MDS, which correlates with the significantly higher clinical IMiD response in del(5q)MDS. As in MM, IMiDs destabilized CD147/MCT1, thus mediating at least in parts, the IMiD-induced anti-tumor effects in del(5q)MDS.

Finally, a zebrafish model was used to evaluate the role of CD147/MCT1 in IMiD-induced teratotoxicity. In zebrafish larvae, thalidomide specifically reduced CD147 protein levels. Moreover, CD147 knock-down led to a dose-dependent teratotoxic phenotype, including pectoral fin malformations, as described for thalidomide-induced teratogenicity (Ito et al., 2010; Mahony et al., 2013), thus underlining the importance of CD147 in IMiD-induced teratotoxicity.

Taken together, this study describes a previously unappreciated chaperone-like function of CRBN, distinguishes CD147 and MCT1 as major mediators of IMiD function and provides a common mechanistic framework explaining both the diverse anti-tumor as well as the teratogenic effects of IMiDs.

2 Introduction

2.1 Multiple myeloma

Multiple myeloma (MM), a B-cell malignancy originating from transformed plasma cells, is one of the entities in which immunomodulatory drugs (IMiDs), a defined group of thalidomide-analogs with anti-proliferative, immunomodulatory and anti-angiogenic properties, have proven highest efficacy so far (Bartlett et al., 2004; Palumbo and Anderson, 2011).

2.1.1 Epidemiology and pathogenesis

With an annual incidence of approximately 5.6 cases per 100,000 inhabitants in western countries, MM accounts for about 1% of all malignancies and 13% of hematologic cancers (Palumbo and Anderson, 2011). With a median age at diagnosis of more than 70 years, it is a disease of the elderly (Palumbo and Anderson, 2011). In recent years, novel therapeutic agents such as IMiDs and proteasome inhibitors have revolutionized therapeutic principles and doubled overall survival in MM patients (Kumar et al., 2008; Palumbo and Anderson, 2011). Nevertheless, MM remains an incurable disease with high replase and mortality rates (Kumar et al., 2008; Palumbo and Anderson, 2011).

Starting from monoclonal terminally differentiated B-cells, an accumulation of mutations and microenvironmental changes leads from the premalignant condition called MGUS (monoclonal gammopathy of undetermined significance), to smoldering myeloma, an asymptomatic early form of MM, and finally to symptomatic intramedullary or extramedullary MM (Fig. 1) (Kuehl and Bergsagel, 2002). The high frequency of translocations and other genetic aberrations in MM likely arises from errors during the rearrangement of immunoglobulin loci during B-cell maturation. For instance, translocations involving the switch region of the immunoglobulin heavy chain locus on chromosome 14, such as t(4;14), t(11;14) or t(14;16), are frequent aberrations involved in early pathogenesis of MM, resulting in deregulation of oncogenes such as FGFR3 (fibroblast growth factor receptor 3), cyclin D1 or c-MAF (musculoaponeurotic fibrosarcoma) (Chesi et al., 1998; Fonseca et al., 2002; Kuehl and Bergsagel, 2002). Secondary translocations drive progression and comprise complex cytogenetic abnormalities, deregulation of MYC, activation of KRAS or mutations in TP53 (Kuehl and Bergsagel, 2002; Palumbo and Anderson, 2011). The aberrations in MM cells result in altered expression of adhesion molecules and growth factor receptors, promoting proliferation and migration and modifying the interaction with the BM microenvironment. Adhesion of MM cells to BM stromal cells or extracellular matrix proteins induces secretion of IL-6, IL-10, VEGF, TNF-α and other cytokines by stromal and MM cells, to promote survival, proliferation and enhanced microvascular density (Fig. 1) (Hideshima et al., 2007; Podar et al., 2001; Podar et al., 2002). Next to the hematopoietic niche, MM cells also alter the osteogenic niche. Via inhibition of osteoblasts and activation of osteoclasts, MM

cells induce characteristic lytic bone lesions, causing pain, pathologic fractures and hypercalcemia (Oranger et al., 2013; Roodman, 2009).

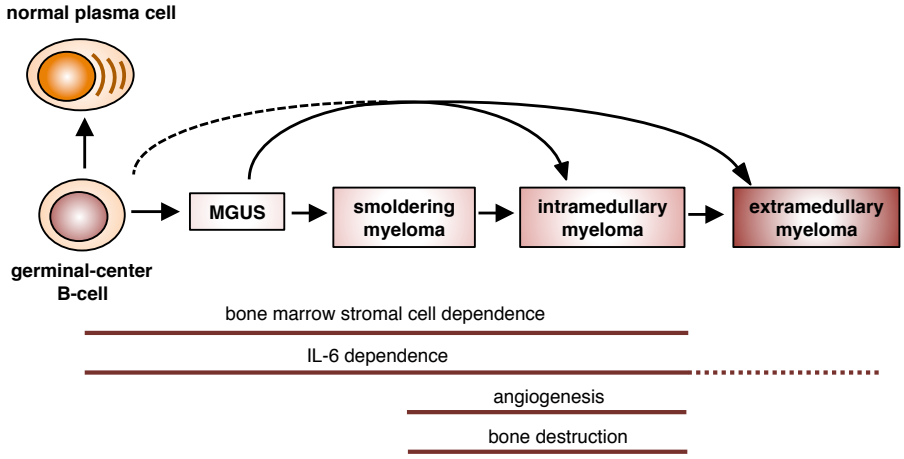

Fig. 1: Development of multiple myeloma. Intra- or extramedullary myeloma (MM) originates from post-germinal-center B-cells either directly (dashed line) or via the premalignant condition MGUS (monoclonal gammopathy of undetermined significance) and the asymptomatic stage of smoldering myeloma. During transition to MM, transformed plasma cells aquire the ability to induce angiogenesis and osteolytic bone lesions. MM cells overcoming their dependence on the BM microenvironment can develop to extramedullary MM. [Adapted from (Kuehl and Bergsagel, 2002)].

2.1.2 Clinical presentation and diagnosis

Diagnosis of MM requires more than 30 mg/dl of monoclonal portein (immunoglobulins or immunoglobulin light chains) in serum and at least 10% of monoclonal plasma cells in the BM (or 30% for nonsecretory myeloma) (Palumbo and Anderson, 2011), while MGUS is characterized by less than 10% monoclonal plasma cells and serum levels of monoclonal protein below 30 mg/dl. Smoldering myeloma meets the diagnostic criteria of MM, but is distinguished from symptomatic MM by absence of organ or tissue impairment (Bergsagel and Kuehl, 2005; Rajkumar and Kumar, 2016; Rajkumar et al., 2015).

The typical clinical symptoms of MM are summarized by the abbreviation CRAB – standing for hypercalcemia, renal impairtment, anemia and bone lesions – and result from organ or tissue damage induced by the uncontrolled proliferation of MM cells and the dysfunctional monoclonal protein, which is frequently referred to as M-protein (Kyle and Rajkumar, 2009; Palumbo and Anderson, 2011). For instance, lytic bone lesions and hypercalcemia originate from MM-mediated osteoclast activation, anemia can result from BM infiltration and renal damage and renal impairment can be caused by hypercalcemia or tubular damage resulting from precipitates of dysfunctional M-protein (Dimopoulos et al., 2008; Kyle et al., 2003; Kyle and Rajkumar, 2009; Oranger et al., 2013; Palumbo and Anderson, 2011).

Initial workup includes routine laboratory testing (blood count, chemical analysis, serum and urine electrophoresis and quantification of monoclonal protein), bone marrow aspiration for

morphologic and cytogenetic analysis, and bone radiographies or low-dose computer tomography scans (Horger et al., 2007; Kyle and Rajkumar, 2009). MM can be staged based on the classification of Durie and Salmon from 1975, taking into account the extent of bone lesions as well as hemoglobin, serum calcium and M-protein levels in serum and urine (Durie and Salmon, 1975), or according to the ISS (International Staging System), which defines three risk groups based on serum β_2-microglobulin and albumin levels (Greipp et al., 2005). Cytogenetics also influence prognosis: chromosomal aberrations in general negatively affect outcome, with specific aberrations such as t(14;16), t(4;14) or del(17p) having particularly poor prognosis (Avet-Loiseau et al., 2007; Fonseca et al., 2009; Palumbo et al., 2015). A revised version of the ISS (R-ISS) now additionally takes into account cytogenetics and LDH (lactate dehydrogenase), defining high-risk disease (R-ISS III) by presence of high β_2-microglobulin (ISS III) and one of the named cytogenetic aberrations or increased LDH, standard-risk disease (R-ISS) by normal β_2-microglobulin (ISS I), absence of high-risk aberrations and normal LDH, and intermediate risk (R-ISS II) by meeting neither criteria for R-ISS I nor for R-ISS III (Palumbo et al., 2015).

2.1.3 Overview on current treatment of MM

Treatment options for MM include steroids, classic chemotherapeutic agents, high-dose (HD) chemotherapy with melphalan followed by autologous stem cell transplantation (ASCT) and diverse novel agents such as thalidomide, lenalidomide and pomalidomie of the IMiD class and proteasome inhibitors, which have altogether significantly improved outcomes of MM patients in the last decade (Kumar et al., 2008; Rajkumar and Kumar, 2016). Treatment of MM, which is indicated as soon as the disease becomes symptomatic according to CRAB criteria (see above), is chosen depending on the risk profile of the disease and patient-specific factors such as age and comorbidities (Fig. 2) (Rajkumar and Kumar, 2016).

The standard of care for patients below 65–70 years without substantial comorbidities is an induction chemotherapy regimen comprising two or three drugs, including at least a novel agent (an IMiD or bortezomib) and steroids, and frequently also a classic chemotherapeutic as doxorubicin or cyclophosphamide, followed by single or tandem HD melphalan and ASCT as consolidation (Fig. 2) (Engelhardt et al., 2014; Palumbo and Anderson, 2011; Rajkumar and Kumar, 2016). After ASCT, maintenance therapy with one of the novel agents can be considered, however only within the scope of clinical studies or off-label (Fig. 2). In young and healthy high-risk patients, autologous SCT can be followed by an allogeneic SCT, which might be curative in very few cases, but is not the standard of care due to high morbidity (Bruno et al., 2007; Koehne and Giralt, 2012; Kroger et al., 2013). In patients older than 65–70 years, which are not eligible for HD therapy, the treatment of choice is melphalan or other another conventional agent in combination with prednisone and one novel agent (Fig. 2) (Palumbo and Anderson, 2011; Rajkumar and Kumar, 2016). Relapsed or refractory disease is treated by combination regimen including novel or classic agents, which the patient had not received previously. Response rates are classically assessed by quantification of M-protein in serum and urine or other parameters

such as percentage of MM cells in BM in asecretory cases. Complete response (CR) is defined by non-detectable M-protein in serum and urine, with stringent CR (sCR) including absence of clonal MM cells in the BM. A very good partial response (VGPR) is defined by ≥ 90% reduction in M-protein levels, and partial response (PR) by ≥ 50% reduction in serum M-protein or ≥ 50% reduction in clonal MM cells in BM in case of asecretory MM (Durie et al., 2006; Kyle and Rajkumar, 2009).

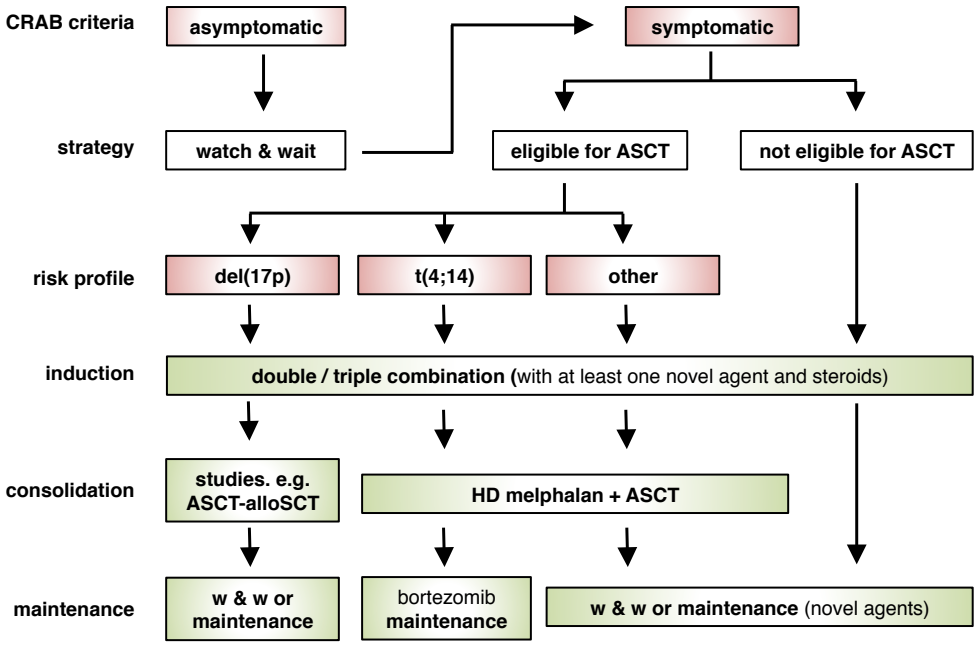

Fig. 2: Treatment strategies in MM. Treatment of MM is initiated when disease becomes symptomatic according to CRAB criteria. Depending on eligibility for autologous stem cell transplantation (ASCT) and the risk profile, induction treatment is either followed by high-dose (HD) melphalan and ASCT, an investigational treatment, maintenance therapy or a watch and wait (w & w) strategy. (Adapted from www.oncopedia.com).

2.2 Myelodysplastic syndrome

Myelodysplastic syndrome (MDS), one of five major entities of myeloid neoplasms, is a malignancy of the hematopoietic stem cell, which is characterized by ineffective erythropoiesis or more generally hematopoiesis, leading to anemia or pancytopenia, with an increased risk of progression to acute myeloid leukemia (AML) (Tefferi and Vardiman, 2009; Vardiman et al., 2009). Besides MM, MDS with deletion of chromosome 5q is the second entitiy, for which IMiDs have been clinically approved given their convincing activity (Shortt et al., 2013; Tefferi and Vardiman, 2009).

2.2.1 Epidemiology and pathogenesis

MDS has an annual incidence of 3.3 cases per 100,000 inhabitants, which is increasing to 20 per 100,000 in people above 70 years of age (Tefferi and Vardiman, 2009). Due to high numbers of unreported or undiagnosed cases, the estimated incidence in the elderly even goes

up to 75 cases per 100,000 (Cogle et al., 2011). MDS is a very heterogenous disease with a 30% overall risk to progress to AML and largely varying survival rates depending on the underlying chromosomal aberrations. Treatment for MDS has long been limited to supportive care or allogeneic SCT as curative option in high-risk disease, and has only recently been extended to novel agents as IMiDs and hypomethylating drugs (Chang et al., 2007; Tefferi and Vardiman, 2009).

MDS arises from hematopoietic stem cells, in which initial mutations set off clonal proliferation. Secondary mutations and epigenetic changes alter the expression of cell-surface receptors, the cytokine response and the interaction with BM stromal cells, finally resulting in ineffective differentiation, increased apoptosis and the MDS-characteristic association of anemia and dysplastic hypercellular BM, while additional mutations can prompt progression to AML (Tefferi and Vardiman, 2009). MDS is thus characterized by both increased proliferation and growth advantage of mutated clones, as well as by abnormal susceptibility to apoptosis and limited responsiveness to growth factors (Nagler et al., 1990). MDS is furthermore associated with increased microvessel densitiy of the BM (Keith et al., 2007), increased levels of pro-inflammatory cytokines, reduced regulatory T-cells and polyclonal or clonal expansion of $CD4^+$ and $CD8^+$ T-cells respectively (Epling-Burnette et al., 2007; Kordasti et al., 2009).

Typical recurrent mutations in MDS include cytogenetic abnormalities such as deletion of chromosome 5q [del(5q)], monosomy 7 or del(7q), trisomy 8 and del(20q), often giving rise to distinct phenotypes (Pozdnyakova et al., 2008; Sole et al., 2005). For instance, del(5q) MDS is characterized by macrocytic anemia, erythroid hypoplasia, a normal or elevated platelet count, hypolobulated megakaryocytes, an indolent clinical course and high response rates to treatment with IMiDs (List et al., 2006; Mohamedali and Mufti, 2009). This phenotype is not yet well understood, but is believed to be caused by haploinsufficiency of genes located on chromosome 5q (Graubert et al., 2009), such as SPARC (secreted portein, acidic, cysteine-rich), a tumorsuppressor, or RPS14, the gene encoding ribosomal protein S14 (Ebert et al., 2008b; Pellagatti et al., 2007). While silencing of RPS14 indeed mimics some aspects of del(5q) MDS (Ebert et al., 2008b), this hypothesis fails to explain other aspects such as the growth advantage of del(5q) cells (Mohamedali and Mufti, 2009). Moreover, ribosomal deficiencies are not specific to del(5q) MDS (Mohamedali and Mufti, 2009), suggesting additional factors. Besides chromosomal aberrations and other mutations, MDS cells display characteristic epigenetic changes such as DNA hypermethylation of transcriptional promotors, thus impeding gene expression and driving disease progression (Jiang et al., 2009).

2.2.2 Diagnosis and classification

MDS, previously named refractory anemia due to its unresponsiveness to the treatment of the time, subsumes a cytogenetically heterogenic group of monoclonal conditions characterized by myelodysplasia. The minimal criterion for diagnosis is the presence of at least 10% dysplastic cells within a specific myeloid lineage, which is not caused by other conditions such as vitamin

deficiencies, viral infections or other malignancies as AML (defined by ≥ 20% myeloblasts in BM or peripheral blood), CMML (chronic myelomonocytic leukemia), or myeloproliferative neoplasms (Tefferi and Vardiman, 2009; Vardiman et al., 2009). MDS was originally classified according to the FAB (French-American-British) system, distinguishing refractory anemia (RA) and refractory anemia with ring sideroblasts (RARS) in case of less than 5% myeloblasts in the BM, refractory anemia with excess of blasts (RAEB) with 5-20% blasts and RAEB "in transformation" (RAEB-T) with 21-30% blasts in the BM (Bennett et al., 1982). The WHO classifcation renamed refractory anemia to refractory cytopenia, included RAEB-T into the AML category and acknowledged multilineage dysplasia and isolated del(5q) MDS as distinct subentities, thus differentiating between refractory cytopenia with unilineage dysplasia, RARS, refractory cytopenia with multilineage dysplasia, RAEB, del(5q) MDS and unclassifiable MDS (Tefferi and Vardiman, 2009).

For estimation of prognosis, the IPSS (International Prognostic Scoring System) differentiates between low, intermediate-1, intermediate-2 and high-risk MDS, with median survival ranging from about 8 years for low-, and less than 1 year for high-risk MDS (Germing et al., 2005). The IPSS takes into account cytogenetics, the percentage of myeloblasts in the BM and the number of hematopoietic lineages affected, with recent refinements additionally including LDH (Germing et al., 2005; Greenberg et al., 1997). Low-risk cytogenetics comprise normal karyotype and isolated deletions of chromosome Y, 5q or 20q, whereas complex karyotypes with more than three anomalies or aberrations of chromosome 7 are defined as high-, and remaining aberrations as intermediate-risk (Greenberg et al., 1997). The WHO classification-based prognostic scoring system (WPSS) additionally considers multilineage dysplasia and red blood cell (RBC) transfusion dependence as adverse prognostic factors (Malcovati et al., 2007).

2.2.3 Overview on current treatment of MDS

Treatment strategies of MDS depend on the risk profile of the disease and aim at symptom control, improval of overall survival and retardation of progression to AML. Therapeutic options include supportive therapy with RBC transfusions, novel agents such as IMiDs or demethylating agents, classic chemotherapeutics such as low-dose cytarabine or intensive AML-like induction chemotherapy, and finally allogeneic SCT. Treatment of low-risk MDS is only required upon symptomatic anemia and focuses on supportive treatment including RBC transfusions, if necessary combined with iron chelators to prevent iron overloading. In patients with low levels of erythropoietin (EPO), the erythropoiesis promoting cytokine, supplementation of EPO can reduce transfusion dependence (Greenberg et al., 2009). In low/intermediate-risk del(5q) MDS, the standard of care includes the IMiD lenalidomide, which successfully reduces transfusion dependence and induces cytogenetic responses in del(5q) MDS, while showing activity only in a small subset of non-del(5q) MDS with impaired erythroid differentiation (Ebert et al., 2008a; Fenaux et al., 2011; List et al., 2006; List et al., 2005; Raza et al., 2008; Toma et al., 2016). High-risk MDS of the elderly not eligible for allogeneic SCT, is treated with DNA

methyltransferase inhibitors such as 5-azacytidine or decitabine, which counteract the DNA hypermethylation, thus successfully achieving hematologic responses including transfusion independence, retarded blastic transformation and improved survival (Fenaux et al., 2009; Kantarjian et al., 2006). In patients with advanced or high-risk disease younger than 60 years of age, allogeneic SCT is the only potentially curative treatment, which is however associated with high treatement-related morbidity and mortality (Chang et al., 2007; Warlick et al., 2009). In case of more than 10% blasts in the BM, AML-like induction chemotherapies are recommended before allogeneic SCT.

2.3 The evolution of immunomodulatory drugs

Immunomodulatory drugs, short IMiDs, are a defined group of glutamic acid derivatives, comprising thalidomide and its analogs lenalidomide and pomalide, which are characterized by a plethora of different functions including immunomodulatory, anti-inflammatory, anti-proliferative, anti-angiogenic, but also teratogenic properties, which nevertheless have become important remedies for different hematological malignancies (Bartlett et al., 2004; Shortt et al., 2013).

2.3.1 Thalidomide, the cause of the "Contergan" scandal

Thalidomide [α-(N-phthalimido)glutarimide] was first synthesized in 1954 by a german company called "Chemie Grünenthal", aiming to develop a non-barbiturate sedative. Due to its strong hypnotic and sedative potency and the absence of adverse effects in murine models, thalidomide was sold as over-the-counter drug named "Contergan" to treat sleep disorders starting from 1957. Given its efficacy against morning sickness in early pregnancy and its alleged safety, it was specifically recommended as anti-emetic and sedative for pregnant women.

Tragically, soon after thalidomide was launched, first reports appeared on severe limb malformations in newborns (Weidenbach, 1959). Over the next years, evidence gradually accumulated that thalidomide was indeed responsible for limb malformations like phokomelia, deformities of eyes or ears and and severe malformations of inner organs in newborns, depending on when women had taken thalidomide during their pregnancy (Mellin and Katzenstein, 1962; Miller and Stromland, 1999; Smithells and Newman, 1992; Speirs, 1962). With 5,000 – 10,000 disabled children, and probably many more miscarriages, "Contergan" caused one of the biggest pharmaceutic scandals in history and was withdrawn from the market in 1961.

Investigations on thalidomide teratotoxicity in different animal models revealed an unexpected species-specificity: whereas thalidomide wasn't teratogenic in mice or rats, it induced malformations in various other species such as xenopus, zebrafish, chicken or non-human primates (Fort et al., 2000; Hendrickx and Sawyer, 1978; Ito et al., 2010; Mahony et al., 2013).

2.3.2 The revival of thalidomide as an immunomodulatory drug

Only few years after being banned from the market, thalidomide experienced an unexpected revival in 1965, when a dermatologist gave leftover thalidomide to a patient with erythema nodosum leprosum (ENL, an inflammatory complication of leprosy) to treat his sleep disorders and surprisingly discovered a significant reduction of inflammantory ENL lesions (Sheskin, 1965). The beneficial effects of thalidomide in ENL were confirmed by a larger study (Iyer et al., 1971), prompting further analyes of the observed anti-inflammatory potential.

Over the next 20 years, different small-scale studies on thalidomide demonstrated efficacy in autoimmune diseases such as rheumatoid arthritis or systemic lupus erythematosus (Atra and Sato, 1993; Gutierrez-Rodriguez, 1984), as well as in graft-versus-host-disease after allogeneic bone marrow transplantation (Vogelsang et al., 1992). In parallel, the biological understanding of the drug increased by discovering that thalidomide inhibits production and secretion of TNF-α (tumor-necrosis-factor alpha), a pro-inflammatory cytokine involved in the pathogenesis of autoimmune, inflammatory, infectious and malignant diseases (Sampaio et al., 1991; Szlosarek and Balkwill, 2003). Independently, thalidomide was found to impede FGF (fibroblast growth factor) and VEGF (vascular endothelial growth factor) induced angiogenesis (D'Amato et al., 1994; Kruse et al., 1998), providing an explanantion for teratotoxicity and suggesting various new clinical applications in diseases such as cancer, which depend on neo-angiogenesis for tumor growth and progression (Bergers and Benjamin, 2003; D'Amato et al., 1994; Folkman, 1971). Later, the drug was found to synergize with TCR (T-cell receptor) induced stimulation of T-cells to enhance IL-2 (interleukin 2) induced T-cell proliferation, IFN-γ (interferon gamma) secretion and cytotoxic T-cell response (Haslett et al., 1998). These findings characterize thalidomide not only as anti-inflammatory agent inhibiting TNF-α or IL-12 secretion (Moller et al., 1997; Sampaio et al., 1991), but rather as immunomodulatory substance, with inhibitory and activatory effects, depeding on the type of immune cell and the stimuli involved (Bartlett et al., 2004).

2.3.3 The anti-cancer potential of thalidomie

Due to its anti-inflammatory, immunomodulatory and particularly anti-angiogenic properties, thalidomide was considered promising as cancer therapeutic. However, it wasn't until a patient with refractory MM was seeking help from experimental treatments, that the anti-tumor activity of thalidomide was revealed. Based on suggestions of Judah Folkman, who discovered the anti-angiogenic effects of thalidomide (D'Amato et al., 1994), the oncologist Bart Barlogie tried thalidomide in this patient in 1997. Although the patient did not respond, Barlogie believed that the anti-angiogenic drug could be beneficial in MM, which is characterized by increased bone marrow (BM) microvessel density (Rajkumar et al., 1999; Vacca et al., 1999). He initiated a clinical trial on thalidomide in advanced MM, revealing remarkable response rates in the range of 30% including few complete remissions in heavily pretreated patients (Singhal et al., 1999).

The potent anti-MM activity was confirmed in further studies showing clinical responses and improved overall survival in refractory MM patients (Barlogie et al., 2001; Juliusson et al.,

2000; Rajkumar, 2000). Notably, thalidomide indeed decreased BM microvessel density in MM patients responding to thalidomide, suggesting a correlation between the anti-MM and the anti-angiogenic activity (Kumar et al., 2004). Combination therapies with dexamethasone or triple combinations with dexamethasone and cyclophosphamide or melphalan further increased response rates in refractory MM and also proved more efficient than standard treatment in untreated MM patients (Cavo et al., 2004; Garcia-Sanz et al., 2004; Palumbo et al., 2006; Palumbo et al., 2001), thus finally leading to approval of thalidomide for MM. Contrary to MM, studies on the efficacy of thalidomide in solid tumors were of limited success with only few partial responses seen in advanced renal cancer or metastatic prostate cancer, while in many other advanced solid malignancies, thalidomide did not have any beneficial effect (Eisen et al., 2000; Figg et al., 2001; Stebbing et al., 2001).

2.3.4 The development of second-generation IMiDs as anti-cancer drugs

The anti-angiogenic and immunomodulatory properties of thalidomide and the rising evidence of its clinical potential prompted the search for analogs with improved anti-cancer or immunological potential and reduced side effects. Based on the thalidomide backbone, various compounds were synthesized and tested in a drug discovery programme conducted by the pharmaceutical company Celgene. Within the group of thalidomide analogs, now called immunomodulatory drugs (IMiDs), two aminophthaloyl-substituted compounds named lenalidomide (formerly CC-5013, Fig. 3) and pomalidomide (formerly CC-4047, Fig. 3), displayed tremendously increased TNF-α inhibitory potential (Muller et al., 1999).

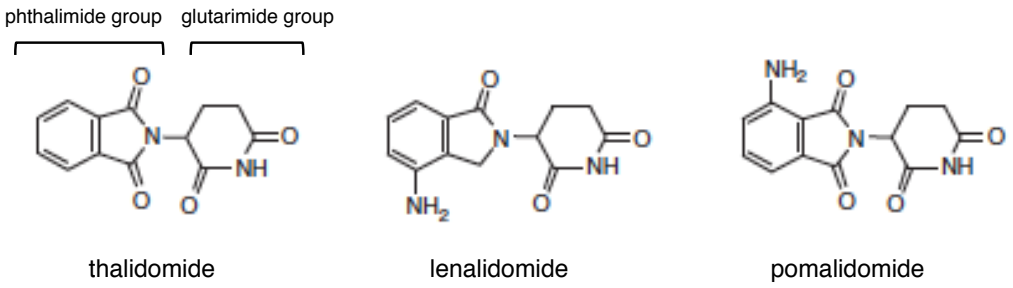

Fig. 3: Chemical structure of thalidomide, lenalidomide and pomalidomide. Immunomodulatory drugs consist of the glutarimide group, identical to all three IMiDs, and a phthalimide group, which is modified by an additional amino group at the fourth carbon of the phthaloyl ring in lenalidomide and pomalidomide. [Adapted from (Shortt et al., 2013)].

Besides significantly higher anti-angiogenic and immunomodulatory potential compared to thalidomide (Bartlett et al., 2004; Lentzsch et al., 2002; Marriott et al., 2002), the novel IMiDs also displayed stronger anti-proliferative effects on myeloma and B-cell lymphoma (Hideshima and Anderson, 2002; Hideshima et al., 2000; Lentzsch et al., 2002). The overall anti-MM potency hence results from multiple effects affecting the tumor cells themselves, the microenvironment and the immune system, with direct induction of growth arrest and apoptosis in MM cells, reduced adhesion of MM to stromal cells, inhibtion of MM-triggered IL-6 and VEGF secretion by the BM,

blocking of VEGF-induced MM cell migration and angiogenesis and T-cell mediated increased NK-cell activity (Gupta et al., 2001; Hideshima et al., 2000; Lentzsch et al., 2002) (Fig. 4).

Altough the exact mechanism of action of IMiDs remained elusive, the second generation IMiDs underwent rapid clinical development given their promising anti-MM activity in preclinical models. As soon as 2002, the first phase I clinical trial on lenalidomide reported impressive response rates of about 70% in refractory MM, with responses even in thalidomide-refractory disease (Richardson et al., 2002). Side effects included myelosuppression and increased risk for thromboembolic disease, while common thalidoimde side effects such as somnolence, constipation, or neuropathy were reported much less (Richardson et al., 2002).

These results set off diverse phase II and III clinicial trials on lenalidomide in MM, MDS, a clonal disease of hematopoietic stem cells which is responsive to thalidomide (Raza et al., 2001; Strupp et al., 2003), and other entities. While these studies were still ongoing, lenalidomide was already granted fast-track approval by the FDA (Food and Drug Administration) for treatment of refractory MM and MDS in the US.

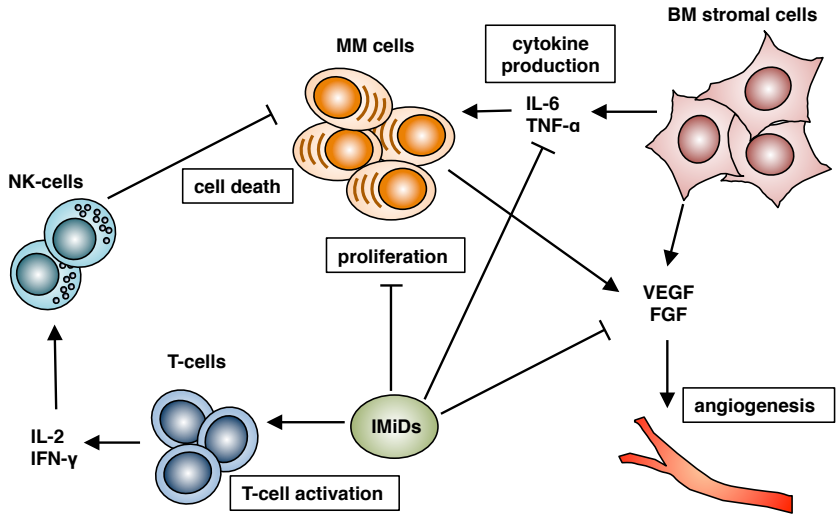

Fig. 4: Different aspects of the anti-MM activity of IMiDs. Immunomodulatory drugs (IMiDs) exert their activity against multiple myeloma (MM) on different levels. They directly inhibit proliferation of MM cells and indirectly affect MM cells via inhibiting cytokine secretion from bone marrow (BM) stromal cells, reducing VEGF (vascular endothelial growth factor) and FGF (basic fibroblast growth factor) secretion, thus targeting angiogenesis. Additionally, IMiDs co-stimulate T-cells, causing MM cell death via activation of natural killer (NK) cells. IL, interleukin; IFN-γ, interferon gamma; TNF-α, tumor necrosis factor alpha. [Adapted from (Bartlett et al., 2004)].

2.3.5 The efficacy of IMiDs in MM and other lympoid malignancies

IMiDs first proved their anti-MM potency in large scale in 2007, when different phase III clinical trials investigating lenalidomide and dexamethasone (Len/Dex) in relapsed/refractory MM confirmed the preliminarly data (Dimopoulos et al., 2007; Richardson et al., 2002; Weber et al., 2007). The high overall response rates (RR) of 60% and the significantly increased progression free (PFS) and overall survival (OS) compared to steroids alone finally led to approval of lenalidomide for treatment of MM also in Europe (Dimopoulos et al., 2007; Weber et al., 2007).

Combination of Len/Dex with other potent anti-MM agents such as adriamycin further boosted the anti-MM efficacy in relapsed or refractory disease, leading to at least VGPR in about 70% of patients (Knop et al., 2009). Bortezomib, a small molecule inhibitor of the proteasome, and central new agent in MM therapy (Rajkumar and Kumar, 2016; Richardson et al., 2005), also proved synergistic in combination with Len/Dex in relapsed or refractory MM, leading to durable responses even in patients refractory to bortezomib or lenalidomide alone (Richardson et al., 2009; Richardson et al., 2014b). The Second-generation proteasome inhibitors carfilzomib and ixazomib were even more efficacious in combination with Len/Dex, boosting ORR to 80% and significantly prolonging PFS in heavily pretreated MM (Moreau et al., 2016; Stewart et al., 2015; Wang et al., 2013). Expectedly, Len/Dex was also highly efficent in newly diagnosed MM (Rajkumar et al., 2005; Zonder et al., 2010), qualifying lenalidomide as first-line therapeutic. In patients not eligible for ASCT, the combination of lenalidomide with prednisone and melphalan, as well as Len/Dex alone proved more efficient than the combination of melphalan, prednisone and thalidomide, thus confirming superiority of lenalidomide over thalidomide (Benboubker et al., 2014; Palumbo et al., 2007). The addition of proteasome inhibitors to Len/Dex further boosted response rates up to 100% with VGPR or better in 70% of patients (Richardson et al., 2010; Roussel et al., 2014). The low side effects and high anti-MM potency additionally distinguish the oral drug lenalidomide as promising agent for maintenance therapy. Indeed, lenalidomide maintenance both after induction with lenalidomide/melphalan/prednisone in patients not eligible for ASCT or after HD melphalan and ASCT, proved highly beneficial, actually doubling the PFS of patients from about 20 to 40 months (Attal et al., 2012; Falco et al., 2013; McCarthy et al., 2012; Palumbo et al., 2014; Palumbo et al., 2012).

By 2009, first clinical studies appeared on pomalidomide, reporting ORR of about 60% in patients with relapsed or refractory MM treated with pomalidomide and low-dose dexamethasone, including RR of 40% in patients resistant to lenalidomide or thalidomide (Lacy et al., 2009). With further studies confirming efficacy of pomalidomide/dexamethasone in heavily pretreated patients, pomalidomide was also approved for treatment in relapsed/refractory MM (Richardson et al., 2014a; San Miguel et al., 2013).

Besides MM, IMiDs also show significant efficacy against other lymphoid malignancies. For instance, lenalidomide treatment of patients with relapsed or refractory aggressive B-cell non-Hodgkin lymphoma (B-NHL) resulted in response in more than one third of patients, including CR in 10% of cases (Wiernik et al., 2008). In relapsed/refractory indolent B-NHL, lenalidomide was slightly less effective, reaching only an ORR of around 20%, including however some durable responses (Witzig et al., 2009). The combination of lenalidomide with rituximab, an anti-CD20 antibody and essential component of B-NHL therapy, was by contrast highly successful in indolent lymphoma, with an ORR of 90% and a CR rate of more than 60%, offering a highly efficient alternative to classic chemotherapy treatment (Fowler et al., 2014).

Among aggressive B-NHLs, mantle cell lymphoma (MCL) was particularly sensitive to lenalidomide monotherapy with RR up to 50% in relapsed/refractory disease, including 20% of

CR (Habermann et al., 2009). Addition of rituximab to lenalidomide significantly raised both ORR and CR rates in relapsed/refractory MCL, as well as in newly diagnosed MCL, where this combination boosted the ORR to more than 90% and the CR rate to more than 60% (Ruan et al., 2015; Wang et al., 2012), thus presenting an efficient alternative to classical chemotherapy. In the US, lenalidomide was already approved for use in relapsed/refractory MCL in light of these results; whereas in the EU, the approval is recommended but still pending.

Finally, in chronic lymphocytic leukemia (CLL), lenalidomide also achieved response rates of around 50% in untreated patients and 30-40% in relapsed/refractors disease, including some cases of CR and some long-term responses, warranting further investigations in this entity (Chanan-Khan et al., 2006; Chen et al., 2011; Ferrajoli et al., 2008; Strati et al., 2013).

2.3.6 The efficacy of IMiDs in MDS and other non-lymphoid malignancies

Next to MM, del(5q) MDS is the second big entitiy in which IMiDs proved to be particularly effective. In MDS, lenalidomide restored efficient eryhtropoiesis leading to transfusion independence in more than 50% of patients at a time where no specific remedy for MDS-related refractory anemia existed (List et al., 2005). Thalidomide was also beneficial in MDS, however response rates were lower than with lenalidomide (Kelaidi et al., 2008; Strupp et al., 2003). Patients with del(5q) MDS responded best to lenalidomide, achieving transfusion-independence in up to 70% of patients (Fenaux et al., 2011; List et al., 2006; List et al., 2005). Importantly, lenalidomide also led to cytogenic responses in up to 70% of patients, with 40% having complete cytogenetic remission (List et al., 2006), suggesting a specific suppression of the del(5q) precursor clone (Sekeres et al., 2008). In non-del(5q) MDS, lenalidomide only achieved reponse rates of 20–30% (Raza et al., 2008; Toma et al., 2016). Although the mechanism of action in del(5q) MDS as well as the factors determining the differences in response between del(5q) and non-del(5q) MDS are not fully understood, lenalidomide is approved and has become an important first-line therapy in lower/intermediate risk del(5q) MDS.

In other myeloid malignancies such as AML, lenalidomide showed response rates of 10–20% in relapsed or refractory cases, including some cases of complete cytogenetic remissions, which is considerable given the aggressiveness of the disease (Blum et al., 2010). Importantly, in case of newly diagnosed AML in the elderly, the CR rates induced by lenalidomie were as high as 50%, suggesting lenalidomide as efficient AML therapy for patients not eligible for intensive chemotherapeutic treatement (Fehniger et al., 2011). In patients with myelofibrosis, lenalidomide and prednisone likewise showed moderate response rates, including some durable clinical and molecular responses (Mesa et al., 2010; Quintas-Cardama et al., 2009), warranting further investigations in these entities.

In contrast to the largely convincing results in lymphoid and myeloid malignancies, the anti-tumor activity of lenaliomide in solid tumors is deceiving. Besides very moderate activity in some entities such as advanced renal cell carcinoma or hepatocellular carcinoma, in which 10-15% of patients responsed to lenalidomide (Choueiri et al., 2006; Safran et al., 2015),

lenalidomide did not show any benefit as mono- or combination therapy in many other entities such as melanoma, colon, ovarian or breast cancer (Eisen et al., 2010; Miller et al., 2007; Segler and Tsimberidou, 2012). Even in prostate cancer, where lenalidomide seemed of potential benefit as monotherapy in phase I/II studies, lenalidomide was even detrimental in a large phase III study when combined with docetaxel in metastatic disease (Keizman et al., 2010; Nabhan et al., 2014; Petrylak et al., 2015).

2.3.7 Overview on the pleiotropic IMiD effects

Overall, IMiDs display a multitude of different effects, contributing to their broad clinical efficacy particularly in the treatment of hematologic neoplasms (Fig. 5).

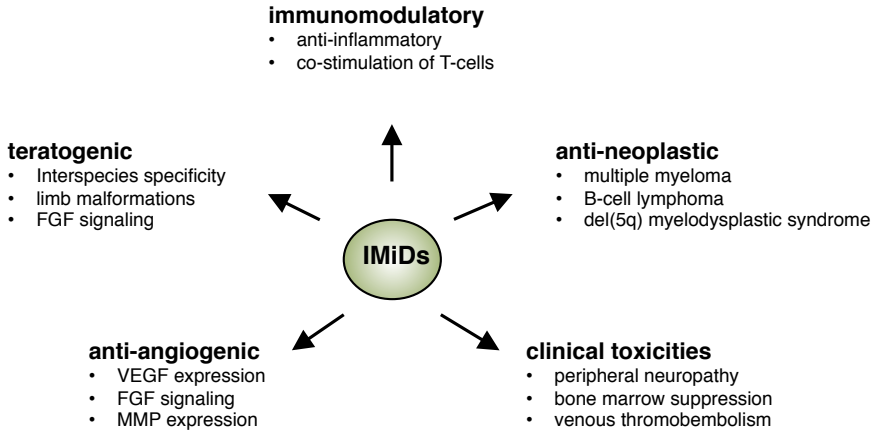

Fig. 5: Overview on IMiD effects. The immunomodulatory drugs (IMiDs) thalidomide, lenalidomide and pomalidomide exert pleiotropic effects including immunomodulatory, antineoplastic, anti-angiogenic and teratogenic activity and are responsible for typical clinical toxicities. VEGF, vascular endothelial growth factor; FGF, fibroblast growth factor; MMP, matrix metalloproteinase. [Adapted from (Shortt et al., 2013)].

For instance, IMiDs inhibit the secretion of LPS-induced inflammatory cytokines as TNF-α, IL-6 and IL-12 (Moller et al., 1997; Sampaio et al., 1991), synergize with IL-2-induced T-cell activation to increase IFN-γ secretion (Haslett et al., 1998) and inhibit stimulus-specific NFκB activation (Majumdar et al., 2002) to result in diverse immunomodulatory effects (Fig. 5). Independently, IMiDs inhibit secretion of different pro-angiogenic and pro-invasive factors such as FGF, VEGF and matrix metalloproteinases (MMP) by MM and BM cells, resulting in reduced motility and invasiveness of cancer cells and represison of angiogenesis (Fig. 5) (D'Amato et al., 1994; Kruse et al., 1998; Segarra et al., 2010). Moreover, IMiDs inhibit osteoclastogengesis and bone-remodeling by reduction of integrin and RANKL expression, contributing to the activity against MM-induced bone lesions (Breitkreutz et al., 2008). In addition to the these microenvironment-related effects, IMiDs also directly inhibit proliferation and induce apoptosis in MM, B-NHL and del(5q) MDS cells (Hideshima and Anderson, 2002; Hideshima et al., 2000; Lentzsch et al., 2002; Pellagatti et al., 2007), together displaying a combined anti-cancer cell and anti-microenvironment activity. Typical clinical side effects include peripheral neuropathy, which is

most prominent in thalidomie, bone marrow suppression, which is more severe with lenalidomide or pomalidomide and increased risk for venous thrombembolism (Fig. 5) (Shortt et al., 2013). Additionally, IMiDs are highly teratogenic substances, leading to a multitude of malformations likely resulting from the anti-angiogenic and anti-invasive effects resulting from VEGF and FGF suppression (Kruse et al., 1998; Mellin and Katzenstein, 1962; Speirs, 1962).

Together, all these discoveries significantly enhanced the understanding of IMiDs, step by step adding new pieces to the puzzle of IMiD biology. However, most of these pieces of evidence were based on correlation and assumptions, and the center piece of the puzzle, an underlying mechanism linking the diverse findings, was still missing until 2010, when Hiroshi Handa and his lab discovered the cellular protein Cereblon (CRBN) as the molecular target of thalidomide, thus making a huge leap forward (Ito et al., 2010).

2.4 The protein Cereblon (CRBN) as molecular target of IMiDs

2.4.1 The structure of CRBN

Cereblon (CRBN) is a ubiquitously expressed highly conserved protein of 442 amino acids (AA) length (Jo et al., 2005; Xin et al., 2008), which localizes to the nucleus, the perinuclear reagion and the cytoplasm, and is found in association with membranes where it possibly adheres via predicted N-myristoylation (Higgins et al., 2004; Ito et al., 2010). CRBN is characterized by a large LON domain (N-terminal domain of the ATP-dependent protease La), which is shared by some proteases and chaperones (Li et al., 2013; Smith et al., 1999).

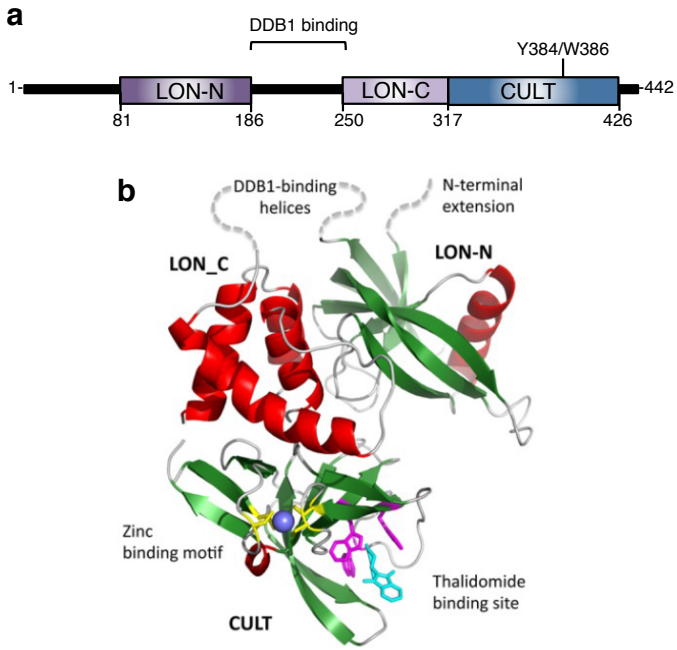

Fig. 6: Structure and domains of CRBN. (a) Schematic of human CRBN, with the N- and C-terminal parts of the LON domain (LON-N and LON-C) separated by DDB1-binding helices, and the CULT (cereblon domain of unknown activity, binding cellular ligands and thalidomide) domain comprising the IMiD-binding pocket. The numbers denote the amino acids; Y384/W386 denotes the residues that disrupt the IMiD binding upon mutation. **(b)** 3D model of CRBN with its different domains; β-strands are marked in green, α-helices in red. [**b** adapted from (Lupas et al., 2015)].

The LON domain, accounting for more than half of the CRBN sequence (AA 81 – 317), is devided in a N- and a C-terminal part (Chamberlain et al., 2014; Lupas et al., 2015), which are separated by a domain responsible for binding of DDB1 (DNA-damage binding protein 1) (Fig. 6) (Chamberlain et al., 2014; Fischer et al., 2014; Ito et al., 2010). Besides the LON domain and the putative N-myristoylation site, CRBN is predicted to have a casein kinase II (CK2) and a protein kinase C (PKC) phosphorylation and a N-glycosylation site, which however have not been validated so far (Higgins et al., 2004). Moreover, the C-terminal of domain of CRBN has a zinc-binding motif, involving four cysteine residues (C323, C326, C391 and C394) (Fig. 6) and a highly conserved hydrophobic pocket essential for IMiD binding (Chamberlain et al., 2014; Fischer et al., 2014; Lupas et al., 2015). The hydrophobic pocket formed by three tryptophan residues and one phenylalanine residue (W380, W386, W400, F402) binds the glutarimide moiety of IMiDs via hydrogen bonds (Chamberlain et al., 2014). Although the tyrosine Y384 is not directly involved in IMiD binding, mutation of the residues Y384 and W386 disrupts IMiD binding, possibly via destabilization of the whole domain (Chamberlain et al., 2014; Ito et al., 2010). The hydrophobic pocket was named TBD (thalidomide-binding domain), or CULT (cereblon domain of unknown activity, binding cellular ligands and thalidomide), and resembles a domain found in some bacterial proteins of unknown function (Lupas et al., 2015) (Fig. 6).

2.4.2 IMiD-independent functions of CRBN

CRBN was first described in 2004, when a nonsense mutation, replacing arginine at position 419 by a premature stop codon, was found responsible for an autosomal recessive nonsyndromic form of mental retardation (Higgins et al., 2004; Higgins et al., 2000). The truncated protein, lacking the last 24 AA including the potential myristoylation site, is expected to have an intact IMiD binding pocket (Chamberlain et al., 2014; Fischer et al., 2014; Higgins et al., 2004). However, the truncation reduced overall protein stability due to increased autoubiquitylation (Xu et al., 2013). Because of its high expression in the brain (cerebrum), its assumed role in cerebral development, memory and learning and the presence of the large LON domain, the protein was named cereblon (Higgins et al., 2004). Later studies in forebrain-specific $CRBN^{-/-}$ knockout mice, which displayed deficits in associative learning, confirmed the importance of CRBN in neuronal development and learning (Rajadhyaksha et al., 2012). Interestingly, CRBN was found to interact with the C-terminal intracellular domains of neuronal ion channels such as large-conductance Ca^{2+}–activated K^{+}–channels (BK_{Ca}) and voltage-gated chloride channels (ClC) to regulate complex formation, membrane expression and ionic currents (Hohberger and Enz, 2009; Jo et al., 2005). Truncated CRBN (R419X) significantly altered expression of BK_{Ca} channels, thus possibly contributing to the observed mental retardation (Higgins et al., 2008).

Additionally, CRBN was reported to inhibit phosphorylation and activation of AMPK (AMP-activated protein kinase), a master regulator of metabolism promoting catabolic processes, via binding to its α-1 subunit (Lee et al., 2011). Accordingly, $CRBN^{-/-}$ knockout mice displayed

increased hepatic AMPK activity and catabolic metabolism, confirming metabolic functions of CRBN (Lee et al., 2013).

Moreover, CRBN was shown to stabilize substrates of the ubiquitin-proteasome system (UPS), which is attributed to inhibition of the UPS via direct binding to a 20S core proteasome subunit (Lee et al., 2012). Other studies reported cytoprotective effects of CRBN in case of UPS dysfunction (Sawamura et al., 2015) and induction of the unfolded protein response (UPR) upon CRBN deletion (Lee et al., 2015), suggesting a protein-stabilizing or cytoprotective function.

2.4.3 CRBN as mediator of IMiD effects

CRBN suddenly got into the research spotlight in 2010, when a Japanese research group around Hiroshi Handa identified CRBN to be the molecular target of thalidomide, essential for mediation of its teratogenic effects (Ito et al., 2010). CRBN silencing in zebrafish and chicken embryos inhibited FGF8 expression and mimicked the teratogenic effects of thalidomide (Ito et al., 2010), suggesting that thalidomide teratogenicity results from disruption of important CRBN functions. Furthermore, CRBN was found to interact with DDB1 (DNA damage-binding protein 1), to form a cullin 4-RING E3 ubiquitin ligase (CRL4) together with CUL4 (cullin 4) and ROC1 (regulator of cullins 1) (Ito et al., 2010). E3 ligases, important players in the UPS, are responsible for recognition and ubiquitylation of specific substrates, leading to proteasomal degradation or functional modification, depending on the type of ubiquitylation (Bassermann et al., 2013; Clague and Urbe, 2010; Hershko and Ciechanover, 1998). E3 ligases of the CRL4 class are multisubunit protein complexes, with CUL4 being the backbone, ROC1 the RING-protein recruiting the E2 ubiquitin ligase, and DDB1 the adaptor binding a DCAF (DDB1-CUL4-associated factor), the actual substrate receptor (Angers et al., 2006). Despite not containing a WD40 domain (domain of 40 amino acids terminating in the amino acids W and D) otherwise characteristic of DCAFs, CRBN was considered to be a DCAF due to its interaction with DDB1 and CUL4 (Angers et al., 2006; He et al., 2006; Lee and Zhou, 2007), and was found to form of a functional $CRL4^{CRBN}$ ligase complex with ubiquitylation activity, which was abrogated by thalidomide (Ito et al., 2010).

Very soon, further studies revealed CRBN expression to be essential for the anti-MM activity of lenalidomide and pomalidomide, thus confirming CRBN as central target of IMiDs with respect to both anti-tumor and teratogenic effects (Lopez-Girona et al., 2012; Zhu et al., 2011). Comparable to IMiD treatment, silencing of CRBN significantly inhibited proliferation of MM cells, confirming the prior hypothesis that IMiDs inhibit crucial CRBN functions (Zhu et al., 2011). MM cells adapting to low CRBN expression, thus surviving the knockdown, displayed IMiD resistance in line with the finding that aquired IMiD-resistance was associated with downregulation of CRBN expression (Lopez-Girona et al., 2012; Zhu et al., 2011). These findings suggest IMiDs to be effective only in a cellular context in which CRBN function is important. Via binding to CRBN, lenalidomide and pomalidomide induced downregulation of IRF4 (interferon-regulatory factor 4) and c-Myc, important transcription factors driving MM proliferation and T-cell activation (Lopez-Girona et al., 2011; Lopez-Girona et al., 2012). These results nicely demonstrate that CRBN is an

essential mediator of IMiD activity, including anti-proliferative, teratogenic and immunomodulatory effects, leaving however open, how CRBN exactly conveys these multiple functions.

2.4.4 IMiDs recruit neo-substrates to the CRL4^{CRBN} ligase

To understand how CRBN mediates IMiD-induced effects, several groups set out to identify novel interactors or substrates of CRBN. Using gene library and mass spectrometry based approaches, IKZF1 (Ikaros) and IKZF3 (Aiolos), two lymphoid-specific transcription factors (Georgopoulos et al., 1994), were identified to be specifically ubiquitylated and degraded upon IMiD treatment (Fig. 7) (Gandhi et al., 2014a; Kronke et al., 2014; Lu et al., 2014; Zhu et al., 2014). While IKZF1/3 are not regulated by CRBN under physiological conditions, lenalidomide binding to CRBN creates a new protein interface with high affinity to IKZF1/3, explaining the lenalidomide-depending binding pattern (Chamberlain et al., 2014; Fischer et al., 2014; Kronke et al., 2014; Lu et al., 2014). Whereas pomalidomide had comparable effects on IKZF1/3 binding and degradation, thalidomide did not significantly affect IKZF1/3 (Gandhi et al., 2014a; Kronke et al., 2015; Zhu et al., 2014). This phenomenon is explained by the C4 amine-group in the phtalimide ring of lenalidomide and pomalidomide, which is not present in thalidomide (see Fig. 3), but assumed to be necessary for interaction of CRBN and IKZF1/3 (Fischer et al., 2014). Given that CRBN forms a CRL4 ubiquitin ligase, it was hypothesized that lenalidomide-dependent binding of IKZF1/3 to CRBN induces ubiquitylation and subsequent proteasomal degradation of IKZF1/3, thus classifying these proteins as neo-substrates of CRL4^{CRBN} (Fig. 7) (Gandhi et al., 2014a; Kronke et al., 2014; Lu et al., 2014; Zhu et al., 2014).

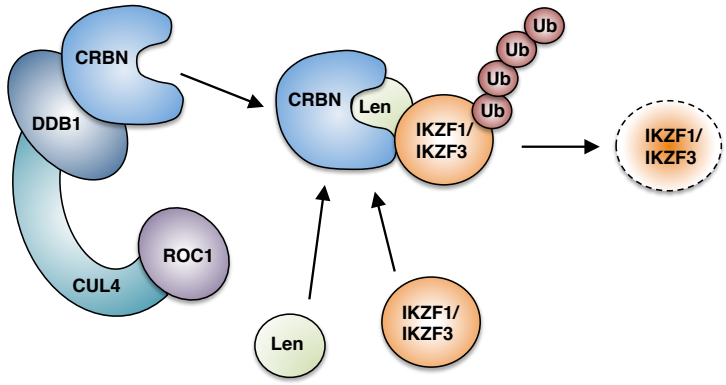

Fig. 7: Model of lenalidomide-specific binding and ubiquitylaiton of IKZF1 and IKZF3 to the CRL4^{CRBN} ligase. CRBN forms a CRL4 E3 ubiquitin ligase together with DDB1, the cullin CUL4 and ROC1, which recruits the E2 ligase. Upon lenalidomide (Len) binding to the hydrophobic pocket within the CULT domain, IKZF1 and IKZF3 bind to the interface of the CRBN-Len complex, resulting in polyubiquitylation and proteasomal degradation. Ub, ubiquitin.

IKZF1 and IKZF3 are important transcription factors in B- and T-cell development, with IKZF3 being involved in plasma cell development and MM cell survival (Cortes and Georgopoulos, 2004; Georgopoulos et al., 1994; Hung et al., 2016; Wang et al., 1998). Knockdown of these proteins led to downregulation of IRF4 and reduced proliferation of MM cells, suggesting that lenalidomide-induced degradation of IKZF1/3 directly contributes to its anti-MM

activity (Kronke et al., 2014; Lu et al., 2014; Zhu et al., 2014). In T-cells, IKZF1/3 are repressors of IL-2 expression, leading to the hypothesis that IMiD-induced degradation of IKZF1/3 and resulting increased IL-2 transcription contributes to the IMiD-characteristic T-cell activation (Gandhi et al., 2014a; Kronke et al., 2014).

Del(5q) MDS and other non-lymphoid malignancies, in which the lymphoid transcription factors are not expressed, are also susceptible to IMiD treatment, suggesting additional mechanisms of action. Indeed, mass spectrometry based studies in myeloid cells found specific ubiquitylation and degradation of CK1-α (casein kinase 1-α), a ubiquitously expressed kinase, upon lenalidomide treatment (Kronke et al., 2015). CK1-α was found to bind to the same lenalidomide-CRBN protein interface as IKZF1/3 (Kronke et al., 2015; Petzold et al., 2016), via a β-hairpin-loop structure with high sequence similarity to a β-hairpin-loop of IKZF1/3 (Petzold et al., 2016). The interface generated by pomalidomide- or thalidomide-binding to CRBN had significantly lower affinity to CK1-α, based on the carbonyl group at the C3 phthalimide position (Fig. 3), making CK1-α a largely lenalidomide-specific target (Petzold et al., 2016). In line with CSNK1a1, the gene coding for CK1-α, being located on chromosome 5q, CK1-α was reported to have lower expression levels in del(5q) than in non-del(5q) MDS (Boultwood et al., 2007). Based on reports that CSNK1a1 haploinsufficiency in del(5q) MDS cells induces stem cell expansion, while homozygous deletion induces stem cell failure (Schneider et al., 2014), and AML cells being more susceptible to CK1-α inhibition than normal hematopoietic stem cells (Jaras et al., 2014), researchers around Benjamin Ebert hypothesized that IMiD-induced degradation of CK-α is responsible for both anti-MDS activity and del(5q)-specificity (Kronke et al., 2015).

Besides the neo-substrates IKZF1/3 and CK1-α, which only bind to $CRL4^{CRBN}$ in presence of lenalidomide, other groups have identified endogenous substrates of CRBN. For instance, MEIS2 (Homeobox protein Meis 2), a transcription factor important for developmental processes, was described to be ubiquitylated and degraded upon binding to $CRL4^{CRBN}$ (Fischer et al., 2014). MEIS2 was shown to compete with IMiDs for binding to the IMiD binding pocket of CRBN, resulting in stabilization of MEIS2 upon IMiD treatment (Fischer et al., 2014). However, the relevance of MEIS2 in both MM and IMiD biology has remained unclear. Another group identified glutamine synthetase as an endogenous substrate of $CRL4^{CRBN}$ (Nguyen et al., 2016), which only binds to CRBN upon glutamine-induced acetylation. Although binding of the acetylated degron required an intact thalidomide-binding pocket, the interaction was not competitive with IMiDs (Nguyen et al., 2016) and has not yet shown relevance for IMiD biology.

Together, the IMiD-induced degradation of IKZF1, IKZF3 and CK1-α explains some immunomodulatory and anti-proliferative effects in MM and del(5q) MDS. However, the three established IMiDs have differing effects towards these proteins, with thalidomide barely affecting IKZF1/3 and CK1-α, and pomalidomide not substantially affecting CK1-α stability (Fischer et al., 2014; Kronke et al., 2015; Petzold et al., 2016). The proposed model therefore fails to provide a common mechanism of action applying to all IMiDs, and the identified substrates do neither explain IMiD-wide effects such as anti-angiogenesis nor address the question of how

teratotoxicity is mediated. The finding, that small molecule drugs can redirect ligase activity of $CRL4^{CRBN}$ against novel substrates, prepresents a previously unknown mechanism of targeted therapy with attractive new perspectives for drug design (Gandhi et al., 2014a; Kronke et al., 2014; Lu et al., 2014; Winter et al., 2015; Zhu et al., 2014). However, this mechanism is in contrast to previous studies, which showed that knockdown of CRBN mimics some IMiD-induced effects, thus supposing an inhibitory effect of IMiDs on CRBN function (Ito et al., 2010; Zhu et al., 2011). Moreover, the clinically observed synergy between IMiDs and proteasome inhibitors such as bortezomib, carfilzomib or ixazomib (Moreau et al., 2016; Richardson et al., 2010; Richardson et al., 2014b; Stewart et al., 2015; Wang et al., 2013) is in conflict to the proposed model, because proteasome inhibition precludes degradation of ubiquitylated proteins and would thus counteract IMiD-induced degradation of IKZF1/3 or CK1-α. A model comprising two different activities of IMiDs – inhibition of physiological functions of CRBN as part of the $CRL4^{CRBN}$ ligase or independent of the ligase complex and induction of novel activities – could possibly reconcile these seemingly opposing findings.

2.5 CD147 and MCT1 as oncogenes with pleiotropic functions

2.5.1 Stuctural characterization of CD147 and MCT1

CD147 (or Basigin) is a highly conserved single-chain type I transmembrane (TM) protein of the immunoglobulin (Ig) superfamily, which was initially identified as tumor surface protein inducing matrix metalloproteinase (MMP) expression in fibroblasts, therefore also named EMMPRIN (extracellular matrix metalloproteinase inducer) (Biswas and Nugent, 1987; Biswas et al., 1995). It is expressed in diverse tissues from neuronal and retinal cells to epithelial and vascular endothial cells, myocard and skeletal muscle, most cells of the hematopoietic system including leukocytes, erythrocytes and thrombocytes and various types of cancer (Weidle et al., 2010). In most of these tissues, CD147 expression is enhanced during development or upon activation (Weidle et al., 2010). The most common isoform of CD147 is made up of 269 AA, containing a signal peptide, an extracellular domain of 186 AA with two Ig-like domains, a highly conserved TM domain of 21 AA and a C-terminal cytoplasmic tail of 40 AA (Fig. 8) (Biswas et al., 1995). Within the Ig-like domains, CD147 has three N-glycosylation sites, which are subsequently glycosylated in the endoplasmatic reticulum (ER) and Golgi during maturation (Sun and Hemler, 2001; Tang et al., 2004a). While the molecular weight of the core protein is 29 kDa, the immature core-glycosylated (CG) CD147 migrates at 35 kDa, and the mature, high-glycosylated (HG) form of CD147 at up to 65 kDa or higher, depending on the cell-type specific degree of glycosylation (Bartlett et al., 2004; Kasinrerk et al., 1992; Tang et al., 2004a). Of note, glycosylation is essential for proper membrane expression and function of CD147, as mutation of N-glycosylation sites leads to retainment of CD147 at the ER and subsequent activation of the unfolded protein response (Huang et al., 2013a). Generally, the cytoplasmic and TM domains are highly conserved and essential for interaction with the monocarboxylate transporters MCT1 and MCT4

(Kirk et al., 2000; Miyauchi et al., 1991). Whereas MCT1 and MCT4 continuously co-localize with CD147, essentially depending on this interaction for membrane expression (Kirk et al., 2000; Le Floch et al., 2011; Poole and Halestrap, 1997), CD147 is stabilized by interaction with MCTs, but is also assumed to form homo-oligomers or interact with different proteins such as integrins or caveolin via their extracellular domains (Curtin et al., 2005; Dai et al., 2009; Deora et al., 2005; Iacono et al., 2007; Yoshida et al., 2000).

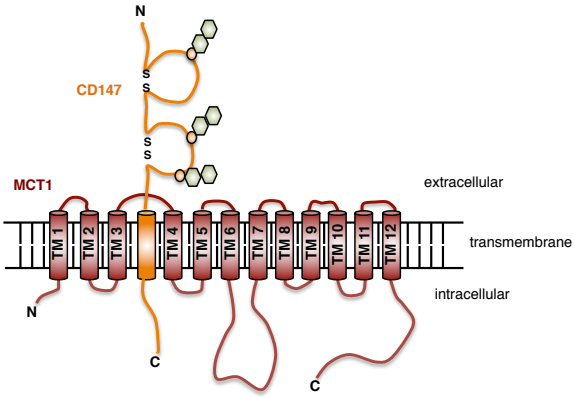

Fig. 8: Schematic of the transmembrane complex of CD147 and MCT1. CD147 (orange) is characterized by a cytoplasmic C-terminus (C), one transmembrane (TM) domain, and an extracellular domain containing two immunoglobulin-like domains (hemicircles) stabilized by disulfide bridges (SS) and three glycosylation sites (small circles) with green hexagons representing attached glycans. MCT1 (red) consists of 12 TM domains, intracellular N- and C-termini and a large intracellular loop between TM 6 and TM 7, likely binding CD147 next to TM3.

Monocarboxylate transporters, transmembrane proteins consisting of 12 TM domains, intracellular N- and C-termini and a large intracellular loop between TM domain 6 and 7 (Fig. 8), catalyze the proton-linked transmembrane-transport of monocarboxylates such as lactate, pyruvate or keton bodies, thus playing a central role in fat, amino acid and particularly carbohydrate metabolism (Halestrap and Price, 1999; Halestrap and Wilson, 2012). Because of its abundance and its metabolic relevance, lactate is the most important substrate (Halestrap, 2013). While MCT1, the best-characterized MCT, is ubiquitously expressed in many tissues including cells of the hematopoietic system, MCT4 is rather expressed upon hypoxia or in cells relying on glycolysis as source of energy such as white sceletal muscle and invasice cancer cells (Halestrap and Wilson, 2012). MCT1 consists of 500 AA, and needs binding to CD147 for stability, maturation and expression at the plasma membrane (Kirk et al., 2000; Le Floch et al., 2011; Poole and Halestrap, 1997). These proteins were found to interact via their TM and intracellular domains, with the third TM domain of MCT1 supposedly lying next to the CD147 TM domain (Fig. 8) (Kirk et al., 2000; Manoharan et al., 2006; Wilson et al., 2002). This protein complex, consisting of either one molecule of each protein, or e.g. a CD147 dimer binding to two MCT1 molecules, is assumed to form at the ER and be processed in ER and Golgi before translocation to the plasma membrane (Kirk et al., 2000; Wilson et al., 2002). While CD147 was initially considered to be primarily a chaperone needed for MCT1 maturation, later studies found

sustained interaction necessary for proper transport acitivity of MCT1 (Wilson et al., 2005; Wilson et al., 2002).

2.5.2 The pleiotropic functions of CD147 and MCT1

Both MCT1 and MCT4 allow import or export of lactate depending on the concentration gradient. While e.g. liver cells import lactate for gluconeogenesis, other cells such as lymphocytes or red blood cells, whose metabolism is largely glycolytic, depend on the export of lactate (Halestrap and Wilson, 2012). Cancer cells, which often grow in a hypoxic environment and also often rely on glycolysis in aerobic conditions (the so-called Warburg effect), likewise depend on the export of lactate, thus frequently overexpressing MCTs (Halestrap and Wilson, 2012; Kennedy and Dewhirst, 2010; Liberti and Locasale, 2016; Parks et al., 2013; Pinheiro et al., 2010).

Besides the MCT-associated functions, CD147 has pleiotropic roles in development, proliferation, adhesion, or migration, mediated by interaction with adhesion molecules on other cells or within the extracellular matrix (Iacono et al., 2007; Weidle et al., 2010). The induction of MMPs, the phenomenon CD147 was initially named EMMPRIN for, is a central effect, important for migratory processes in e.g. development or angiogenesis, but also for cancer cell invasion. For instance, CD147 can induce expression and secretion of various MMPs from fibroblasts but also from tumor cells themselves (Biswas et al., 1995; Guo et al., 1997; Sun and Hemler, 2001). This induction is assumed to base upon homotypic interactions between CD147 molecules on tumor and stroma cells (Sun and Hemler, 2001). Importantly, CD147 can also be released from the cell surface by shedding of microvesicles or via intra-membrane cleavage by MMPs, thus allowing induction of MMP secretion and angiogenesis beyond direct cell-cell contact (Egawa et al., 2006; Millimaggi et al., 2007; Sidhu et al., 2004; Tang et al., 2004b). Interestingly, forced expression of CD147 in fibroblasts in absence of tumor cells also induced MMP secretion, suggesting an autocrine component (Li et al., 2001). The observed pro-angiogenic function of CD147 likely results from distinct activities: while induction of MMPs facilitates angiogenesis via degradation of the extracellular matrix, CD147 also induces VEGF secretion from stromal and tumor cells independent of MMPs, and moreover, CD147 is highly expressed on endothelial cells, directly promoting angiogenesis (Chen et al., 2009; Su et al., 2009; Tang et al., 2005; Voigt et al., 2009). With angiogenesis and migration being essential in development, knockout of CD147 resulted in impairment of sensory and memory functions, comparable to the effects of the CRBN nonsense mutant responsible for mild mental retardation (Higgins et al., 2004; Naruhashi et al., 1997). Hematopoietic cells, which also depend on migration, express high levels of CD147 particularly on activated B- and T-cells as well as on granulocytes, monocytes and macrophages. While CD147 was shown to be involved in T-cell activation and immunological synapse formation (Hu et al., 2010), the reported upregulation of CD147 in activated T-cells did however display inhibitory effects on T-cell proliferation (Biegler and Kasinrerk, 2012), which is in contrast to the

growth-promoting effects of CD147 in diverse hematopoietic and cancer cells (Arendt et al., 2012; Riethdorf et al., 2006), suggesting a particular role of CD147 in T-cell biology.

Together, the pro-proliferative, pro-invasive and pro-angiogenic properties of CD147 and MCT1 are highly advantageous for growth and progression of cancer cells. The frequent CD147 overexpression observed in cancer indeed proved highly relevant for neoangiogenesis via VEGF and MMP induction (Bougatef et al., 2009; Chen et al., 2012; Riethdorf et al., 2006; Tang et al., 2005). Accordingly, overexpression of CD147 and MCTs often is a negative prognostic factor, assumed to also mediate chemotherapy resistance (Futamura et al., 2014; Huang et al., 2013b; Stenzinger et al., 2012; Toole and Slomiany, 2008). Given the oncogenic properties of CD147 and MCT1, specific inhibitors are under development and have already shown promising anti-cancer activity, reducing proliferation, invasion and angiogenesis (Baba et al., 2008; Frederick et al., 2016; Le Floch et al., 2011; Polanski et al., 2014; Walter et al., 2016; Xu et al., 2007b), thus selectively targeting cancer cells while barely affecting non-transformed cells (Baba et al., 2008).

2.5.3 CD147 and MCT1 in hematologic malignancies

With CD147 and MCT1 being expressed in many hematopoietic cells in the physiological state, these proteins are frequently expressed at even higher levels in hematologic malignancies. Particularly MM was reported to display high expression levels of both CD147 and MCT1, which increase stepwise from normal plasma cells to MGUS and finally to overt MM, and also correlate with disease progression (Arendt et al., 2012; Walters et al., 2013). High levels of CD147 induced proliferation of MM cells, while silencing of CD147 significantly inhibited MM cell proliferation (Arendt et al., 2012). Likewise, inhibition of MCT1 resulted in decreased MM proliferation and reduced lactate efflux from MM cells (Walters et al., 2013). Togeher with destabilization of CD147 upon MCT1 silencing and vice versa, these studies confirmed the importance of the CD147-MCT1 transmembrane complex for proliferation and viability in MM (Arendt et al., 2012; Walters et al., 2013). Furthermore, CD147 was shown to mediate extravasation and homing of MM cells to the BM in a MMP-dependent manner (Zhu et al., 2015). Via shedding of CD147-rich microvesicles, MM cells were moreover capable of promoting pro-proliferative and pro-invasive effects beyond direct cell-cell contacts (Arendt et al., 2014). In line with increased CD147 abundance, MM patients also displayed increased concentrations of MMPs in the BM as compared to healthy controls (Urbaniak-Kujda et al., 2016), confirming the relevance of CD147 for both direct MM cell proliferation and MM microenvironment. Importantly, antibody-mediated targeting of CD147 and targeting of MCTs via small molecule inhibitors both proved efficient in reduction of MM cell proliferation and tumor growth, further distinguishing CD147 and MCT1 as promising target structures in MM (Hanson et al., 2015; Zhu et al., 2015).

Beyond MM, CD147 was moreover found to promote growth and proliferation in AML, where co-expression of CD147 and VEGF indicated poor prognosis (Fu et al., 2010; Gao et al., 2015). Likewise, CD147 is assumed to be important in pathogenesis of B-cell acute lymphoblastic leukemia, anaplastic large cell lymphoma and Hodgkin's disease (de Vries et al., 2010; Thorns et

al., 2002), suggesting that CD147 and MCT1 are important oncogenes in most hematological malignancies.

2.6 Aim of the study

IMiDs, which have emerged as important therapeutics against MM, del(5q)MDS and further hematologic and non-hematologic malignancies, were shown to exert their pleiotropic anti-tumor as well as their teratotoxic effects via CRBN (Ito et al., 2010; Lopez-Girona et al., 2012; Zhu et al., 2011). Recent reports described CRBN to form a CRL4 E3 ubiquitin ligase complex, which binds and subsequently degrades the transcription factors IKZF1/3 in presence of lenalidomide (Kronke et al., 2014; Lu et al., 2014). However, both the physiological function of CRBN, as well as a common mechanism of action mediating the well-described antiproliferative, immunomodulatory, anti-angiogenic but also teratotoxic effects of IMiDs has largely remained elusive.

Given this background, the aim of this study was to identify novel interactors of CRBN and thereby further elucidate its physiological function and the mode of action of IMiDs. To this end, an unbiased screen combining affinity purification of CRBN with mass spectrometric (MS) analyses was to be performed. Once binding to promising candidates was confirmed, the influence of CRBN as well as IMiD treatment on the abundance and activity of the protiens were to be analyzed and the molecular mechanism underlying the observed effects was to be reveiled. Next, the role of the identified interactors generally in MM and del(5q)MDS biology and more specifically in IMiD response and resistance was to be assessed. Besides IMiD-sensitive and resistant cell lines, studies in primary material and in a complementary mouse model were plannted for further examination of the *in-vivo* relevance of the identified mechanism. Finally, the potential involvement of the identified interactors in IMiD-induced teratotoxicity was to be assessed using a suitable teratotoxicity model.

Overall, via identification of novel CRBN interactors, this study aimed to gain further insight into IMiD biology, thus eventually providing new biomarkers predicting IMiD response or idenfiying new target structures for molecular therapies.

3 Results

This study was performed as collaborative project in the research group of Prof. Dr. Florian Bassermann at Klinikum rechts der Isar (TUM) together with help from collaborators at other institutes. In order to ensure a comprehensive understanding of the project, relevant data obtained by other researchers is also presented here; the respective contributions are indicated in the text and figure legends.

3.1 IMiDs destabilize CD147 and MCT1 via inhibition of CRBN binding

3.1.1 CRBN binds to CD147 and MCT1

CRBN is the molecular target of IMiD drugs such as thalidomide, lenalidomide and pomalidomide and is essential for mediation of both their pleiotropic anti-tumor and teratotoxic effects (Ito et al., 2010; Lopez-Girona et al., 2012; Zhu et al., 2011). Despite recent advances, many open questions regarding IMiD biology as well as the physiological function of CRBN remain.

In order to identify novel CRBN interactors, an unbiased screen combining tandem affinity purification (TAP) with mass spectrometric (MS) analyses was performed. TAP comprises two subsequent purification steps, thus increasing specificity, while however reducing sensitivity. To allow for TAP, CRBN was cloned into an expression vector with a C-terminal tandem-Strep-single-Flag tag [C-SF-TAP-pcDNA3.0 (Gloeckner et al., 2007)]. For large scale TAP, 2 x 10^9 HEK293T cells were transfected with C-SF-CRBN or, as controls, non-tagged CRBN or empty vector (EV). The lysates were subjected to immobilization on Strep-Tactin beads, followed by elution with desthiobiotin and subsequent anti-Flag immunoprecipitation followed by elution with 3x-FLAG peptide. 5% of the Flag-eluates were separated by SDS-PAGE and visualised by silver staining (Fig. 9a). The remaining eluates were analyzed at the MS facility at the Department for Proteomics and Bioanalytics (TUM) in collaboration with Prof. B. Küster and Dr. S. Lemeer.

The MS analysis resulted in a list of detected peptides from 1412 different proteins, which were ranked according to their peptide spectrum match (PSM) count in relation to the two controls. After first sorting for proteins, which were specifically detected in the sample and not present in the controls, typical contaminants from tandem-Strep-Flag TAP purifications were omitted from further analysis in a second step. Besides established interactors as DDB1 and CUL4A/CUL4B, the resulting list of 36 specific interactors included CD147 [also known as EMMPRIN (extracellular matrix metalloproteinase inducer) or Basigin] and monocarboxylate transporter 1 (MCT1), which form a transmembrane complex. Given that CD147 and MCT1 are involved in different IMiD-associated biological processes such as proliferation, invasion or angiogenesis (Weidle et al., 2010) and ranked among the top candidates in the final MS list, they were clearly considered as the most promising candidates.

a

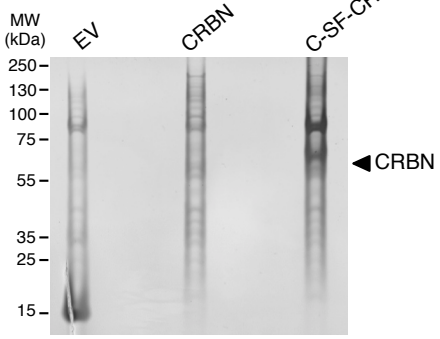

b **CD147**

Sequence	Mascot Ion score	Modifications	Start	Stop
(K)GGVVLKEDALPGQK(T)	88.64		58	71
(K)EDALPGQK(T)	58.06		64	71
(K)SSEHINEGETAMLVcK(S)	78.3	Carbamidomethyl (+57)	112	127
(K)SESVPPVTDWAWYK(I)	56.25		128	141
(R)FFVSSSQGR(S)	41.36		158	166
(R)SELHIENLNmEADPGQYR(C)	87.48	Oxidation (+16)	167	184
(K)GSDQAIITLR(V)	66.62		192	201
(R)RKPEDVLDDDDAGSAPLK(S)	83.3		233	250

c **MCT1**

Sequence	Mascot Ion score	Modifications	Start	Stop
(K)SITVFFK(E)	40		39	45
(K)DLHDANTDLIGRHPK(Q)	55,97		225	239
(K)DLHDANTDLIGR(H)	81,49		225	236
(R)LNDMYGDYK(Y)	54,99		412	420
(K)KESKEEETSIDVAGKPNEVTK(A)	61,98		459	479
(K)ESKEEETSIDVAGKPNEVTK(A)	52,8		460	479

Fig. 9: Mass spectrometric (MS) analysis of tandem-affinity purified CRBN. (a) Silver stained gel of tandem affinity purified (TAP) CRBN. C-terminally tandem-Strep-single-Flag-tagged CRBN (C-SF-CRBN) was expressed in HEK293T cells and purified by TAP: after immobilization on Strep-Tactin beads and elution with desthiobiotin in the first step, CRBN was immunoprecipitated with anti-Flag resin and eluted with 3x-Flag octapeptide in the second step. Parallel purifications from HEK293T cells transfected with either empty vector (EV) or a non-tagged CRBN construct served as controls. 5% of the final Flag eluate was separated by SDS-PAGE and visualized by silver staining. The arrow points to the prominent band at the expected size of CRBN. MW, molecular weight. **(b,c)** Amino acid sequences of unique peptides of CD147 **(b)** and MCT1 **(c)** as identified by MS together with modifications and Mascot ion score. C, carbaminomethyl; m, oxidation. [MS data for **b** and **c** provided by Dr. S. Lemeer and Prof. B. Küster].

MS analysis detected eight unique peptides corresponding to CD147 (IPI00019906) and six unique peptides corresponding to MCT1 (IPI00024650) (Fig. 9b, c). CD147 consists of 269 amino acids (AA) and the detected peptides covered large parts of its intra- and extracellular domain. In case of MCT1, a protein of 500 AA with total 12 transmembrane (TM) domains, the peptides corresponded to the C-terminal and three further intra- and extracellular domains.

In order to validate CD147 and MCT1 as interactors of CRBN, bi-directional immunoprecipitaion (IP) experiments were performed. First, endogenous CRBN was precipitated from MM1.S cells, a human MM cell line, using a customed anti-CRBN antibody. An unspecifc IgG antibody served as control. Immunoblot analyses showed co-immunoprecipitation (co-IP) of endogenous CD147 and MCT1 with CRBN (Fig. 10a). Interestingly, the core-glycosylated (CG) immature form of CD147 showed a relatively stronger binding to CRBN than the high-glycosylated (HG) mature form (Fig. 10a), suggesting preferred interaction of CBRN with immature protein. To confirm binding, reciprocal IPs were performed with Flag-tagged CD147 and MCT1 expressed in HEK293T cells and precipitated from whole cell lysates by Flag-IP using Flag-M2 beads. Immunoblot analyses showed co-IP of endogenous CRBN with both Flag-CD147 and Flag-MCT1, while no signal was detected in the empty vector (EV) control (Fig. 10b, c)

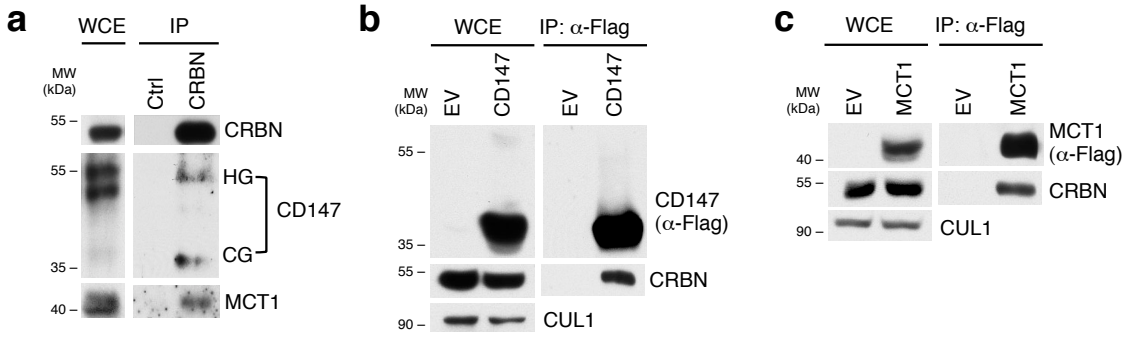

Fig. 10: CRBN binds to CD147 and MCT1. (a) Immunoprecipitation of endogenous CRBN from MM1S cells. Whole cell extracts (WCE) were subjected to immunoprecipitation with anti-CRBN or control IgG antibodies and analyzed by immunoblotting using the indicated antibodies. **(b,c)** Immunoprecipitation of Flag-CD147 **(b)** and Flag-MCT1 **(c)**. HEK293T cells were transfected with Flag-CD147, Flag-MCT1 or empty vector control (EV) and subjected to Flag-IP. Immunoprecipitates were analyzed by immunoblotting with the indicated antibodies. MW, molecular weight.

After confirmation of specific binding of CRBN to both CD147 and MCT1, complementary *in-vitro* interaction studies were performed by Dr. V. Fernández-Sáiz to rule out indirect binding via unknown third proteins. Both CD147 and MCT1 were translated *in-vitro* using a eukaryotic cell-free transcription/translation system (see chapter 6.3.10) and marked radioactively by incorporation of [^{35}S]-Methionine, while a GST-CRBN fusion protein was expressed in bacterial cells and purified using Glutathion Sepharose beads (see chapter 6.3.9.1). Interaction studies were perfomed by incubating GST-CRBN or empty GST beads with *in-vitro* translated CD147 and MCT1. The bound protein fractions were separated by SDS-PAGE and visualized by autoradiography for radioactively labeled CD147 and MCT1 or Coomassie staining for GST/GST-CRBN. As expected, both CD147 and MCT1 were significantly enriched in the GST-CRBN bound fraction compared to control, confirming direct interaction (Fig. 11). Of note, the *in-vitro* translated CD147 is not glycosylated and therefore only presents as one (non-glycolsylated) protein band.

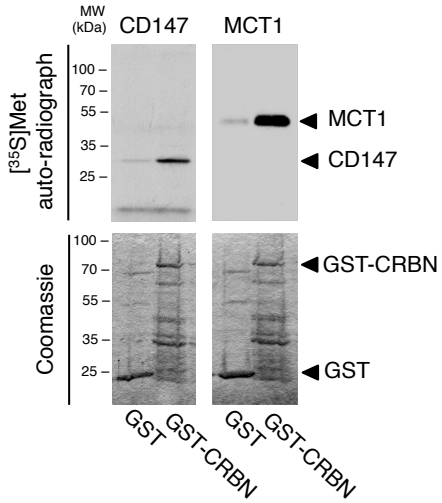

Fig. 11: CBRN binding to CD147 and MCT1 is direct. GST-pulldown assays of recombinant GST-CRBN or empty GST incubated with *in-vitro* translated, ^{35}S-labeled CD147 and MCT1 proteins. Bound protein fractions were visualized by autoradiograpy, GST and GST-CRBN were visualized using Coomassie staining. [Data provided by Dr. V. Fernández-Sáiz].

3.1.2 CRBN interacts with the intracellular domains of CD147 and MCT1

Once specific and direct interaction between CRBN and both CD147 and MCT1 was confirmed, mapping experiments followed to identify the specific interacting domains. As CD147 and MCT1 are membrane proteins, CRBN could either bind to the intracellular, the transmembrane or the extracellular domain. With CRBN localizing to the cytoplasm and nucleus and possibly associating with membranes due to an N-myristoylation site (Higgins et al., 2004; Ito et al., 2010), interaction with the intracellular domains seemed most plausible. Mapping studies were thus restricted to the intracellular parts of CD147 and MCT1. GST- tagged fragments of the cytoplasmatic C-terminus of CD147 (comprising AA 230 – 269) and both the middle cytoplasmic loop (AA 188-262) and the C-terminal cytoplasmatic tail (AA 444-500) of MCT1 were expressed in bacteria and purified via Glutathione Sepharose beads. Figure 12a depicts the structure of CD147 and MCT1 and the chosen GST-fusion fragments. The purified beads with bound GST-tagged protein fragments were used for pulldown experiments in whole cell extracts of MM1.S cells. Immunoblot analysis of bound fractions revealed binding of CRBN to the C-termini of CD147 and MCT1, but not to the middle cytoplasmic loop of MCT1 (Fig. 12b).

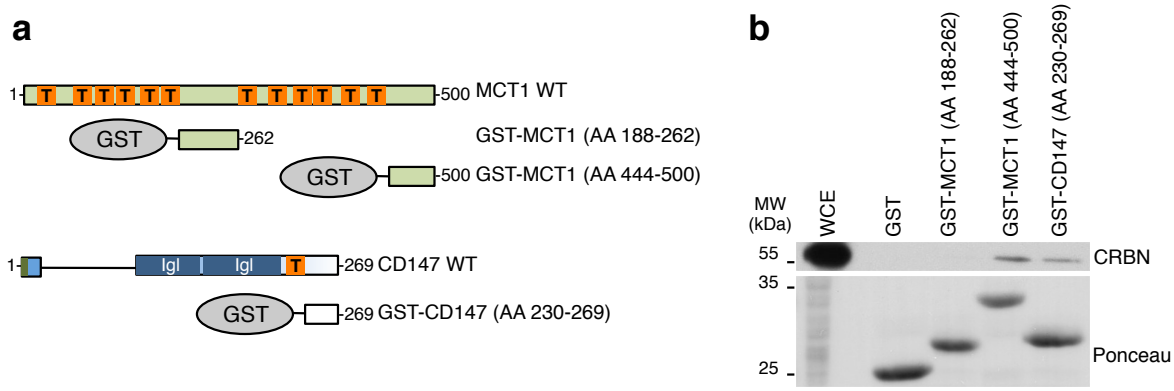

Fig. 12: CRBN binds to the C-terminal intracellular domains of CD147 and MCT1. (a) Schematic overview of full-length human CD147 and MCT1 proteins and the GST-tagged fragments of their intracellular domains. T, transmembrane domain; IgI, immunoglobulin-like domain **(b)** GST pull-downs with the indicated fragments of CD147 and MCT1 in whole cell extracts (WCE) of MM1.S cells. Precipitates were subjected to immunoblot analyses.

3.1.3 Lenalidomide competes with CD147 and MCT1 for CRBN binding

Recently identified CRBN substrates such as IKZF1/3 and CK1-α are described to predominantly bind CRBN in presence of lenalidomide (Kronke et al., 2015; Kronke et al., 2014; Lu et al., 2014). In order to investigate if lenalidomide affects the binding of CD147 and MCT1 to CRBN, different affinitiy purification experiments were performed. First, HEK293T cells were transfected with constructs coding for Flag-CD147, Flag-MCT1, Flag-IKZF3 or empty vector control (EV) and treated with lenalidomide or vehicle for 24 hrs. Before harvest, DSS (disuccinimidyl suberate) was added to the cells for 45 min to crosslink interacting proteins (see chapter 6.2.3.4). Whole cell extracts were subjected to Flag-IPs using Flag-M2 beads and subsequent immunoblot analysis. As expected and previously described, CRBN only bound to

IKZF3 in presence of lenalidomide (Fig. 13a). CD147 and MCT1 showed the opposite behavior: both CD147 and MCT1 bound to CRBN in absence of lenalidomide (see also Fig. 10-12), whereas lenalidomide treatment completely abrogated the interaction (Fig. 13a).

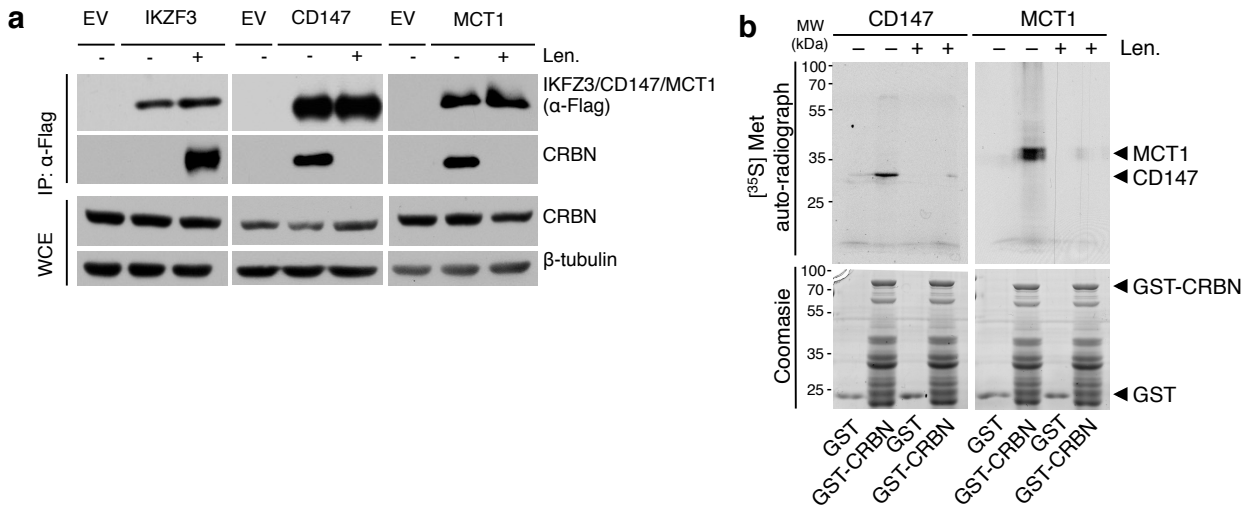

Fig. 13. Lenalidomide competes with CD147 and MCT1 for binding to CRBN. (a) Immunoprecipitation (IP) of Flag-tagged IKFZ3, CD147, and MCT1 from whole cell extracts (WCE) of HEK293T cells transfected with the according expression constructs or empty vector control (EV) and treated with 100 µM lenalidomide (Len.) or vehicle as indicated. Proteins were crosslinked *in-vivo* using DSS. Bound protein fractions were subjected to immunoblot analysis. **(b)** GST-pulldown assays of recombinant GST-CRBN with *in-vitro* translated and ^{35}S-labeled CD147 and MCT1 proteins incubated with solvent or lenalidomide (100 µM) as indicated. Bound proteins were visualized by autoradiograpy and GST-proteins by Coomassie staining. [Data provided by Dr. V. Fernández-Sáiz].

To confirm that lenalidomide impedes direct interaction between CRBN and CD147/MCT1, binding experiments with *in-vitro* translated, radioactively labeled CD147 and MCT1 (see Fig. 11), were repeated in presence and absence of the drug. As expected, CD147 and MCT1 bound to GST-CRBN in absence of lenalidomide, while *in-vitro* incubation with 100 µM lenalidomide almost completely blocked interaction (Fig. 13b), thus characterizing CD147 and MCT1 as physiological direct interactors of CRBN, which are outcompeted by IMiD treatment.

The competitive binding pattern could result from competition for the same binding motif within CRBN, or, alternatively, from IMiD-induced alteration of CRBN folding or structure omitting further interaction with CD147/MCT1. However, IMiD binding to CRBN was not reported to distort the entire protein (Chamberlain et al., 2014; Fischer et al., 2014), making competition for binding to the hydrophobic IMiD binding pocket more likely (see chapter 2.4.1). To analyse if CD147 and MCT1 indeed bind to the same motif, GST-pulldown assays were performed with a CRBN mutant harboring the Y384A and W386A mutations (CRBN$^{YW/AA}$), which disrupt the IMiD binding pocket (see chapter 2.4.1) (Fischer et al., 2014; Ito et al., 2010). For pulldown experiments, HEK293FT cells with CRISPR/Cas9-induced knockout of CRBN (HEK293FT CRBN$^{-/-}$) were transfected to express either wildtype CRBN, the CRBN$^{YW/AA}$ mutant or control, and treated with lenalidomide or vehicle. Respective lysates were subjected to GST-pulldown assays with GST-tagged C-terminal intracellular fragments of CD147 and MCT1 as described above (Fig. 12). Notably, the interaction between wildtype CRBN and CD147/MCT1 was inhibited by lenalidomide, whereas the

CRBN$^{YW/AA}$ mutant failed to bind CD147 or MCT1 independent of lenalidomide (Fig. 14), thus confirming the hypothesis of competitive binding and characterizing the IMiD binding pocket as binding site of CD147 and MCT1.

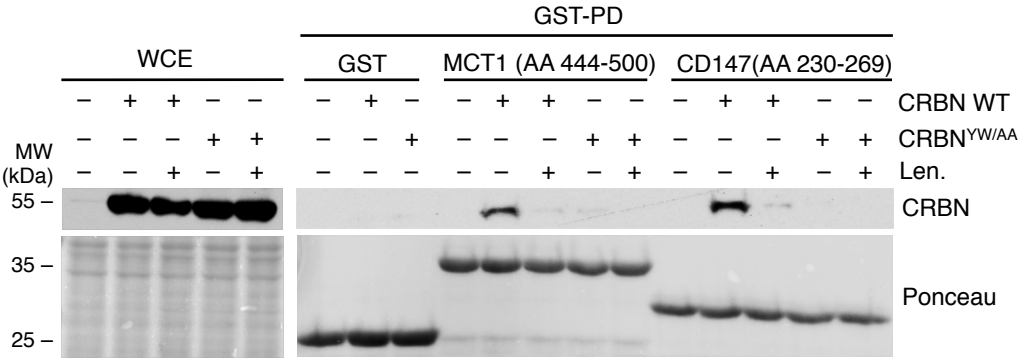

Fig. 14: CD147 and MCT1 bind to the IMiD binding pocket of CRBN. GST-pulldowns using the indicated GST-tagged fragments of CD147 and MCT1 or empty GST, which were incubated with whole cell extracts (WCE) of CRBN$^{-/-}$ HEK293FT cells transfected to express wildtype (WT) CRBN, the IMiD binding-defective CRBN$^{YW/AA}$ mutant or empty vector. Lenalidomide (Len.;100 µM) or vehicle was added to cells in culture and to WCE as indicated. Precipitates were subjected to immunoblot analysis; Ponceau staining served as loading control.

3.1.4 CRBN promotes stabilization of CD147 and MCT1

CRBN is described to be a DCAF (DDB1-CUL4-associated fctor), the substrate-binding unit of CRL4 ubiquitin ligases, and exert ubiquitin ligase activity within the CRL4^{CRBN} complex (see chaper 2.4.3 and 2.4.4). The lenalidomide-induced degradation of IKZF1/3 and CK1-α is attributed to CRL4^{CRBN}-mediated ubiquitylation, followed by proteasomal degradation of these substrates (Kronke et al., 2015; Kronke et al., 2014; Lu et al., 2014).

In order to test wether CD147/MCT1 are physiological substrates, which are targeted for degradation by the CRL4^{CRBN} ligase, the impact of modified CRBN expression on CD147/MCT1 stability was examined. First, MM1.S cells were lentivirally infected with two independent shRNA constructs targeting CRBN or a scrambled control shRNA. If CD147 and MCT1 were classic ligase substrates, silencing of CRBN would result in decreased degradation and increased stability. Surprisingly, immoblot analyses showed the opposite: both CD147 and MCT1 levels significantly decreased upon CRBN knockdown (Fig. 15a), suggesting a stabilizing effect of CRBN and arguing against a classic ligase-substrate interaction. To further inquire the relation of CRBN to CD147/MCT1 stability, MM1.S cells were lentivirally infected to overexpress either wildtype CBRN or the IMiD-binding defective CRBN$^{YW/AA}$ mutant. In line with the knockdown data, immunoblot analysis of whole cell extracts showed increased abundance of both CD147 and MCT1 upon CRBN overexpression, whereas expression of CRBN$^{YW/AA}$ did not have any effect on CD147 and MCT1 (Fig. 15b). Together, these data suggest that CRBN promotes stabilization of CD147 and MCT1 via direct interaction.

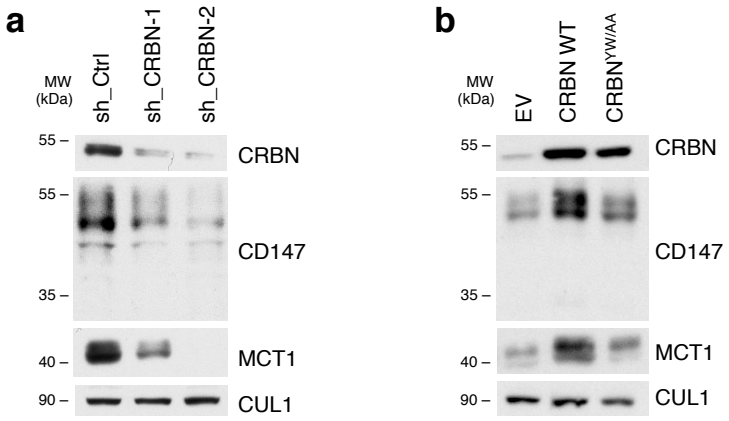

Fig. 15: CRBN stabilizes CD147 and MCT1. (a,b) Immunoblot analyses of MM1.S cells, which were lentivirally infected with two independent shRNAs against CRBN (sh_CRBN-1 and -2) or a control shRNA (sh_Ctrl) **(a)**, or with expression constructs coding for wildtype (WT) CRBN, $CRBN^{YW/AA}$, or empty vector (EV) **(b).** Whole cell extracts were subjected to immunoblot analysis using the indicated antibodies.

3.1.5 Lenalidomide destabilizes CD147 and MCT1

If CRBN stabilizes CD147 and MCT1 (Fig. 15) while lenalidomide abrogates the interaction of these proteins (Fig. 13, 14), it is conceivable that lenalidomide destabilizes CD147 and MCT1. To test this hypothesis, MM1.S cells were treated with increasing doses of lenalidomide, ranging from 0 to 100 µM. Immunoblot analyses of whole cell extracts indeed showed a decrease of CD147 and MCT1 protein abundance under lenalidomide treatment (Fig 16), comparable to the effects of CRBN silencing (Fig. 15a). Lenalidomide-induced destabilization of CD147 and MCT1 was dose-dependent, with significant effects already at concentrations as low as 1,25 µM (Fig. 16a). IKZF3 expression levels were also dramatically reduced unter lenalidomide (Fig. 16), in accordance with published data (Kronke et al., 2014; Lu et al., 2014).

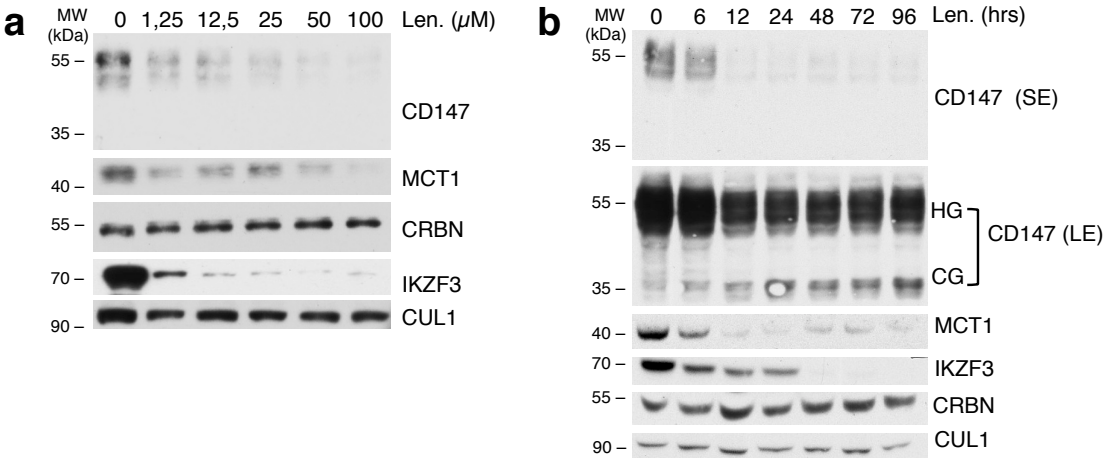

Fig. 16: Lenalidomide destabilizes CD147 and MCT1 in a dose- and time-dependent manner. (a,b) Immunoblot analyses of MM1.S cells. treated with the indicated concentrations of lenalidomide (Len.) for 72 hrs **(a)** or with 10 µM Len. for the indicated times **(b).** HG, high-glycosylated; LG, low-glycosylated; SE, short exposure; LE, long exposure. [Data for **a** provided by M.Heider].

In a complementary approach, MM1.S cells were treated with 10 µM lenalidomide for up to 96 hrs to investigate the time course of CD147/MCT destabilization. Immunoblots of cells harvested at predefined timepoints revealed first effects on MCT1 and CD147 abundance as early as 6–12 hrs after onset of treatment (Fig. 16b). Interestingly, the immature core-glycosylated (CG) form of CD147 accumulated, while the mature high-glycosylated (HG) form decreased with time (Fig. 16b).

3.1.6 Lenalidomide-induced destabilization of CD147/MCT1 depends on CRBN

Given the competition between CD147/MCT1 and IMiDs for CRBN binding (Fig. 13,14) and the destabilization of CD147 and MCT1 upon CRBN silencing or lenalidomide treatment (Fig. 15a, 16), it is likely that the lenalidomide-induced effects depend on CRBN. To investigate this hypothesis, the effect of lenalidomide on wildtype (WT) MM1.S cells was compared to the effect on MM1.S cells with CRISPR/Cas9 induced CRBN knockout (clone T11 and T21 of MM1.S CRBN$^{-/-}$). In accordance with the findings in sh_CRBN expressing MM1.S cells (Fig. 15a), expression levels of CD147 and MCT1 were significantly lower in CRBN$^{-/-}$ cells as compared to WT controls (Fig. 17a). Despite reduced overall CD147 abundance in MM1.S CRBN$^{-/-}$ cells, immature CG-CD147, which accumulated under lenalidomide (Fig. 16b), was more abundant in the CRBN$^{-/-}$ context (Fig. 17a), suggesting a block in maturation from CG- to mature HG-CD147.

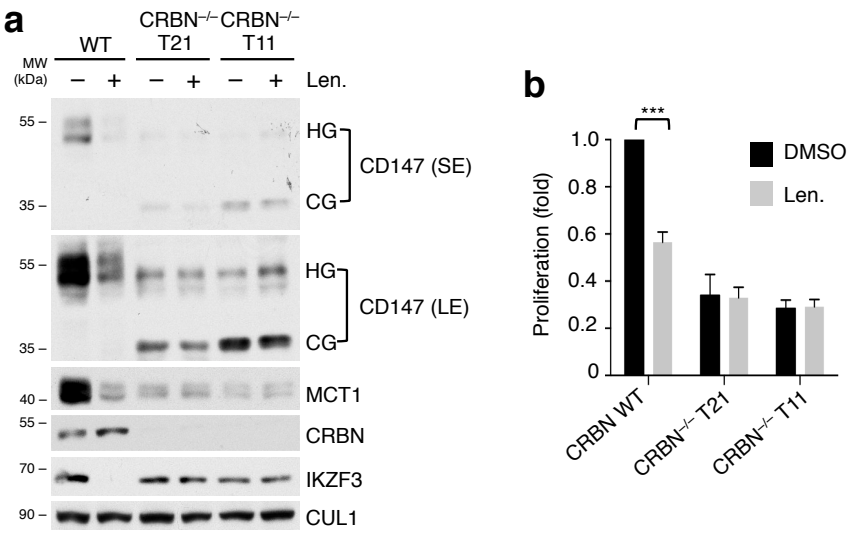

Fig. 17: Lenalidomide-induced destabilization of CD147 and MCT1 depends on CRBN. (a) Immunoblot analysis of wildtype (WT), and two CRBN$^{-/-}$ (T11, T21) MM1.S lines, treated with 10 µM lenalidomide (Len.) or vehicle (DMSO) for 96 hrs as indicated. Whole cell extracts were subjected to immunoblot analysis using the indicated antibodies. HG, high-glycosylated; LG, low-glycosylated; SE, short exposure; LE, long exposure. **(b)** Proliferation of cells described in **(a)** as determined by counting of viable cells after 96 hrs oftreatment using the trypan blue exclusion method. Cell counts are presented in relation to the counts of WT cells under DMSO treatment. (n = 3 independent experiments with two technical replicates each, data is presented as mean ± S.D.). ***, $P < 0.001$; one-sample t-test.

In accordance with previous results (Fig. 16), lenalidomide induced destabilization of CD147 and MCT1 in WT MM1.S cells (Fig. 17a). By contrast, lenalidomide did not further reduce

the already low expression levels of MCT1 and CD147 in CRBN$^{-/-}$ cells (Fig. 17a). These results demonstrate that lenalidomide-induced destabilization of CD147 and MCT1 depends on CRBN, in line with the proposed model that lenalidomide and CD147/MCT1 compete for CRBN binding. As expected, lenalidomide-induced destabilization of IKZF3 was only observed in wildtype and not in CRBN$^{-/-}$ MM cells (Fig. 17a). In contrast to CD147 and MCT1 however, IKZF3 was equally expressed in wildtype and CRBN$^{-/-}$ MM1.S cells, consistent with its role as "neo-substrate", which only interacts with CRBN in presence of lenalidomide without being regulated by CRBN in the physiological context (Kronke et al., 2014; Lu et al., 2014).

Importantly, MM1.S CRBN$^{-/-}$ cells, which displayed low expression of CD147 and MCT1, proliferated much slower than WT MM1.S cells (Fig. 17b), consistent with previous data that silencing of CRBN or CD147/MCT1 is anti-proliferative in MM cells (Arendt et al., 2012; Zhu et al., 2011). Moreover, the low proliferation rates of CRBN$^{-/-}$ cells were not further reduced by lenalidomide, while growth of highly proliferating MM1.S WT cells with high expression of CRBN, CD147 and MCT1, was markedly inhibited by lenalidomide (Fig. 17b). Overall, these results confirm that the anti-MM effects of IMiDs depend on CRBN (Zhu et al., 2011) and suggest that lenalidomide-induced destabilization of CD147/MCT1 depends on CRBN and correlates with anti-MM efficacy.

3.1.7 CD147 and MCT1 destabilization occurs on a post-transcriptional level

Given the direct binding of CRBN to CD147 and MCT1 (Fig. 10–14), the CRBN-mediated stabilization or lenalidomide-induced destabilization respectively (Fig. 15–17), are most plausibly mediated on a post-translational level. In light of IKZF1/3 being transcription factors, additional experiments were however performed to confirm this hypothesis and exclude transcriptional effects. To evaluate the impact of lenalidomide on transcription of CD147 and MCT1, RNA of MM1.S cells treated with lenalidomide or vehicle was extracted, reverse transcribed and subjected to qPCR analysis using specific primers for CRBN, CD147 and MCT1. Importantly, mRNA levels of CD147 and MCT1 did not decrease under lenalidomide treatment (Fig. 18a), strengthening the evidence for post-transcriptional destabilization. Interestingly, both CRBN and CD147 mRNA levels even seemed to moderately increase under lenalidomide (Fig. 18a), an effect, which might result from compensatory mechanisms trying to counteract loss of CD147.

To rule out any other correlation between IKZF1/3 and CD147/MCT1, MM1.S cells were lentivirally infected with constructs encoding shRNAs specific for IKZF1 or IKZF3, or an unspecific control shRNA. Despite efficient knockdown of IKZF1 and IKZF3 in immunoblot analyses of respective lysates, no change of CD147 and MCT1 protein levels was observed (Fig. 18b). Overall, these results are in line with previous experiments, suggesting that lenalidomide destabilizes CD147 and MCT1 on a post-transcriptional level and independent of IKZF1/3.

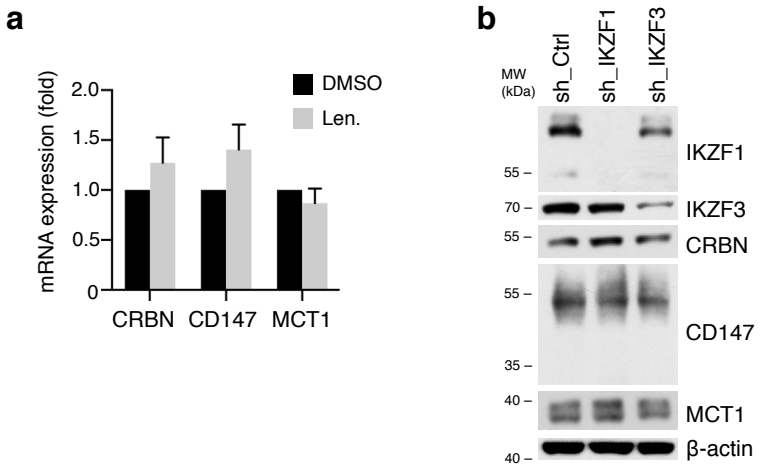

Fig. 18: Destabilization of CD147 and MCT1 is post-transcriptional and independent of IKZF1/3. (a) Real-time qPCR analysis on RNA extracted from MM1.S cells treated with 10 µM lenalidomide (Len.) or vehicle (DMSO) for 96 hrs. Total RNA was reverse transcribed and subjected to real-time qPCR analysis using specific primers for *CRBN*, *CD147*, *MCT1* or *ARPP* as internal control. The mRNA amount in the DMSO treated sample was set as 1 (n = 3 independent experiments with 2 technical replicates each, mean ± S.D.) [Data provided by M. Heider]. **(b)** Immunoblot analysis of MM1.S cells, which were lentivirally infected with shRNA constructs targeting IKZF1 (sh_IKZF1), IKZF3 (sh_IKZF3) or control (sh_Ctrl).

3.1.8 Destabilization of CD147 and MCT1 is a class-specific effect of IMiDs

As thalidomide and pomalidomide, the other two established IMiDs, bind to the same binding pocket within CRBN (Chamberlain et al., 2014; Fischer et al., 2014; Ito et al., 2010; Kronke et al., 2015), these drugs are supposed to outcompete CD147 and MCT1 in analogy to lenalidomide, resulting in destabilization. In order to investigate if CD147/MCT1 destabilization indeed is a class-wide effect of IMiDs or rather specific to lenalidomide, MM1.S cells were treated with 500 µM thalidomide, 10 µM lenalidomide, 100 nM pomalidomide or vehicle (DMS0) for 96 hrs. The relatively high concentration of thalidomide was chosen based on preliminary experiments testing different concentrations as to their cellular effects. Due to the low solubility of thalidomide in aqueous solution, the effective concentration in solution is expected to be much lower than 500 µM. Immunoblot analysis of MM1.S cells treated with the respective IMiDs or vehicle indeed demonstrated significant destabilization of CD147 and MCT1 under thalidomide, lenalidomide and pomalidomide (Fig.19), suggesting a general drug-class specific effect, which is in accordance with the proposed mechanism of competitive binding.

Importantly, IKZF1 and IKZF3 levels were not affected by thalidomide (Fig.19). In fact, IKZF1/3 degradation was initially only described for lenalidomide (Kronke et al., 2014; Lu et al., 2014), and structural data suggested that IKZF1/3 binding required an amine-group at C4 of the phtalimide ring of IMiDs (see chapter 2.4.4), which is common to lenalidomide and pomalidomide, but not thalidomide (Fischer et al., 2014). Together, these results identify destabilization of CD147 and MCT1 as an IMiD-wide class-specific effect, while destabilization of IKZF1/3 is restricted to lenalidomide and pomalidomide. Therefore, IKZF1/3 degradation can only be responsible for some effects of lenalidomide and pomalidomide, but not for the typical effects

attributed to all IMiDs. Instead, CD147 and MCT1, which were destabilized by all established IMiDs (Fig. 19), might be important mediators of common IMiD effects, given their diverse tumor-promoting properties (see chapter 2.5.2).

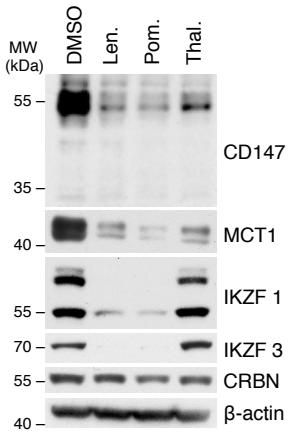

Fig. 19: Destabilization of CD147 and MCT1 is a class-specific effect of IMiDs. Immunoblot analysis of whole cell extracts of MM1.S cells treated with 10 µM lenalidomide (Len.), 100 nM pomalidomide (Pom.), or 500 µM thalidomide (Thal.) for 96 hrs. MW, molecular weight.

3.2 CD147/MCT1 destabilization is independent of CRL4 ligase function

3.2.1 IMiD-induced destabilization of CD147/MCT1 is independent of CUL4

The relation of CRBN to CD147 and MCT1 differs in many aspects from its relation to the previously described targets IKZF1/3 and CK1-α. While the latter are ubiquitylated and degraded once lenalidomide or pomalidomide promote their binding to CRBN (Kronke et al., 2015; Kronke et al., 2014; Lu et al., 2014), CRBN physiologically interacts with CD147 and MCT1 to stabilize them (see chapter 3.1). The relation between CRBN and CD147/MCT1 hence does not fulfill the criteria of classic E3 ligase-substrate interactions. However, ubiquitylation does not necessarily lead to proteasomal degradation. K63-linked polyubiquitylation and particularly monoubiquitylation of proteins typically modifies binding properties or intracellular localization (Hicke, 2001; Nakagawa and Nakayama, 2015). Against this background, the observed stabilizing effect of CRBN (Fig. 15a, 17) could result from non-proteolytic, stabilizing ubiquitlyation of CD147 and MCT1, or be mediated by an E3-ligase-independent function of CRBN.

To investigate wether the stabilizing effect of CRBN and the IMiD-induced destabilization of CD147 and MCT1 depend on $CRL4^{CRBN}$ ligase activity, MM1.S cells were infected with specific shRNA constructs directed against CUL4A or CUL4B, the two paralogs of CUL4, which is the scaffold protein of CRL4 ubiqutin ligases (see Fig. 7). The MM1.S cells, in which CRL4 ligase activity was impeded by knockdown of CUL4A or CUL4B, were treated with 10 µM lenalidomide or vehicle (DMSO) for 96 hrs. Efficient knockdown on the protein level was confirmed by immunoblot analysis (Fig. 20a). In contrast to CBRN silencing (Fig. 15a, 17a), neither baseline

levels of CD147 and MCT1, nor lenalidomide-induced destabilization were affected by knockdown of CUL4A or CUL4B (Fig. 20a), suggesting CRL4 independence of the CRBN-mediated effects.

As expected, silencing of CUL4A or CUL4B did not affect baseline IKZF3 levels either. Contrary however, and in discordance to the effects of CRBN knockdown (Fig. 17a), CUL4A/B knockdown did not significantly hinder lenalidomide-induced degradation of IKZF3 (Fig. 20a). Assuming that IKZF3 is ubiquitylated by $CRL4^{CRBN}$ (Kronke et al., 2014; Lu et al., 2014) these results were surprising and the underlying cause remains unclear. Hypothetically, other CRL ligases might compensate for reduced CRL4 activity, thus maintaining degradation of IKZF3.

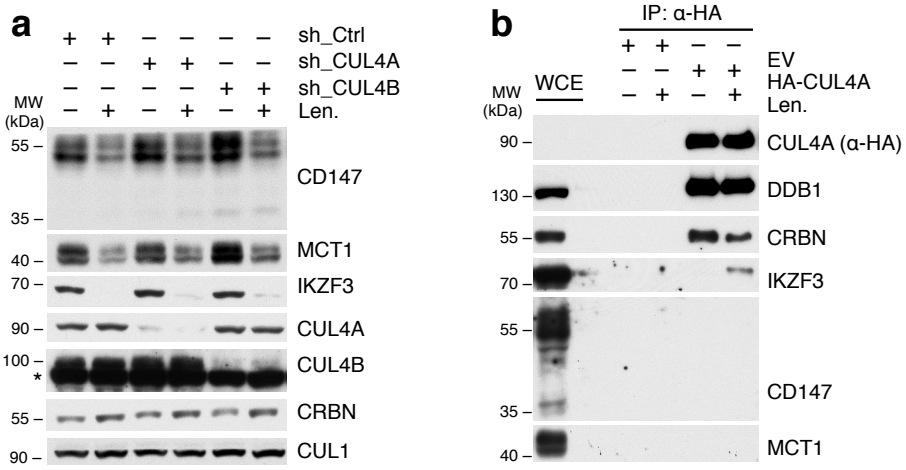

Fig. 20: IMiD-induced destabilization of CD147/MCT1 is independent of the CRL4 ligase. (a) Immunoblot analysis of MM1.S cells infected with lentiviral shRNA constructs targeting CUL4A (sh_CUL4A) or CUL4B (sh_CUL4B) or a scrambled control (sh_Ctrl). Cells were treated with 10 µM lenalidomide (Len.) or vehicle (DMSO) for 96 hrs as indicated. The asterisk denotes an unspecific band of the CUL4B antibody. **(b)** Immunoprecipitation (IP) of HA-CUL4A which was purified from HEK293T cells using HA-beads and incubated with MM1.S whole cell extracts (WCE) treated with 100 µM Len. or vehicle as specified. Bound protein fractions were subjected to immunoblot analysis.

To investigate if CD147 and MCT1 acutally interact with the $CRL4^{CRBN}$ ligase or maybe bind to CRBN in a non CRL-context, CUL4A immounoprecipitates were analyzed for association with CD147/MCT1 and IKZF3. HA-beads with bound HA-CUL4A purified from HEK293T cells or control HA-beads were therefore incubated with MM1.S lysates in presence of lenalidomide or vehicle (DMSO). As expected, DDB1 and CRBN bound to CUL4A independent of lenalidomide, confirming proper assembly of the $CRL4^{CRBN}$ complex (Fig. 20b). By contrast, IKZF3 was only co-purified with CUL4A in presence of lenalidomide, in accordance with previous data (Fig. 13a), while CD147 and MCT1 were not retrieved in any of the CUL4A precipiates (Fig. 20b). Overall, these results provide evidence that CRBN-mediated stabilization of CD147/MCT1 as well as IMiD-induced destabilization do not depend on CRL4 E3 ligase function or any CRBN-mediated ubiquitylation and suggest that CD147 and MCT1 might actually bind to a subset of CRBN not in complex with DDB1 and CUL4.

3.2.2 CRBN forms a ligase-independent complex with CD147 and MCT1

Given the ubiquitin-independence of CRBN-mediated stabilization of CD147/MCT1 (Fig. 20a), the failure of CD147/MCT1 to purify with the CRL4 complex (Fig. 20b), and considering the strikingly different behavior and binding properties of CD147/MCT1 and IKZF1/3, it is conceivable that CRBN fulfills distinct cellular functions as part of different complexes. On the one hand, CRBN would be involved in protein ubiquitylation and degradation as part of the $CRL4^{CRBN}$ E3 ligase, while on the other hand, CRBN could have functional roles outside the CRL4 ligase.

To validate the hypothesis that CRBN forms different complexes within the cell, chromatography experiments were performed by Dr. V. Fernández-Sáiz. To this end, Flag-tagged CRBN, CD147, MCT1, CUL4A and DDB1 were expressed in HEK293T cells, purified by Flag-IP, eluted and incubated with lenalidomide or vehicle before loading on Superose 6 columns for size exclusion chromatography (see chapter 6.3.12) As speculated, CRBN was indeed found to fractionate in two different complexes in absence of lenalidomide (Fig. 21). On the one hand, CRBN co-migrated with DDB1 and CUL4A in a complex of approximately 300 kDa, corresponding to the molecular weight of the CRL4 complex, while on the other hand, it migrated with CD147 and MCT1 in a complex of approximately 120 kDa, roughly corresponding to the molecular weight of the CRBN-CD147/MCT1 complex (Fig. 21). Importantly, lenalidomide treatment completely disrupted the CRBN-CD147/MCT1 complex, while not affecting integrity of the $CRL4^{CRBN}$ complex comprising CRBN, DDB1 and CUL4A (Fig. 21). Together, these findings support the hypothesis that CRBN has at least a dual function, one within the CRL4 ligase, and a distinct ligase-independent function that mediates e.g. stabilization of CD147 and MCT1.

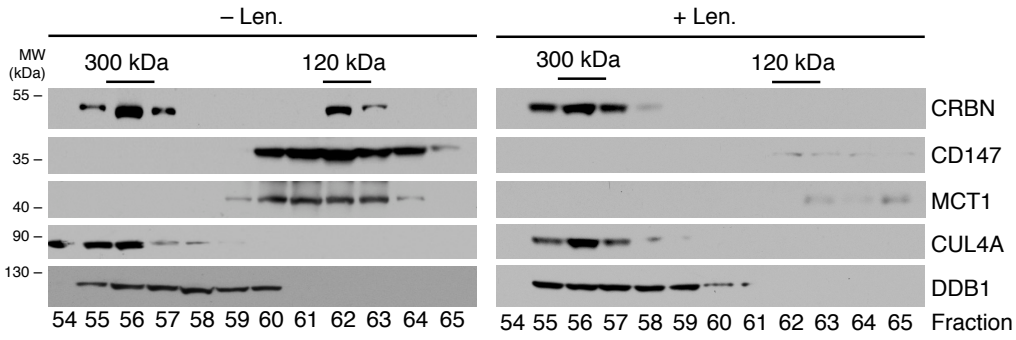

Fig. 21: CRBN forms a CRL4-independent complex with CD147 and MCT1. Gel filtration chromatography of CRBN-complexes that were purified by Flag-IP from HEK293T cells overexpressing Flag-CRBN, CD147, MCT1, CUL4 and DDB1. Proteins were eluted by Flag peptide and either left untreated (left) or exposed to 100 µM lenalidomide (right) prior to loading onto a calibrated Superose 6 sizing column. Analysis of resulting fractions (250 µl) was performed by immunoblotting subsequent to protein precipitation. The apparent molecular sizes of the peak-complexes are shown. [Data provided by Dr. V. Fernández-Sáiz].

3.3 CRBN promotes maturation of CD147 and MCT1

3.3.1 CRBN promotes membrane localization of CD147 and MCT1

Different hypotheses are conceivable to explain how binding to CRBN could stabilize CD147 and MCT1 and increase their abundance. CRBN could either increase stability and abundance by assisting in initial folding, complex assembly, maturation or transport across membranes, or inhibit degradation via e.g. interfereing with endocytosis or recycling. Importantly, CRBN contains a large LON domain, which is shared by some proteases and chaperones (Fischer et al., 2014; Smith et al., 1999) such as the mitochondrial Lon protease, which has chaperone-like functions promoting assembly of mitochondrial membrane complexes (Pinti et al., 2016; Rep et al., 1996). It is thus conceivable that CRBN has comparable chaperone-like functions promoting maturation of the CD147/MCT1 complex. Data showing preferred interaction of CRBN with immature core-glycosylated (CG) CD147 (Fig. 10a) and accumulation of this immature form unter lenalidomide treatment or CRBN knockdown (Fig. 16b, 17a), further supports the model that CRBN binds to early forms to promote their maturation.

As membrane proteins are translated at the endoplasmatic reticulum (ER), mature in the ER and Golgi and finally reach the plasma membrane in a mature form, blocking of maturation would result in accumulation at the ER, als already shown for CD147 and MCT1 (Huang et al., 2013a; Kirk et al., 2000). To assess whether CRBN knockdown affects subcellular localization of CD147 and MCT1, immunofluorescence (IF) experiments were performed with HeLa cells stably expressing an shRNA construct targeting CRBN or a scrambled control. The cells were transfected with tagged CD147 and MCT1 constructs, which were visualized by indirect IF staining (see chapter 6.2.8). Indeed, control HeLa cells showed co-localization of CD147 and MCT1 at the plasma membrane (Fig. 22a). In HeLa cells with depletion of CRBN by contrast, both CD147 and MCT1 did not properly localize to the plasma membrane, but instead accumulated in a perinuclear compartment (Fig. 22a), confirming the hypothesis that CRBN is necessary for maturation and membrane localization of CD147 and MCT1. DNA was stained with DAPI to visualize the nucleus. Quantification of cells with proper membrane expression of CD147 and MCT1 from three independent experiments confirmed significantly lower membrane localization of CD147/MCT1 in the CRBN knockdown context compared to control (Fig. 22c).

The perinuclear compartment, in which CD147 and MCT1 accumulate upon CRBN knockdown (Fig. 22a), is likely to be the ER, given the localization and pattern shown in IF. To verify this assumption, IF experiments were repeated as described above, with replacement of DAPI by an *in-vivo* ER tracker, a fluorescent dye accumulating in the ER. While CD147 and MCT1 primarily localized to the membrane in control cells, both proteins accumulated at the ER upon CRBN depletion (Fig. 22d), allowing the assumption that CRBN is needed for stabilization and maturation of early forms of CD147 and MCT1 at the ER.

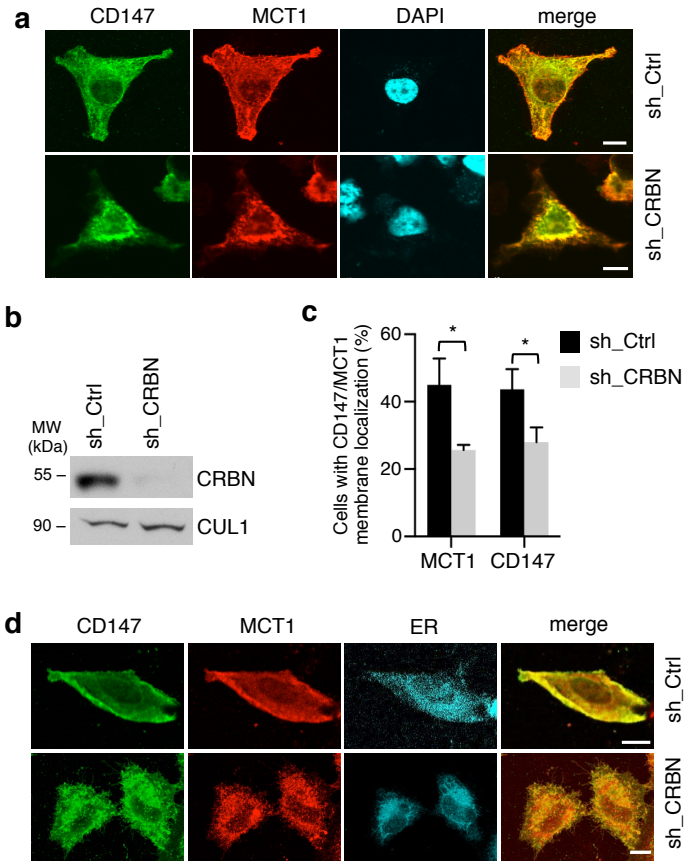

Fig. 22: CRBN promotes membrane localization of CD147 and MCT1. (a) Immunofluorescence (IF) staining of HeLa cells expressing shRNAs targeting CRBN (sh_CRBN) or control (sh_Ctrl), which were transfected with constructs encoding HA-CD147 and Flag-MCT1. After incubation with antibodies to HA (green) and Flag (red), DNA was stained with DAPI (blue) and IF slides were analyzed by confocal microscopy. Scale bars represent 10 µm. **(b)** Immunoblot analysis of whole cells extracts of HeLa cells shown in **a** using the indicated antibodies. **(c)** Quantification of cells with membrane localization of CD147 and MCT1 from the experiment described in **a** equalized with two independent experiments (n = 3 experiments with 100 cells counted per experiment, error bars are mean ± S.D.). *, $P < 0.05$ by Student's t-test. [Data for **a** and **c** provided by Dr. B.S. Targosz]. **(d)** Immunofluorescence (IF) staining of HeLa cells as described in **a**, which were incubated with an ER-tracker (blue) prior to fixation with paraformaldehyde and incubation with antibodies to HA (green) and Flag (red). ER, endoplasmatic reticulum. Scale bars represent 10 µm.

Since non-adherent cells such as MM cells are not suitable for IF analysis, flow cytometry was chosen to validate the obtained data in MM. To only stain CD147 on the cell surface, cells were not permeabilized prior to analysis (see chapter 6.2.7.1). As expected, staining of wildtype (WT) and CRBN$^{-/-}$ MM1.S cells with anti-CD147 or isotype control antibodies demonstrated clearly higher surface expression of CD147 in WT cells as compared to the CRBN$^{-/-}$ context (Fig. 23a,b). Quantification of CD147 median fluorescence intensities (MFI) in CRBN$^{-/-}$ and WT MM1.S confirmed significance of the observed differences in surface expression (Fig. 23b).

In a complementary approach, MM1.S WT cells were treated with 10 µM lenalidomide or vehicle (DMSO) and evaluated for CD147 surface expression by flow cytometry. Consistent with previsous data and in analogy to the effects of CRBN silencing, surface expression of CD147 significantly decreased under lenalidomide treatment (Fig. 23c). Since all MCT1 binding

antibodies detect intracellular parts of the protein, staining of MCT1 was not possible without permeabilization, and was therefore not carried out.

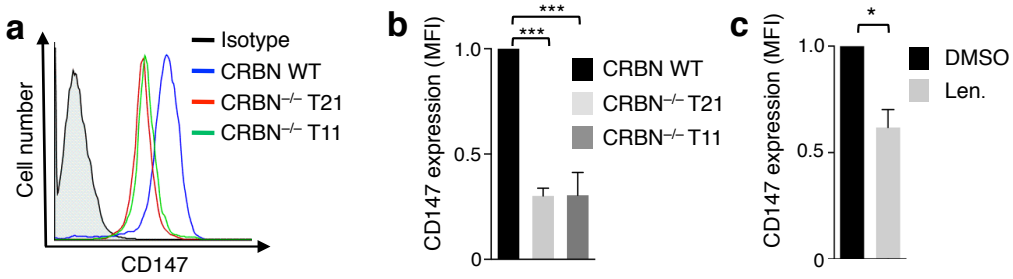

Fig. 23: Cell surface expression of CD147 in MM cells is promoted by CRBN and inhibited by IMiDs. (a) Flow cytometric analysis of cell surface expression of endogenous CD147 in wildtype (WT) MM1.S cells and two CRBN$^{-/-}$ MM1.S clones (T11, T21). The cells were incubated with anti-CD147 or isotype control antibody and a FITC-tagged secondary antibody. Data is depicted as histogram analysis of FL1 (FITC) signal intensity. **(b)** Quantification of CD147 median fluorescence intensities (MFI) of MM1.S cells described in **a**, presented as CD147/isotype ratios (n = 3 independent experiments, error bars are mean ± S.D.). ***, $P < 0.001$ by one sample t-test. **(c)** Cell surface expression of endogenous CD147 in MM1.S cells treated with 10 µM lenalidomide (Len.) or DMSO as evaluated by flow cytometry. Quantification of CD147 MFI presented as CD147/isotype ratios (n = 3 independent experiments, mean ± S.D.). *, $P < 0.05$ by one sample t-test.

3.3.2 CRBN interacts with immature forms of CD147 and MCT1

If CRBN binds to CD147 and MCT1 at the ER to promote their maturation, it is assumable that CRBN preferably interacts with freshly translated immature proteins, as already indicated by increased binding to CG-CD147 (Fig. 10a).

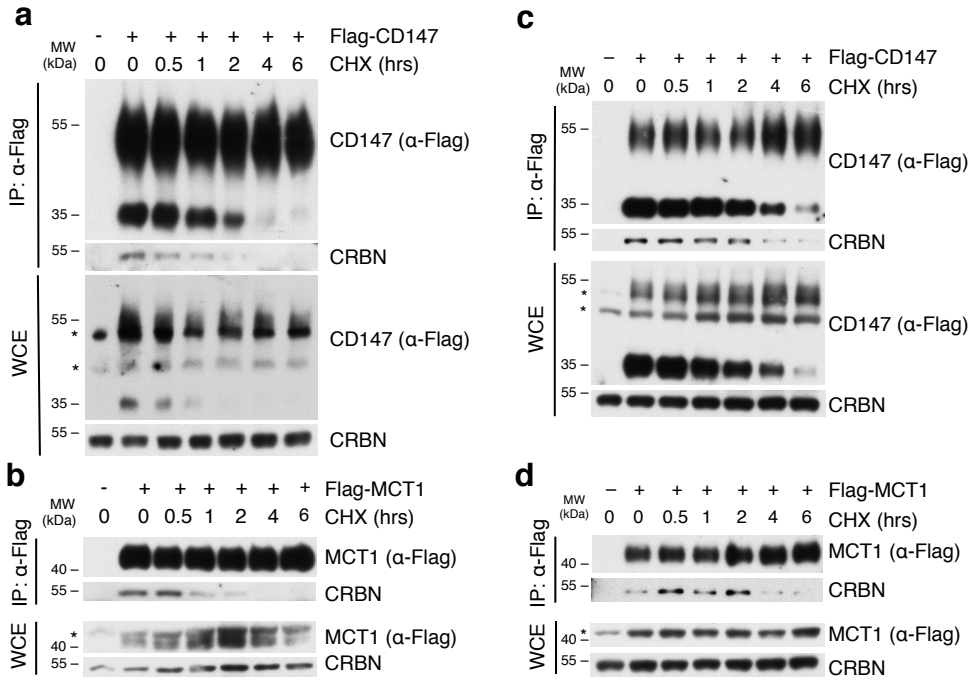

Fig. 24: CRBN binds to freshly translated CD147 and MCT1. Flag-immunoprecipitations (IP) of Flag-CD147 **(a, c)** or Flag-MCT **(b, d)** from whole cell extracts (WCE) of MM1.S **(a, b)** or U266 MM cells **(c, d)** lentivirally infected to express Flag-CD147 **(a, c)** or Flag-MCT1 **(b, d)**. Cells were treated with 100 µg/ml cycloheximide (CHX) for the indicated periods of time. Flag-IPs were subjected to immunoblot analysis using the indicated antibodies. The asterisks denote unspecific bands of the Flag antibody.

To verify this assumption, two different human MM cell lines, MM1.S and U266, were lentivirally infected to express Flag-tagged CD147, Flag-tagged MCT1 or empty vector as control, and treated with cycloheximide (CHX), and inhibitor of protein translation (see chapter 6.2.3.2). Aliquots were harvested after different periods of time and subjected to Flag-IP. If CRBN preferably interacts with immature proteins, binding is expected to be stronger in untreated cells, and decline with longer CHX treatment, as proteins mature. As previously shown, CBRN co-purified with CD147 and MCT1 in untreated cells (Fig. 10b,c; 12b; 13a; 14; 24). With increasing time of CHX treatment by contrast, CRBN binding was indeed gradually lost, despite stable protein levels in whole cell lysates (Fig. 24 a-d), confirming the hypothesis that CRBN interacts with freshly translated immature CD147 and MCT1. Of note, the extent of CRBN binding to CD147 correlated well with the abundance of immature CG-CD147, which was progressively lost under prolonged CHX treatment (Fig. 24a, c), providing further evidence that CRBN preferentially interacts with immature CD147.

3.3.3 IMiD treatment and CRBN silencing inhibit CD147 maturation

In order to further investigate the impact of CRBN on CD147 maturation, Dr. V. Fernández-Sáiz performed pulse-chase experiments with radioactively labeled CD147, whose differential glycosylation allows distinction of immature and mature protein by immunoblotting. MM1.S cells stably expressing two different shRNAs targeting CRBN or a control shRNA were radioactively labeled with L-[^{35}S]-Methionine/Cysteine (see chapter 6.3.11). Samples were harvested at defined time points up to 24 hrs after pulsing and endogenous CD147 was immunoprecipitated and visualized by autoradiography. As expected, CD147 was gradually glycosylated, evolving from the immature CG form to the mature HG form within 24 hrs (Fig. 25a). Upon CRBN silencing by contrast, a high percentage of CD147 persisted as immature CG form, with only a small fraction undergoing maturation (Fig. 25a), thus underlining the importance of CRBN for proper maturation of CD147.

An analogous approach investigated the effect of lenalidomide treatment on CD147 maturation. MM1.S cells, pulsed with radioactive L-[^{35}S]-Methionine/Cysteine as described above, were therefore incubated with 10 µM lenalidomide or vehicle (DMSO) for up to 24 hrs. While DMSO treatment did not affect CD147 maturation, autoradiography of immunprecipitated CD147 showed substantially impaired glycosylation and maturation under lenalidomide treatment (Fig. 25b), comparable to the effects of CRBN silencing (Fig. 25a)

To confirm CRL4 ligase-independence of the observed effects on CD147 maturation, pulsed cells were additionally exposed to MLN4924, an inbititor of CRL E3 ligases. Importantly, MLN4924 had no effect on CD147 maturation and did not alter lenalidomide activity (Fig. 25b), thus further underscoring ubiquitin-independence of the observed effects.

Altogether, the binding of immature proteins at the ER and the observed effects on CD147 maturation suggest that CRBN exerts a chaperone-like function towards CD147 and MCT to promote their proper maturation, complex assembly and membrane expression.

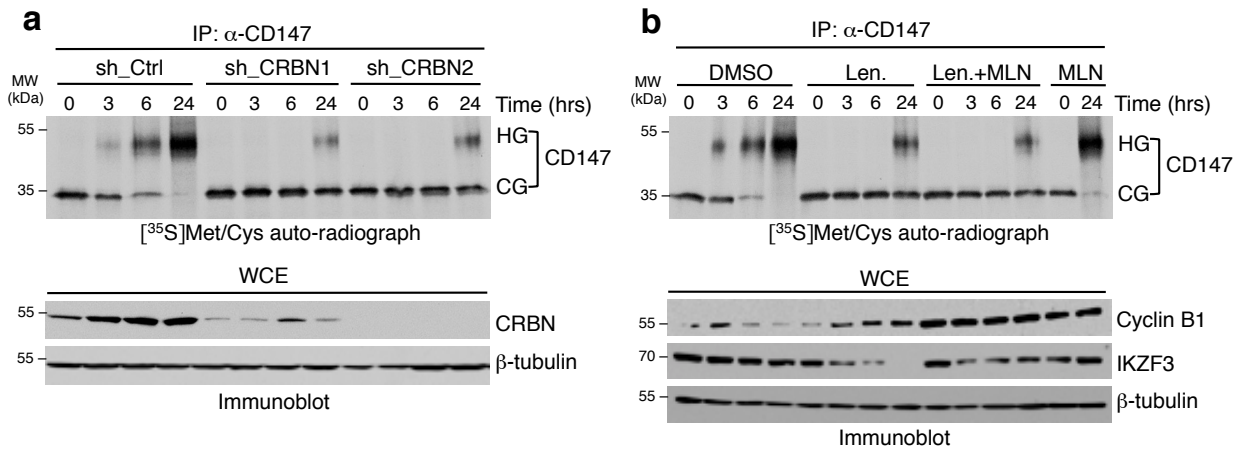

Fig. 25: CD147 maturation depends on CRBN. (a) Autoradiographic analysis (top) of CD147 immunoprecipitates (IPs) from MM1.S cells, which were lentivirally infected with the indicated shRNA constructs targeting CRBN (sh_CRBN1 and sh_CRBN2) or control (sh_Ctrl). Cells were pulsed with ^{35}S-Methionine/Cystein and chased for the indicated periods of time. Whole cell lysates (WCE) were analyzed by immunoblotting using the specified antibodies (bottom). **(b)** Autoradiography (top) of CD147 IPs from MM1.S cells pulsed with ^{35}S-Methionine/Cystein, treated with 10 µM lenalidomide (Len.) or vehicle (DMSO) and/or 10 µM MLN4924 (MLN) as indicated, and chased for the specified times. WCE were subjected to immunoblot analysis (bottom). CG, core glycosylated; HG, high glycosylated. [Data provided by Dr. V. Fernández-Sáiz].

3.4 IMiDs mediate anti-myeloma activity via CD147/MCT1 destabilization

3.4.1 CD147/MCT1 destabilization correlates with IMiD sensitivity

The performed experiments established CD147 and MCT1 as proteins whose maturation and membrane expression are promoted by CBRN in a chaperone-like way, and whose binding to CRBN is outcompeteted by IMiDs, resulting in destabilization. In light of the importance of CD147 and MCT1 for MM cell proliferation and survival (Arendt et al., 2012; Walters et al., 2013; Zhu et al., 2015), it is conceivable that IMiD-induced destabilization of these proteins substantially contributes to the anti-MM effects of IMiDs.

To investigate the functional role of CD147 and MCT1 destabilization for IMiD-specific biological and therapeutic effects, different MM cell lines with described lenalidomide-sensitivity (MM1.S, U266, AMO1, L363) or -resistance (KMS12BM, RPMI 8226, JJN3, INA-6) (Gandhi et al., 2014a; Kronke et al., 2014; Lu et al., 2014) were analyzed with regard to proliferation as well as CD147 and MCT1 stability unter lenalidomide treatment. As expected, treatment with 10 µM lenalidomide significantly impaired proliferation of sensitive cell lines compared to DMSO treated controls (Fig. 26a): after 96 hrs of lenalidomide treatment, overall cell counts dropped to 40-70%, depending on the cell line, while 144 hrs of treatment suppressed cell counts to 10-45% in relation to controls (Fig. 26a). Resistant cells by contrast were not significantly affected by lenalidomide treatment (Fig. 26a). Immunoblot analysis of respective cell lines confirmed the previously described destabilization of CD147 and MCT1 upon lenalidomide exposure (Fig. 16, 17a, 19, 20) in sensitive lines (Fig. 26b). Strikingly, these effects were not observable in resistant cell lines, suggesting a connection between CD147/MCT1 destabilization and IMiD activity (Fig. 26b, c).

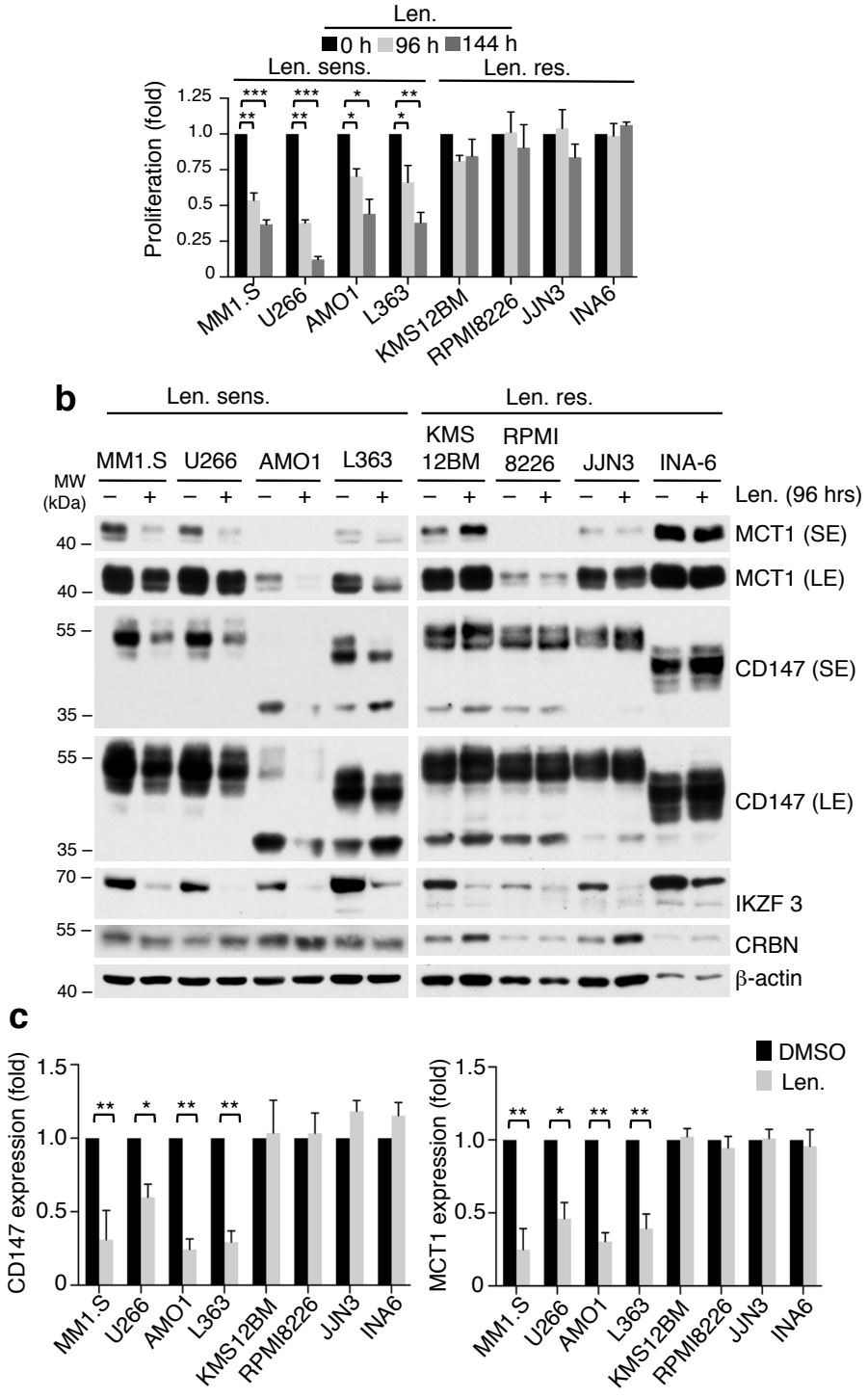

Fig. 26: IMiD-induced destabilization of CD147 and MCT1 is restricted to IMiD sensitive cells. (a) Proliferation of lenalidomide (Len.) sensitive (MM1S, U266, AMO1, L363) and resistant (KMS12BM, RPMI8226, JJN3, INA-6) MM cell lines treated with DMSO or Len. (10 µM). Viable cells were counted at indicated time points using the trypan-blue exclusion method; results are presented in relation to DMSO treated controls (n = 3 independent experiments with 2 technical replicates each, mean ± S.D.). *, $P < 0.05$; **, $P < 0.01$; ***, $P < 0.001$ by one sample t-test. **(b)** Immunoblot analysis of Len. sensitive (Len.sens.) and Len. resistant (Len.res.) MM cells described in **a** that were treated with DMSO or 10 µM Len. for 96 hrs. Whole cell extracts were probed using the indicated antibodies. SE, short exposure; LE, long exposure. **(c)** Quantification of CD147 and MCT1 expression levels of immunoblots shown in **b** averaged with two additional independent experiments (n = 3 independent experiments, mean ± S.D.). Results are presented in relation to DMSO controls. *, $P < 0.05$; **, $P < 0.01$; ***, $P < 0.001$ by one sample t-test. [Data provided by M. Heider].

In contrast to CD147 and MCT1, which were destabilized only in sensitive cell lines, IKZF3 degradation was observed equally in sensitive and resistant MM cells (Fig. 26b), which is in accordance with previous studies (Lu et al., 2014; Zhu et al., 2014). IKZF3 degradation does hence not correlate with the anti-proliferative response, questioning both the biological relevance of this mechanism as well as its utility as biomarker for IMiD sensitivity. CD147/MCT1 destabilization on the contrary clearly correlated with IMiD response, arguing for its biological relevance and potential use as predictor of IMiD response.

To test the hypothesis that IMiDs do not affect CD147 and MCT1 stability in resistant cell lines, experiments were extended to murine cells, which are intrinsically resistant to IMiDs, possibly resulting from an altered IMiD binding pocket (Kronke et al., 2015). Treatment of murine cells with lenalidomide or pomalidomide at concentrations highly active in sensitive human MM cell lines (Fig. 26a, b), did not affect proliferation of neither Ba/F3 cells, a mouse pro-B cell line, nor of X63AG8.653 cells, a murine myeloma cell line, at 96 hrs (Fig. 27a). Immunblotting of the respective whole cell lysates did not reveal any change of CD147 or MCT1 abundance after lenalidomide or pomalidomide treatment in comparison to DMSO control (Fig. 27b), confirming the correlation between IMiD sensitivity and CD147/MCT1 destabilization.

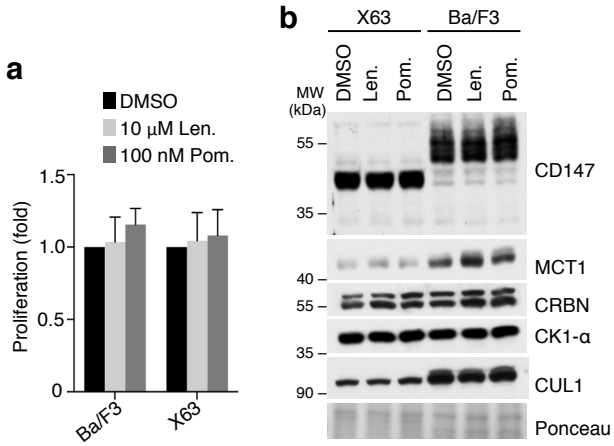

Fig. 27: IMiDs have no effect on proliferation and CD147/MCT1 stability in mouse cells. (a) Proliferation of the mouse myeloma cell line X63AG8.653 (X63) and mouse pro-B cell line Ba/F3 treated with DMSO, 10 µM lenalidomide (Len.) or 100 nM pomalidomide (Pom.) for 96 hrs. Viable cells counted using the trypan blue exclusion method are depicted in relation to DMSO control (n = 3 independent experiments with 2 technical replicates each, data is presented as mean ± S.D.). **(b)** Immunoblot analysis of whole cell lysates of murine cells described in **a**, which were treated with DMSO, 10 µM Len. or 100 nM Pom for 96 hrs.

3.4.2 CD147 and MCT1 are essential for proliferation and viability of MM cells

In order to investigate if CD147/MCT1 destabilization, which was found to correlate with IMiD sensitivity (Fig. 26), could be directly responsible for IMiD-mediated anti-MM activity, CD147 and MCT1 were silenced in MM cells. Both lenalidomide-sensitive and -resistant MM cell lines were infected with shRNA constructs targeting CD147, MCT1 or scrambled control. After verification of efficient knockdown (Fig. 28a), the cells were subjected to proliferation assays. In agreement with previous reports demonstrating the relevance of CD147 and MCT1 for MM

survival and proliferation (Arendt et al., 2012; Walters et al., 2013; Zhu et al., 2015), knockdown of either CD147 or MCT1 significantly reduced viability and proliferation in all analyzed MM cell lines, independent of their sensitivity or resistance to lenalidomide (Fig. 28b). These results confirm that CD147 and MCT1 are vital for proliferation and viability of MM cells in general and strengthen the hypothesis that CD147 and MCT1 are central mediators of the anti-MM effects of IMiDs.

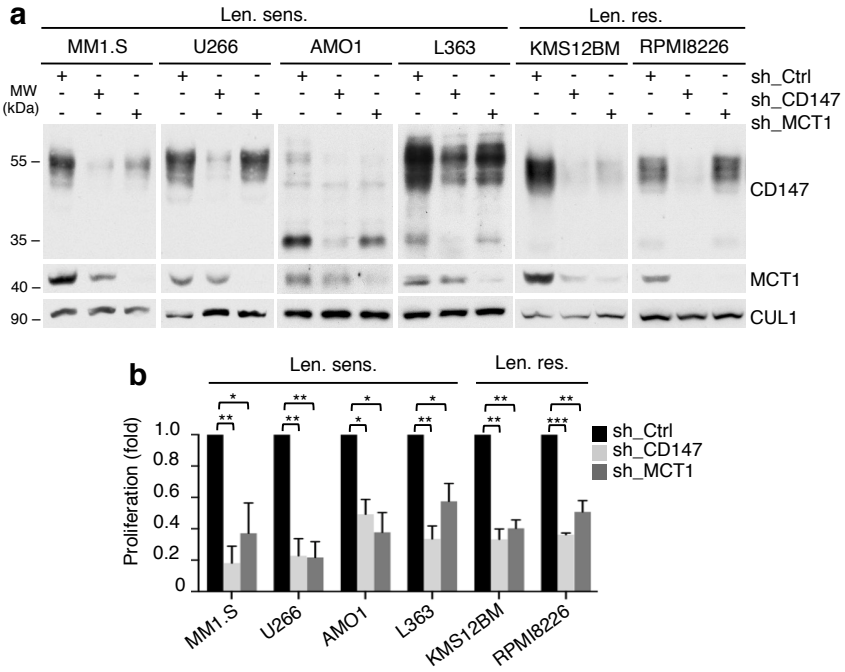

Fig. 28: CD147 and MCT1 are essential for MM proliferation and viability. (a) Immunoblot analysis of whole cell extracts of lenalidomide-sensitive (Len. sens.) and -resistant (Len. res.) MM cell lines, which were lentivirally infected with shRNA constructs targeting CD147 (sh_CD147), MCT1 (sh_MCT1) or control (sh_Ctrl). **(b)** Proliferation analysis of MM cell lines described in **a**, in which CD147, MCT1 or control was silenced using the indicated constructs. Viable cells counted using the trypan blue exclusion method 6 days after infection are presented in relation to control (n = 3 independent experiments with 2 technical replicates each, mean ± S.D.). *, $P < 0.05$; **, $P < 0.01$; ***, $P < 0.001$ by one sample t-test. [Data partly provided by M. Heider].

3.4.3 Overexpression of CD147/MCT1 attenuates IMiD effects

If IMiDs exert their anti-proliferative effects via destabilization of CD147 and MCT1, overexpression of these proteins could maybe counteract the anti-proliferative effects. According to the proposed model that IMiDs outcompete CD147 and MCT1 from binding to CRBN, forced expression of CD147 and MCT1 is however not expected to completely rescue the phenotype, as overexpressed CD147 and MCT1 supposedly still depend on CRBN for maturation.

To test these hypotheses and investigate the effects of induced CD147/MCT1 expression, MM1.S cells were double-infected with lentiviral particles encoding CD147 and MCT1 or empty vector control. Due to low transduction rates, double-infected cells were purified by FACS (fluorescence activated cell sorting) and subsequently expanded for further analysis. When exposed to lenalidomide, CD147/MCT1 overexpressing MM1.S cells were indeed more resistant to the anti-proliferative effects of IMiDs (Fig. 29a). While cell counts of lenalidomide treated

control cells were already reduced by 40% compared to DMSO treatment, proliferation of CD147/MCT1 overexpressing cells was only reduced by 10% after 72 hrs of lenalidomide treatment (Fig. 29a), showing a protective effect of CD147/MCT1 overexpression. With prolonged time of treatment, lenalidomide also reduced proliferation of CD147/MCT1 overexpressing MM cells more effectivly, in line with the model that transgenically expressed CD147 and MCT1 still depend on CRBN for maturation.

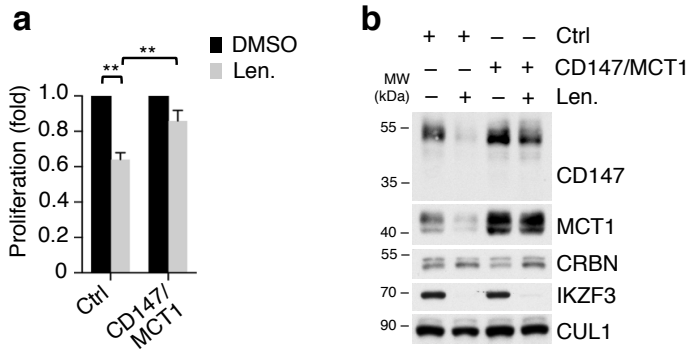

Fig. 29: Forced expression of CD147 and MCT1 counteracts the anti-proliferative effects of IMiDs. (a) Proliferation of MM1.S cells that were double-infected with the indicated lentirviral constructs to induce forced expression of CD147 and MCT1 or empty vector control (Ctrl). Purified cells were treated with DMSO or 10 µM lenalidomide (Len.) for 72 hrs as specified (n = 3 independent experiments with 2 technical replicates each, data is presented as mean ± S.D.). **, $P < 0.01$ by one sample t-test. **(b)** Representative immunoblot analysis of whole cell lysates of cells described in **a** that were treated with DMSO or 10 µM Len. for 72 hrs.

Immunoblot analysis of respective MM1.S cells confirmed stable overexpression of CD147 and MCT1 (Fig. 29b). Importantly, after 72 hrs of lenalidomide treatment, CD147 and MCT1 were already markedly destabilized in control cells, whereas no significant changes in CD147 or MCT1 abundance were yet observed in CD147/MCT1 overexpressing cells (Fig. 29b). As for proliferation, increased time of lenalidomide exposure eventually also destabilized CD147 and MCT1 in overexpressing cells, in line with the proposed model. Notably, the levels of CD147 and MCT1 expression closely correlated with the respective proliferation rates (Fig. 29a, b), further underlining the relevance of CD147 and MCT1 for MM cell proliferation. By contrast, IKZF3 degradation was not affected by overexpression of CD147/MCT1 and did not reflect the different proliferation rates (Fig. 29b). Overall, these results showing that forced expression of CD147/MCT1 attenuates the anti-proliferative effects of IMiDs at early time points, confirm the central role of CD147 and MCT1 in IMiD response.

3.4.4 IMiDs reduce VEGF and MMP7 secretion via CD147 destabilization

Besides direct anti-proliferative effects, which correlate with CD147/MCT1 destabilization (Fig. 26, 29), IMiDs also exert various other anti-tumor effects with possible relation to CD147 and MCT1, such as anti-angiogenic and anti-invasive properties (D'Amato et al., 1994; Kruse et al., 1998; Segarra et al., 2010). As CD147 has been described to promote angiogenesis via induction of VEGF and enhance migration and invasion via induction of matrix metalloproteinases

(MMPs) (Chen et al., 2009; Sun and Hemler, 2001; Tang et al., 2005), both anti-angiogenic and ant-proliferative effects of IMiDs could possibly be mediated via CD147 and MCT1.

In order to test this hypothesis, the influence of IMiDs on VEGF and MMP7, a matrix metalloproteinase constitutively secreted by MM cells (Barille et al., 1999), was investigated via quantification of secreted proteins in cell culture supernatants. Lenalidomide-sensitive and resistant MM cell lines were treated with DMSO or 10 µM lenalidomide for 96 hrs and subsequently incubated in fresh medium (with DMSO or lenalidomide) for 3 hrs. After independent harvesting of supernatants and corresponding cell pellets, concentration of VEGF or MMP7 was determined in supernatants using enzyme linked immunosorbent assays (ELISAs) and normalized to the protein concentration in lysates of the according cell pellets.

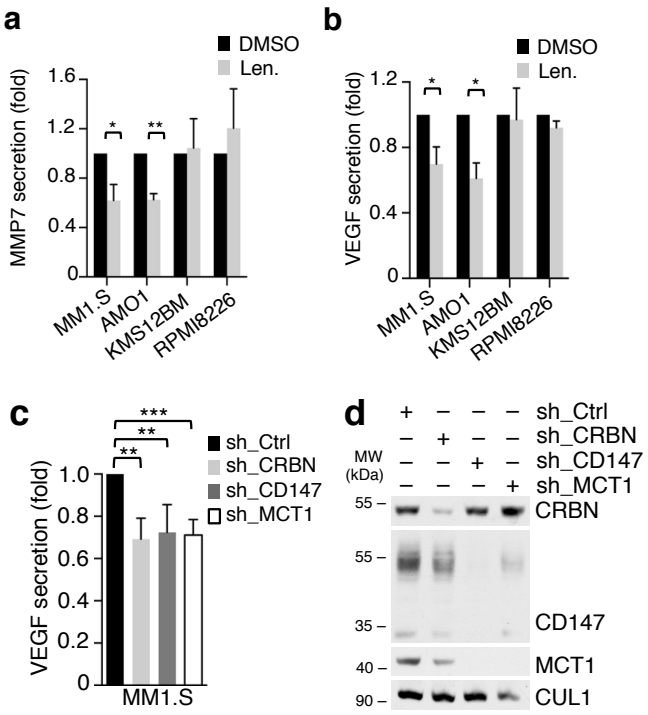

Fig. 30: IMiDs inhibit secretion of MMP7 and VEGF via CD147 destabilization. Analysis of MMP7 **(a)** and VEGF **(b)** secretion of lenalidomide-sensitive (MM1.S, AMO1) or -resistant MM cell lines (KMS12BM, RPMI8226) treated with DMSO or 10 µM lenalidomide (Len.) for 96 hrs before incubation with fresh medium (with DMSO or Len.) for 3 hrs. MMP7 and VEGF concentration in cell culture supernatants was measured by ELISA and normalized to protein concentration of respective pellets. Results are shown in relation to DMSO control. (n = 3 independent experiments with 2 technical replicates each, data is presented as mean ± S.D.). *, $P < 0.05$; **, $P < 0.01$ by one sample t-test. **(c)** Analysis of VEGF concentration in cell culture supernatants of MM1.S cells lentivirally transduced with shRNA constructs targeting CRBN, CD147, MCT1 or control (sh_Ctrl), using ELISAs as described above. (n = 5 independent experiments with 2 technical replicates each, mean ± S.D.). **, $P < 0.01$; ***, $P < 0.001$ by one sample t-test. **(d)** Representative immunoblot analysis of whole cell lysates from MM cells described in **c**. [Data provided by M. Heider].

In line with the data on CD147/MCT1 destabilization, lenalidomide treatment significantly reduced MMP7 and VEGF secretion in lenalidomide-sensitive cells, while MMP7 and VEGF secretion remained unchanged in lenalidomide-resistant cell lines, in which CD147/MCT1 is not destabilized (Fig. 30a, b), suggesting a causal relationship.

To investigate if IMiD-induced reduction of VEGF secretion is functionally linked to the CRBN-CD147/MCT1 axis, MM1.S cells were lentivirally infected with shRNA constructs to silence CRBN, CD147, MCT1 or control. Importantly, knockdown of any of the named proteins significantly reduced VEGF secretion as detected by ELISAs (Fig. 30c, d). Overall, these results strongly support the hypothesis that VEGF- and MMP7-mediated anti-proliferative and anti-angiogenic properties of IMiDs are, at least to some extent, mediated by CD147 destabilization.

3.4.5 IMiDs reduce cellular lactate export via MCT1 destabilization

The main function of MCT1 is the transmembrane transport of lactate, which can occur in both directions, depending on concentration gradients (Halestrap and Wilson, 2012). In cancer cells, whose energy production is often based on anaerobic or aerobic glycolysis (Warburg effect) instead of oxidative phosphorylation, the export of lactate, the resulting metabolite from glycolysis, becomes essential. IMiD-induced destabilization of MCT1 could therefore negatively impact glycolysis via inhibition of lactate export.

To evaluate if IMiDs indeed affect lactate export via MCT1 destabilization, lenalidomide-sensitive and -resistant cell lines were treated with DMSO or different doses of lenalidomide (10 µM or 100 µM) for 72 hrs. For determination of intracellular lactate levels, resullting cell pellets were lysed and subjected to lactate measurement in the Department of Clinical Chemistry at Klinikum rechts der Isar. Lactate concentrations were normalized to protein concentration in the respective cell pellet. In line with destabilization of MCT1, lenalidomide significantly reduced lactate efflux in lenalidomide-sensitive cells lines, leading to elevated intracellular lactate (Fig. 31a). Importantly, the increase of intracellular lactate was dose-dependent (Fig. 31a), just as the destabilization of MCT1 (Fig. 16a). Consistent with unchanged MCT1 levels, lenalidomide had no effect on lactate levels in resistant MM cell lines (Fig. 26, 31a).

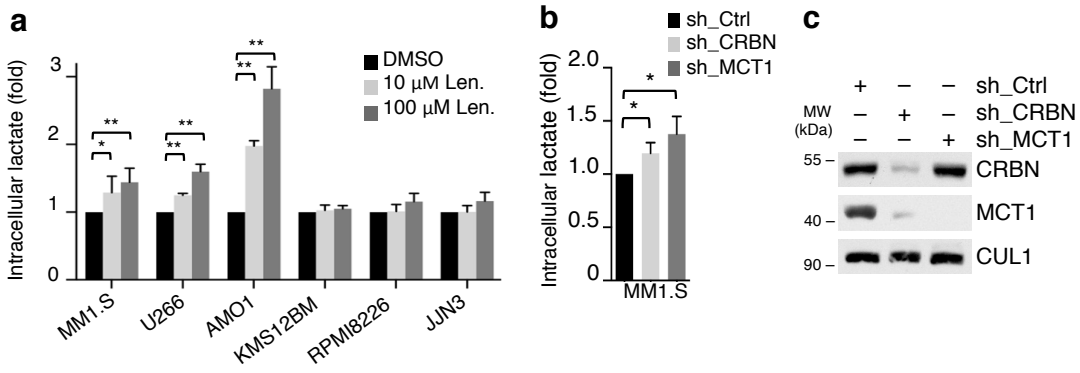

Fig. 31: IMiDs inhibit lactate export via MCT1 destabilization. (a) Analysis of intracellular lactate in IMiD-sensitive (MM1.S, U266, AMO1) and resistant MM cell lines (KMS12MB, RPMI8226, JJN3), which were treated with DMSO, 10 µM or 100 µM lenalidomide (Len.) for 72 hrs. Lactate levels in cell lysates, as determined by the cobas 800 instrument, were normalized to protein concentration. Results are shown in relation to DMSO control (n = 3 independent experiments with 2 technical replicates each; mean ± S.D.). *, $P < 0.05$; **, $P < 0.01$ by one sample t-test. **(b)** Analysis of intracellular lactate levels in MM1.S cells, which were lentivirally infected with shRNA constructs silencing CRBN, MCT1 or control. Lactate levels were determined as described in **a** (n = 4 independent experiments with 2 technical replicates each; mean ± S.D). *, $P < 0.05$ by one-sample t-test. **(c)** Representative immunoblot analysis of MM1.S cells described in **b**, using the specified antibodies. [Data provided by M. Heider].

To confirm the causal relation between destabilization of MCT1 and reduced lactate export, MM1.S cells were infected with lentiviral particles encoding shRNA contructs targeting CRBN, MCT1 or control and subjected to analysis of intracellular lactate. Consistent with previous results, silencing of either CRBN or MCT1 gave rise to a significant increase of intracellular lactate (Fig. 31b, c). These results provide evidence that IMiDs decrease cellular lactate efflux via destabilization of MCT1 to inhibit glycolysis and thus tumor cell metabolism.

3.4.6 CD147 and MCT1 are important IMiD targets *in-vivo*

After thorough investigation of IMiD-induced effects on CD147/MCT1 and the relevance of CD147/MCT1 in MM cell proliferation and viability in cell culture models, the proposed mechanism was investigated *in-vivo* in different mouse models. Endogenous mouse models were not suitable for evaluation of the proposed mechanism, given that murine cell lines were resistant to lenalidomide and pomalidomide (Fig. 27), consistent with the reported intrinsic IMiD resistantance of mice (Kronke et al., 2015). Instead, xenograft models, which are based on the transplantation of human cancer cells into immunodeficinent mice, were chosen for this study.

First, the relevance of CD147 and MCT1 for *in-vivo* tumor growth was investigated using MM1.S cells double-infected with shRNA contructs targeting CD147 and MCT1 or a scrambled control. In order to overcome differences in tumor growth between individual mice, identical cell numbers of control and experimental condition were injected into opposite flanks of immunodeficinent NOD/SCID mice (left: control; right: sh_CD147/sh_MCT1). The MM cells were injected together with Matrigel to assure formation of compact subcutaneous tumors, which are convenient for monitoring of tumor growth. Tumor growth was followed by examination and palpation of subcutaneous tumors. On a fixed day after injection, all injected mice bearing tumors underwent a PET (positron emission tomography) scan with FDG (^{18}F-fluorodeoxyglucose, a radioactively labeled glucose molecule), allowing detection of glucose uptake, which is significantly increased in tumor cells. The obtained FDG-PET images clearly showed dramatically reduced tumor growth upon knockdown of CD147 and MCT1 (arrow 2 in Fig. 32a). The PET-based quantitatification of metabolic volumes confirmed significantly reduced tumor growth upon CD147/MCT1 silencing across all mice (Fig. 32b). Isolation of the xenografted tumors from sacrificed mice further visualized the striking differences in size between control and sh_CD147/sh_MCT1 MM1.S xenografts (Fig. 32c). Comparison of tumor weight of all analyzed mice confirmed the highly significant differences in tumor growth (Fig. 32d). CD147 and MCT1 therefore seem at least as relevant for *in-vivo* as for *in-vitro* growth of MM1.S cells (Fig. 28, 32).

Isolated and fixed xenograft tumors were sent to the Institute of Pathology in Würzburg, where PD Dr. M. Rudelius performed immunohistochemical (IHC) analysis. Staining with anti-CD147 and anti-MCT1 antibodies confirmed efficient knockdown of both proteins in xenograft tumors (Fig. 32e). Constistent with MMP7 being a downstream effector of CD147, knockdown of CD147 and MCT1 was detrimental to MMP7 expression and secretion in the xenograft tumors (Fig. 32e), thus confirming functional *in-vivo* relevance of CD147 and MCT1.

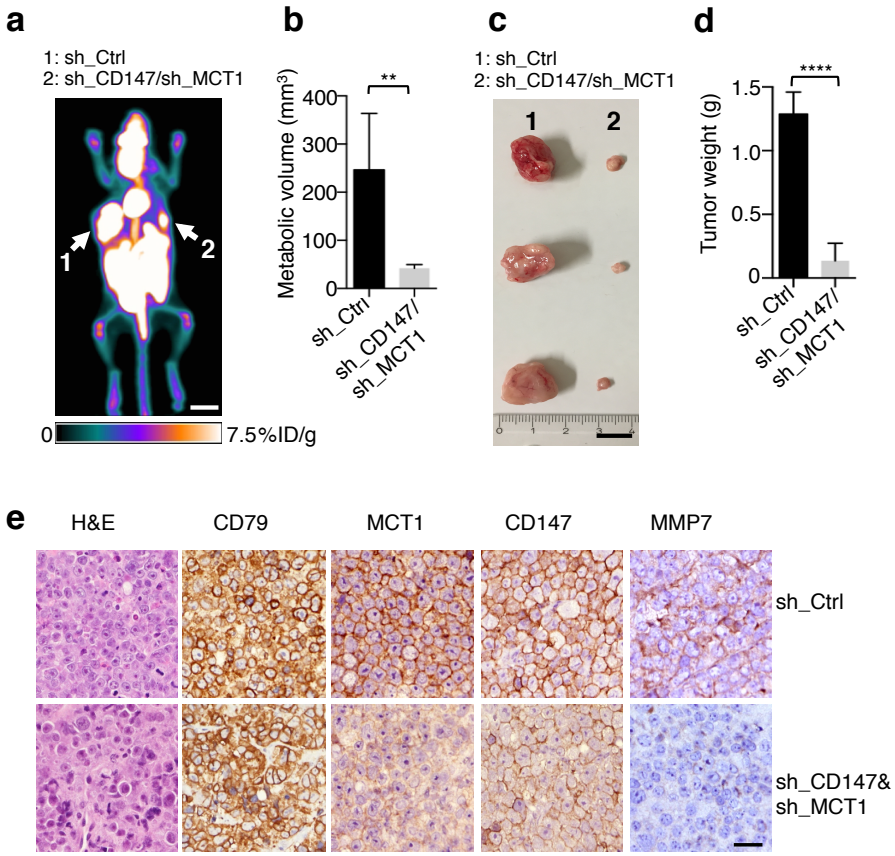

Fig. 32: CD147 and MCT1 promote growth of MM cells *in-vivo*. (a) Representative FDG-PET (^{18}F-fluorodeoxyglucose; positron emission tomography) image of a NOD/SCID mouse which was subcutaneously injected with human MM1.S cells which were lentivirally transduced with either control shRNA constructs (1) or shRNA constructs targeting CD147 and MCT1 (2) prior to grafting. Images were taken at 28 days post injection. White arrows point to xenograft tumors. Color scale, percentage of injected dose per gram (% ID/g). Scale bar, 10 mm. **(b)** Quantification of metabolic tumor volume by FDG uptake of control tumors (sh_Ctrl) or tumors with silenced CD147/MCT1 (sh_CD147/sh_MCT1) (n = 5 tumors per condition, data is presented as mean ± S.D.). **, $P < 0.01$ by student's t-test. **(c)** Picture of three different pairs of xenograft tumors from sacrificed mice injected with MM1.S cells expressing a control shRNA (1) or shRNAs targeting CD147 and MCT1 (2), as described in **a**. Scale bar, 10 mm. **(d)** Quantification of tumor weight of xenografted tumors described in **a** and pictured in **c** (n = 5 tumors per condition, data is presented as mean ± S.D.). ****, $P < 0.0001$ by student's t-test. **(e)** Immunohistochemistry (IHC) of representative xenograft tumors described above using the indicated antibodies and stainings. H&E (hematoxylin and eosin stain) visualizes histomorphology. CD79 is a marker of B- and plasma cells. Scale bar, 20 µm. [IHC Data for **e** provided by PD Dr. M. Rudelius].

If CD147 and MCT1 are important for tumor growth *in-vivo*, lenalidomide treatment could inhibit growth of MM xenograft tumors via destabilization of CD147 and MCT1. To investigate if lenalidomide destabilizes CD147 and MCT1 *in-vivo* to mediate its *in-vivo* anti-proliferative effects, a second MM xenograft experiment was designed in analogy to the *in-vitro* experiment in which overexpression of CD147 and MCT1 attenuated IMiD-induced anti-proliferative effects (Fig. 29).

As for the *in-vitro* approach, MM1.S cells were lentivirally infected with overexpression constructs coding for CD147 and MCT1 or an empty vector control. Equal numbers of overexpression or control MM1.S cells were injected into opposite flanks of NOD/SCID mice, as decribed above for the previous experiment. Once the MM cells were grafted, tumor growth was

closely monitored. Consistent with reduced tumor growth upon CD147 and MCT1 silencing in the previous experiment (Fig. 32), the tumors overexpressing CD147/MCT1 grew faster than the controls, confirming the pro-proliferative effect of CD147 and MCT1.

Once both overexpression and control tumors reached at least 5 mm in diameter, mice were randomized to receive either lenalidomide (30 mg/kg) or vehicle on a daily basis. Close monitoring of tumor growth by daily caliper-based measurement revealed that lenalidomide retarded growth of control xenograft tumors, while not inhibiting growth of CD147 and MCT1 overexpressing tumors at early time points (Fig. 33a), confirming that overexpression of CD147 and MCT1 protects from IMiD-induced cytotoxicity in analogy *in-vivo*.

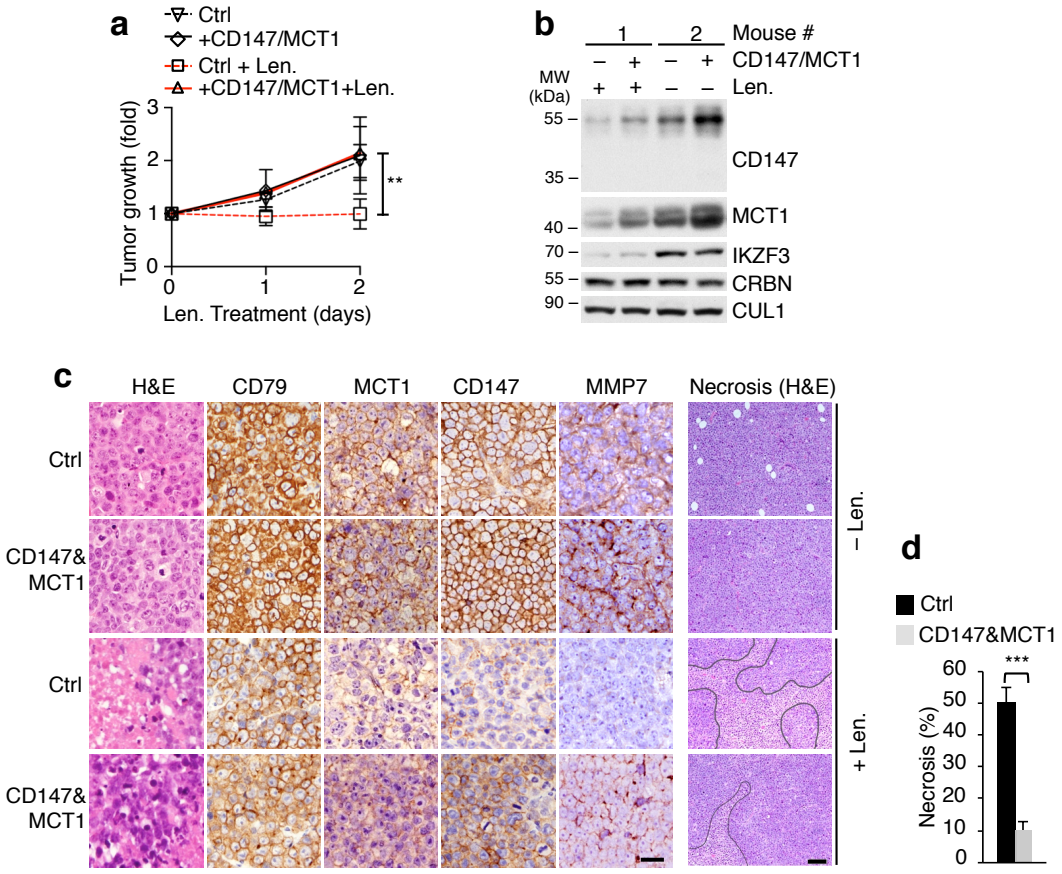

Fig. 33: IMiDs destabilize CD147 and MCT1 *in-vivo* to inhibit MM growth. (a) Growth of xenograft tumors in NOD/SCID mice, which were subcutaneously injected with human MM1.S cells lentivirally transduced with either empty vector control or onstructs inducing forced expression of CD147 and MCT1. Once both tumors reached 5 mm in diameter, mice were treated with vehicle or lenalidomide (Len.) 30mg/kg as specified and tumor growth was monitored by measurement of length and width. Calculated tumor volumes are shown in relation to baseline volumes before treatment (n = 4 tumors per condition without Len., n = 4 tumors per condition plus Len., mean ± S.E.M.). **, $P < 0.01$ by student's t-test. **(b)** Immunoblot analysis of representative xenograft tumors from mice described in **a** using the indicated antibodies**. (c)** Immunohistochemistry of representative MM1.S xenograft tumors derived from mice described in **a** visualizing histomorphology (H&E), plasma cell origin (CD79), CD147, MCT1 and MMP7 expression (left panel). Scale bar, 20 µm. Necrotic areas in xenografted tumors from mice treated with lenalidomide are encircled in H&E stainings (right panel). Scale bar, 100 µm. **(d)** Quantification of necrotic areas in Len.-treated xenograft tumors. Analysis was performed in 10 HPF (high power fields) of each stain. (n = 4 tumors per condition, values represent mean ± S.D.). ***, $P < 0.001$ by student's t-test. [IHC Data for **c** and **d** provided by PD Dr. M. Rudelius].

To investigate if lenalidomide also destabilized CD147 and MCT1 *in-vivo*, the isolated xenograft tumors were splitted to be either lysed for immunoblot analysis or fixed for subsequent IHC. Both immunoblot and IHC analysis confirmed persistent overexpression of CD147 and MCT1 in xenograft tumors (Fig. 33b, c) and additionally showed clear destabilization of CD147 and MCT1 upon lenalidomide treatment (Fig. 33b, c). As in the *in-vitro* setting (Fig. 29), the destabilization was more pronounced in control cells (Fig. 33b, c). Moreover, the expression levels of CD147 correlated with its downstream target MMP7 (Fig. 33c): while MMP7 staining was stronger in the overexpression xenografts, it was almost completely lost in control cells treated with lenalidomide, whereas its expression was only slightly reduced in overexpression tumors after IMiD treatment (Fig. 33c). In line with the differences in growth between control and overexpression tumors under lenalidomide (Fig. 33a), the percentage of necrotic areas observable in histomorphological H&E (hematoxylin and eosin) stainings were also highly diverging (Fig. 33c, d): while only few necrotic areas were visible in CD147/MCT1 overexpressing tumors after lenalidomide treatment, among 50% of the control tumors were necrotic (Fig. 33c, d), thus confirming the vital importance of CD147 and MCT1 for mediation of IMiD effects *in-vivo*.

3.4.7 IMiDs destabilize CD147 and MCT1 in primary patient cells

All previous experiments suggest a central role of CD147 and MCT1 in IMiD biology. To further strengthen the clinical relevance of this mechanism, complementary experiments were performed with primary patient cells. To this end, remaining bone marrow (BM) samples from MM patients, who underwent BM aspiration for diagnostic purposes, were collected from the routine hematology lab of the III. Medical Department. The samples were derived from patients at first diagnosis or with refractory or relapsed disease, and clinical data regarding their response to lenalidomide was collected in order to correlate the *in-vitro* behavior to clinical behavior *in-vivo*.

Starting from the BM samples, MM cells were enriched via purification of $CD138^+$ cells using CD138 MACS (magnetic activated cell sorting) beads (see chapter 6.2.4.1). The $CD138^+$ cells were taken into culture, treated with DMSO or 10 µM of lenalidomide for 4 days and analyzed by flow cytometry. If possible, aliquots were harvested for immunoblot analysis.

For flow cytometric analysis, the primary MM cells were incubated with antibodies to detect plasma cell origin (CD38/CD138), antibodies against CD147 or an isotype control IgG and annexin V and PI to detect apoptosis (see chapter 6.2.7.4). Strikingly, CD147 surface expression decreased upon *in-vitro* lenalidomide treatment in primary cells derived from patients with documented lenalidomide response, while CD147 expression was not altered in cells derived from lenalidomide-resistant patients (Fig. 34a). In line with these findings, the percentage of viable (annexin V^- and PI^-) cells was significantly reduced by lenalidomide in sensitive cells, whereas no increased apoptosis was detected in resistant cells (Fig. 34b). Hence, IMiD-induced reduction of CD147 expression *in-vitro* correlated with lenalidomide-induced apoptotis and clinical lenalidomide-sensitivity, thus underlining the clinical relevance of the mechanism and strengthening the potential of CD147/MCT1 destabilization as predictor of IMiD response.

Immunoblot analysis of those patients for which enough material was available, confirmed this correlation (Fig. 34c): all samples derived from lenalidomide-sensitive patients demonstrated destabilization of CD147 and MCT1 upon lenalidomide exposure, whereas cells derived from resistant patients showed stable expression levels of both proteins (Fig. 34c).

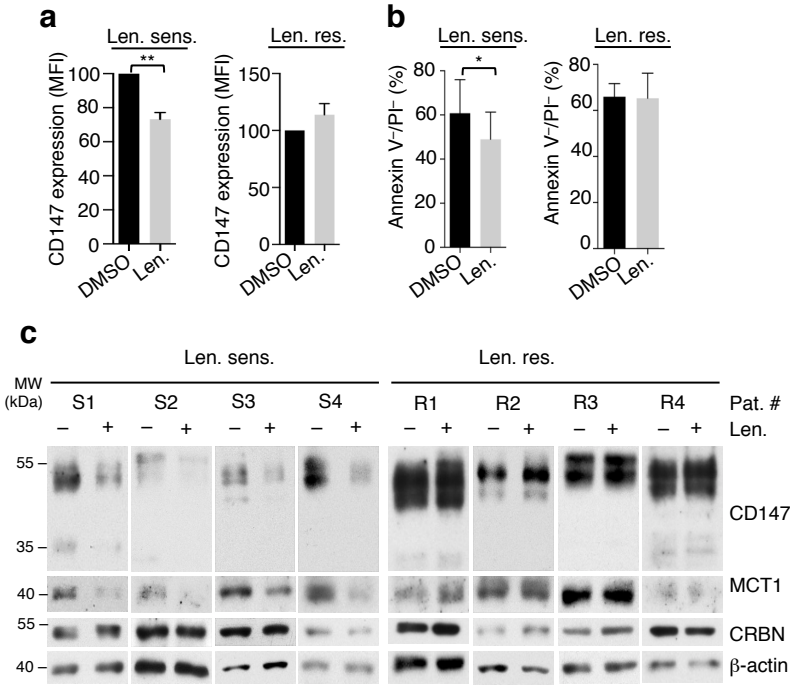

Fig. 34: IMiD-induced destabilization of CD147 and MCT1 correlates with clinical response. (a) Flow cytometric analysis of CD147 cell surface expression in purified primary CD138$^+$ MM cells derived from patients with either lenalidomide-sensitive (Len.sens.) or -resistant disease (Len.res). Purified MM cells were treated with DMSO or 10 µM lenalidomide for 96 hrs before analysis. Data is shown as mean fluorescence intensity (MFI) of CD147 in relation to isotype control (Len. sensitive: n = 5, Len. resistant: n = 5; mean ± S.E.M.). **, $P < 0.01$ by one-sample t-test. **(b)** Quantfication of viable cells characterized by negative annexin V/PI staining (Annexin$^-$/PI$^-$) in flow cytometric analysis of cells described in **a** (len. sensitive: n = 5, len resistant: n = 5; mean ± S.E.M.). *, $P < 0.05$ by student's t-test. **(c)** Immunoblot analyses of primary MM cells derived from subjects with either Len. sensitive (patient S1-S4) or resistant disease (patient R1-R4) that were cultured and treated as described in **a.**

3.5 IMiD activity in del(5q) MDS is mediated via CD147 and MCT1

Next to MM, where IMiDs are central components of current therapeutic guidelines due to their high clinical anti-MM activity (Dimopoulos et al., 2007; Lacy et al., 2009; Rajkumar and Kumar, 2016), lenalidomide is furthermore approved for treatment of del(5q) myelodysplastic syndrome (MDS) (Fenaux et al., 2011). Importantly, the efficacy of lenalidomide is largely restricted to the MDS subentity with deletion of chromosome 5q [del(5q) MDS], where lenalidomide achieves response rates of 60-70% or higher and currently is the first-line treatment in lower risk disease (Fenaux et al., 2011; List et al., 2006). By contrast, in cases of MDS without deletion of chromosome 5q [non-del(5q) MDS], lenalidomide is much less effective and only achieves response rates of 20-30% (Raza et al., 2008; Toma et al., 2016).

3.5.1 Overexpression of CD147 and MCT1 is vital for del(5q) MDS

If CD147 and MCT1 were central mediators of IMiD activity in MDS, these proteins would be expected be of vital importance in this entity and maybe show differing expression in non-del(5q) and del(5q) MDS to explain the differences in lenalidomide response. Besides few reports on CD147 in AML (Fu et al., 2010; Gao et al., 2015), there is however currently no information on CD147 and MCT1 expression in MDS.

To investigate the potential role of CD147 and MCT1 in anti-MDS activity of IMiDs, expression of both proteins was first to be verified in MDS-derived cells. Altough MDS cell lines are generally hard to establish due to the biology of the disease, cells lines from MDS RAEB (refractory anemia with excess blasts) cases or from MDS-derived AML are available. A panel of different del(5q) MDS/AML cell lines (MDSL, KG1) and non-del(5q) MDS/AML lines (SKK-1, SKM-1) was thus analyzed by immunoblotting for baseline expression levels of CD147 and MCT1. Strikingly, both del(5q) MDS cell lines showed high expression levels of CD147 and MCT1 (Fig. 35a), whereas both non-del(5q) MDS cell lines displayed significantly lower levels of CD147 and particularly MCT1 (Fig. 35a). If non-del(5q) MDS lines are characterized by low levels of CD147 and MCT1, these cells likely do not depend on these proteins for growth, whereas relative CD147/MCT1 overexpression in del(5q) MDS lines suggests importance of these proteins for proliferation and/or viability.

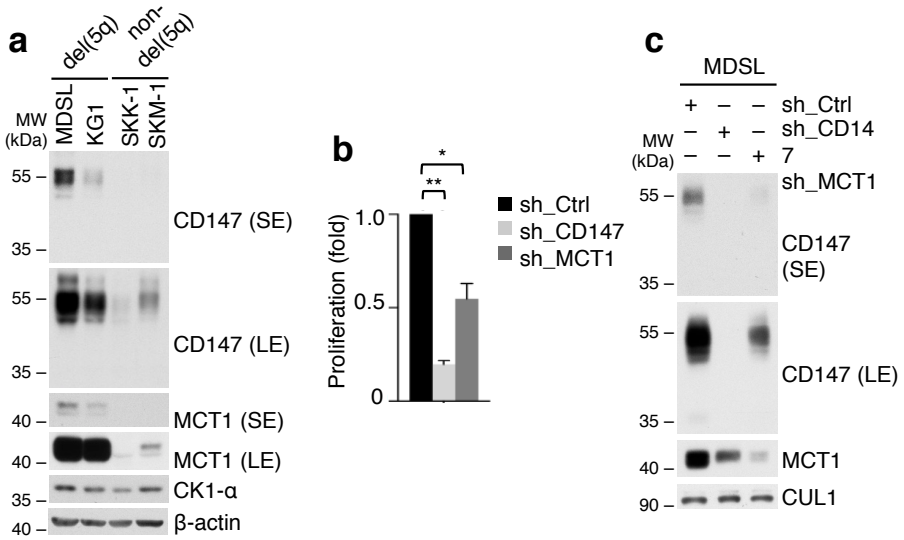

Fig. 35: Overexpression of CD147 and MCT1 drives proliferation of del(5q) MDS cells. (a) Immunoblot analysis of whole cell lysates of the specified del(5q) (MDSL, KG1) and non-del(5q) MDS cell lines (SKK-1, SKM-1) using the indicated antibodies. **(b)** Proliferation of MDSL cells which were transduced with lentiviral shRNA contructs to silence CD147 (sh_CD147), MCT1 (sh_MCT1) or control (sh_Ctrl). Viable cells were counted using the trypan blue exclusion method and are depicted in relation to control (n = 3 independent experiments with 2 technical replicates each; data is presented as mean ± S.D.). *, $P < 0.05$; **, $P < 0.01$ by one sample t-test. **(c)** Immunoblot analysis of MDSL cells described **(b)** using the indicated antibodies.

To evaluate the importance of CD147 and MCT1 for proliferation and survival in del(5q) MDS cell lines, MDSL cells were lentivirally infected with shRNA constructs targeting either CD147, MCT1 or control. As in MM cells (Fig. 28), knockdown of either CD147 or MCT1 severly inhibited proliferation of MDSL cells (Fig. 35b, c), confirming that CD147 and MCT1 are of vital importance for viability and proliferation of del(5q) MDS cells.

The kinase CK1-α, which is described to be a target of lenalidomide in MDS (Kronke et al., 2015), is encoded on chromosome 5q. Therefore, lower CK1-α levels were expected in del(5q) MDS, explaining the increased lenalidomide-sensitivity in this subentity (Kronke et al., 2015). However, in the analyzed del(5q) and non-del(5q) MDS lines, there was no obvious difference in CK1-α expression on the protein level (Fig. 35a).

Together, these experiments indicate an important role of CD147 and MCT1 for del(5q) MDS cell proliferation and suggest that diverging CD147/MCT1 levels might indeed be responsible for the differences in IMiD response between del(5q) and non-del(5q) MDS, while CK1-α, which was previously reported to be haploinsufficient in del(5q) MDS (Kronke et al., 2015; Schneider et al., 2014), showed equal levels in the analyzed del(5q) and non-del(5q) cells.

3.5.2 IMiDs mediate anti-del(5q) MDS activity via CD147/MCT1 destabilization

After confirmation of CD147 and MCT1 expression and relevance in del(5q) MDS, exemplary cell lines for del(5q) and non-del(5q) MDS were treated with lenalidomide or pomalidomide to analyze their impact on cell proliferation and CD147/MCT1 abundance.

In line with the data in MM cell lines (Fig. 26), proliferation of the lenalidomide-sensitive MDSL cell line (Matsuoka et al., 2010) was significantly inhibited by lenalidomide and pomalidomide, whereas the non-del(5q) MDS cell line SKK was not affected (Fig. 36a). In accordance with the anti-proliferative effects, both CD147 and MCT1 were destabilized by lenalidomide and pomalidomide in MDSL cells, while the almost undetectable levels of CD147 and MCT1 in SKK cells remained unchanged (Fig. 36b). Of note, CK1-α was not only destabilized in del(5q) cells, but also in non-del(5q) cells (Fig. 36b), which did not respond to IMiD treatement. Moreover, pomalidomide had stronger anti-proliferative effects in MDSL cells than lenalidomide, whereas the degradation of CK1-α was more pronounced after lenalidomide exposure, arguing against a significant role of CK1-α in mediation of IMiD effects in del(5q) MDS.

To assess whether forced expression of CD147 and MCT1 can attenuate the antiproliferative effects of IMiDs on del(5q) MDS, MDSL cells were double-infected with lentiviral expression constructs coding for CD147 and MCT1 or empty vector control and treated with DMSO or lenalidomide (10 µM). Assessment of proliferation indeed revealed differences between the named conditions, particularly at early time points. While proliferation of control cells was already markedly reduced after 48 hrs of lenalidomide treatment, no anti-proliferative effects were yet visible in CD147/MCT1 overexpressing cells (Fig. 36c, left panel), suggesting protective effects of CD147/MCT1 in analogy to the experiments in MM1.S cells (Fig. 29, 33). After 96 hrs of

treatment, anti-proliferative effects of lenalidomide became observable also in CD147/MCT1 overexpressing cells (Fig. 36c, right panel), as CD147 and MCT1 continue to be destabilized by lenalidomide. Nevertheless, cell counts of CD147/MCT1 overexpressing cells were still significantly higher compared to control cells after 96 hrs of lenalidomide treatment (Fig. 36c, right panel). Together, these results correspond to the results in the MM context and confirm CD147 and MCT1 as important mediators of IMiD response also in del(5q) MDS.

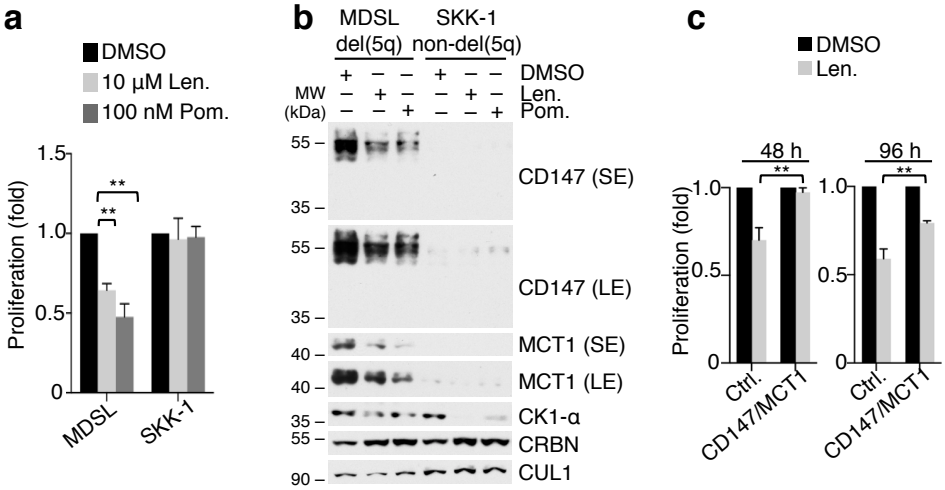

Fig. 36: Destabilization of CD147 and MCT1 mediates antiproliferative effects in del(5q)MDS. (a) Proliferation of the del(5q) cell line MDSL and the non-del(5q) line SKK-1, which were treated with DMSO, 10 µM lenalidomide (Len.) or 100 nM pomalidomide (Pom.). Viable cells were counted at 96 hrs using the trypan-blue exclusion method; results are presented in relation to DMSO treated controls. (n = 3 independent experiments with 2 technical replicates each, mean ± S.D.). **, $P < 0.01$ by one sample t-test. **(b)** Immunoblot analysis of whole cell lysates of the indicated MDS cell lines treated with DMSO, Len. or Pom. for 144 hrs using the indicated antibodies. **(c)** Proliferation of MDSL cells that were lentivirally infected with empty vector control (Ctrl) or expression constructs coding for CD147 and MCT1. Sorted cells were treated with DMSO or 10 µM lenalidomide and counted after 48 hrs (left panel) or 96 hrs (right panel) of treatment using the trypan blue exclusion method. Results are shown in relation to DMSO controls (n = 3 independent experiments with 2 technical replicates each, mean ± S.D.). **, $P < 0.01$ by student's t-test.

3.5.3 Lenalidomide reduces CD147 levels in patient-derived del(5q) MDS cells

In order to confirm the data resulting from cell culture models in primary patient cells, bone marrow (BM) samples from del(5q) and non-del(5q) patients as well as from patients with del(5q) MDS currently undergoing lenalidomide treatment were investigated regarding their CD147 surface expression. To this end, anti-CD147 antibodies were integrated in the normal diagnostic flow cytometry panel of the routine hematology lab of the III. Medical Department. Thus, information on CD147 expression was acquired with clinical flow cytometric analyses in the rountine lab and resulting data was analyzed by Prof. Dr. K.Götze (see chapter 6.2.7.3).

The resulting flow cytometric data indeed revealed differences in CD147 surface expression between subjects with del(5q) MDS and non-del(5q) MDS. Interestingly, within different BM subpopulations, CD147 was particularly overexpressed in the $CD45^{low}/CD235\alpha^{+}$ erythropoietic compartment of del(5q) MDS in comparison to non-del(5q) MDS samples (Fig. 37). Consistent with the cell line based data, lenalidomide treatment significantly reduced the average

CD147 surface expression in erythroid cells derived from del(5q) MDS patients, resulting in expression levels comparable to those in non-del(5q) MDS samples (Fig. 37).

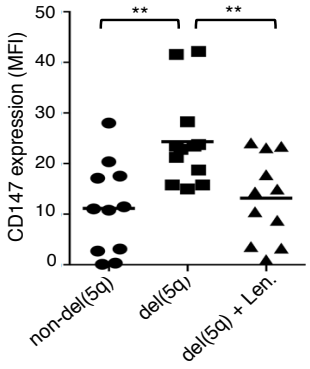

Fig. 37. Lenalidomide reduces CD147 expression in del(5q) MDS to the levels in non-del(5q) MDS. Flow cytometric analysis of CD147 surface expression on $CD45^{low}/CD235\alpha^{+}$ erythroid cells in bone marrow samples from non-del(5q) (circles), del(5q) (squares) or del(5q) MDS patients under lenalidomide (Len.) treatment (triangles). Each circle, square or triangle represents one patient. Data are shown as median fluorescence intensity (MFI) relative to matched isotype control. **, $P < 0.01$; one-way ANOVA. [Data provided by Prof. Dr. K.Götze].

MDS is mainly characterized by ineffective erythropoiesis, which is efficiently restored upon lenalidomide treatment via inhibition of monoclonal del(5q) erythroid progenitors (Giagounidis et al., 2014; Sekeres et al., 2008). Given the patient-derived data, it is conceivable that CD147 is indeed responsible for these effects. CD147 overexpressing, hyperproliferative erythroid precursor cells from del(5q) MDS patients might be incapable to properly differentiate to mature erythrocytes. Lenalidomide could then inhibit proliferation of these CD147 overexpressing clones to allow growth of healthy, properly maturating erythroid cells.

3.5.4 IMiD-induced destabilization of CD147 targets del(5q) erythropoiesis

In order to confirm the hypothesis that lenalidomide specifically targets CD147 in erythroid cells in the del(5q) MDS context, complementary *in-vitro* experiments with patient derived cells were performed by A.K. Garz in the lab of Prof. Dr. K.Götze (III. Medical Department at Klinikum rechts der Isar).

For *in-vitro* differentiation along the eryhtroid lineage, $CD34^{+}$ hematopoietic precursor cells were isolated from BM samples from del(5q)MDS patients, which had undergone diagnostic BM aspiration. The MACS-purified $CD34^{+}$ cells were taken into culture in serum-free medium supplemented with five growth factors (KIT-ligand, FLT-3-ligand, thrombopoietin, IL-3 and IL-6; see chapter 6.2.4.2) and incubated with DMSO or 10 µM lenalidomide. After 7 days, erythropoietic differentiation was induced by addition of erythropoietin for another 7 days (Fig. 38a, upper panel). Using flow cytometric analysis, CD147 surface expression and apoptosis were evaluated in different compartments of the myeloid and particularly erythroid lineage using respective antibodies as described in chapter 6.2.7.5. Strikingly, lenalidomide specifically induced apoptosis in erythroid precursor cells ($CD36^{+}$) from del(5q) MDS patients, whereas non-erythroid cells ($CD36^{-}CD235\alpha^{-}$) of the same patients did not undergo apoptosis upon lenalidomide

treatment (Fig. 38a, b). In correlation with the data on apoptosis, lenalidomide-induced reduction of CD147 surface expression was also restricted to CD36$^+$ cells of the early eryhtroid lineage, while non-erythroid cells maintained stable CD147 expression (Fig. 38a). Within the CD36$^+$ cells, loss of CD147 expression moreover directly correlated with increased apoptosis (Fig. 38c), suggesting that CD147 destabilization and subsequent apoptosis might represent the mechanism by which lenalidomide specifically targets non-functional del(5q) erythropoietic precursor clones.

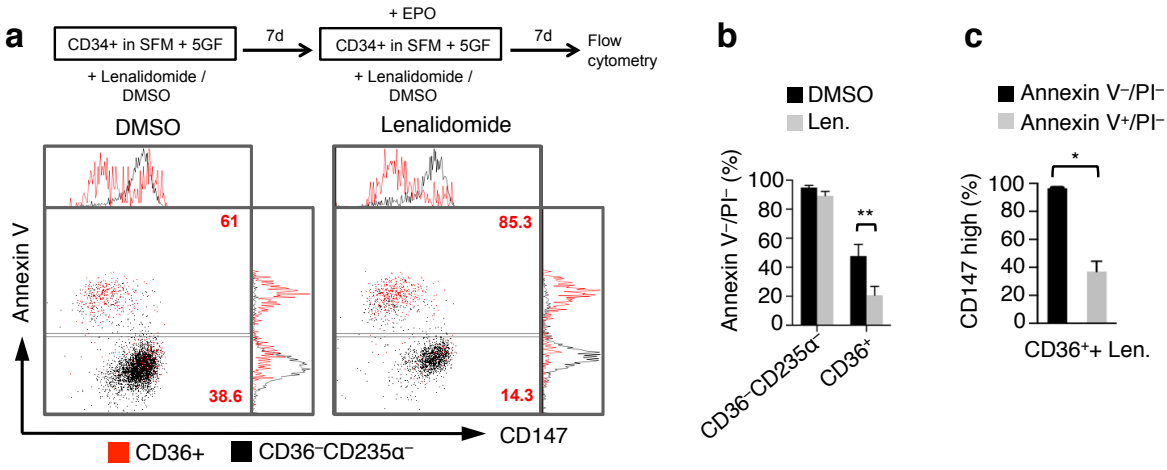

Fig. 38: Lenalidomide targets del(5q) erythroid progenitors by destabilization of CD147. (a) Schematic of the performed experiment (top): BM-derived CD34$^+$ cells from del(5q) MDS patients were differentiated *in-vitro* along the eryhtoid lineage in serum free medium (SFM) supplemented with 5 growth factors (5GF) comprising KIT-ligand, FLT3-ligand, TPO, IL-3, and IL-6 and treated with DMSO or lenalidomide (10 µM) as indicated. Erythropoietin (EPO) was added on d 7. Representative flow cytometric analysis (bottom) of apoptosis (marked by annexin V) and CD147 surface expression in non-erythroid (CD36$^-$CD235α$^-$, black) and early erythroid (CD36$^+$, red) compartments derived from BM samples of del(5q) MDS patients, which were processed as described above. An overlay of dot plots and according histogram analyses are shown. **(b)** Quantification of viable (annexin V$^-$/ PI$^-$) cells after DMSO or lenalidomide (Len.) treatment in non-erythroid (CD36$^-$ CD235α$^-$) and early erythroid (CD36$^+$) cells described in **a.** Data are presented as mean of the experiment shown in **a** and two further independent samples (n = 3 independent experiments, mean ± S.D.). $^{**}P < 0.01$ by Student's t-test. **(c)** Quantification of CD147 expression in viable (annexin V$^-$/PI$^-$) and apoptotic (annexin V$^+$/PI$^-$) CD36$^+$ erythroid cells treated with Len. as described in **a** (n = 3 independent experiments, mean ± S.D.). $^{*}P < 0.05$ by Student's t-test. [Data provided by A.K. Garz].

Overall, obtained data identifies destabilization of CD147 and MCT1 as central mechanism by which IMiDs mediate their anti-proliferative and general anti-cancer effects both in MM as well as in del(5q) MDS, two of the central clinical entitites responsive to IMiD treatment.

3.6 Thalidomide induced teratotoxicity is mediated via CD147

Besides efficient anti-cancer activity comprising anti-proliferative, anti-invasive and anti-angiogenic properties, which are believed to be largely mediated via CD147 and MCT1 destabilization based on the previous experiments, IMiDs are furthermore characterized by teratoxic effects (Ito et al., 2011; Ito et al., 2010; Mahony et al., 2013). Given that proliferation, angiogenesis and invasion are important processes during development, it was hypothesized that the CRBN-CD147/MCT1 axis could also be responsible for IMiD-induced teratogenicity.

3.6.1 Knockdown of CD147 phenocopies thalidomide-induced teratotoxic effects

In order to investigate if the teratoxic effects of IMiDs result from destabilization of CD147/MCT1, zebrafish was chosen as model system. This model was repeatedly used to study the teraotoxic effects of IMiDs and demonstrate the CRBN-dependence of thalidomide-induced teratotoxicity (Ito et al., 2010; Mahony et al., 2013). As mentioned before, mice are intrinsically resistant to IMiDs and therefore not suitable to study IMiD-induced teratotoxicity (Ito et al., 2010). All zebrafish experiments were performed by Dr. B. Schmid and Dr. F. van Bebber at the DZNE (Deutsches Zentrum für Neurodegenerative Erkrankungen).

Before investigation of the CRBN-CD147/MCT1 axis in zebrafish, the data on thalidomide-mediated teratotoxicity was reproduced for verification and establishment of a reference phenotype. As previously described, treatment of zebrafish larvae with thalidomide indeed resulted in a complex teratotoxic phenotype at 3 days post fertilization (dpf) including smaller heads, smaller eyes and reduced size of pectoral fins in the vast majority of treated larvae (Fig. 39a, b) (Ito et al., 2010; Mahony et al., 2013).

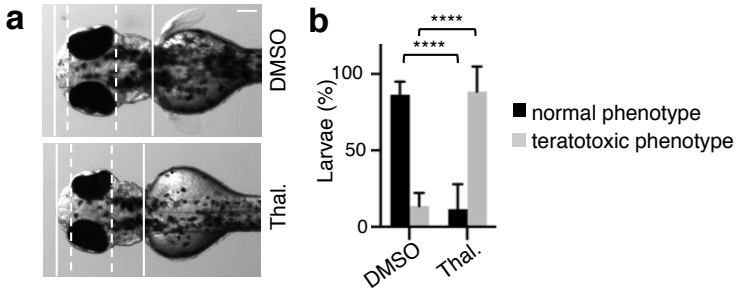

Fig. 39: Thalidomide induces teratotoxic effects in zebrafish including reduced head, eye and fin size. (a) Representative images of zebrafish larvae at 3 dpf (days post fertilization), which were treated with either DMSO or 400 µM thalidomide (Thal.), anterior to the left, dorsal view. Dotted lines demarcate the eyes; solid lines the head. Scale bar, 100 µm. **(b)** Quantifications of larvae as described in **a** with normal eye size (normal phenotype) or reduced eye size (teratoxic phenotype) (n = 9 independent experiments with 10 larvae each per condition and experiment, mean ± S.D). ****, $P < 0.0001$ by Student's t-test. [Data provided by Dr. F.v.Bebber].

If the mechanism of IMiD-induced destabilization of CD147 and MCT1 is transferable to zebrafish and if moreover, IMiD-induced teratotoxicity is mediated by destabilization of CD147 and MCT1, knockdown of either of these proteins should have comparable teratotoxic effects as thalidomide. Given that there is a variety of different isoforms of monocarboxylate transporters in zebrafish without evidence which isoform is functionally relevant, knockdown experiments in zebrafish were restricted to CD147, which has three described isoforms. For knockdown, two different morpholinos (MOs) were designed to target all isoforms of zebrafish (zf) CD147 mRNA: one morpholino binding to the splice-junction between exon 3 and intron 3 (splice MO), and one binding to the ATG start codon (ATG MO) (see chapter 5.8.4).

Different concentrations (0.1 mM or 0.25 mM) of both morpholinos were injected in into zebrafish larvae shortly after fertilization (see chapter 6.5.2.2). Strikingly, morpholino-induced knockdown of CD147 phenocopied the teratoxic effects observed with thalidomide (Fig. 40a). Both CD147 morpholinos induced a dose-dependent reduction of head, eye and fin size of

zebrafish embryos at 3 dpf (Fig. 40a, b), suggesting a central role of CD147 during development of zebrafish. Quantifications of zebrafish with reduced eye size as parameter for teratotoxic phenotype confirmed significance of the observed effects (Fig. 40b).

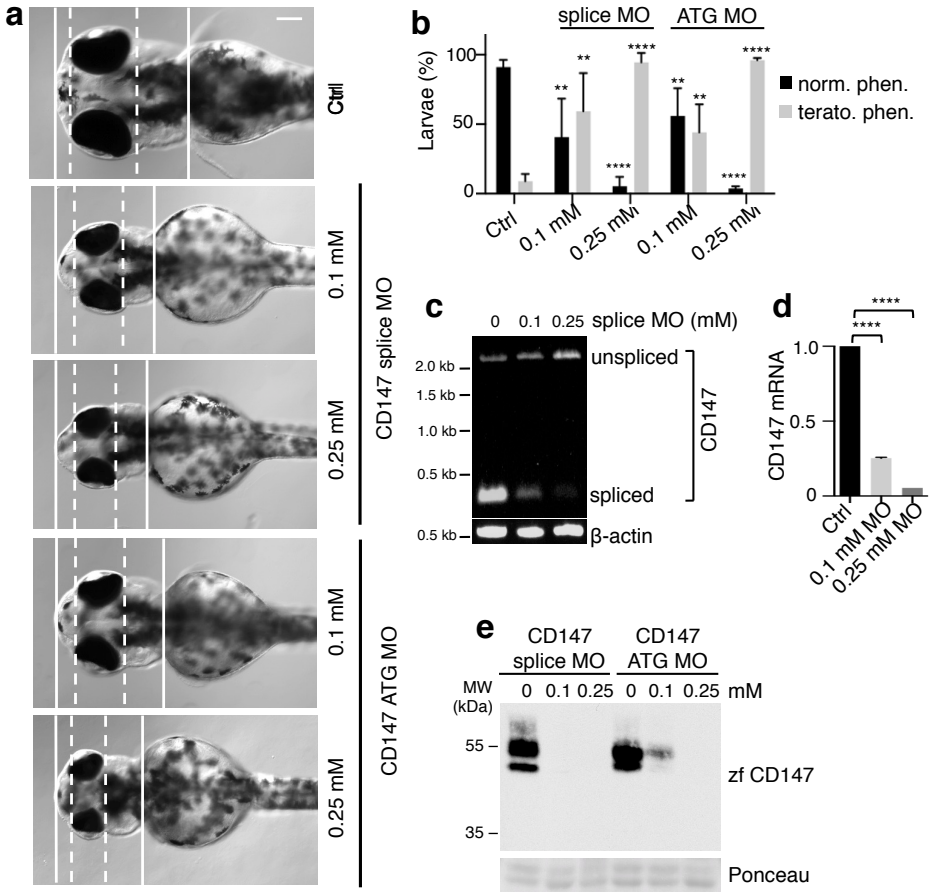

Fig. 40: Knockdown of CD147 phenocopies thalidomide-induced teratotoxicity in a dose-dependent manner. **(a)** Representative images of zebrafish larvae at 3 dpf (days post fertilization), which were injected with two different CD147 morpholinos (splice MO, ATG MO) at the indicated concentrations or left untreated (Ctrl). Anterior to the left, dorsal view. Dotted lines demarcate the eyes; solid lines the head. Scale bar, 100 µm. **(b)** Quantifications of larvae described in **a** with normal eye size (norm. phen.) or reduced eye size (terato. pheno.) (n = 3 independent experiments for 0.1 mM, 0.25 mM splice MO, and 0.1 mM ATG MO; n = 4 for 0.25 mM ATG MO and Ctrl, with 50 larvae per condition and experiment, data presented as mean ± S.D). Significance levels are in comparison to the control group. **, $P < 0.01$; ****, $P < 0.0001$ by Student's t-test. **(c)** Semiquantitative RT-PCR based on cDNA from zebrafish larvae at 3dpf, injected with 0.1 or 0.25 mM of CD147 splice MO (targeting the border of exon3/intron3) or untreated control. PCR was performed with a CD147 fw primer in exon 3 and rv primer in exon 5, amplifying the spliced form of 341 bp and the non-spliced form of 2387 bp. PCR with primers for β-actin served as control. **(d)** Real-time qPCR analysis on cDNA from zebrafish described in **c**, with a CD147 fw primer in exon 3 and a rv primer in exon 4. The amount of mRNA in the control sample was set as 1. (n = 3 independent experiments with 10 larvae per condition and two technical replicates, mean ± S.D.). ****, $P < 0.0001$ by one-sample t-test. **(e)** Immunoblot analysis of extracts from zebrafish larvae at 3 dpf, which were injected with the indicated CD147 morpholinos at the indicated concentrations and probed using a custom anti-zfCD147 antibody. Ponceau staining was used as loading control. [Data for **a** and **b** provided by Dr. F.v.Bebber].

Because no specific antibody detecting zfCD147 was commercially available, the knockdown efficiency of CD147 was first investigated via PCR. Of note, morpholinos only inhibit translation and do not lead to degradation of mRNA, therefore standard qPCR approaches

evaluating mRNA abundance are not suitable. Instead, PCR primers were chosen to differentiate between properly spliced CD147 and unspliced CD147 as readout for efficiency of the CD147 splice MO. After extraction and reverse transcription of RNA from zebrafish larvae treated with 0.1 mM or 0.25 mM splice MO, or untreated control larvae, semiquantitative RT-PCRs were performed using either a combination of a forward primer in zfCD147 exon 3 and a reverse primer in exon 5, or a combination of primers to amplify β-actin mRNA as control. As expected, the CD147 splice MO resulted in significant reduction of correctly spliced CD147 mRNA (341 bp length), while non-spliced mRNA (2387 bp length) accumulated in a dose-dependent manner (Fig. 40c). In a complementary approach, qPCR analysis was performed using a forward primer in exon 3 and a reverse primer in exon 4, thereby amplifying only the correctly spliced form of CD147 in qPCR. In accordance with the semiquantitative approach, qPCR also demonstrated dose-dependent reduction of correctly spliced CD147 mRNA upon treatment with the CD147 splice MO (Fig. 40d), thus confirming efficient knockdown of CD147. Once a custom antibody was produced for zfCD147, a dose-dependent knockdown of CD147 by both splice MO and ATG MO was furthermore confirmed on protein levels (Fig. 40e).

3.6.2 The teratotoxic potential of IMiDs correlates with destabilization of CD147

In addition to the described morphological abnormalities, thalidomide was more specifically shown to downregulate expression of FGF8 (fibroblast growth factor 8) in the fin buds of zebrafish embryos (Ito et al., 2010), thus impeding proper fin development. As further read-out for the specificity of the observed teratotoxic effects of CD147 knockdown (see Fig. 40), FGF8 expression in fin buds was investiaged in the context of CD147 knockdown. To this end, zebrafish larvae, which were injeceted with morpholinos targeting CD147 or left untreated, were fixed at 2 dpf and hybridized with an FGF8 specific probe. Indeed, knockdown of CD147 resulted in almost complete loss of FGF8 expression in the apical ectodermal ridge (AER) of the fin buds (Fig. 41a, b, left panel each), in analogy to the published effects of thalidomide (Ito et al., 2010), thus strengthening the evidence that thalidomide-induced teratotoxicity is mediated via CD147.

In human MM cells, not only thalidomide, but also lenalidomide and pomalidomide significantly destabilized CD147 (Fig. 19). If the same was true in zebrafish, these IMiDs would also be expected to have teratotoxic effects in this model; however a recent publication describes lenalidomide and pomalidomide to be non-teratogenic in zebrafish (Mahony et al., 2013). To verify these results, zebrafish embryos, which were treated with DMSO, thalidomide, lenalidomide or pomalidomide, were subjected to FGF8 *in-situ* hybridization. In accordance with published data, thalidomide downregulated expression of FGF8 in the AER, while lenalidomide and pomalidomide by contrast did neither induce any remarkable malformations nor affect FGF8 expression (Fig. 41a, b, right panel each).

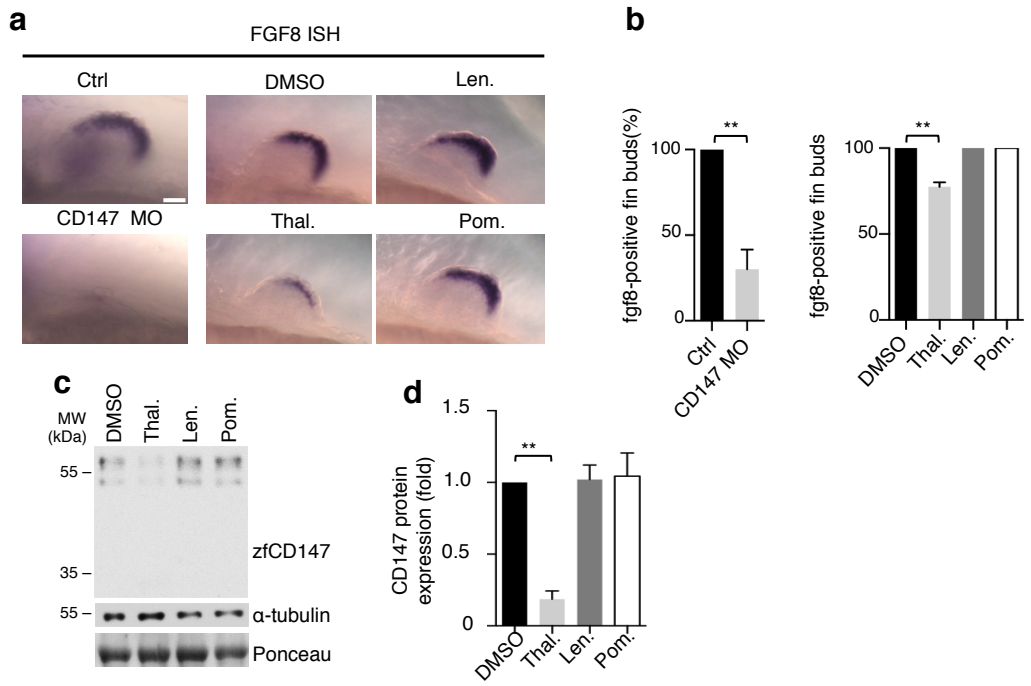

Fig. 41: IMiD-induced teratotoxicity correlates with knockdown of CD147. (a) Representative *in-situ* hybridizations (ISH) using an antisense RNA probe for FGF8 in wildtype zebrafish (Ctrl), in larvae injected with CD147 MO, or larvae treated with DMSO, 772 µM lenalidomide (Len.), 400 µM thalidomide (Thal.), or 219 µM pomalidomide (Pom.). Images show lateral views of the fin buds of embryos at 2 days post fertilization (dpf). Scale bar, 10 µm. **(b)** Quantification of FGF8 positive fin buds in zebrafish embryos described in **a** (n = 3 with 10 larvae per condition and experiment for IMiD vs. DMSO treatment and 50 larvae per condition and experiment for MO-injections or control, mean ± S.D.). **, $P < 0.01$ by one sample t-test. **(c)** Immunoblot analysis of extracts from zebrafish embryos at 3 dpf, which were treated with DMSO, Thal., Len. or Pom. at concentrations as in **a**, using the indicated antibodies and ponceau staining as loading control. **(d)** Quantification of zfCD147 protein levels of immunoblots shown in **c,** averaged with two additional independent experiments (n = 3 independent experimets with 10 larvae per condition, data is mean ± S.D.). **, $P < 0.01$ by one-sample t-test. [Data for **a** and **b** provided by Dr. F.v.Bebber].

Aiming to solve this supposed paradoxon, a custom antibody was generated against zebrafish CD147 to investigate the effects of different IMiDs on CD147 stability in zebrafish. Surprisingly, immunoblot analysis of zebrafish extracts showed significant destabilization of zfCD147 upon thalidomide treatment, whereas no effect on CD147 abundance was observed after exposure to lenalidomide or pomalidomide (Fig. 41c, d). The reasons why the latter efficiently destabilize CD147 and MCT in human, but not in zebrafish, are unclear, but might be explained by reduced affinities of these IMiDs to zebrafish CRBN. Neverthelss, the clear correlation between IMiD-induced destabilization of CD147 and the teratotoxic potential of the respective IMiD (Fig. 41) further distinguishes CD147 as central mediator of IMiD teratotoxicity. Thus, the CRBN-CD147/MCT1 axis does not only seem essential for the anti-tumor activities of IMiDs, but also responsible for their teratotoxicity.

4 Discussion

The molecular mechanism by which thalidomide mediates its teratotoxic and pleiotropic anti-tumor and immunomodulatory functions has remained elusive over decades. Despite development of highly active analogs as lenalidomide and pomalidomide, which have revolutionized treatment of some hematological malignancies in recent years, the anti-angiogenic, anti-proliferative and anti-invasive properties were only incompletely understood, and a common underlying meachanism connecting the pleiotropic effects was missing. The discovery of CRBN as molecular target of thalidomide and other immunomodulatory drugs (Ito et al., 2010) made a huge step forward in understanding IMiD biology, however, questions as to how CRBN mediates the diverse IMiD properties remained. Recently, neo-substrates such as the lymphoid transcription factors IKZF1 and IKZF3 and the kinase CK1-α were identified to bind to the $CRL4^{CRBN}$ E3 ubiquitin ligase in presence of lenalidomide or pomalidomide, but not thalidomide, resulting in ubiquitylation and degradation of these proteins (Gandhi et al., 2014a; Kronke et al., 2015; Kronke et al., 2014; Lu et al., 2014; Zhu et al., 2014). Although the IMiD-induced ubiquitylation and degradation of IKZF1/3 and CK1-α explains some of the anti-proliferative and immunomodulatory properties of lenalidomide and pomalidomide, many open questions remained, particularly with regard to the pleiotropic anti-angiogenic and anti-proliferative properties, and the still unexplained teratotoxic effects.

Starting from an unbiased, mass spectrometry based screen, this study identified CD147 and MCT1, which form a transmembrane complex frequently overexpressed in diverse malignancies to regulate tumor growth, metabolism, angiogenesis and invasion (Halestrap and Wilson, 2012; Weidle et al., 2010), as novel physiological interactors of CRBN and highly relevant mediators of IMiD effects. CRBN was found to stabilize CD147 and MCT1 in a chaperone-like manner, independent of CRL4 ubiquitin ligase function.

CRBN bound to immature forms of CD147 and MCT1 at the ER to promote complex formation, maturation, and membrane expression of CD147 and MCT1, which proved vital for proliferation and survival of MM and del(5q) MDS cells. By competing with CD147 and MCT1 for binding to the IMiD binding pocket of CRBN, IMiDs disrupted the CRBN-CD147/MCT1 complex, leading to destabilization and reduced membrane expression of CD147/MCT1, thus exhibiting anti-proliferative, anti-angiogenic and anti-invasive effects. Destabilization of CD147 was additionally found responsible for mediation of thalidomide-induced teraotoxicity in the zebrafish model. Therefore, this study provides for the first time a common mechanism of action underlying the pleiotropic anti-tumor and the teratotoxic effects of IMiDs.

The identified chaperone-like function of CRBN and the formation of protein complexes independent of the previously described $CRL4^{CRBN}$ ubiquitin ligase, suggests a dual activity of CRBN comprising ligase-dependent and ubiquitin- and CRL4-independent chaperone-like functions. Importantly, such a dual function provides an explanation for the observed syngergistic

anti-MM activity of IMiDs in combination with proteasomal inhibitors such as bortezomib, carfilzomib and ixazomib, which would be expected to antagonize the function of the $CRL4^{CRBN}$ ligase and its effects on IKZF1/3 and CK1-α (Moreau et al., 2016; Richardson et al., 2009; Richardson et al., 2010; Richardson et al., 2014b; Stewart et al., 2015; Wang et al., 2013).

While degradation of the neo-substrates IKZF1/3 and CK1-α strongly varies between specific IMiDs, thus not representing a class-wide effect (Kronke et al., 2015), destabilization of CD147 and MCT1 is common to thalidomide, lenalidomide and pomalidomide in human. This study is hence the first to identify a class-wide mechanism of action common to all IMiDs.

Finally, this study demonstrates a clear correlation between destabilization of CD147/ MCT1 and response to IMiDs, suggesting CD147/MCT1 and their IMiD-induced destabilization as potential biomarkers for IMiD response. Given the cell surface localization, CD147 is accessible to clinical evaluation by flow cytometry. Moreover, the cell surface expression distinguishes CD147 and MCT1 as accessible therapeutic targets both in IMiD-sensitive and –resistant disease.

4.1 CRBN exerts a dual function

4.1.1 CRBN mediates IMiD functions beyond targeting of neo-substrates

The most important publications on the molecular mechanism of IMiDs in the last years focused on the ubiquitin ligase function of CRBN as part of the $CRL4^{CRBN}$ E3 ubiquitin ligase, and the neo-substrates IKZF1/3 and CK1-α (Chamberlain et al., 2014; Fischer et al., 2014; Gandhi et al., 2014a; Kronke et al., 2015; Kronke et al., 2014; Lu et al., 2014; Zhu et al., 2014). The very appealing novel concept that small molecule inhibitors induce specific binding and ubiquitylation of otherwise hardly targetable oncogenes (Kronke et al., 2015; Kronke et al., 2014; Lu et al., 2014) set off a veritable hype and quest for novel IMiD analogs targeting other previously undruggable proteins (Winter et al., 2015). However, the focus on neo-substrates and ligase-associated functions of CRBN misses out central other aspects of IMiD biology and CRBN physiology.

With different neo-substrates for each IMiD, this concept fails to provide a common mechanism of action explaining the typical class-wide effects of IMiDs such as immunomodulatroy, anti-angiogenic or the infamous teratotoxic properties. Furthermore, the focus on neo-substrates leaves the question concerning the physiological function of CRBN completely unanswered. Interestingly, previous studies already showed that inactivation of CRBN is responsible for some of the typical anti-MM and teratotoxic effects of IMiDs, suggesting that IMiDs interfere with physiological CRBN functions (Ito et al., 2010; Zhu et al., 2011). These findings and the data on the neo-substrates could be united in a model postulating a dual activity of IMiDs, which comprises interference with physiological CRBN functions and induction of novel functions such as the specific degradation of neo-substrates.

Importantly, the current study confirms the hypothesis of a compound effect of IMiDs and uncovers the stabilization of CD147 and MCT1 as highly relevant physiological function of CRBN, which is disrupted by IMiD treatment, thus leading to destabilization of CD147 and MCT1. In contrast to neo-substrates such as IKZF3, which only bound to CRBN in presence of lenalidomide (Fig. 13) in accordance with previous studies (Chamberlain et al., 2014; Fischer et al., 2014; Gandhi et al., 2014a; Kronke et al., 2014; Lu et al., 2014), CD147 and MCT1 were discovered to be physiological interactors which bound to CRBN under normal conditions and were outcompeted by IMiD treatment (Fig 13, 14). Although other physiological CRBN interactors such as large-conductance Ca^{2+}–activated K^{+}–channels (BK_{Ca}) or voltage-gated chloride channels (ClC) had been previously described (Hohberger and Enz, 2009; Jo et al., 2005), CD147 and MCT1 are the first physiological CRBN interactors highly relevant for mediation of IMiD effects.

With regard to membrane expression and stability of CD147 and MCT1, MM cell proliferation, VEGF secretion or lactate transport, CRBN silencing had the same detrimental effects as IMiD treatment (Fig. 17, 22, 23, 30, 31), suggesting that the observed anti-angiogenic, anti-proliferative and metabolic effects result from inhibition of physiological CRBN activities and not from degradation of any neo-substrates. $CRBN^{-/-}$ MM1.S cells for instance, which proliferated far less that their wildtype counterparts, displayed markedly reduced levels of CD147 and MCT1 but equal IKZF3 levels (Fig. 17), leading to the hypothesis that the anti-proliferative effects in MM might predominantly result from CRBN inhibition and associated CD147/MCT1 destabilization and not from IMiD-induced IKZF1/3 degradation. However, knockdown of IKZF1 or IKZF3 also reduced MM cell growth (Kronke et al., 2014; Lu et al., 2014), without affecting CD147, MCT1 or CRBN expression (Fig. 18b), suggesting that the anti-MM activity of IMiDs is indeed a compound effect resulting from inhibition of physiological CRBN functions with subsequent destabilization of CD147 and MCT1 on the one hand, and from degradation of neo-substrates on the other hand. The overall effects of a given IMiD drug would thus result from inhibition of physiological CRBN functions, which are expected to be common to all current IMiDs, and specifc effects of each drug, possibly resulting from targeting of differing neo-substrates.

4.1.2 CRBN exerts ligase-independent chaperone-like functions

Diverse experiments were performed within this study to investigate the underlying mechanism of the observed stabilizing effect of CRBN towards CD147 and MCT1. Although protein ubiquitylation generally leads to proteasomal degradation of the respective protein, K63-linked polyubiquitylation chains or e.g. monoubiquitylation do not lead to degradation, but instead are reported to modulate protein function, binding properties or intracellular localization of a given protein (Clague and Urbe, 2010; Hershko and Ciechanover, 1998; Nakagawa and Nakayama, 2015). The observed effects on CD147 and MCT1 stability could therefore be mediated either by some kind of stabilizing mono- or polyubiquitylation exerted by CRBN as part of the $CRL4^{CRBN}$

ligase complex, or via a completely independent mechanism. Experiments impeding CRL4-associated ligase activity via knockdown of CUL4A or CUL4B however demonstrated that neither stabilization of CD147 and MCT1, nor their IMiD-induced destabilization were dependent on CRL4 ligase function (Fig. 20a). Together with size exclusion chromatography based experiments showing two distinct complexes of CRBN, one in association with DDB1 and CUL4 as CRL4 ligase, and a second CRL4-independent complex of CRBN with CD147 and MCT1 (Fig. 21), it was concluded, that CRBN exerts its stabilizing effects in a ubiquiting- and ligase-independent manner.

Proteins promoting stabilization and assisting in maturation of other proteins are generally called chaperones or are at least attributed chaperone function. The observed binding of CRBN to early forms of CD147 and MCT1 (Fig. 24), the accumulation of CD147 and MCT1 at the ER upon CRBN silencing (Fig. 22) and moreover, the clear retardation of CD147 maturation and glycosylation upon CRBN silencing or lenalidomide treatment (Fig. 25), moreover confirmed a chaperone-like activity of CRBN towards CD147 and MCT1. Notably, the large LON domain, which makes up for more than half of the CRBN protein (Fig. 6), is common to some proteases and chaperones (Li et al., 2013; Smith et al., 1999) and might thus represent the structural basis for chaperone-like acitivity of CRBN.

Interestingly, there have been some hints in the literature suggesting chaperone-like functions of CRBN already prior to this study. For instance, CRBN was found to be recruited to aggregations of misfolded proteins and have cytoprotective properties in case of disturbed protein homeostasis (Sawamura et al., 2015). The same study also showed interaction of CRBN with heat shock protein 70 (HSP70), one of the major cellular chaperone proteins assisting in folding of nascent polypeptide chains (Hartl, 1996; Sawamura et al., 2015). The mitochondrial Lon protease was also found to interact with HSP70 to meditate chaperone activity (Kao et al., 2015), suggesting a LON-domain dependent interaction with proteins of the heat shock family as mechanism underlying the observed chaperoning activity of CRBN. Moreover, other membrane proteins, including ion channels with multiple transmembrane domains such as the Cystic fibrosis transmembrane conductance regulator (CFTR), structurally resembling to MCT1, were found to be dependent on HSP90 and associated co-chaperones for maturation and membrane expression (Loo et al., 1998; Wang et al., 2006), making a comparable mechanism conceivable for CD147 and MCT1.

Nevertheless, the underlying mechanism of CRBN-induced stabilization of CD147 and MCT1 currently remains elusive. Although the above named studies suggest cooperation of CRBN with established heat shock proteins, thus making CRBN a co-chaperone of e.g. HSP70 or HSP90, it is also conceivable that CRBN exerts protein-stabilizing functions independent of other chaperone complexes. For instance, CRBN binding could induce e.g. necessary sterical changes in the transmembrane proteins, allowing proper folding and complex formation, or influence the vesicle-mediated transport from ER to Golgi. The verification of these hypotheses will be subject

of future studies, which will hopefully help to elucidate the exact mechanism underlying the chaperone-like functions of CRBN.

Another important question remaining to be addressed, is how and where the different CRBN-containing complexes form in the cell and if interchange exists. Currently, it is unclear if CRBN exists in parallel in CRL4 dependent and independent complexes within the same cellular compartment, or if CRBN has different functions depending on its subcellular localization. CRBN is localized in the nucleus, the cytoplasm and the perinuclear region possibly corresponding to the ER (Higgins et al., 2004; Ito et al., 2010). It could thus be hypothesized, that CRBN e.g. forms a CRL4 ligase in the nucleus, where it targets the transcripton factors IKZF1/3 or the kinase CK1-α, which localizes to nucleus and cytoplasm, while rather exerting CRL4-independent chaperone-like functions in the cytoplasm or associated to the ER. All these questions will have to be elucidated in further studies, thus improving the understanding of CRBN and also IMiD biology.

4.1.3 The dual function explains synergism of MiDs and proteasomal inhibitors

Before the discovery of CRL4 E3 ligase-independent functions of CRBN, the highly synergistic anti-MM activity of IMiDs and proteasome inhibitors (PI) observed in various clinical studies could not be explained and was even in conflict with the current models of drug activity. Lenalidomide and pomalidomide were assumed to mediate their anti-MM efficacy predominantly via ubiquitylation and subsequent degradation of IKZF1 and IKZF3 (Gandhi et al., 2014a; Kronke et al., 2014; Lu et al., 2014; Zhu et al., 2014). Importantly, the degradation of polyubiquitylated IKZF1/3 was clearly shown to be proteasome dependent, and treatment with MG132, a potent PI, reversed the IMiD-induced degradation (Lu et al., 2014). By contrast, clinical studies found the combination of the established PIs bortezomib, carfilzomib and ixazomib with either of the IMiDs to be highly effective (Moreau et al., 2016; Richardson et al., 2009; Richardson et al., 2010; Richardson et al., 2014b; Roussel et al., 2014; Stewart et al., 2015; Wang et al., 2013). The combination therapies were even capable of overcoming resistance to monotherapy of either of the substances (Richardson et al., 2009; Richardson et al., 2014b). Furthermore, the combination of lenaliomide, dexamethasone and bortezomib was potent enough to achieve some degree of response in all treated patients, approaching an overall response rate of 100% in untreated MM (Richardson et al., 2010).

These findings demonstrate that the clinical efficacy of IMiDs is not counteracted by PIs; by contrast, they display a high degree of synergism. Whereas the underlying mechanism could not be explained by previous models, the identification of chaperone-like effects of CRBN disclosed proteasome-independent functions not counteracted by PI, thus providing an explanation for the observed synergy. For instance, IMiD-mediated inhibition of chaperone-like CRBN functions might synergize with PIs by increasing the cellular stress response. PIs are known to induce the unfolded protein response (UPR), resulting from accumulation of unfolded and damaged proteins, which cannot be degraded by the ubiquitin-proteasome system in presence of PIs (Nikesitch et al., 2016; Obeng et al., 2006). Importantly, the induction of the UPR

is believed to be the central anti-MM activity of PIs, inducing cell stress and finally apoptosis (Nikesitch et al., 2016; Obeng et al., 2006). Meanwhile, it is conceivable that inhibition of chaperone-like CRBN functions also induces cellular stress via accumulation of misfolded, immature proteins – specifically with respect to CD147 and MCT1. Although it has not yet been studied if IMiDs induce ER stress or the UPR, a recent publication describes that depletion of CRBN activates the UPR (Lee et al., 2015), supporting the prior hypothesis. Moreover, CRBN overexpression was shown to protect from PI induced cell death, while CRBN silencing increased the cytotoxicity of PIs (Sawamura et al., 2015). Given that IMiDs have the same effect towards CD147 and MCT1 as CRBN silencing (Fig. 16, 17, 30-31), it can be hypothesized, that IMiDs indeed activate the UPR in analogy to CRBN silencing (Lee et al., 2015; Sawamura et al., 2015), thus synergizing with PIs in induction of cellular stress and activation of the UPR. To verify this hypothesis, it will be interesting to analyze markers of the UPR, after PI treatment, IMiD treatment and combination treatments.

4.2 Destabilization of CD147 and MCT1 mediates central IMiD effects

The central finding of this study, besides decription of novel, ligase-independent CRBN functions, is the identification of CD147 and MCT1 as important mediators of IMiD effects in MM, del(5q) MDS and also in the context of teratogenicity, thus defining one common mechanism underlying most of the known IMiD effects.

4.2.1 Destabilization of CD147 and MCT1 mediates central anti-tumor effects

IMiDs exert various activities including immunomodulatory, anti-angiogenic, anti-invasive, anti-proliferative and unfortunately also teratotoxic activity (Fig. 5) (Bartlett et al., 2004; Shortt et al., 2013). For many years, the overall IMiD activity seemed like a potpourri of different well described anti-cancer and immunomodulatory properties, without a common mechanism linking these effects to each other. It was generally assumed that IMiDs exert their function via different mechanisms and target proteins, until CRBN was described as their molecular target mediating anti-proliferative, immunomodulatory and teratotoxic effects (Ito et al., 2010; Zhu et al., 2011). Given the initially scarce data on CRBN however, the mechanisms by which CRBN mediates IMiD effects only start to be understood.

With identification of CD147 and MCT1 as CRBN-dependent target proteins of IMiDs, this study is the first one to describe proteins as IMiD effectors, whose properties are as broad as the diverse effects of IMiDs (Iacono et al., 2007; Weidle et al., 2010). For instance, IMiDs are known to inhibit angiogenesis via repression of both FGF and VEGF secretion from tumor cells and associated stromal cells (D'Amato et al., 1994; Kruse et al., 1998), while CD147 promotes secretion and activation of VEGF and MMPs from tumor and stroma cells (Biswas et al., 1995; Chen et al., 2012; Guo et al., 1997; Tang et al., 2005; Voigt et al., 2009). This study further confirmed that IMiDs inhibit VEGF and MMP7 secretion from MM cells via destabilization of

CD147/MCT1 (Fig. 30) and moreover showed that knockdown of CD147 results in suppression of FGF (Fig. 41). It can thus be assumed, that the anti-angiogenic activity of IMiDs results from destabilization of CD147. Besides activation of MMP secretion (Biswas et al., 1995), which is necessary for migration and invasion, CD147 moreover interacts with integrins to promote cell motility (Curtin et al., 2005; Weidle et al., 2010). This allows the conlcusion, that the anti-invasive potential of IMiDs, which was reportet to include reduction of integrin expression, cellular migratory potential and expracellular MMP activity (Segarra et al., 2010), can also be explained by destabilization of CD147.

The direct anti-proliferative effects of IMiDs observed in MM or del(5q) MDS cells as shown in this study (Fig. 17, 26, 29, 35, 36) and also previously described (Hideshima et al., 2000; Pellagatti et al., 2007; Quach et al., 2010; Zhu et al., 2011), can moreover be sufficiently explained by destabilization of CD147 and MCT1, which are overexpressed in MM and del(5q) MDS and proved to be essential for cell viabilitiy and proliferation in this (Fig. 28, 35) and previous studies (Arendt et al., 2012; Arendt et al., 2014; Walters et al., 2013). The described indirect anti-MM effects of IMiDs (Fig. 4), which include inhibition of angiogenesis and altered interaction with BM stromal cells likely also result from destabilization of CD147 and associated inhibition of VEGF secretion and integrin activity. The observed IMiD-induced inhibition of osteoclasts, which is beneficial for MM patients with lytic bone lesions, is likewise mediated via reduction of integrin expression (Breitkreutz et al., 2008), and thus likely induced by CD147 destabilization.

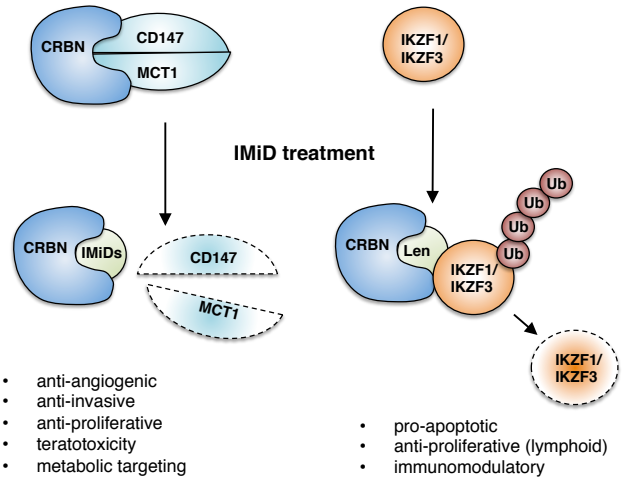

Fig. 42: Model of the compound IMiD-mediated functions. Under physiological conditions (top), CRBN binds to CD147 and MCT1 to promote stabilization and complex formation (top left), while IKZF1/3 and other neo-substrates do not interact with CRBN (top right). Upon IMiD treatment (bottom), IMiDs bind to the IMiD binding pocket of CRBN, thus outcompeting CD147 and MCT1 from binding to CRBN, which results in destabilization of the protein complex (bottom, left), thus mediating anti-angiogenic, anti-invasive, anti-proliferative, teratotoxic and metabolic functions. In parallel, binding of lenalidomide or pomalidomide to CRBN induces recruitment of the neo-substrates KZF1/3 to CRBN (bottom, right), leading to their ubqiuitylation and degradation, which finally results in pro-apoptotic, anti-proliferative and immunomodulatory effects. Overall, IMiD effects are suggested to be the result of at least these two independent mechanisms of action.

Although not specifically addressed in this study, there is also some evidence that CD147 is involved in mediation of immunomodulatory IMiD functions, as recent studies found CD147 to be involved in T-cell activation and immunological synapse formation (Hu et al., 2010) while being specifically expressed in a highly suppressive subset of T-regulatory cells (Solstad et al., 2011). IMiD-induced destabilization of CD147 could therefore inhibit activity of suppressive T-cells, thus leading to the observed IMiD-linked T-cell activation (Bartlett et al., 2004; Haslett et al., 1998).

Taken together, the destabilization of CD147 and MCT1 seems largely responsible for mediation of the pleiotropic anti-cancer effects of IMiDs, including anti-angiogenic, anti-proliferative, anti-invasive and maybe also immunomodulatory properties (Fig. 42). Together with the data on neo-substrates such as IKZF1/3, this results in a model of dual IMiD activity: while destabilization of CD147 and MCT1 mediates most of the described functions, IMiD-induced degradation of IKZF1/3 adds further anti-proliferative and immunomodulatory effects to the overall activity of IMiDs (Fig. 42).

4.2.2 Destabilization of CD147 and MCT1 inhibits cancer cell metabolism

Besides revealing that major IMiD functions such as anti-angiogenic, anti-invasive and direct anti-proliferative properties are largely mediated by destabilization of CD147, this study additionally describes a novel, previously unappreciated metabolic function of IMiDs, arising from destabilization of MCT1 and consecutive inhibition of lactate transport (Fig. 31).

Most cancer cells, including MM and MDS cells, frequently grow in hypoxic conditions and rely on anaerobic or aerobic glycolysis to meet their high energy demand, thus making the export of lactate, the final product of glycolysis, essential for maintenance of cellular homeostasis and pH (Colla et al., 2010; Liberti and Locasale, 2016; Parks et al., 2013). The distorted cancer cell metabolism makes metabolic targeting a promising approach in cancer therapy, which is currently subject of intense investigations (Parks et al., 2013). MCT1 has been shown to be essential for lactate export in many tumors, which, together with its frequent overexpression in MM and other malignancies, makes it one of the most interesting target proteins to interfere with cancer cell metabolism (Parks et al., 2013; Pinheiro et al., 2010; Walters et al., 2013). Indeed, siRNA-induced silencing of MCT1 or inhibition via small molecule inhibitors led to decreased lactate export, accumulation of intracellular lactate and reduced proliferation in MM and other cancers in this and previous studies (Fig. 31) (Polanski et al., 2014; Walters et al., 2013), thus confirming the efficacy of metabolic targeting. Via destabilization of MCT1, this study found IMiDs to inhibit cellular lactate efflux in analogy to direct MCT1 inhibition, leading to significantly increased intracellular lactate levels in IMiD-sensitive MM cells (Fig. 31). Importantly, this study is the first to report an association of IMiDs with lactate transport and cancer metabolism in general, thus adding metabolic targeting to the large panel of diverse IMiD activities.

4.2.3 Destabilization of CD147 mediates teratotoxic effects

Next to the various anti-tumor effects which are mediated by destabilization of CD147 and MCT1, the same mechanism was found responsible for the teratotoxicity of IMiDs in a zebrafish model. While there had been different hypotheses and pieces of evidence regarding the mechanism of IMiD-mediated teratotoxicity so far, the current study adds a new piece to the puzzle, confirming previous models and functionally connecting the previously described findings.

For instance, once thalidomide was identified to inhibit angiogenesis via supression of FGF and VEGF (D'Amato et al., 1994; Kruse et al., 1998), it was hypothesized that the anti-angiogenic effects of thalidomide could be responsible for the observed teratotoxic malformations. Indeed, the antiangiogenic activity correlated with the teratotoxic potential, and thalidomide treated rabbit embryos displayed deformed limb bud vasculature (D'Amato et al., 1994). Additionally, thalidomide was described to induce down-regulation of surface adhesion receptors such as integrins, thus inhibiting cell migration and differention, leading to severe disturbances of embryonic development (McCarty, 1997; Neubert et al., 1996; Nogueira et al., 1996). The observed suppression of adhesion proteins with consecutive inhibition of cell motility could either represent an independent mechanism responsible for teratotoxicity next to anti-angiogenesis, or be the common basis of both phenomena. Later, knockdown of CRBN was shown to induce similar teratotoxic malformations as thalidomide, including severe suppression of FGF8 expression in the fin buds of developing zebrafish (Ito et al., 2010).

The current study now demonstrates that thalidomide destabilizes CD147 in zebrafish, and that knockdown of CD147 leads to similar malformations and suppression of FGF8 expression in fin buds as thalidomide treatment (Fig. 40, 41), thus establishing CD147 as central mediator of IMiD teratotoxicity. Importantly, the identification of CD147 as mediator of teratotoxicity unites all previously described findings under a common mechanism. Knockdown of CRBN results in destabilization of CD147 (Fig. 17a), thus explaining the teratotoxic effects of CRBN knockdown (Ito et al., 2010). The observed thalidomide-mediated suppression of FGF8 is assumed to likewise result from CD147 destabilization, as CD147 has identical effects. Moreover, CD147 is known to interact with integrins to promote cell migration (Curtin et al., 2005; Delyon et al., 2015; Li et al., 2012; Weidle et al., 2010), and induce angiogenesis via induction of VEGF and MMP secretion (Chen et al., 2009; Su et al., 2009; Tang et al., 2005; Voigt et al., 2009). Destabilization of CD147 results in reduced migration and angiogenesis via inhibiton of the named processes, thus explaining the large majority of the findings described in the context of thalidomide teratotoxicity.

Notably, the teraotoxic potential of an IMiD correlated with its impact on CD147 within the same species (Fig. 41), thus further strengthening CD147 as central mediator of IMiD-induced teratotoxitiy. While all three established IMiDs destabilized CD147 and MCT1 in human (Fig. 19), only thalidomide showed destabilization and by consequence teratotoxicity in zebrafish (Fig. 41). The reasons for these differences remain unclear and make part of the larger mystery regarding

the striking inter-species variance of IMiD activity (Fort et al., 2000; Hendrickx and Sawyer, 1978; Ito et al., 2010; Lopez-Girona et al., 2012; Mahony et al., 2013). One hypothesis might be that alterations of the IMiD binding pocket in different species result in different affinities to the respective IMiDs; however further research will be necessary to understand these variances. Until the underlying reasons for the diverging activity of IMiDs in different species are elucidated, no conclusions can be drawn from one species to another with respect to the teratogenic potential of an IMiD. Importantly, a recent report likewise showing that only thalidomide, but not lenalidomide or pomalidomide, are teratotoxic in zebrafish (Mahony et al., 2013), prompted the hypothesis that lenalidomide and pomalidomide could also lack teratogenic potential in general. However, pomalidomide had teratotoxic actitivity in rats and rabbits (D'Amato et al., 2013; Lopez-Girona et al., 2012), and given that destabilization of CD147 seems responsible for IMiD-mediated teratogenic effects, pomalidomide would certainly be expected to be teratogenic in human, where it induced the strongest destabilization of CD147 of all three IMiDs (Fig. 19). Although not providing an explanation for the inter-species differences of IMiD teratogenicity, this study however suggests destabilization of CD147 as marker to predict teratogenicity within a certain species, as knockdown of CD147 on the one hand clearly induces teratotoxicity, and, on the other hand, IMiD induced destabilization of CD147 clearly correlated with the teratotoxic potential in zebrafish (Fig. 41). This correlation needs to be validated in further species, but if it proves true, it would be the first species-specific predictor of IMiD induced teratogenicity.

4.3 Potential biomarkers for IMiD response

4.3.1 Currently discussed biomarkers for IMiD response

Currently, there is no established marker to identify patients that could benefit from IMiD treatment. Instead, IMiDs are directly administered and clinical response is evaluated weeks later by quantification of M-protein in serum or percentage of MM cells in the BM. A biomarker clearly predicting IMiD response could thus help to avoid that non-responding patients undergo weeks of treatment without clinical benefit.

So far, there have been different attempts to establish indicators for IMiD response, but all remained controversial. For instance, degradation of IKZF1/3 and CK1-α was observed in both IMiD-sensitive and resistant MM or MDS lines respectively (Fig. 26, 36), in accordance with previous studies (Lu et al., 2014), therefore being useless as predictor of response. Regarding baseline levels of IKZF1/3, one study using a murine xenograft model with MM1.S cells found high IKZF1/3 baseline levels to correlate with acquired IMiD resistance (Ocio et al., 2015), whereas another study investigating MM cell lines and primary patient cells, identified low IKZF1 levels to predict poor IMiD response (Zhu et al., 2014). Mechanistically, both scenarios are conceivable: high IKZF1/3 abundance could compensate potential IMiD-induced loss and thus explain resistance, while low IKZF1/3 levels could indicate a relative irrelevance of these in transcription factors in the respective tumor cell, making them indifferent to changes in IKZF1/3

abundance. Together, these opposing findings on the predictive role of baseline IKZF1/3 levels do however not allow clear conclusions and need to be further investigated.

CRBN itself has also been investigated regarding its potential as biomarker to predict IMiD response. In cell culture models, acquired or intrinsic IMiD resistance correlated with low CRBN expression (Lopez-Girona et al., 2012; Zhu et al., 2011). In analogy, clinical studies found high CRBN expression on the transcriptional level to be associated with improved response to thalidomide, lenalidomide or pomalidomide in MM, while low CRBN expression correlated with IMiD resistance (Bedewy and El-Maghraby, 2014; Broyl et al., 2013; Heintel et al., 2013; Schuster et al., 2013). An immunohistochemistry based study confirmed high CBRN expression on the protein level to be predictive of superior response to thalidomide or lenalidomide, whereas no correlation between CRBN expression and response to non-IMiD treatement could be observed in MM (Huang et al., 2014). Beyond MM, high transcriptional levels of CRBN were found to distinguish generally IMiD sensitive del(5q) disease from largely IMiD-resistant non-del(5q) MDS and to additionally correlate with lenalidomide-response in del(5q) MDS (Jonasova et al., 2015). By contrast, other studies did not find any correlation between lenalidomide response and CRBN expression on the protein level in MM cell lines (Gandhi et al., 2014b; Greenberg et al., 2013). Moreover, sequencing of CRBN in MM cell lines and patient derived MM cells did not reveal any recurrent mutation in CRBN or DDB1 genes in neither IMiD-sensitive nor IMiD-resistant MM lines or patient-derived primary cells, suggesting CRBN-independent mechanisms of resistance (Thakurta et al., 2013). Taken together, there is some evidence that low CRBN expression correlates with IMiD resistance, while high CRBN expression is associated with IMiD response (Bedewy and El-Maghraby, 2014; Broyl et al., 2013; Heintel et al., 2013; Huang et al., 2014; Schuster et al., 2013). However, CRBN expression on mRNA level fails to correlate with protein levels (Gandhi et al., 2014b), thus limiting the results of the named studies, which used different non-standardized methods to analyze CRBN expression. Moreover, different splice variants of CRBN were found to complicate assessment of CRBN expression (Gandhi et al., 2014b; Lode et al., 2013). Hence, proper evaluation of CRBN expression as biomarker for IMiD response requires a standardized, validated method such as the recently established dual color immunohistochemistry assay, and analysis of large patient collectives, before any clear conclusions can be drawn (Gandhi et al., 2014b; Lode et al., 2013; Ren et al., 2015).

4.3.2 Destabilization of CD147 and MCT1 as predictor of IMiD response

Compared to all these findings, the IMiD-induced destabilization of CD147 and MCT1, which is deemed responsible for mediation of central IMiD properties such as anti-angiogenic and anti-proliferative effects, showed a strikingly clear correlation with IMiD sensitivity. While IMiD-induced destabilization of CD147 and MCT1 was observed in all MM and MDS cells responding to IMiD treatment (Fig. 26, 36), CD147 and MCT1 levels were stable under IMiD treatment in all IMiD-resistant cell lines, in which neither proliferation, nor VEGF or MMP7 secretion, nor lactate efflux were affected by IMiDs (Fig. 26, 30, 31). The observed clear and full correlation between

IMiD-sensitivity and destabilization of CD147 and MCT1 was confirmed in patient-derived MM cells (Fig. 34), thus further distinguishing the specificity and importance of CD147/MCT1 destabilization for IMiD effects and making CD147/MCT1 destabilization the probably most promising predictor of IMiD sensitivity so far.

Overall protein levels of CD147 and MCT1 did by contrast not to correlate with IMiD sensitivity in MM cell lines (Fig. 26), while in MDS, IMiD activity was restricted to the del(5q) subentitiy displaying significantly higher CD147 and MCT1 expression levels than non-del(5q) MDS (Fig. 35, 36). These findings lead to the hypothesis, that expression of CD147 and MCT1 is necessary for cells to be potentially susceptible to IMiDs and IMiD-induced CD147 destabilization, while the overall protein abundance does not necessarily correlate with IMiD sensitivity. However, analyses of patient samples are necessary before drawing any conclusions on the potential of baseline CD147/MCT1 expression as biomarker for IMiD response.

Destabilization of CD147/MCT1 thus remains the most promising biomarker predicting IMiD response. Unfortunately, assessment of destabilization requires two subsequent analyses (before and after IMiD exposure), which complicates the procedure. However, it might be worth the effort if the results allow clear-cut distinction between sensitive and resistant disease, as suggested by the data of this study. Importantly, CD147 and MCT1 are easily evaluable by e.g. flow cytometry due to their cell surface localization. Shedding and intramembrane cleavage of CD147 (Egawa et al., 2006; Sidhu et al., 2004) moreover allow e.g. ELISA-based assessment of free CD147 in serum, which has already been described for other diseases (Lee et al., 2016; Yanaba et al., 2012). While isolation of MM cells followed by *in-vitro* IMiD treatment and flow cytometry analysis, as performed in this study (Fig. 34), would be possible but likely too laborious for clinical routine, comparison of e.g. free CD147 in serum before and after initial IMiD treatment could allow early conlusions on IMiD sensitivity. Detailed protocols and analysis of larger patient cohorts will however be necessary to determine the clinical utility of CD147/MCT1 destabilization as predictive biomarker of IMiD response.

4.4 CD147 and MCT1 as targets for cancer therapy beyond IMiDs

4.4.1 Targeting of CD147 and MCT1 in non-hematological malignancies

The cell surface expression of CD147 and MCT1, which makes these proteins easily accessible for diagnostic purposes, also renders these proteins easily accessible for targeted therapeutics such as antibodies. The broad oncogenic properties of CD147 and MCT1 together with their frequent overexpression in various tumors (Halestrap and Wilson, 2012; Pinheiro et al., 2010; Riethdorf et al., 2006; Weidle et al., 2010) indeed characterize these proteins as attractive therapeutic targets and it is not surprising, that antibodies directed against CD147 and small molecule inhibitors of MCT function are already in preclinical or even early clinical development.

For instance, specific anti-CD147 antibodies inhibited MMP and VEGF secretion and reduced tumor growth, invasion and angiogenesis in human breast cancer and hepatocellular

carcinoma (HCC) xenograft models, additionally killing cancer cells via antibody-dependent cell cytotoxicity (ADCC) (Walter et al., 2016; Xu et al., 2007b). Also in squamous cell cancer, inhibitory anti-CD147 antibodies proved to inhibit cell proliferation and migration as efficiently as siRNA-mediated knockdown (Frederick et al., 2016). In addition to the anti-CD147 antibodies, a specific small moleculre inhibitor, AC-73, was found to inhibit CD147 dimerization and reduce motility and invasion of HCC cells (Fu et al., 2016). Notably, Chinese researchers already tested anti-CD147 therapy in early clinical trials, showing some anti-HCC activity of an anti-CD147 antibody coupled to radioactive iodine (Chen et al., 2006; Xu et al., 2007a). Importantly, antibody-mediated targeting of CD147 was shown to also impede MCT1 function in colon cancer and melanoma cell lines, reducing lactate transport and increasing acidity, thus inducing cell death (Baba et al., 2008). Likewise, direct inhibition of MCT1 by small molecule inhibitors such as AR-C155858, SR13800 or AZD3965 suppressed lactate export, glycolysis and tumor growth in different cancer cell lines including lymphoma cells (Doherty et al., 2014; Le Floch et al., 2011; Polanski et al., 2014). Importantly, cell death induced by inhibition of CD147 and MCT1 was largely restricted to tumor cells and was not detected in non-transformed cells (Baba et al., 2008), making this approach even more attractive.

4.4.2 Targeting of CD147 and MCT1 in hematological malignancies

In hematologic malignancies, there is only few data on anti-CD147 or anti-MCT1 directed treatment, despite different reports on the vital role of CD147 and MCT1 for proliferation, metabolism, migration and homing of MM, AML or B-NHL cells (Arendt et al., 2012; de Vries et al., 2010; Fu et al., 2010; Gao et al., 2015; Thorns et al., 2002; Walters et al., 2013; Zhu et al., 2015). At least, one study reported antibody-mediated targeting of CD147 to efficiently inhibit MM cell migration and activation (Zhu et al., 2015), while another study showed that the MCT1 inhibitor AR-C155858 induces cell death in MM via accumulation of intracellular lactate and associated reduced intracellular pH (Hanson et al., 2015).

This current study now additionally emphasizes the central role of CD147 and MCT1 in both MM and del(5q) MDS, showing that downregulation of either of these proteins severly impedes MM and MDS cell proliferation, VEGF and MMP secretion, lactate transport and *in-vivo* tumor growth (Fig. 28, 30–32, 35). Importantly, CD147 and MCT1 proved vital for proliferation in all investigated MM and MDS cells expressing these proteins, independent of their IMiD sensitivity. Targeting of CD147 or MCT1 could thus be used als alternative to IMiDs in potentially IMiD sensitive entities, which might be particularly attractive if these agents displayed a more preferable safety profile than IMiDs. Moreover, anti-CD147/anti-MCT1 directed therapy could be combined with IMiDs to increase anti-cancer efficacy, and, most importantly, targeting of CD147 and MCT1 promises to be an effective therapeutic approach in IMiD refractory patients, which genereally do not have many therapeutic options left.

As with all anti-cancer therapies, side effects will have to be considered. Although a recent study described an anti-CD147 antibody to specifically induce cell death in tumor cells, while not

affecting non-transformed fibroblasts (Baba et al., 2008), potential side effects are still conceivable. For instance, the described tumor-specificity likely results from differences in metabolism: while most cancer cells depend on glycolysis and thus lactate export, fibroblasts and many other cells and tissues conduct oxidative phosphorylation, making them less dependent on lactate transport (Baba et al., 2008). However, several non-malignant cells such as many cells of the hematopoietic and the central nervous system largely depend on glycolysis for energy production, thus limiting the cancer-specificity of MCT1 inhibition. Moreover, with CD147 and MCT1 being ubiquitously expressed in many tissues (Halestrap and Wilson, 2012; Iacono et al., 2007), specific targeting of these proteins likely brings about some side effects, which possibly overlap with some of the IMiD-induced side effects. Notably, as CD147 and MCT1 were found to mediate the teratotoxicity of IMiDs (Fig. 40, 41), clinical evaluation of anti-CD147 and anti-MCT1 directed therapy will have to take into account these potentially dramatic side effects.

Nevertheless, this study strongly encourages the development and clinical evaluation of anti-CD147 and anti-MCT1 agents in the treatment of IMiD-sensitive and IMiD-resistant MM, del(5q) MDS and other malignancies displaying enhanced expression of CD147 and MCT1.

5 Materials

5.1 Instruments

Analytical balance ABJ 220	Kern & Sohn GmbH
Aqualine water bath	Lauda-Brinkmann
Centrifuge Multifuge 3SR+	Thermo Scientific™
Cobas Integra® 8000	Roche Diagnostics GmbH
Concentrator plus	Eppendorf AG
Cool-Centrifuge 5417R	Eppendorf AG
CyAn™ ADP Analyzer	Beckman Coulter®
Cytomics FC 500 analyzer	Beckman Coulter®
Digital Sonifier® 250D	Branson-Emerson
E-Box VX2 Imager	VILBER
FACSCalibur™	BD Biosciences
FACSAria™ II	BD Biosciences
FluoView FV10i	Olympus
Fridges and lab freezers	Liebherr
HERAcell® 150i CO_2-Incubator	Thermo Scientific™
HERAfreeze ™	Thermo Scientific™
Hypercassettes ™	Amersham / GE Healthcare
Innova® 40 shaker for bacteria	New Brunswick™ / Eppendorf AG
Inveon Micro PET system	Siemens Medical Solutions
Invitrogen Chamber for Ready Gels	Invitrogen™
Light cycler® 480 system	Roche Diagnostics GmbH
LS4800 liquid nitrogen tank	Taylor-Wharton Lab Systems
LTQ Orbitrap Velos mass spectrometer	Thermo ScientificTM
MACS MultiStand	Miltenyi Biotec
Magnetic thermo stirrer RCT basic	IKA® Laboratory Equipment
Microscope Axiovert 40 CFL	Carl Zeiss AG
MidiMACS™ Separator	Miltenyi Biotec
Mini-PROTEAN® Tetra Cell SDS electrophoresis system	Bio-Rad Laboratories
Mini-Sub® Cell GT system for agarose electrophoresis	Bio-Rad Laboratories
Multifuge 3SR+	Thermo Scientific™
NanoLC-Ultra	Eksigent
NanoPhotometer®	Implen GmbH
Neubauer hemocytometer	Paul Marienfeld GmbH
Novex® Mini cell system for precast NuPAGE gels	Thermo Scientific™
peqSTAR2x gradient thermocycler	Peqlab Life Science
pH-meter pH720 InoLab	WTW GmbH

Pipetman neo (P10N, P20N, P100N, P200N, P1000N)	Gilson®
Polymax 1040 platform shaker	Heidolph Instruments
PowerPac™ Basic power supply	Bio-Rad Laboratories
PowerPac™ HC power supply	Bio-Rad Laboratories
Precision balance 572 -37	Kern & Sohn GmbH
Rotating Wheel 3000	Fröbel Labortechnik
Safety cabinet HERAsafe® KS	Thermo Scientific
Scanner V750 Pro	Epson®
SDS-gel Electrophoresis chamber Mini-Protean	Bio-Rad Laboratories
Sorvall® RC-5B centrifuge (rotors SS-24 & GS-3)	Du Pont Instruments
SRX-101A developer	Konica-Minolta
Superose 6 PC 3.2/30 analytical column	GE Healthcare
Tabletop centrifuge 5424	Eppendorf AG
Thermo block MBT 250	Kleinfeld Labortechnik
Thermomixer compact	Eppendorf AG
Trans Blot Cell Blotting chamber	Bio-Rad Laboratories
Tumbling roller mixer RM5	Neolab

5.2 Consumables

3mm CHR paper (Whatman™)	GE Healthcare
Cell Scraper	SARSTEDT AG
CELLSTAR® cell culture flasks (50ml; 250ml; 550ml)	Greiner Bio-One GmbH
CELLSTAR® serological pipettes (5ml; 10ml; 25ml)	Greiner Bio-One GmbH
CELLSTAR® sterile PP tubes (15ml; 50ml)	Greiner Bio-One GmbH
CL-XPosure™ Films	Thermo Scientific™
CryoPure Tubes (1,6ml)	SARSTEDT AG
CULTUBE™ sterile culture tubes T406-2A	Simport®
Flexi-PCR-Tubes (0,2ml)	Kisker Biotech GmbH
LS Columns	Miltenyi Biotec
Pipette tips (10 µl; 200 µl; 1000µl)	SARSTEDT AG
PVDF membrane (Immobilon®-P)	Merck Millipore
Micro-fine insulin syringes	BD Medical
SafeSeal micro tubes (1,5ml; 2,0ml)	SARSTEDT AG
Sterican® disposable needles (26G x1“)	B. Braun Melsungen AG
Syringes Injekt® (10ml)	B. Braun Melsungen AG
Syringe filters 0,45 µm	TPP Techno Plastic Products
Tissue culture dishes (100 x 20mm)	CORNING
Tissue culture dishes (150 x 20mm; 6-well)	TPP Techno Plastic Products
UVette® cuvettes (50-2000µl)	Eppendorf AG
Vasofix® saftey catheter	B. Braun Melsungen AG

x-well tissue culture chambers (2-well; 4-well)	SARSTEDT AG

5.3 Chemicals and reagents

[γ-^{32}P]Adenosine 5'-triphosphate (γATP)	Hartmann Analytics
β-Mercaptoethanol	Sigma-Aldrich™
3x FLAG® Peptide	Sigma-Aldrich™
Acetic acid	Carl Roth GmbH
Acetone	Carl Roth GmbH
Adefodur developer solution	Adefo Chemie GmbH
Adefo-Fix fixer solution	Adefo Chemie GmbH
Adenosintriphosphate (ATP)	Sigma-Aldrich™
Agarose NEEO	Carl Roth GmbH
Albumin fraction V (BSA)	Carl Roth GmbH
Ammonium persulfate (APS)	Carl Roth GmbH
Ampicillin	Carl Roth GmbH
ANTI-FLAG® M2 Affinity Gel	Sigma-Aldrich™
ANTI-HA Affnity Matrix	Roche Diagnostics GmbH
Aprotinin from bovine lung	Sigma-Aldrich™
Aqua ad injectabilia, sterile	B. Braun Melsungen AG
Bacto™ Agar	BD Biosciences
Bacto™ Trypton	BD Biosciences
Bacto™ Yeast Extract	BD Biosciences
BES buffered saline, pH 7.1	Sigma-Aldrich™
Bromphenol blue	Sigma-Aldrich™
Calcium chloride ($CaCl_2$)	Sigma-Aldrich™
Carboxymethylcellulose	Sigma-Aldrich™
Coomassie Brilliant Blue	Carl Roth GmbH
Cycloheximide (CHX)	Sigma-Aldrich™
Deoxynucleotide triphosphate (dNTP) mix (10mM)	Thermo Scientific™
Dimethyl sulfoxide (DMSO)	Carl Roth GmbH
Disuccinimidyl suberate (DSS)	Thermo Scientific™
DNA Loading Dye (6x)	Thermo Scientific™
ER tracker blue white DPX	Thermo Scientific™
Ethanol	Merck Millipore
Ethidium bromide	Carl Roth GmbH
Ethylendiamintetraacedtic acid (EDTA)	Sigma-Aldrich™
FACS Flow	BD Biosciences
Gluthatione Sepharose™ 4B	GE Healthcare
Glycine	Carl Roth GmbH
Glycerol	Sigma-Aldrich™

Glycerol 2-phosphate disodium salt hydrate (G2P)	Sigma-Aldrich™
HEPES	SERVA Electrophoresis GmbH
Hexanucleotide Mix (10x)	Roche Diagnostics GmbH
Hydrochloric acid (HCl) 32%	Carl Roth GmbH
Isopropanol	Carl Roth GmbH
Isopropyl β-D-1-thiogalactopyranoside (IPTG)	Sigma-Aldrich™
Kanamycin sulfate	Sigma-Aldrich™
L-[^{35}S]-Cysteine	Hartmann Analytics
L-[^{35}S]-Methionine	Hartmann Analytics
L-Glutathione	Sigma-Aldrich™
Lenalidomide	Selleck Chemicals
Leupeptin	Sigma-Aldrich™
Lipofectamine® 2000 Reagent	Thermo Scientific™
Lysozyme from chicken egg white	Sigma-Aldrich™
Magnesium chloride ($MgCl_2$)	Sigma-Aldrich™
Matrigel Basement Membrane Matrix	BD Bioscience
Methanol (J.T.Baker®)	Avantor™ Performance Materials
MLN4924	Selleck Chemicals
Nonidet P40, 10%	Roche Diagnostics GmbH
NuPAGE® MES SDS Running Buffer	Invitrogen™
Okadaic acid	Sigma-Aldrich™
Paraformaldehyde (PFA)	Sigma-Aldrich™
PBS Dulbecco (powder)	Biochrom Merck Millipore
Phenylmethylsulfonyl fluoride (PMSF)	Sigma-Aldrich™
Polybrene (hexadimethrine bromide)	Sigma-Aldrich™
Ponceau S solution	Sigma-Aldrich™
Pomalidomide	Selleck Chemicals
Potassium chloride (KCl)	Sigma-Aldrich™
ProLong® GOLD antifade reagent with DAPI	Thermo Scientific™
Propidium iodide (PI)	Sigma-Aldrich™
Protein A Sepharose CL-4B	GE Healthcare
Protein G Agarose, Fast Flow	Sigma-Aldrich™
Protein G Sepharose, Fast FLow	GE Healthcare
Rotiphorese® NF-Acrylamide/Bis-Solution 40% (29:1)	Carl Roth GmbH
Skim milk powder	Sigma-Aldrich™
SOC medium	New England Biolabs®
Sodium acetate	Merck Millipore
Sodium azide (NaN_3)	Merck Millipore
Sodium chloride (NaCl)	Carl Roth GmbH
Sodium citrate	Sigma-Aldrich™

Sodium dihydrogenphosphat	Merck Millipore
Sodium dodecylsulfate (SDS)	SERVA Electrophoresis GmbH
Sodium fluoride (NaF)	Sigma-Aldrich™
Sodium hydroxid (NaOH)	Carl Roth GmbH
Sodium orthovanadate (Na_3VO_4)	Sigma-Aldrich™
Soybean trypsin inhibitor	Sigma-Aldrich™
Strep-Tactin® Superflow 50%	IBA Life Sciences
Strep-tag® elution buffer (10x) with Desthiobiotin	IBA Life Sciences
SuperSignal® Stable Peroxide Solution	Thermo Scientific™
SuperSignal® Luminol/Enhancer Solution	Thermo Scientific™
Tetramethylethylenediamine (TEMED)	Sigma-Aldrich™
Thalidomide	Sigma-Aldrich™
Tosyl-L-lysyl-chloromethyl ketone hydrochloride (TLCK)	Sigma-Aldrich™
Tosyl-phenylalanyl-chloromethyl ketone (TPCK)	Sigma-Aldrich™
Trichloroacetic acid (TCA)	Sigma-Aldrich™
Tris(hydroxymethyl)aminomethane (TRIS)	Carl Roth GmbH
Tris buffered saline (TBS) (10X)	Sigma-Aldrich™
Triton™ X-100	Sigma-Aldrich™
Trypsin inhibitor from soybean	Sigma-Aldrich™
Tunicamycin	Sigma-Aldrich™
Tween 20	Sigma-Aldrich™
Tween 80	Sigma-Aldrich™
UltraPure™ TBE buffer (10x)	Thermo Scientific™

5.4 Cell culture media and supplements

β-Mercaptoethanol 50mM	Gibco® by Life Technologies™
ACK Lysing Buffer	Gibco® by Life Technologies™
Biocoll Separating Solution	Biochrom Merck Millipore
BIT9500 Serum Substitute	StemCell™ Technologies
Bovine Serum (BS)	Biochrom Merck Millipore
Dulbecco's Modified Eagle's Medium (DMEM)	Gibco® by Life Technologies™
Erythropoietin (EPO), human	Janssen-Cilag GmbH
Fetal Bovine Serum (FBS) Gold	Biochrom Merck Millipore
Flt-3 Ligand, human	R&D Systems™
HBSS (Hank's Balanced Salt Solution) 10X	Gibco® by Life Technologies™
HEPES Buffer Solution (1M)	Gibco® by Life Technologies™
Interleukin 3 (IL-3), murine	R&D Systems™
Interleukin 3 (IL-3), human	R&D Systems™
Interleukin 6 (IL-6), human	Sigma-Aldrich™
Iscove's Modified Dulbecco's Media (IMDM)	Gibco® by Life Technologies™

Kit Ligand, human	R&D Systems™
L-Glutamine 200mM (100X)	Biochrom Merck Millipore
Opti-MEM® I, reduced serum media	Invitrogen™
Phosphate buffered saline (PBS), 10X, sterile	Gibco® by Life Technologies™
Penicillin/ Streptomycin (100X)	Gibco® by Life Technologies™
RPMI 1640	Gibco® by Life Technologies™
Thrombopoietin (TPO), human	R&D Systems™
Trypan Blue Stain (0,4%)	Gibco® by Life Technologies™
Trypsin-EDTA (10X) solution	Biochrom Merck Millipore
Versalyse®	Beckman Coulter

5.5 Enzymes

AgeI	Thermo Scientific™
Antarctic Phosphatase	New England Biolabs®
BamHI	Thermo Scientific™
Benzonase® Nuclease	Sigma-Aldrich™
DNase I	Sigma-Aldrich™
EcoRI	Thermo Scientific™
NotI	Thermo Scientific™
Ribonuclease A	Sigma-Aldrich™
Pfu Ultra II DNA Polymerase	Agilent Technologies
PNGase F	New England Biolabs®
SalI	Thermo Scientific™
SuperScript III Reverse Transcriptase	Invitrogen™ by Thermo Scientific™
T4 DNA Ligase	Roche Diagnostics GmbH
XbaI	Thermo Scientific™
XhoI	Thermo Scientific™

5.6 Antibodies

5.6.1 Commercially available unconjugated primary antibodies

α-tubulin (#T6199)	mouse	Sigma-Aldrich™
α/β-tubulin (#2148)	rabbit	Cell Signaling Technology®
β-actin (#A-1978)	mouse	Sigma-Aldrich™
CD147 (8D6; #sc-21746)	mouse	Santa Cruz Biotechnology®
CD147 (H-200; #sc-13976)	rabbit	Santa Cruz Biotechnology®
CD79 (JCB-117; # M7050)	mouse	Dako by Agilent Technologies
Chk1 (#2360)	mouse	Cell Signaling Technology®
c-MYC (9E10; #sc-40)	mouse	Santa Cruz Biotechnology®
CUL1 (2H4C9; #32-2400)	mouse	Sigma-Aldrich™

CUL4A (#A300-739A)	rabbit	Bethyl Laboratories
CUL4B (#12916-1-AP)	rabbit	Proteintech™
Cyclin B1 (#4138)	rabbit	Cell Signaling Technology®
DDB1 (#A300-462A)	rabbit	Bethyl Laboratories
FLAG (#F7425)	rabbit	Sigma-Aldrich™
FLAG-M2 (#F3165)	mouse	Sigma-Aldrich™
HA (16B12; #MMS-101P)	mouse	Covance
HA (Y-11; #sc-805)	rabbit	Santa Cruz Biotechnology®
IgG control (#P120-101)	rabbit	Bethyl Laboratories
IKZF1 (#5443)	rabbit	Cell Signaling Technology®
IKZF3 (#12720)	rabbit	Cell Signaling Technology®
IRF4 (M-17; #sc-6059)	goat	Santa Cruz Biotechnology®
MCT1 (#AB-3538P)	rabbit	Merck Millipore
MCT1 (H-70; #sc-50324)	rabbit	Santa Cruz Biotechnology®
MMP7 (#ab4044)	rabbit	Abcam
murine CD147 (M-190; #sc-25531)	rabbit	Santa Cruz Biotechnology®
murine MCT1 (M-45; #sc-50325)	rabbit	Santa Cruz Biotechnology®
p21 (#OP64)	mouse	Merck Millipore

5.6.2 Customed primary antibodies

CRBN	rabbit	Innovagen
Immunogenic peptides: amino acids 1-19 and 424-437 of human CRBN: MAGEDQQDAAHNMGNHLPC; CPTIDPTEDEISPDK		
zebrafish CD147	rabbit	Innovagen
Immunogenic peptides: C-terminal peptide of zebrafish CD147 (Isoform3): CATNHKDKNVRQRNSN		

5.6.3 Conjugated secondary antibodies

anti-goat IgG, HRP-linked (#sc-2020)	Santa Cruz Biotechnology ®
anti-mouse IgG Alexa Fluor 488	Invitrogen™
anti-mouse IgG Alexa Fluor 594	Invitrogen™
anti-rabbit IgG Alexa Fluor 488	Invitrogen™
anti-rabbit IgG Alexa Fluor 594	Invitrogen™
ECL™ anti-mouse IgG, HRP-linked	GE Healthcare
ECL™ anti-protein-A, HRP-linked	GE Healthcare
ECL™ anti-rabbit IgG, HRP-linked	GE Healthcare
Streptavidin eFluor®450 (#48431782)	eBioscience

5.6.4 Conjugated primary antibodies

Annexin V- APC	BD Biosciences

CD3-PECy5 (clone UCHT1)	Beckman Coulter®
CD7-PE (clone 8H8.1)	Beckman Coulter®
CD14-PECy5 (clone RM052)	Beckman Coulter®
CD19-PECy7 (clone J4.119)	Beckman Coulter®
CD33-PC5.5 (clone D3HL60.251)	Beckmann Coulter®
CD33-PE (clone D3HL60.251)	Beckman Coulter®
CD34-FITC (#581/CD34)	BD Biosciences
CD34-PECy7 (clone 581)	Beckman Coulter®
CD34 microbeads	Miltenyi Biotec
CD36-APC Cy7 (clone 336213)	BioLegend
CD38-biotin (#130092288)	Miltenyi Biotec
CD38 microbeads	Miltenyi Biotec
CD45 PE Cy7 (clone HI30)	eBioscience
CD45-ECD (clone J33)	Beckman Coulter®
CD138-biotin (#130099162)	Miltenyi Biotec
CD147-FITC (clone HIM6)	BD Biosciences
CD147-PE (clone HIM6)	BD Biosciences
CD235α-biotin (clone HIR2)	eBioscience
CD235α -PE (clone 11E4B-7-6)	Beckman Coulter®
mouse IgG1k-PE (clone MOPC-21)	BD Biosciences

5.7 Kits

Calibration Kit MWGF200	Sigma-Aldrich™
DC™ Protein Assay	Bio-Rad Laboratories
GeneJET™ Gel Extraction Kit	Thermo Scientific™
GeneJET™ PCR Purification Kit	Thermo Scientific™
Human MMP7 ELISA Kit	Sigma-Aldrich™
Human VEGF ELISA Kit	Sigma-Aldrich™
LightCycler 480 SYBR Green I Master	Roche Diagnostics GmbH
peqGOLD Plasmid Miniprep Kit	Peqlab Life Science
QIAGEN Plasmid Maxi Kit	Qiagen
QIAshredder™ homogenizer Kit	Qiagen
QuikChange Site-Directed Mutagenesis Kit	Stratagene
Rapid DNA Dephos & Ligation Kit	Roche Diagnostics GmbH
RNeasy Mini Kit	Qiagen
SilverQuest™ Silver Staining Kit	Thermo Scientific™

5.8 Oligonucleotides

All oligonucleotides were purchased from Eurofins Genomics.
Morpholino oligomers were purchased from Gene Tools, LLC.

5.8.1 Cloning oligonucleotides

(Ko = Kozak sequence + ATG; St = incl. STOP-Codon; no_St = no STOP-Codon)

CRBN_BamHI_fw	5'-CCCGGATCCGCCGGCGAAGGAGATCAG-3'
CRBN_BamHI_fw_Ko	5'- CCCGGATCCGCCACCATGGCCGGCGAAGGAGATC-3'
CRBN_BamHI_rv_St	5'-CCCGGATCCTTACAAGCAAAGTATTAC-3'
CRBN_BamHI_rv_no_St	5'- CCCGGATCCCAAGCAAAGTATTACTTTG-3'
CRBN_NotI_rv_St	5'-CCCGCGGCCGCTTACAAGCAAAGTATTAC-3'
CRBN_NotI_rv_no_St	5'-CCCGCGGCCGCCAAGCAAAGTATTACTTTG-3'
CRBN_XhoI_fw	5'-CCCCTCGAGGCCGGCGAAGGAGATCAG-3'
CRBN_XhoI_fw_Ko	5'-CCCCTCGAGGCCACCATGGCCGGCGAAGGAGATC-3'
CRBN_XbaI_fw_Ko	5'-CCGTCTAGAGCCACCATGGCCGGCGAAGGAGATC-3'
CRBN_Y384A_fw	5'-CACAGCTGGTTTCCTGGGGCTGCCTGGACTGTTGCCCAG-3'
CRBN_Y384A_rv	5'-CTGGGCAACAGTCCAGGCAGCCCCAGGAAACCAGCTGTG-3'
CRBN_W386A_fw	5'-GGTTTCCTGGGTATGCCGCGACTGTTGCCCAGTGTAAG-3'
CRBN_W386A_rv	5'-CTTACACTGGGCAACAGTCGCGGCATACCCAGGAAACC-3'
CD147_BamHI_fw_Ko	5'-CCCGGATCCGCCACCATGGCGGCTGCGCTGTTCG-3'
CD147_230_BamHI_fw	5'-CCCGGATCCGAGAAGCGCCGGAAGCCCGAGGAC-3'
CD147_230_BamHI_fw_Ko	5'-CCCGGATCCGCCACCATGGAGAAGCGCCGGAAGCCCG-3'
CD147_BamHI_rv_St	5'-CCCGGATCCTCAGGAAGAGTTCCTCTGGCG-3'
CD147_269_EcoRI_rv_St	5'-CGGGAATTCCTAGGAAGAGTTCCTCTGGCGGACG-3'
CD147_269_XhoI_rv _St	5'-CGGCTCGAGCTAGGAAGAGTTCCTCTGGCGG-3'
CD147_XhoI_fw_Ko	5'-CCCCTCGAGGCCACCATGGCGGCTGCGCTGTTCG-3'
CD147_XbaI_fw_Ko	5'-CCCTCTAGAGCCACCATGGCGGCTGCGCTGTTC-3'
CUL4a_BamHI_fw_Ko	5'-CCCGGATCCGCCACCATGCTCTACAAGCAACTGC-3'
CUL4a_ XhoI_rv_St	5'-CCCCTCGAGTCAGGCCACGTAGTGGTACTG-3'
DDB1_KpnI_fw_Ko	5'-CCCGGTACCGCCACCATGTCGTACAACTACGTG-3'
DDB1_SalI_fw	5'-CCCGTCGACTTCGTACAACTACGTGGTAACGGCC-3'
DDB1_SalI_rv_St	5'-CCCGTCGACCTAATGGATCCGAGTTAGCTCCTC-3'
DDB1_XbaI_rv_St	5'-CCCTCTAGACTAATGGATCCGAGTTAGCTCCTC-3'
DsRed_BamHI_fw	5'-CCCGGATCCGCCACCATGGATAGCACTGAGAAC-3'
DsRed_BamHI_rv_St	5'-CCCGGATCCCTACTGGAACAGGTGGTGG-3'
DsRed_KpnI_rv_St	5'-CCCGGTACCCTACTGGAACAGGTGGTGG-3'
MCT1_BamHI_fw_Ko	5'-CCCGGATCCGCCACCATGCCACCAGCAGTTGGAGGTCC-3'
MCT1_BamHI_fw	5'-CCCGGATCCCCACCAGCAGTTGGAGGTCC-3'
MCT1_188_BamHI_fw	5'-CCCGGATCCTGCTGTGTTGCTGGAGCCCTC-3'
MCT1_444_BamHI_fw	5'-CCCGGATCCAATTATCGACTTTTGGCAAAAG-3'
MCT1_BamHI_rv_St	5'-CCCGGATCCTCAGACTGGACTTTCCTCCTCC-3'
MCT1_SalI_rv_St	5'-CGGGTCGACTCAGACTGGACTTTCCTCCTCC-3'
MCT1_XbaI_fw	5'-CCCTCTAGACCACCAGCAGTTGGAGGTCC-3'
MCT1_XbaI_ fw_Ko	5'-CCCTCTAGAGCCACCATGCCACCAGCAGTTGGAG-3'

MCT1_XhoI_fw_Ko	5'-CGCCTCGAGGCCACCATGCCACCAGCAGTTGGAGG-3'
MCT1_XhoI_ rv_St	5'-CGGCTCGAGTCAGACTGGACTTTCCTCCTCC-3'
MCT1_262_XhoI_rv_St	5'-CCCCTCGAGTCAGCCTCTGTGGGTGAATAGG-3'
zfCD147_BamHI_fw	5'-CCCGGATCCGCCACCATGGAAAAGAAGCTCTTTGG-3'
zfCD147_XhoI_rv	5'-CCCCTCGAGTCAGTTGGAGTTTCTTTGCC-3'

5.8.2 qPCR and semiquantitative RT-PCR primers

CRBN (human):	fw: 5'-ACAGCTGGTTTCCTGGGTATGC-3';
	rv: 5'-ACAGAGCAGATCGCGTTAAGCC-3'
MCT1 (human):	fw: 5'-TGGCTGTCATGTATGGTGGAGGTC-3';
	rv: 5'-GAAGCTGCAATCAAGCCACAGC-3'
CD147 (human):	fw: 5'-GATCACTGACTCTGAGGACAAGGC-3';
	rv: 5'-TGCGAGGAACTCACGAAGAACC-3'
ARPP (human):	fw: 5'-GCACTGGAAGTCCAACTACTTC-3';
	rv: 5'-TGAGGTCCTCCTTGGTGAACAC-3'
CD147 (zebrafish):	fw: 5'-AGGCCACTATTGGGTCAAGAATGGAAAGAAAATC-3' (ex 3);
(RT-PCR)	rv: 5'-CCGTTCTCCTGCATCAGGAAGCTTGAAC-3' (ex 5)
β-actin (zebrabfish):	fw: 5'-TGTTTTCCCCTCCATTGTTGG-3';
(RT-PCR)	rv: 5'-TTCTCCTTGATGTCACGGAC-3'
CD147 (zebrafish):	fw: 5'-ACAGACTCCTATGCTGAACACT-3' (ex 3);
	rv: 5'-CAATTGTGGCATTGGCCTGA-3' (ex 4)
RPL13A (zebrafish):	fw: 5'-ATTGTGGTGGTGAGGTGTGA-3';
	rv: 5'-CATTCTCTTGCGGAGGAAG-3'

5.8.3 shRNA sequences

CRBN:	(#1)	5´-CGCTGGCTGTATTCCTTATAT-3´
	(#2)	5´-CCAGAAACATCTACTTGGGTA-3' (Kronke et al., 2014)
CD147:		5´-GTACAAGATCACTGACTCTGA-3' (Le Floch et al., 2011)
MCT1:		5´-GCAGGGAAAGATAAGTCTAAA-3' (Birsoy et al., 2013)
IKZF1:		5´-CTACGAGAAGGAGAACGAAAT-3' (Lu et al., 2014)
IKZF3:		5´-GCCTGAAATCCCTTACAGCTA-3' (Lu et al., 2014)
CUL4A:		5'-GCAGAACTGATCGCAAAGCAT-3' (Lo et al., 2012)
CUL4B:		5'-GCCATGAAAGAAGCATTTGAA-3' (Lo et al., 2012)
Control/scramble:		5´-CCTAAGGTTAAGTCGCCCTCG -3'

5.8.4 zebrafish morpholinos

CD147 splice MO:	5'- aagaggtgaagaacatacAAGTGTT-3' (exonic sequence in upper case)
CD147 ATG MO:	5'-GCGCCAAAGAGCTTCTTTTCCATGC -3'

5.9 Plasmids

C-SF-TAP-pcDNA3.0	Prof. Dr. M.Ueffing (Gloeckner et al., 2007)
N-SF-TAP-pcDNA3.0	Prof. Dr. M.Ueffing (Gloeckner et al., 2007)
C-SF-TAP-pcDNA3.0 -CRBN	this study, cloned by R.Eichner
N-SF-TAP-pcDNA3.0 -CRBN	this study, cloned by R.Eichner
pCS2+	Dr. F. van Bebber
pCS2+ -zfCD147	this study, cloned by R.Eichner
pCS2+ -GFP-MCT1	this study, cloned by R.Eichner
pCS2+ -MCT1	this study, cloned by R.Eichner
pcDNA3.1(+) zeo	Thermo Scientific^{TM}
pcDNA3.1-CRBN	this study, cloned by R.Eichner
pcDNA3.1- CRBN$^{YW/AA}$	this study, cloned by Dr. V.Fernandez-Saiz
pcDNA3.1-CD147	this study, cloned by R.Eichner
pcDNA3.1-MCT1	this study, cloned by M.Heider
pcDNA3.1-FLAG	Prof. Dr. F. Bassermann
pcDNA3.1-HA	Prof. Dr. F. Bassermann
pcDNA3-C-FLAG-CD147	Prof. Dr. K. Kadomatsu
pcDNA3-C-HA-CD147	Prof. Dr. K. Kadomatsu
pcDNA3-N-FLAG-MCT1	this study, cloned by R.Eichner
pcDNA3-N-HA-MCT1	this study, cloned by R.Eichner
pcDNA3-HA-IKZF3	Prof. Dr. B. Ebert
pcDNA3-FLAG-IKZF3	this study, cloned by R.Eichner
pcDNA3-HA2-CUL4A	Addgene (#19907), Yue Xiong
pcDNA3-FLAG-DDB1	Addgene (#19918), Yue Xiong
pEGFP-C3	Clontech Laboratories
pEGFP-C3-MCT1	this study, cloned by R.Eichner
pGEX-4T2	GE Healthcare
pGEX-4T2_CRBN	this study, cloned by M.Heider
pGEX-4T2-mMCT1(AA 188-262)	this study, cloned by R.Eichner
pGEX-4T2-cMCT1(AA 444-500)	this study, cloned by R.Eichner
pGEX-4T2-cCD147(AA 230-269)	this study, cloned by R.Eichner
VSV-G	Addgene (#14888), Tannishtha Reya
GAG/POL	Addgene (#14887), Tannishtha Reya
pMIGR1	Addgene (#27490), Warren Pear
pMIGR1-MCT1	this study, cloned by R.Eichner
pMIGR1-N-FLAG-MCT1	this study, cloned by R.Eichner
pMIdsred	Dr. T. Brummer
pMIdsred-CD147	this study, cloned by R.Eichner
pMIdsred-C-FLAG-CD147	this study, cloned by R.Eichner
psPAX2	Addgene (#12260), Didier Trono

pMD2.G	Addgene (#12259), Didier Trono
pLKO.1 TRC cloning vector	Addgene (#10878), David Root
pLKO.1- Puro-sh_scramble	Addgene (#1864), David Sabatini
pLKO.1- dsred-sh_scramble	this study, cloned by M.Heider
pLKO.1- dsred-shMCT1	this study, cloned by M.Heider
pLKO.1- dsred-shCD147	this study, cloned by R.Eichner
pLKO.1- dsred-shCRBN-1	this study, cloned by R.Eichner
pLKO.1- dsred-shCRBN-2	this study, cloned by R.Eichner
pLKO.1- dsred-shIKZF1	this study, cloned by R.Eichner
pLKO.1- dsred-shIKZF3	this study, cloned by R.Eichner
pLKO.1- dsred-shCUL4A	this study, cloned by R.Eichner
pLKO.1- dsred-shCUL4B	this study, cloned by R.Eichner
pHIV-EGFP	Addgene (#21373), Bryan Welm
pHIV-EGFP-CRBN	this study, cloned by M.Heider
pHIV-EGFP-CRBN$^{YW/AA}$	this study, cloned by M.Heider
pHIV-EGFP-N-FLAG-MCT1	this study, cloned by R.Eichner
pHIV-EGFP-MCT1	this study, cloned by R.Eichner
pHIV-dsred	this study, cloned by M.Heider
pHIV-dsred-C-FLAG-CD147	this study, cloned by R.Eichner
pHIV-dsred-CD147	this study, cloned by R.Eichner

5.10 Standards for DNA and protein electrophoresis

GeneRuler 1kb DNA Ladder	Thermo Scientific™
PageRuler Plus Prestained Protein Ladder	Thermo Scientific™

5.11 Bacteria

BL21(DE3) Competent E. coli	New England Biolabs
NEB 5-alpha F´I_q Competent E. coli	New England Biolabs

5.12 Cell lines

AMO1	human MM cell line	DSMZ (ACC-538)
Ba/F3	murine pro-B cell line	DSMZ (ACC-300)
HEK293T	human embryonic kidney cell line	ATCC (CRL-3216)
HEK293FT CRBN$^{-/-}$	CRBN knock-out HEK293FT	kind gift of Prof. WG Kaelin
HeLa	human cervix carcinoma cell line	ATCC (CCL-2)
INA6	human MM cell line	kind gift of Prof. U Keller
JJN3	human MM cell line	DSMZ (ACC-541)
KG-1	human del(5q)MDS cell line	DSMZ (ACC-14)

KMS-12-BM	human MM cell line	DSMZ (ACC-551)
L363	human MM cell line	DSMZ (ACC-49)
MDSL	human del(5q)MDS cell line	kind gift of Prof. K. Tohyama
MM1.S	human MM cell line	ATCC (CRL-2974)
MM1.S CRBN$^{-/-}$	CRBN knock-out MM1.S	kind gift of Prof. WG Kaelin
RPMI 8226	human MM cell line	DSMZ (ACC-402)
SKK-1	human non-del(5q) MDS cell line	kind gift of Prof. M. Buschbeck
SKM-1	human non-del(5q) MDS cell line	kind gift of Prof. M. Buschbeck
U266	human MM cell line	DSMZ (ACC-9)
X63AG8.653	murine MM cell line	DSMZ (ACC-43)

5.13 Mice

NOD/SCID (NOD.CB17/AlhnRj-*Prkdc*^{scid}/Rj)	Janvier Labs

5.14 Patient samples

Fresh bone marrow samples from muliple myeloma patients (with IMiD senstive or refractory disease) as well as from non-del(5q) and del(5q) MDS patients (with or without IMiD treatment) were obtained with informed consent and in compliance with the institutional review board at the Faculty of Medicine of the Technical University of Munich. The samples were aquired at our site (Klinikum rechts der Isar) as well as from collaborators in other german centers. As such, additional MDS samples were received from Prof. Dr. U. Platzbecker (Technical University Dresden) as well as Prof. Dr. U. Germing (Heinrich Heine University Düsseldorf), and MM samples from PD Dr. C. Langer (University of Ulm), Prof. Dr. S. Knop and Prof. Dr. H. Einsele (both University of Würzburg).

5.15 Solutions and buffers

All listed buffers were prepared with aqua dest., unless specified otherwise.

Annexin/PI buffer:	1 M HEPES 2.5 M NaCl 1.62 mM $CaCl_2$
Binding Buffer (*in-vitro* binding):	PBS (1×) 0.1% NP-40 0.5 mM DTT 10% glycerol + protease inhibitors
Blocking Buffer (Western Blot):	PBS (1×) 0.1% Tween 20 5% skim milk powder

Coomassie Destain (1×):	45% methanol 10% acetic acid
Coomassie Staining (1×):	45% methanol 10% acetic acid 0.25% Coomassie brilliant blue
E3 (zebrafish medium)	5 mM NaCl 0.17 mM KCl 0.33 mM $CaCl_2$ 0.33 mM $MgSO_4$
Freezing medium:	FBS 10% DMSO
FACS-Buffer (1×):	PBS (1×) 2% FBS
HF2+ Buffer (1×):	HBSS (1×) 5% heat-inactivated FBS 1% Pen/Strep 1mM HEPES 10 µM β-mercaptoethanol
IF-Buffer (1×):	PBS (1×) 0.5% Tween 20
Inhibitors (final concentrations):	1 µg/ml aprotinin 1 mM DTT 10 mM G2P 1 µg/ml leupeptin 0.1 mM PMSF 0.1 mM Na_3VO_4 10 µg/ml soybean trypsin inhibitor 5 µg/ml TLCK 10 µg/ml TPCK
Laemmli Buffer (5×):	300 mM Tris (pH 6.8) 50% glycerol 10% SDS

	5% β-mercaptoethanol 0.05% bromphenolblue
Luria-Bertani (LB) medium (1×):	1% Bacto Tryptone 0.5% Bacto Yeast Extract 170 mM NaCl
Luria-Bertani (LB)-agar plates:	LB medium 1.5% Bacto Agar
Lysis Buffer (1×):	50 mM Tris (pH 7.5) 150 mM NaCl 0.1% NP40 1 mM EDTA 5 mM $MgCl_2$ 5% Glycerol + protease inhibitors
250 mM lysis buffer (1×):	50 mM Tris (pH 7.5) 250 mM NaCl 0.1% Triton X-100 1 mM EDTA 50 mM NaF + protease inhibitors
NETN Buffer (1×) :	20 mM Tris (pH 8,0) 100 mM NaCl 1 mM EDTA 0.5% NP40 1 mM PMSF + protease inhibitors
SDS-PAGE Seperating Gel Buffer (1×):	1.5 M Tris (pH 8.8)
SDS-PAGE Stacking Gel Buffer (1×):	0.5 M Tris (pH 6.8)
SDS Running Buffer (10×):	250 mM Tris (pH 7.5) 1.92 M glycine 1% SDS

SDS Transfer Buffer (1×):	48 mM Tris (pH 7.5) 39 mM glycine 20% methanol
Stripping Buffer (Western Blot):	62.5 mM Tris (pH 6.8) 0.867% β-Mercaptoethanol 2% SDS
Washing Buffer (Western Blot):	PBS (1×) 0.1% Tween 20

5.16 Software and database tools

BLAST Basic local alignment search tool	NCBI
CellQuest™ Pro (flow cytometry software)	BD Biosciences
Excel (data analysis software)	Microsoft Office
FlowJo (flow cytometry analysis software)	Tree Star
Image J (image analysis software)	open source
Kaluza® Flow Analysis Software	Beckman Coulter®
MacVector (sequence analysis software)	MacVector
Mascot Distiller v2.2.1	Matrix Science, UK
Primer-BLAST	NCBI
Prism (data analysis software)	Graph Pad Software
QuantPrime	Max-Planck Institute for plant physiology
Unicorn software	GE Healthcare

6 Methods

6.1 Molecular biology techniques

6.1.1 Polymerase chain reaction (PCR)

The polymerase chain reaction (PCR) allows for *in-vitro* amplification of specific DNA sequences, based on repeated cycles of DNA-denaturation, annealing of specific primers and elongation by a thermoresistant DNA polymerase (Mullis and Faloona, 1987).

The reaction mix for standard PCRs contained 100 ng of template DNA, 10 pmol each of forward (fw) and reverse (rv) primers, 1 µl dNTPs (10mM each), 1 µl Pfu Ultra II DNA Polymerase and 5µl of the according 10× reaction buffer in a final volume of 50 µl. The temperature for denaturation was 95°C, annealing temperatures varied between 55-65°C depending on the melting temperature of the primers, and elongation was carried out at 72°C for 1-2 min depending on the length of the sequence.

6.1.2 Agarose gel electrophoresis and gel purification

In an agarose gel, DNA can be separated in the electric field according to its size and visualised by addition of a fluorescent DNA-intercalating agent as ethidium bromide (EtBr).

For 1% agarose gels, as used in this study, agarose was dissolved in the appropriate volume of electrophoresis buffer (1× TBE), boiled, supplemented with EtBr and cooled down in a gel chamber. DNA samples mixed with 6× DNA loading dye were loaded together with a marker (DNA ladder) prior to electrophoresis. EtBr stained DNA visualized under UV-light. For cloning purposes, digested DNA fragments were cut out with a scalpel under UV light and purified using the GeneJet Gel Extraction Kit (Thermo Scientific) according to the manufacturer's instructions.

6.1.3 Molecular cloning

Molecular cloning, a method to generate and amplify recombinant DNA plasmids, comprises insertion of specific DNA sequences (called inserts) generated e.g. by PCR into a vector (e.g. a plasmid) using restriction enzymes and DNA ligases, and subsequent transformation of the plasmid into bacteria, from where the amplified product can be isolated.

6.1.3.1 Digestion of DNA with restriction enzymes

Restriction enzymes recognize and cleave DNA at defined palindromic sequences, resulting in sticky- or blunt-end DNA fragments. All restriction enzymes used in this study produced single-stranded DNA overhangs (sticky ends) facilitating annealing and ligation.

For cloning or analytical purposes, 0,5- 3 µg DNA (plasmids and/or inserts) were digested using 0,5-1 µl of restriction enzyme in the respective buffer for 1-2 hrs at 37°C. Buffers for double digests were chosen according to the manufacturer's instructions.

6.1.3.2 DNA dephosphorylation and ligation

DNA phosphatases cleave off the 5' terminal phosphate from nucleic acids, preventing re-ligation of cleaved DNA. In this study, this step was only performed in case of single-cut plasmids or use of enzymes with compatible ends. DNA ligases catalyze formation of phosphodiester bonds, thus ligating two DNA strands (e.g. plasmid and insert) together.

DNA dephosphorylation and ligation was done using the Rapid DNA Dephos & Ligation Kit (Roche; containing rAPid Alkaline Phosphatase and T4 DNA Ligase), according to the manufacturers instructions. For ligation, insert and plasmid were mixed at molar ratio of at least 3:1, with 50-100 ng of the restricted vector and an overall amount of DNA not exceeding 200 ng. For ligation, the DNA was mixed with the according buffers and the T4 ligase in a total volume of 20 µl for 5 min at RT.

6.1.3.3 Transformation of competent bacteria

Transformation denominates the process of plasmid incorporation into bacteria, which subsequently amplify plasmids independent of their genomic DNA. For efficient transformation, bacteria need to be in a state of competence, which can experimentally be reached by e.g. specific chemical treatment increasing membrane permeability.

In this study, chemically competent NEB® 5-alpha Competent E. coli (New England Biolabs) were used for transformations. 2 µl of the respective ligation mix (see chapter 6.1.3.2) or, in case of re-transformations, 10-100 ng of plasmid DNA, were added to 30 µl of competent bacteria and incubated on ice for 30 min. Heat shock at 42°C for 45 sec, necessary for plasmid uptake, was followed by a 2 min incubation on ice. Subsequently, SOC medium was added and the bacteria were allowed to recover at 37°C for 30-60 min before plating on LB agar plates and incubating at 37°C over night. To allow growth of transformed bacteria only, LB plates contained antibiotics according to the resistance gene encoded in the plasmid. Next, single clones were picked and inoculated in LB medium with antibiotics for growth at 37°C and 200 rpm.

Transformation of BL21(DE3) Competent E. coli (New England Biolabs) for expression of recombinant proteins was performed in the same way.

6.1.3.4 Isolation of DNA from bacteria

Amplified plasmid DNA from bacteria was purified using commercially available plasmid purification kits. Depending on the amount of bacterial culture, either the peqGOLD Plasmid Miniprep Kit (Peqlab Life Science) or the QIAGEN Plasmid Maxi Kit (Qiagen) was used according to the manufacturer's instructions.

After cloning, test digests using suitable restrictions enzymes were performed and positive clones were sent for sequencing. For long-term storage of positive clones, an aliquot of the bacterial culture was mixed 1:1 with glycerol and frozen at -80°C.

6.1.4 Mutagenesis PCR

Site directed mutagenesis is a PCR-based method to induce specific mutations, such as point mutations, deletions or insertions, in double-stranded plasmid DNA.

In this study, specific mutations were introduced to cDNA using the QuikChange Site-Directed Mutagenesis Kit (Stratagene) according to the manufacturer's instructions. Two complementary mutation primers of 35-40 bp length were designed to carry the desired mutated base pair(s) in the middle and be flanked by sequences compatible to the cDNA sequence on both sides of the mutation. These primers and the original cDNA plasmid were subject to a PCR reaction (see chapter 6.1.1), resulting in an amplified plasmid carrying the desired mutation. Before transformation in competent bacteria (see chapter 6.1.3.3), the template plasmid was removed from the sample by incubation with DpnI, an enzyme cleaving methylated DNA. Positive clones were assed by sequencing of purified plasmids.

6.1.5 RNA extraction from eukarotic cells

For analysis of gene expression on the transcriptional level, mRNA needs to be extracted, a process which needs to be performed on ice and using RNase-free solutions because of the omnipresence of RNases.

In this study, total RNA from MM cell lines was extracted using the RNeasy Mini Kit (Qiagen), which depends on reversible binding of RNA to silica-membrane spin columns, according to the manufacturer's instructions. Isolation of total RNA from zebrafish larvae was performed using a two-step protocol: the tissue lysate was first homogenized using the QIAshredder, before RNA was extracted with help of the RNeasy Mini Kit as stated above. RNA concentration in the final eluates was measured spectrophotometrically.

6.1.6 Reverse transcription (RT) and RT-PCR

Reverse transcriptases are enzymes of viral origin, synthesizing complementary DNA (cDNA) based on an RNA template in a process called reverse transcription (RT). Resulting cDNA is the basis of different gene expression analyses such as quantitative PCR.

To obtain cDNA, 1 µg of extracted RNA (see chapter 6.1.5) was reversed transcribed using oligo-dT primers, which allow specific transcription of mRNA via annealing to polyA-tails, dNTPs and the SuperScript III Reverse Transcriptase according to the manufacturer's protocol: after primer annealing at 42°C for 5 min, cDNA was synthesized at 72°C for 60 min.

Semiquantitative RT-PCRs were performed to detect differentially spliced mRNAs of zebrafish *CD147* (*zfCD147)*. With the CD147 splice morpholino (spliceMO) targeting the border of exon 3 to intron 3 of *zfCD147*, thus inhibing access of the splicing machinery, PCRs with a fw primer in exon 3 and a rv primer in exon 5, amplify either a short spliced or a much longer unspliced sequence. RT-PCRs were performed using the primers denoted in chapter 5.8.4, and cDNA from spliceMO-treated or control zebrafish following the standard PCR protocol (see

chapter 6.1.1), with only 25 cycles to prevent saturation. As reference, PCRs were performed on the same cDNA using primers for *β-actin* before equal percentages of each PCR reaction were subjected to gel electrophoresis and visualized under UV-light.

6.1.7 Quantitative PCR

Quantitative PCR (qPCR), or real-time qPCR, is a PCR-based method using flurochromes to monitor the amount of amplified DNA in real-time after each PCR cycle. SYBR Green is a common qPCR dye, unspecifically binding double-stranded DNA to form a DNA-SYBR Green complex absorbing blue and emitting green light. Fluorescence intensity thus correlates with the amount of DNA, allowing quantification of gene expression in relation to reference genes.

In this study, qPCR was performed on a LightCycler 480 instrument using the LightCycler 480 SYBR Green I Master (both Roche), according to the manufacturer's instructions, with reverse transcribed cDNA from MM cell lines or zebrafish larvae (see chapter 6.1.6) as template. Specific qPCR primers were designed with the help of the QuantPrime software (Arvidsson et al., 2008) or the primer-BLAST platform (http://www.ncbi.nlm.nih.gov/tools/primer-blast/) to amplify short sequences (around 100 bp) of *CD147*, *MCT1*, *CRBN* or *ARPP* (acidic ribosomal phosphoprotein P0), which was used as reference. For qPCR of spliced *zfCD147*, respective primers in exon 3 and exon 4 were designed using the same tools, and *RPL13A* (ribosomal protein L13a) was used as reference. Primer sequences are listed in chapter 5.8.2.

6.2 Cell culture and cell-based assays

6.2.1 Culture of suspension and adherent cell lines

All cell lines and primary cells used in this study were cultured in a humidified incubator with 5% CO_2 at 37°C. The adherent cell lines HEK293T, CRBN$^{-/-}$ HEK293FT and HeLa were grown in Dulbecco's modified Eagle's medium (DMEM) with GlutaMAX (containing L-alanyl-L-glutamine, a stabilized form of L-glutamine), supplemented with 1% penicillin-streptomycin (P/S) and 10% bovine serum (BS) for HEK293T or 10% fetal bovine serum (FBS) for HeLa. The human MM cell lines MM1.S, MM1.S CRBN$^{-/-}$, U266, KMS 12BM, RPMI 8226, JJN3, L363, AMO1 and INA-6, the murine MM cell line X63AG8.653, the murine pro-B cell line Ba/F3 as well as the human del(5q)MDS/AML cell lines MDSL and KG-1 and the non-del(5q) AML/MDS lines SKK-1 and SKM-1 were cultured in RPMI-1640 with GlutaMAX, 10% heat-inactivated FBS and 1% P/S. Medium for INA-6 cells was supplemented with 2 ng/ml human IL-6; medium for Ba/F3 cells with 2 ng/ml murine IL-3 and medium for MDSL cells with 50 µM β-mercaptoethanol, 2 mM L-glutamine, 10 mM HEPES and 10 ng/ml IL-3.

Suspension cells were seeded at a density of 1×10^5 cells/ml in cell culture flasks and splitted every 2-3 days at a ratio of 1:5 – 1:10 depending on cell growth. Adherent cells lines were grown in tissue culture dishes and splitted at densities of 80–90% at a ratio of 1:2 – 1:5. For

passaging, cells were washed in PBS, incubated with trypsin for 5 min at 37°C, resuspended, centrifuged and plated in fresh growth medium.

The trypan blue exclusion method was used to determine cell count and viability. After staining of cells in a 1:1 mix with trypan blue, a dye only penetrating and thus coloring dead cells, viable cells were counted using a Neubauer hemocytometer.

6.2.2 Freezing and thawing of cells

Cells can be cryoconserved using a cryoprotectant such as DMSO (dimethyl sulfoxide), which enters the cell to prevent crystallization, damage and cell lysis. For long-term storage, exponentially growing cells were pelleted, resuspended at a concentration of $1–10\times10^6$ cells/ml in FBS with 10% DMSO (freezing medium) and aliquoted in cryotubes. To avoid damage to the cell membrane by rapid freezing, the cryotubes were transferred to the -80°C freezer in a freezing container with isopropanol assuring a cooling rate of 1°C/min. After at least 24 h at -80°C, the cells were transferred to liquid nitrogen for long-term storage.

While unfreezing, it is important to rapidly wash out DMSO, which can be toxic at prolonged exposures. Accordingly, cells were rapidly thawed at 37°C, diluted in the respective growth medium, centrifuged and plated in fresh growth medium.

6.2.3 Treatment with drugs and inhibitors

6.2.3.1 IMiD treatment

Thalidomide, lenalidomide and pomalidomide, the three established IMiDs, were dissolved in DMSO, aliquoted and stored at -20°C; new solutions were prepared every 3 months.

For IMiD treatment, suspension cell lines were generally seeded at 1×10^5 cells/ml and incubated with thalidomide, lenalidomide or pomalidomide or vehicle (DMSO) at different concentrations for 6–144 hrs depending on the experimental setting. For incubation times longer than 72 hrs, cells were splitted every 2-3 days (depending on the cell line) and placed in fresh medium supplemented with fresh inhibitors.

To assess viability and proliferation under IMiD treatment, viable cells were counted at different time points using the trypan blue exclusion method and set in relation to control cells.

6.2.3.2 Inhibition of protein translation

Cycloheximide (CHX), a compound inhibiting protein biosynthesis via interference with translational elongation, was dissolved in 100% ethanol at a concentration of 100 mg/ml and freshly prepared before an experiment.

For time courses studying the binding of CRBN to MCT1 and CD147 depending on the maturity of proteins, CHX was added to cells at a final concentration of 100 µg/ml for up to 6 hrs, and aliquots were harvested at defined time points.

6.2.3.3 Inhibition of Cullin-RING ligase function

Cullin, the scaffold protein of Cullin-RING E3 ubiquitin ligases (CRLs), needs to be conjugated with NEDD8, a ubiquitin-like molecule, for proper ligase function. MLN4924, an inhibitor of the NEDD8 activating enzyme, thus allows functional inhibition of all CRLs.

To test the CRL-dependence of maturation or IMiD-induced destabilization of CD147, MLN4924 was added to the cells at a final concentration of 10 µM for 24 hrs. MLN4924 was dissolved in DMSO, aliquoted and stored at -20°C.

6.2.3.4 Protein crosslinking

Protein crosslinkers, covalently linking closely interacting proteins, are useful tools for analysis of low affinity protein interactions. DSS (disuccinimidyl suberate) is a membrane-permeable protein crosslinker with amine-reactive ester groups, crosslinking amines to amines. It can be applied to living cells to crosslink proteins *in-vivo.*

For immunoprecipitations of crosslinked proteins, DSS was dissolved in DMSO and added to the cells at a final concentration of 1 mM. After 45 min incubation at RT, the reaction was quenched by addition of 20 mM Tris-HCl (pH 7.5). Subsequent cell lysis was performed according to the standard protocol (see chapter 6.3.1), with 50 mM HEPES (pH 7.5) instead of Tris-HCl in the lysis buffer.

6.2.4 Isolation and culture of primary patient cells

Leftover material from diagnostic bone marrow (BM) aspirations from MM and MDS patients was collected with informed consent and in compliance with the institutional review board at the Faculty of Medicine of TUM. Collected samples were analysed by flow cytometry or sorted for plasma or progenitor cells depending on the disease and the experiments.

6.2.4.1 Patient-derived primary MM cells

Primary MM cells were purified from BM samples of MM patients (at first diagnosis, with refractory disease or at relapse) using magnetic bead selection for $CD138^+$ cells according to the manufacturer's instructions.

Briefly, heparin-BM samples were diluted 1:1 with HF2+ buffer (see chapter 5.15) and carefully layered on 10 ml Biocoll Separating Solution, allowing separation of cellular and liquid components of blood or BM according to their denisity. After centrifugation (without brakes) at 2100 rpm for 15 min, mononuclear cells were collected from the interphase of plasma and Biocoll layers. The cells were washed, counted and resuspended in 80 µl HF2+ buffer per 2×10^7 cells, before 20 µl magnetic CD138 microbeads per 2×10^7 cells were added. After 30 min incubation at 4°C, stained cells were washed, resuspended in 500 µl HF2+ buffer and pipetted onto an equilibrated LS MACS column placed into a MACS separator. After washing three times to remove unlabelled cells, the column was detached from the separator and retained $CD138^+$ cells were flushed out with 5 ml buffer using a plunger. The isolated MM cells were taken into culture

at 1×10^5 cells/ml in IMDM GlutaMAX with 20% heat-inactivated FBS and 1% P/S, followed by a 4 day incubation with 10 µM lenalidomide or vehicle (DMSO).

6.2.4.2 Patient-derived hematopoietic stem cells

In order to analyze the effects of lenalidomide on erythropoiesis in del(5q) MDS, $CD34^+$ hematopoietic precursor cells were isolated from del(5q) MDS patients and stimulated to undergo erythropoietic differentiation *in-vitro* following a published protocol (Tehranchi et al., 2003).

Mononuclear cells were isolated from BM aspirates from del(5q) MDS patients as described above (see chapter 6.2.4.1). Subsequently, $CD34^+$ cells were purified using CD34 microbeads according to the manufacturer's instructions and in analogy to the procedure described for CD138 microbeads (see chapter 6.2.4.1). Purified precursor cells were seeded in 2 ml serum free medium (SFM) containing 80% IMDM GlutaMAX, 20 % BIT9500 Serum Substitute and the following human cytokines: 100 ng/ml Kit-Ligand (KL), 100 ng/ml Flt-3-Ligand (FL), 25 ng/ml TPO, 10 ng/ml IL-3 and 10 ng/ml IL-6. Additionally, 10 µM of lenalidomide or vehicle (DMSO) was added to the cells. On day 7, erythropoietin was added to the cultures at a final concentration of 2 IU/ml to stimulate erythropoiesis. Every third day, half of the volume was replaced with fresh medium, cytokines and inhibitors. On day 14,vcells were harvested for flow cytometric analysis.

6.2.5 Transfection of eukaryotic cells

Transfection, the introduction of DNA (e.g. plasmids) or RNA (e.g. siRNA) into eukaryotic cells, requires formation of complexes, which are endocytosed by the cell, induction of transient membrane pores allowing entry of nucleic acids, or packing of the DNA or RNA in liposomes, which fuse with the plasma membrane.

In this study, transfection of HEK293T cells was performed using the calcium phosphate method, while HeLa cells were transfected using Lipofectamine, a cationic lipid. Viurs-mediated transfer of nucleic acids is called transduction and is described in chapter 6.2.6.

6.2.5.1 Calcium phosphate method

The calcium phosphate method, a classical method for chemical transfection (Graham and van der Eb, 1973), is based on the formation of small DNA-binding complexes of positively charged calcium and negatively charged phosphate, which are incorporated after adhesion to the cell surface.

For transfection of a standard 10 cm tissue culture dish of HEK293T cells (at 60-70% confluency), 10-15 µg of plasmid DNA was diluted in dH_2O to a final volume of 450 µl, before 50 µl $CaCl_2$ were added to a final concentration of 250 mM. After 5 min incubation at RT, allowing binding of Ca^{2+} ions to negatively charged DNA, 500 µl BES [N,N-Bis-(2-hydroxyethyl)-2-aminoethansulfonic acid) buffered in NaCl and Na2HPO$_4$ to pH 7.1] were added carefully drop by drop while constantly turning the tube. After formation of precipitates during 20 min incubation at

RT, the complexes were dropped on the cells, were they adhere to the plasma membrane to be endocytosed. The medium was exchanged after 4 hrs of incubation at 37°C to re-establish a physiological pH. Cells were harvested 24-36 hrs after transfection, depending on the experiment. For optimal results, $CaCl_2$ and BES were prepared in advance and stored at -20°C.

6.2.5.2 Lipofectamine

Lipofection describes the liposome-mediated transfer of DNA or RNA (Felgner et al., 1987). Lipofectamine, a common lipofection reagent, contains cationic lipids binding to negatively charged nucleic acids to form DNA-containing liposomes, together with neutral helper lipids. The positive surface charges allow binding and fusion with the negatively charged plasma membrane.

In this study, HeLa cells were transfected with Lipofectamine 2000 according to the manufacturer's instructions. Briefly, cells were transfected at a confluency of 60-70% in P/S-free medium. DNA and Lipofectamine were diliuted independently in serum-free Opti-MEM, incubated for 5 min, mixed and incubated for another 20 min at RT before addition to the cells. To avoid toxicity, the medium was changed after 3 hrs.

6.2.6 Viral transduction of cells

Viral transduction is method to transfer nucleic acids to eukaryotic cells using modified viral vectors. Besides offering high efficiency rates even in hardly transfectable cells, retro- or lentiviral systems allow stable expression via integration of transduced DNA into the genome. Synthesis of viral particles is carried out in eukaryotic cells expressing all necessary viral genes. To prevent self-replicating viruses, the information for assembly of a functional virion is not encoded on one viral plasmid. Instead, packaging enzymes and envelope glycoproteins are coded on independent plasmids which need to be co-transfected, or stably expressed in transgenic "packaging"-cell lines. In this study, retro- and lentiviral particles were produced in HEK293T cells transfected with three independent viral plasmids.

6.2.6.1 Production of viral particles

Retroviral vectors based on the MiGR1 (MSCV-IRES-GFP) construct were combined with the packaging plasmid pcDNA MLV GAG/POL (coding for Gag and Pol) and the envelope plasmid VSV-G (coding for VSV-G), while lentiviral vectors based on the pLKO.1 plasmid or the pHIV-EGFP plasmid were combined with psPAX (coding for Gag_HIV) as lentiviral packaging plasmid and pMD2.G (coding for VSV-G) as envelope plasmid. For virus production, a 10 cm plate of HEK293T cells was transfected at 60-70% confluency with 20 µg of the respective viral plasmid, 15 µg of the packaging plasmid and 5 µg of the envelope plasmid using the calcium phosphate method (see chapter 6.2.5.1). After 4 hrs of incubation, the medium was changed to DMEM with 10% FBS and P/S. At 24 hrs, the supernatant was collected and replaced by 10 ml of target cell growth medium. At 48 hrs, the viral supernatant was collected, passed through a 0.45 µm filter and used for spin infection right away or stored at 4°C up to 1 week.

6.2.6.2 Retro- and lentiviral transduction of cells

For infection of non-adherent cells such as MM and MDS cell lines, 1×10^6 cells were plated in 1 ml of growth medium per well of a 6-well plate. 2 ml of viral supernatant was added and polybrene was supplemented to a final concentration of 8 µg/ml. Polybrene, a commercial name for hexadimethrine bromide, is a cationic polymer facilitating interaction of virions and the cell surface (Davis et al., 2002). To increase efficiency, the cells were subjected to spin-infection at 1000 rpm for 30 min at 32°C and subsequently incubated with the viral supernatant for 24 hrs before plating in fresh medium. Cells with low transduction rates were subjected to a second spin-infection with fresh viral supernatants. Adherent cells like HeLa were plated one day prior to spin infection to achieve a conflency of 50-60% at the day of infection. Transduction efficiency was evaluated 3 days after infection using flow cytometry (see the following chapter 6.2.7).

6.2.7 Flow cytometry

Flow cytometry, a laser-based technique for characterization of cells at single-cell resolution, is broadly used for analysis and cell sorting. In a stream of fluid, single cells pass lasers and detectors, measuring fluorescent signals from e.g. fluorochrome-coupled antibodies or expressed flurochromes, and physical properties such as size and granularity of single cells.

6.2.7.1 Flow cytometry of cell lines

For flow cytometric analysis of CD147 cell surface expression, MM1.S cells treated with 10 µM lenalidomide or DMSO for 72 hrs, or MM1.S wildtype as well as MM1.S $CRBN^{-/-}$ cells, were washed in FACS buffer (see chapter 5.15) and incubated on ice with an anti-CD147 antibody (clone 8D6) or IgG2a control isotype antibody at final concentrations of 10 µg/ml for 30 min. After washing twice, an Alexa Fluor 594 conjugated secondary antibody was added for 30 min at a dilution of 1:1000 in FACS buffer. After washing, cells were analyzed on a FACSCalibur.

Resulting data was analyzed with FlowJo software. CD147 expression in the viable cell population (as gated in the FSC vs. SSC gate to exclude debris and cell doublets) was compared by histogram analysis. Median fluorescence intensity (MFI) of CD147 relative to its matched isotype-control was calculated for each sample.

6.2.7.2 Fluorescence activated cell sorting

FACS (fluorescene activated cell sorting) describes the sorting of cells based on their flow cytometric properties and fluorescent markers.

In this study, FACS was used in case of insufficient transduction rates to purify infected cells (expressing DsRed-Express2 or eGFP as fluorochromes) in order to work with a homogenous cell population. The cut-off for sorting was a transduction rate of 70-80%.

FACS was performed on a FACSAria cell sorter in the Flow Cytometry Unit in the Department of Microbiology, Klinikum recht der Isar. For sorting, the cells were washed, resuspended in FACS buffer at a concentration of $1–10\times10^6$ cells/ml, filtered and stored on ice until sorting; sorted cells were recovered in FBS and taken into culture in normal growth medium.

6.2.7.3 Flow cytometry of patient-derived MDS bone marrow samples

Flow cytometric analyses of bone marrow (BM) from MDS patients were performed in the routine hematology lab of the III. Medical Department, Klinikum recht der Isar, where a FITC-tagged antibody for CD147 was added to the routine MDS antibody panel.

Fresh BM samples from patients with non-del(5q)MDS, del(5q)MDS or del(5q)MDS under lenalidomide treatement were collected in heparin and treated with VersaLyse Lysing Solution according to the manufacturer's instructions to lyse erythrozytes. Subsequently, cells were stained with the follwoing anti-human monoclonal fluorochrome-conjugated antibodies: CD45-ECD (clone J33), CD33-PE (clone D3HL60.251), CD14-PECy5 (clone RM052), CD7-PE (clone 8H8.1), CD3-PECy5 (clone UCHT1), CD19-PECy7 (clone J4.119), CD7-PE, CD235α -PE (clone 11E4B-7-6), CD34-PECy7 (clone 581) and CD147-FITC (clone HIM6) following the manufacturer's instructions and the standard protocols of the routine laboratory. After staining and washing, BM samples were analyzed on a Cytomics FC 500.

Obtained data was analyzed using the Kaluza Flow Analysis Software. Monocytes, lymphocytes, granulocytes, progenitor cells and $CD45^{low}/CD235\alpha^{+}$ cells were identified using a CD45 vs. SSC gating strategy. Within the lymphocyte gate, gates were placed on $CD19^{+}$ B-cells, $CD3^{+}$ T-cells and $CD3^{-}CD7^{+}$ NK cells. Further gates were placed on $CD33^{+}$ granulocytes, $CD14^{+}$ monocytes, $CD45^{low}CD33^{+}CD34^{+}$ progenitor cells and $CD45^{low}/CD235\alpha^{+}$ erythropoiesis. CD147 expression within the $CD45^{low}/CD235\alpha^{+}$ erythropoietic population was determined by histogram analysis and median fluorescence intensity (MFI) of CD147 relative to isotype-matched control was calculated for each patient.

6.2.7.4 Flow cytometry of patient-derived myeloma cells

Isolation and culture of patient-derived primary MM cells is described in chapter 6.2.4.1. After 4 days of culture in presence of 10 µM lenalidomide or vehicle (DMSO), cells were collected and washed in HF2+ buffer (for buffers see chapter 5.15). After resuspension in 100 µl Annexin/PI buffer, the cells were incubated with CD138-biotin and CD38-biotin antibodies at a 1:10 dilution for 10 min at 4°C according to the manufacturer's instructions. After washing, 2 µl Streptavidin-eFlour450 and 2,5 µl CD147-PE (clone HIM6) or 10 µl of isotype control mIgG1k-PE antibody were added to a final volume of 100 µl in Annexin/PI buffer for 20 min. For detection of apoptosis and necrosis, 2 µl APC-conjugated annexin V and 1 µl propidium iodide (PI) was added to each sample. Annexin V binds to phosphatidylserin, a phospholipid localized on the cytosolic side of the plasma membrane, which only flips to the cell surface during apoptosis, while PI is a membrane-impermeable, fluorescent DNA-intercalating agent only reaching and staining DNA in dead cells. Stained cells were analyzed on a CyAn ADP LxP8 cytometer.

Data was analyzed using FlowJo software. After gating on the main cell population in the initial FSC vs. SSC gate (excluding debris and cell doublets), the gate was set on $CD38^{+}/CD138^{+}$ myeloma cells within the PI^{-} and thus viable cell population. Within this gate, CD147 expression was calculated as MFI in relation to its isotype control both in the overall $CD38^{+}/CD138^{+}$ cell

population and separately in the viable annexin$^-$ and the apoptotic annexin$^+$ subset, allowing to detect changes in CD147 expression in viable vs. apoptotic cells. Patients with more than 50% of PI$^+$ cells in the controls were excluded from further analysis.

6.2.7.5 Flow cytometry of patient-derived MDS progenitor cells

The isolation and culture of hematopoietic stem cells derived from MDS patients is described in chapter 6.2.4.2. The respective experiments incl. flow cytometry were performed by A.-K. Garz in the lab of Prof. Götze (III. Medical Department, Klinikum rechts der Isar).

After *in-vitro* differentiation and treatment, cells were collected and washed with Annexin/PI buffer. Subsequently, cells were stained with CD34-FITC (clone 581/CD34), CD147-PE (clone HIM6), CD33-PC5.5 (clone D3HL60.251), CD45 PE Cy7 (clone HI30), CD36-APC Cy7 (clone 336213) and primary CD235-α-biotin (clone HIR2) antibodies together with and secondary streptavidin eFluor®450, according to manufacturer's instructions. APC-conjugated annexin V and PI were added to detect apoptosis/necrosis. Flow cytometry was performed on a CyAn ADP LxP8, using single stained samples for compensation.

The data was analyzed using FlowJo software. After excluding debris and doublets, CD147 expression was analysed within the PI$^-$ subset in both annexin$^+$ and annexin$^-$ populations in CD36$^+$ erythroid precursor cells as well as CD36$^-$CD235-α$^-$ non-erythroid cells.

6.2.8 Immunofluorescence

Immunofluorescence is a technique to visualize subcellular structures or proteins using fluorescent markers such as fluorochrome-coupled antibodies and a fluorescence microscope detecting the fluorescent signals.

In this study, wildtype HeLa cells or HeLa cells stably expressing shRNA constructs targeting CRBN or control, were plated in chambers on glass coverslips and transfected with constructs expressing HA-CD147, Flag-MCT1 or HA-MCT1 and/or Flag-CRBN using Lipofectamine (see chapter 6.2.5.2). 24 hrs after transfection, the cells were washed in PBS and fixed in ice-cold methanol at -20°C for 20 min. Subsequently, cells were blocked with IF buffer with 5% FBS for 20 min at RT before incubation with anti-HA (mouse; clone 16B12) and anti-Flag (rabbit) antibodies at a 1:500 dilution in IF buffer for 1h. After washing, Alexa Fluor 488 or Alexa Fluor 594 conjugated anti-rabbit and anti-mouse secondary antibodies were added at a 1:1000 dilution for 45 min at RT and protected from light. The chambers were removed after washing, and 1 drop of ProLong GOLD antifade reagent with DAPI was placed on the cells before placing a coverslip on top. The antifade reagent preserves the fluorescent signal and DAPI coutnerstians the DNA. In experiments visualizing the ER, the ER tracker blue white DPX was added to cells in culture for 30 min according to the manufacturer's instructions. After fixation in 4% PFA, the cells were processed as described above. Images were taken using the laser-scanning confocal microscope FluoView FV10i.

6.3 Protein Biochemistry

6.3.1 Cell lysis

For analysis of cellular proteins, cell samples need to be lysed in suitable buffers that disrupt cellular organelles, keep proteins in solution and prevent their degradation. Unless indicated otherwise, fresh or frozen cell samples were lysed in standard lysis buffer with fresh protease inhibitors (see chapter 5.15), at a volume suitable for the pellet size. After 20 min incubation on ice, the lysate was centrifuged for 15 min at 14,000 rpm and 4°C to separate from debris. Protein concentration in supernatants was measured using the colorimetric Bio-Rad DC protein assay, which is based on the Lowry method (Lowry et al., 1951), according to the manufacturer's instructions. Finally, Laemmli buffer (see chapter 5.15) was added to denature proteins via SDS and stabilize the sample.

6.3.2 SDS polyacrylamid gel electrophoresis (SDS-PAGE)

SDS polyacrylamide gel electrophoresis (SDS-PAGE) is a gel-based method to separate proteins in an electric field according to their electrophoretic mobility. In presence of SDS, tertiary structures are overcome and proteins are coated in negative charge, thus migrating according to their molecular weight.

Gels were prepared freshly before use. For a 10% separating gel, 4.8 ml of H_2O, 2.5 ml of 40% acrylamide, 2.5 ml of 1,5 M Tris (pH 8.8), 100 µl of 10% SDS, 100 µl of 10% APS and 4 µl TEMED were mixed and allowed to polymerize in a gel caster. The stacking gel mixture, consisting of 3 ml H_2O, 550 µl acrylamide, 1.25 ml of 0.5 M Tris (pH 6.8), 50 µl of 10% SDS and 10% APS and 5 µl TEMED, was polymerized on top. Proteins samples and a molecular weight marker were loaded onto SDS-polyacrylamid gels (15–25 µg protein per slot) and subjected to gel electrophoresis in running buffer at 80–150 V. After PAGE, proteins were visualized within the gel (see chapter 6.3.3) or transferred to a membrane for immoblot analysis (see chapter 6.3.4).

6.3.3 Silver- and Coomassie stainings

Proteins within a poly-acrylamide gel can be visualized using silver- or Coomassie staining. Silver staining is based on the conversion of silver ions, which bind to amino acid functional groups, to metallic silver. Coomassie is a blue triphenylmethane dye, which after staining and subsequent destaining, is only retained by proteins. While Coomassie allows detection of about 50 ng of protein, silver staining is up to 50 times more sensitive.

In this study, silver staining was performed using the SilverQuest Silver Staining Kit according to the manufacturer's instructions. For Coomassie staining, polyacrylamide gels were incubated in Coomassie staining solution on a shaker over night and destained by washing repeatedly in Coomassie destaining solution (for solutions see chapter 5.15).

6.3.4 Immunoblot analysis (Western Blot)

Immunoblot analysis is a method to specifically detect membrane-bound proteins using specific antibodies. Proteins separated by SDS-PAGE were transferred to polyvinylidene difluoride (PVDF) membranes, which bind proteins via hydrophobic and polar interactions. The transfer was done by electroblotting in blotting buffer (see chapter 5.15) either at 100 V for 1 h or at 30 V over night. For analysis of protein loading, the membrane was colored with Ponceau, a diazo dye reversibly staining protein. After destaining in washing buffer (WB) and blocking in 5% milk in WB for 30 min, the membranes were incubated with primary antibodies diluted in 5% milk or 5% BSA in WB for 2 hrs at RT or ≥ 4 hrs at 4°C on a roller mixer. After washing (3×10 min) in WB, membranes were incubated with the respective HRP (horse raddish peroxidase)-coupled secondary antibody at a dilution of 1:5000 in 5% milk for 30 min at RT. After washing again (3×10 min), membranes were developed using ECL (enhanced chemoluminescence) and exposed to photosensitive films. The ECL method is based on chemiluminescent HRP substrates, giving rise to luminescent signals at the site of bound secondary antibody. Quantification of immunoblot signals was performed on low saturation exposures using Quantity One software.

6.3.5 Stripping of membranes

In order to re-probe a PVDF membrane with another antibody, the previously bound primary and secondary antibodies can be removed via incubation with a denaturing buffer containing SDS and β-mercaptoethanol in a process called stripping.

After reactivation in methanol, membranes were incubated in stripping buffer (see chapter 5.15) at 65°C for 30-45 min. After shaking for another 15 min at RT and subsequent washing in PBS (4×15 min), the membrane was ready for blocking and incubation with a new antibody.

6.3.6 Immunoprecipitations

Immunoprecipitation (IP) is a method to purify proteins using specific antibodies. The antibodies can either be covalently coupled to agarose or sepharose beads, or applied together with beads conjugated to protein A or G, binding rabbit or mouse antibodies, respectively.

IPs were performed from whole cell lysates in standard lysis buffer (see chapter 6.3.1). For Flag-IPs of Flag-tagged proteins or HA-IPs from HA-tagged proteins, lysates were incubated with Flag-M2 or HA-7 agarose beads respectively. Before use, the beads were washed (2× in PBS and 2× in lysis buffer) and diluted 1:1 in lysis buffer to obtain a slurry suspension. Per sample (300-500 µl of cell lysate), 20 µl of slurry beads were added and incubated for 2 hrs at 4°C on a rotating wheel. After washing the beads in lysis buffer (3×) to reduce unspecific binding, 80 µl of Lämmli buffer was added to the sample. For IPs of endogenous proteins, 4 µg of the respective antibodies and 20 µl slurry beads coupled to protein A or G were added to each sample. Incubation and washing steps were performed as described. Where indicated, DMSO or lenalidomide was added to the lysis buffer at the concentration used in cell culture. Lysis and

Flag-IP in experiments using DSS as crosslinker (see chapter 6.2.3.4) were performed in the same way, with the only difference being 50 mM HEPES instead of Tris-HCl in the lysis buffer.

6.3.7 Tandem affinity purification

Tandem affinity purification (TAP), a common approach to purify proteins for subsequent mass spectrometric analysis of bound interactors, describes the combination of two subsequent affinity purification steps, which increases specificity of the interaction.

In this study, a combination of Strep-affinity purification (AP) and Flag-IP was chosen for TAP of CRBN. CRBN was cloned into a C-terminal tandem-Strep-single-Flag-tag construct (C-SF-CRBN) (Gloeckner et al., 2007). For TAP, approximately 2×10^9 HEK293T cells grown to a density of 60-70% were transfected with either the C-SF-CRBN construct, a non-tagged CRBN overexpression construct or an empty vector control using the calcium phosphate method (see chapter 6.2.5.1) and harvested 24 hrs later. Lysis was performed in standard lysis buffer as described above. To include proteins from less accessible cellular compartments, lysates were passed through 22G and 26G syringe needles and additionally sonicated. The supernatants were incubated with Strep-Tactin Superflow resin for 2 hrs at 4°C. After washing in lysis buffer, bound proteins were eluted twice using desthiobiotin elution buffer for 10 min each at RT. Next, the eluate was subjected to a second precipitation using Flag-M2 beads for 1 h at 4°C, followed by washing (1× in lysis buffer, 1× in TBS) and three consecutive elution steps using 250 µg/ml 3×Flag peptide in TBS buffer for 10 min at RT. The three elutions were pooled, and proteins were precipitated by incubation with TCA at a ratio of 1:10 at 4°C over night. After centrifugation at 13,500 rpm for 10 min at 4°C, the protein pellet was washed with 500 µl cold acetone, centrifuged again and finally vacuum dried. 5% of the purification was resuspended in Lämmli buffer for silver gel staining, the remaining dried protein sample was sent for mass spectrometric analysis to collaborators at the Department of Proteomics and Bioanalytics at TUM.

6.3.8 Mass spectrometric analyses

Mass spectrometry (MS) is a method to measure the mass and charge of substances. In case of protein analysis, peptides resulting from enzymatic digestion (e.g. by trypsin) are ionized and separated according to their mass-to-charge ratio in an electric or magnetic field. Based on the detected spectra, peptides are identified by correlation to the mass-to-charge ratio of known peptides (generated by the respective enzyme), enabling identification of the protein of origin.

MS analysis of affinitiy purified CBRN with bound proteins was performed by Dr. Simone Lemeer in the group of Prof. Dr. Bernhard Küster at the Department of Proteomics and Bioanalytics at TUM. Peptides were generated by in-gel trypsin digestion, dried and dissolved in 0.1% formic acid (FA). Subsequently, liquid chromatography coupled mass spectrometry (LC-MS/MS) was performed by coupling a nanoLC-Ultra high-performance liquid chromatography instrument to a LTQ Orbitrap Velos mass spectrometer, using a 110 min gradient from 0 to 40% solution B (0.1% FA in AcN) as decribed previously (Baumann et al., 2014; Fernandez-Saiz et al.,

2013). For peptide and protein identification, peak lists were extracted from raw files using the Mascot Distiller v2.2.1 software and subsequently searched against the Human IPI database (v3.68, 87061 entries) using Mascot (v2.3.0) with carbamidomethyl cysteine as a fixed modification and phosphorylation of serine or threonine and oxidation of methionin as variable modifications. Precursor tolerance was set to 5 ppm and fragment ion tolerance to 0.02 Da. Trypsin/P was specified as the proteolytic enzyme with up to 2 missed cleavage sites allowed.

6.3.9 GST-protein experiments

Glutathione S-transferase (GST) is an enzyme of 211 amino acids, which is commonly used as protein-tag due to its high affinity for glutathione. GST-fusion proteins are produced in bacteria and purifiied by glutathione-coated beads, which can be used for pulldown experiments.

6.3.9.1 GST-protein induction and purification

To express GST-tagged proteins, respective genes were cloned in the pGEX-4T2 bacterial expression vector and transformed in *E. Coli* BL21. Expression of the fusion protein is under the control of the LAC promoter, which is blocked by the Lac repressor molecule. Isopropyl-β-D-thiogalactopyranoside (IPTG) binds to the repressor, thus inducing conformational changes, which release the repressor to enable protein expression. Precultures of positive BL21 clones, which were grown in LB^{AMP} media over night, were diluted 1:10 in fresh LB medium (without Amp) to a final volume of 100 ml and allowed to grow. After 1 h and at an optical densitiy (OD_{600}) of 0.4 - 0.6, indicating exponential bacterial growth, IPTG was added to a final concentration of 1 mM for 3.5 hrs to induce protein expression. Subsequently, bacteria were harvested by centrifugation and frozen at -80°C.

For purification of GST-tagged proteins, the frozen pellets were resuspended in NETN buffer (see chapter 5.15) and passed through a 22 G syringe. After incubation with 100 µg/ml lysozyme for 30 min for breakage of the cell wall, the sample was sonicatied (10 pulses of 51% amplitude of 1 sec and 0.5 sec pause). After centrifugation at 9500 rpm at 4°C for 15 min, the supernatatent was incubated with Glutathion Sepharose 4B beads for 1.5 hrs at 4°C. The beads with bound GST-tagged proteins were washed (4×) and stored in NETN buffer at 4°C. Abundance of the purified proteins was analyzed by SDS-PAGE followed by Coomassie staining.

6.3.9.2 GST-pulldown experiments

Before using the purified GST-tagged proteins bound to Glutathion Sepharose 4B beads (see chapter 6.3.9.1) for pulldown-experiments, the beads were washed four times in lysis buffer. Subsequently, lysates of MM1.S or HEK293T cells (for lysis see chapter 6.3.1) were incubated with the bead-bound GST-fusion proteins or bead-bound GST as control. After an incubation of 2 hrs at 4°C and subsequent washing (3× in lysis buffer), Lämmli was added to the beads and pulled-down proteins fractions were analyzed by immunoblotting. For binding studies with lenalidomide, the drug or DMSO were added to the lysis buffer during pulldown and washing steps. For *in-vitro* binding assays, purified GST-CRBN was incubated with ^{35}S-labeled, *in-vitro*

translated CD147 or MCT1 in binding buffer (see chapter 5.15). After washing, bound protein fractions were separated by SDS-PAGE and analyzed by autoradiography.

6.3.10 *In-vitro* protein translation (IVT)

In-vitro protein translation (IVT), the cell-free biosynthesis of proteins, allows production of pure protein for e.g. interactions studies, as well as radioactive labeling of a protein of interest.

In this study, CD147 and MCT1 were translated *in-vitro* using the eukaryotic cell-free TNT T7 Quick-Coupled Transcription/Translation system, which comprises RNA polymerases, nucleotides, salts, the RNase inhibitor RNasin, amino acids and reticulocyte lysate solution (from reticulocytes, the precursors of erythrocytes), thus offering coupled transcription and translation in a single tube. This kit drives transcription from T7 promotors, therefore 0.2 – 2.0 µg of T7 driven CD147 or MCT1 expression plasmids were added to 50 µl of the TNT Quick Master Mix for 90 min at 30°C. For radioactive labeling, 0.2 mCi/ml L-[^{35}S]-Methionine was added to the sample.

6.3.11 Pulse-chase analysis

Pulse-chase analysis allows tracking of cellular processes or e.g. proteins over time using e.g. radioactive labeling. The described experiments were performed by Dr. V. Fernandez-Saiz.

To investigate CD147 maturation over time, MM1.S cells were labelled with L-[^{35}S]-Methionine/Cystein as described previously (Fernandez-Saiz et al., 2013). Briefly, MM1.S cells treated with lenalidomide or DMSO, or infected with shRNA constructs to knockdown CRBN or control, were washed (3× in PBS) and incubated in methionine- and cysteine-free DMEM for 1 h at 37°C. For labeling of newly translated proteins, the cells were incubated for 45 min with methionine- and cysteine-free DMEM containing 0.2 mCi/ml L- [^{35}S]-Met/Cys. After washing (3× in PBS), the cells were incubated with DMEM up to 24 hrs and aliquots were harvested at defined timepoints. Where indicated, lenaliomide, MLN4924 or DMSO was added to the medium.

6.3.12 Size exclusion chromatography (SEC)

Size-exclusion chromatography (SEC) is a technique to separate proteins or protein complexes in aqueous solutions according to their size. The fractionation is achieved by letting proteins pass through a colomn with differently sized pores, resulting in varied passing times for differently sized proteins. SEC experiments were performed by Dr. V. Fernandez-Saiz together with help from Brigitte Nuscher at the DZNE (Deutsches Zentrum für Neurodegenerative Erkrankungen) in Munich.

For SEC of CRBN complexes, HEK293T cells were transfected with Flag-tagged CRBN, CD147, MCT1, CUL4A and DDB1 expressing constructs. After harvest and lysis, CRBN-complexes were immunoprecipitated using Flag-M2 beads (see chapter 6.3.6) and eluted by competition with 3×Flag peptide in TBS buffer. Purified proteins were incubated at 25°C for 30 min with of lenalidomide or DMSO and loaded on a calibrated Superose 6 PC 3.2/30 analytical

column. Chromatography was performed at 4°C at 0.3 ml/min in TBS buffer. Elution volumes were measured by peak integration using Unicorn software. For immunoblot analysis, the proteins of each fraction were precipitated using TCA and resuspended in a reduced volume.

6.4 Biological assays

6.4.1 Enzyme-linked immunosorbent assay (ELISA)

The enzyme-linked immunosorbent assay (ELISA) is an antibody-based method to detect and quantify soluble antigens. The most common application is the sandwich ELISA, based on immobilized antibodies on a plate binding respective antigens from a sample. After addition of a second antigen-binding antibody and an enzyme-coupled secondary antibody, incubation with the enzyme's substrate gives rise to a detectable signal correlating with the quantity of the antigen.

To investigate secretion of VEGF and MMP7, two downstream targets of CD147, their abundance in cell culture supernatants was analyzed using ELISAs. MM cell lines pretreated with 10 µM lenalidomide or DMSO for 96 hrs, or lentivirally infected with shRNA constructs targeting CD147, CRBN or control, were incubated for 3 hrs in fresh medium (with lenalidomide or DMSO as indicated) before supernatant and cell pellets were harvested and snap-frozen in liquid nitrogen. VEGF and MMP7 concentrations in cell culture supernatants were determined using commercially available ELISA kits (see chapter 5.7) according to the manufacturer's instructions. Protein concentration in the cellular lysates was used for normalization.

6.4.2 Lactate measurements

Lactate, the end-product of anaerobic glycolysis, can be exported from the cell via monocarboxylate transporters as MCT1. In this study, intracellular lactate levels of MM cells were measured with the help of Prof. Dr. P. Luppa on a cobas 8000 instrument, a device used for clinical routine analyses in the Department of Clinical Chemistry, Klinikum rechts der Isar.

MM cell lines treated with 10 or 100 µM lenalidomide or DMSO for 96 hrs or lentivirally infected with shRNA constructs against MCT1, CRBN or control, were harvested and washed in PBS before lysis in 250 mM lysis buffer (see chapter 5.15 and 6.3.1). Each lysate was split in three: two aliquots (technical replicates) were subjected to immediate lactate measurement on the cobas 8000 instrument, while the third aliquot was used to determine protein concentration, allowing normalization of lactate levels.

6.5 Animal experiments

6.5.1 Murine xenograft experiments

Mouse models are central preclinical models in cancer research, allowing evalution of tumor growth and treatment effects *in-vivo.* Given that IMiDs are not active in mouse, xenogeneic

tumor models based on transplantation of human cell lines into immunodeficient mice, seemed most adequate to evaluate the *in-vivo* relevance of CD147/MCT1.

The xenograft mouse experiments were performed with female NOD.CB17/AlhnRj-*Prkdc*^{scid}/Rj (NOD/SCID) mice at 8–12 weeks of age. The mice of one experiment were from the same charge, and per condition, a group size of at least four animals was chosen. All mouse experiments were were approved by the responsible regional authority (Regierung von Oberbayern) and were performed in accordance with local animal protection standards.

6.5.1.1 Animal care

Female NOD/SCID mice were kept in groups of 4-6 animals per cage in specific mouse facilities at the ZPF (Zentrum für Präklinische Forschung), which follow a 12 h day and night rhythm and underlie strict hygienic standards. Food and water was supplied according to the standards of the ZPF at Klinikum rechts der Isar and animal care was provided by trained staff.

6.5.1.2 Preparation of cells and xenograft injection

For xenograft experiments, MM1.S cells were either lentivirally infected with knockdown or overexpression constructs. In the first approach, MM1.S cells were co-transduced with two shRNA constructs targeting CD147 or MCT1, or a control shRNA. Because of the high infection rates together with reduced viability resulting from CD147/MCT1 knockdown, viral infection was done 2 days prior to xenograft injection. In the second setting, MM1.S cells were co-infected with viral particles for induced expression of CD147 and MCT1, or control. Because of low transduction efficiencies, double-infected MM1.S cells were sorted for double positivitly (EGFP and DsRed-Express2) using FACS and expanded for transplantation thereafter.

At the day of injection, 1×10^7 cells were washed per tumor, resuspended in 50 µl PBS and mixed on ice with Matrigel Basement Membrane Matrix at a 1:1 ratio directly before injection. A final volume of 100 µl was injected subcutaneously into the flank of female NOD/SCID mice, which were anesthetized with isoflurane. In order to have experimental condition and control in the same subjects, each animal was injected with both control and overexpression or knockdown cells on opposite flanks.

6.5.1.3 Monitoring of tumor growth and drug treament

Growth of the xenograft tumors was carefully monitored by palpation, first twice per week, later on a daily basis. As soon as tumors became detectable, their diameter was measured by caliper. Once both control and CD147/MCT1 overexpression tumors reached at least 5 mm in diameter, mice were randomly assigned to receive either daily lenalidomide at a dose of 30 mg/kg (dissolved in 0,5% carboxymethylcelluose and 0,25% Tween 80 in deionized water) or vehicle only. A volume of 100 µl of drug or vehicle was administered daily by oral gavage. Due to the limited stabilitiy in aqueous solution, lenalidomide was freshly prepared directly before use. Under treatment, both length (L) and width (W) of the tumors were measured daily using a caliper. The metric tumor volume (V) was estimated using the following equation: $V = (L \times W^2) \times$

0.5. Once a tumor reached a maximal diameter of 15 mm, the predefined endpoint for terminal disease, the mouse was sacrificed.

6.5.1.4 PET-analysis and evaluation

Positron emission tomography (PET) is a method for functional imaging based on positron-emitting radionuclides, which can be coupled to molecules such as glucose, resulting in e.g. ^{18}F-fluorodeoxyglucose (FDG), which is commonly used for metabolic imaging.

In this study, PET-analyses of xenografted mice were performed with the help of Sybille Reder at the Small Animal Imaging Unit in the Department of Nuclear Medicine at Klinikum rechts der Isar. All mice of the shCD147/shMCT1 cohort were subjected to PET-imaging on day 28 after tumor cell inoculation. 2 hrs before imaging, mice were fasted to reduce blood glucose levels. For PET, anesthetized mice received 100 µl of FDG by tail vein injection at an activity dose of 5–10 MBq. After allowing accumulation of the radiotracer for 60 min, mice were imaged for a 15 min static acquisition on a Inveon Micro-PET system. Metabolic tumor volume was calculated based on a semiautomated three-dimensional region of interest of isocontour 50% around the maximum activity of the tumor.

6.5.1.5 Necropsy

After reaching the predefined end point (tumor size ≥ 15 mm), mice were anesthetized using isoflurane and sacrificed using the cervical dislocation method. The subcutaneous xenograft tumors were dissected from the surrounding tissues, weighed and measured (max. lengths and width). For further analysis, the tumors were divided: one part was fixed in 4% PFA for immunohistochemical analysis, the other part was passed through 70 µm cell strainers, washed in PBS and frozen for immunoblot analysis. If xenograft tumors were smaller than 4-5 mm in diameter, the entire tumor was fixed in PFA.

6.5.1.6 Immunohistochemical analysis of xenograft tumors

Immunohistochemical (IHC) analyses of xengraft tumors were performed by PD Dr. Martina Rudelius at the Institute of Pathology (University of Würzburg). IHC describes the detection of antigens in tissue sections using specific antibodies.

Samples of xenograft tumors fixed in 4% PFA were sent to the Institute of Pathology in Würzburg, where the samples were processed according to standard procedures of the institute. The tumors were first paraffinzed and cut into sections using a microtome. After deparaffinization and rehydration, the sections were incubated for 7 min with preheated 10 mM citrate buffer (pH 6.0) or EDTA buffer (pH 9.0) in a pressure cooker for antigen retrieval. For IHC, the slides were subsequently incubated with CD147 antibody (clone H-200) at a dilution of 1:200, MCT1 antibody (clone H-70) at a dilution of 1:100, CD79 antibody (clone JCB-117) or MMP7 antibody at a dilution of 1:50 for 1 h at RT. Signal detection was performed using the Dako REAL detection system according to the suppliers' recommendations. Hematoxylin and eosin staining was performed following standard protocols.

6.5.2 Zebrafish experiments

Zebrafish is an established model to study IMiD induced teratoxocity (Ito et al., 2010; Mahony et al., 2013) and was therefore chosen to investigate CD147 in IMiD-mediated teratotoxicity. All zebrafish experiments were performed by Dr. Frauke van Bebber in the group of Dr. Bettina Schmid at the DZNE (Deutsches Zentrum für Neurodegenerative Erkrankungen) in Munich, in accordance with animal protection standards of the LMU Munich. All experiments were approved by the responsible regional authority (Regierung von Oberbayern).

6.5.2.1 Animal care and drug treatment

The zebrafish wildtype strain AB was used for all experiments. Zebrafish embryos were kept at 28.5°C in E3 media (see chapter 5.15) supplemented with 5-10% methylene blue. Fertilized embryos at 3 hrs post fertilization (hpf) were randomly split in groups of 10 for subsequent IMiD treatment. The control group was transferred into E3 medium containing 0.1% DMSO, while treatment groups were kept in E3 medium with final concentrations of 400 µM thalidomide, 772 µM lenalidomide or 219 µM pomalidomide, in analogy to previous publications (Ito et al., 2010; Mahony et al., 2013). The larvae were kept in the named conditions at 28.5 °C for up to 3 days depending on the experiment. The sample size of 10 was chosen based on a pilot experiment.

6.5.2.2 Morpholino injection

Morpholino oligomers, called morpholinos, are synthetic nucleic acid analogs used for knockdown of gene expression in embryonic systems. They consist of normal nucleic acid bases, but instead of deoxyribose rings, they have a backbone of methylenemorpholine rings, which are linked by phosphorodiamidate groups and not phosphates (Summerton, 1999; Summerton and Weller, 1997). Due to this structure, morpholinos can bind to complementary RNA sequences, but cannot be degraded by DNases or RNases. Therefore, morpholinos are much more stable than normal oligonucleotides and can persist for up to 5 days in the developing embryo. Contrary to siRNA, the binding of morpholinos to e.g. mRNA does not induce its degradation; instead, morpholinos merely block the access of proteins to mRNA, thus inhibiting translation.

For knockdown of CD147 in zebrafish, two independent antisense morpholinos of 25 bp length were designed: one to target the splice junction between exon 3 and intron 3 (spilce MO), thus inhibiting correct splicing, and one to target the ATG start codon (ATG MO), thus inhibiting initiation of translation. Sequences are listed in chapter 5.8.4. At the single-cell stage, zebrafish embryos were injected with 2–4 pl of 0.1 mM or 0.5 mM splice MO or ATG MO using a microinjection system according to standard procedures. Injected eggs and controls were cultured at 28°C in E3 buffer for up to 3 days. For each experiment, 50 eggs were injected per condition.

6.5.2.3 Evaluation of phenotypes

In the literature, the thalidomide-induced teratotoxic phenotype in zebrafish, which includes smaller eyes and smaller pectoral fins, was described at 3 dpf (days post fertilization)

(Ito et al., 2010; Mahony et al., 2013). Therefore, zebrafish larvae treated with IMiDs or DMSO or injected with CD147 morpholinos were microscopically examined for signs of teratotoxicity at 3 dpf. A reduced eye size of at least 20% at 3 dpf was considered significant and determined as parameter to quantify teratotoxicity. For microscopy and quantification, zebrafish larvae were anesthetized with tricaine methanesulfonate (0.016% w/v) and mounted in 3% methylcellulose on coverslips. Images were taken using an Axioplan2 compound microscope. All surviving larvae at 3 dpf were included in the analyses.

6.5.2.4 *In-situ* hybridisation (ISH)

In-situ hybridization (ISH) describes the detection of specific DNA or RNA sequences in tissue sections based on hybridization with labeled complenetary DNA probes. In case of small specimen as e.g. zebrafish embryos, the entire embryo can be stained (whole-mount ISH).

FGF8 is a downstream target of thalidomide, whose expression in the fin buds of zebrafish is significantly reduced after thalidomide treatment, thus causing the typical teratotoxic fin malformations (Ito et al., 2010). In this study, FGF8 expression in the apical ectodermal ridge (AER) of the fin buds was analyzed at 2 dpf in embryos treated either with DMSO, thalidomide, lenalidomide or pomalidomide (see chapter 6.5.2.1) or treated with CD147 splice MO vs. control (see chapter 6.5.2.2). Embryos were fixed in 4% PFA at 2 dpf and ISH was performed with an antisense probe detecting zebrafish *FGF8* mRNA using a standard protocol (Schmid et al., 2013). DIC images of fin buds were taken using a Zeiss compound microscope with a Zeiss Plan-Apochromat 10x/0.45 lens.

6.6 Statistical analysis

All quantified experiments were performed in triplicate, meaning three independent biological replicates. For ELISAs, lactate measurements, qPCR and proliferation data, two or three technical replicates were measured per biological replicate. Quantification of Western Blots resulted from three independent experiments. The non-quantified western blot data generally shows results representative for at least two independent experiments. Statistical analyses of the results were performed with the GraphPad Prism software. Depending on the data, significance was calculated using the Student's t-test, one-sample t-test or one-way ANOVA, according to assumptions of the test. Statistical analysis of relative ratios was performed using one-sample t-tests with hypothetical means of 1.0. The error bars shown in the figures represent the mean ± standard deviation (S.D.). The *P* values are denoted in the figure legends where a statistically significant difference was found: *, $P < 0.05$; **, $P < 0.01$; ***, $P < 0.001$; ****, $P < 0.0001$.

7 Literature

Angers, S., Li, T., Yi, X., MacCoss, M.J., Moon, R.T., and Zheng, N. (2006). Molecular architecture and assembly of the DDB1-CUL4A ubiquitin ligase machinery. Nature *443*, 590-593.

Arendt, B.K., Walters, D.K., Wu, X., Tschumper, R.C., Huddleston, P.M., Henderson, K.J., Dispenzieri, A., and Jelinek, D.F. (2012). Increased expression of extracellular matrix metalloproteinase inducer (CD147) in multiple myeloma: role in regulation of myeloma cell proliferation. Leukemia *26*, 2286-2296.

Arendt, B.K., Walters, D.K., Wu, X., Tschumper, R.C., and Jelinek, D.F. (2014). Multiple myeloma dell-derived microvesicles are enriched in CD147 expression and enhance tumor cell proliferation. Oncotarget *5*, 5686-5699.

Arvidsson, S., Kwasniewski, M., Riano-Pachon, D.M., and Mueller-Roeber, B. (2008). QuantPrime--a flexible tool for reliable high-throughput primer design for quantitative PCR. BMC bioinformatics *9*, 465.

Atra, E., and Sato, E.I. (1993). Treatment of the cutaneous lesions of systemic lupus erythematosus with thalidomide. Clinical and experimental rheumatology *11*, 487-493.

Attal, M., Lauwers-Cances, V., Marit, G., Caillot, D., Moreau, P., Facon, T., Stoppa, A.M., Hulin, C., Benboubker, L., Garderet, L.*, et al.* (2012). Lenalidomide maintenance after stem-cell transplantation for multiple myeloma. N Engl J Med *366*, 1782-1791.

Avet-Loiseau, H., Attal, M., Moreau, P., Charbonnel, C., Garban, F., Hulin, C., Leyvraz, S., Michallet, M., Yakoub-Agha, I., Garderet, L.*, et al.* (2007). Genetic abnormalities and survival in multiple myeloma: the experience of the Intergroupe Francophone du Myelome. Blood *109*, 3489-3495.

Baba, M., Inoue, M., Itoh, K., and Nishizawa, Y. (2008). Blocking CD147 induces cell death in cancer cells through impairment of glycolytic energy metabolism. Biochem Biophys Res Commun *374*, 111-116.

Barille, S., Bataille, R., Rapp, M.J., Harousseau, J.L., and Amiot, M. (1999). Production of metalloproteinase-7 (matrilysin) by human myeloma cells and its potential involvement in metalloproteinase-2 activation. J Immunol *163*, 5723-5728.

Barlogie, B., Desikan, R., Eddlemon, P., Spencer, T., Zeldis, J., Munshi, N., Badros, A., Zangari, M., Anaissie, E., Epstein, J.*, et al.* (2001). Extended survival in advanced and refractory multiple myeloma after single-agent thalidomide: identification of prognostic factors in a phase 2 study of 169 patients. Blood *98*, 492-494.

Bartlett, J.B., Dredge, K., and Dalgleish, A.G. (2004). The evolution of thalidomide and its IMiD derivatives as anticancer agents. Nat Rev Cancer *4*, 314-322.

Bassermann, F., Eichner, R., and Pagano, M. (2013). The ubiquitin proteasome system - Implications for cell cycle control and the targeted treatment of cancer. Biochim Biophys Acta.

Baumann, U., Fernandez-Saiz, V., Rudelius, M., Lemeer, S., Rad, R., Knorn, A.M., Slawska, J., Engel, K., Jeremias, I., Li, Z.*, et al.* (2014). Disruption of the PRKCD-FBXO25-HAX-1 axis attenuates the apoptotic response and drives lymphomagenesis. Nature medicine.

Bedewy, A.M., and El-Maghraby, S.M. (2014). Do baseline Cereblon gene expression and IL-6 receptor expression determine the response to thalidomide-dexamethasone treatment in multiple myeloma patients? Eur J Haematol *92*, 13-18.

Benboubker, L., Dimopoulos, M.A., Dispenzieri, A., Catalano, J., Belch, A.R., Cavo, M., Pinto, A., Weisel, K., Ludwig, H., Bahlis, N.*, et al.* (2014). Lenalidomide and dexamethasone in transplant-ineligible patients with myeloma. N Engl J Med *371*, 906-917.

Bennett, J.M., Catovsky, D., Daniel, M.T., Flandrin, G., Galton, D.A., Gralnick, H.R., and Sultan, C. (1982). Proposals for the classification of the myelodysplastic syndromes. Br J Haematol *51*, 189-199.

Bergers, G., and Benjamin, L.E. (2003). Tumorigenesis and the angiogenic switch. Nat Rev Cancer *3*, 401-410.

Bergsagel, P.L., and Kuehl, W.M. (2005). Molecular pathogenesis and a consequent classification of multiple myeloma. J Clin Oncol *23*, 6333-6338.

Biegler, B., and Kasinrerk, W. (2012). Reduction of CD147 surface expression on primary T cells leads to enhanced cell proliferation. Asian Pacific journal of allergy and immunology / launched by the Allergy and Immunology Society of Thailand *30*, 259-267.

Birsoy, K., Wang, T., Possemato, R., Yilmaz, O.H., Koch, C.E., Chen, W.W., Hutchins, A.W., Gultekin, Y., Peterson, T.R., Carette, J.E.*, et al.* (2013). MCT1-mediated transport of a toxic molecule is an effective strategy for targeting glycolytic tumors. Nat Genet *45*, 104-108.

Biswas, C., and Nugent, M.A. (1987). Membrane association of collagenase stimulatory factor(s) from B-16 melanoma cells. Journal of cellular biochemistry *35*, 247-258.

Biswas, C., Zhang, Y., DeCastro, R., Guo, H., Nakamura, T., Kataoka, H., and Nabeshima, K. (1995). The human tumor cell-derived collagenase stimulatory factor (renamed EMMPRIN) is a member of the immunoglobulin superfamily. Cancer Res *55*, 434-439.

Blum, W., Klisovic, R.B., Becker, H., Yang, X., Rozewski, D.M., Phelps, M.A., Garzon, R., Walker, A., Chandler, J.C., Whitman, S.P.*, et al.* (2010). Dose escalation of lenalidomide in relapsed or refractory acute leukemias. J Clin Oncol *28*, 4919-4925.

Bougatef, F., Quemener, C., Kellouche, S., Naimi, B., Podgorniak, M.P., Millot, G., Gabison, E.E., Calvo, F., Dosquet, C., Lebbe, C.*, et al.* (2009). EMMPRIN promotes angiogenesis through hypoxia-inducible factor-2alpha-mediated regulation of soluble VEGF isoforms and their receptor VEGFR-2. Blood *114*, 5547-5556.

Boultwood, J., Pellagatti, A., Cattan, H., Lawrie, C.H., Giagounidis, A., Malcovati, L., Della Porta, M.G., Jadersten, M., Killick, S., Fidler, C.*, et al.* (2007). Gene expression profiling of CD34+ cells in patients with the 5q- syndrome. Br J Haematol *139*, 578-589.

Breitkreutz, I., Raab, M.S., Vallet, S., Hideshima, T., Raje, N., Mitsiades, C., Chauhan, D., Okawa, Y., Munshi, N.C., Richardson, P.G.*, et al.* (2008). Lenalidomide inhibits osteoclastogenesis, survival factors and bone-remodeling markers in multiple myeloma. Leukemia *22*, 1925-1932.

Broyl, A., Kuiper, R., van Duin, M., van der Holt, B., el Jarari, L., Bertsch, U., Zweegman, S., Buijs, A., Hose, D., Lokhorst, H.M.*, et al.* (2013). High cereblon expression is associated with better survival in patients with newly diagnosed multiple myeloma treated with thalidomide maintenance. Blood *121*, 624-627.

Bruno, B., Rotta, M., Patriarca, F., Mordini, N., Allione, B., Carnevale-Schianca, F., Giaccone, L., Sorasio, R., Omede, P., Baldi, I.*, et al.* (2007). A comparison of allografting with autografting for newly diagnosed myeloma. N Engl J Med *356*, 1110-1120.

Cavo, M., Zamagni, E., Tosi, P., Cellini, C., Cangini, D., Tacchetti, P., Testoni, N., Tonelli, M., de Vivo, A., Palareti, G., *et al.* (2004). First-line therapy with thalidomide and dexamethasone in preparation for autologous stem cell transplantation for multiple myeloma. Haematologica *89*, 826-831.

Chamberlain, P.P., Lopez-Girona, A., Miller, K., Carmel, G., Pagarigan, B., Chie-Leon, B., Rychak, E., Corral, L.G., Ren, Y.J., Wang, M., *et al.* (2014). Structure of the human Cereblon-DDB1-lenalidomide complex reveals basis for responsiveness to thalidomide analogs. Nature structural & molecular biology *21*, 803-809.

Chanan-Khan, A., Miller, K.C., Musial, L., Lawrence, D., Padmanabhan, S., Takeshita, K., Porter, C.W., Goodrich, D.W., Bernstein, Z.P., Wallace, P., *et al.* (2006). Clinical efficacy of lenalidomide in patients with relapsed or refractory chronic lymphocytic leukemia: results of a phase II study. J Clin Oncol *24*, 5343-5349.

Chang, C., Storer, B.E., Scott, B.L., Bryant, E.M., Shulman, H.M., Flowers, M.E., Sandmaier, B.M., Witherspoon, R.P., Nash, R.A., Sanders, J.E., *et al.* (2007). Hematopoietic cell transplantation in patients with myelodysplastic syndrome or acute myeloid leukemia arising from myelodysplastic syndrome: similar outcomes in patients with de novo disease and disease following prior therapy or antecedent hematologic disorders. Blood *110*, 1379-1387.

Chen, C.I., Bergsagel, P.L., Paul, H., Xu, W., Lau, A., Dave, N., Kukreti, V., Wei, E., Leung-Hagesteijn, C., Li, Z.H., *et al.* (2011). Single-agent lenalidomide in the treatment of previously untreated chronic lymphocytic leukemia. J Clin Oncol *29*, 1175-1181.

Chen, Y., Gou, X., Ke, X., Cui, H., and Chen, Z. (2012). Human tumor cells induce angiogenesis through positive feedback between CD147 and insulin-like growth factor-I. PLoS One *7*, e40965.

Chen, Y., Zhang, H., Gou, X., Horikawa, Y., Xing, J., and Chen, Z. (2009). Upregulation of HAb18G/CD147 in activated human umbilical vein endothelial cells enhances the angiogenesis. Cancer letters *278*, 113-121.

Chen, Z.N., Mi, L., Xu, J., Song, F., Zhang, Q., Zhang, Z., Xing, J.L., Bian, H.J., Jiang, J.L., Wang, X.H., *et al.* (2006). Targeting radioimmunotherapy of hepatocellular carcinoma with iodine (131I) metuximab injection: clinical phase I/II trials. International journal of radiation oncology, biology, physics *65*, 435-444.

Chesi, M., Bergsagel, P.L., Shonukan, O.O., Martelli, M.L., Brents, L.A., Chen, T., Schrock, E., Ried, T., and Kuehl, W.M. (1998). Frequent dysregulation of the c-maf proto-oncogene at 16q23 by translocation to an Ig locus in multiple myeloma. Blood *91*, 4457-4463.

Choueiri, T.K., Dreicer, R., Rini, B.I., Elson, P., Garcia, J.A., Thakkar, S.G., Baz, R.C., Mekhail, T.M., Jinks, H.A., and Bukowski, R.M. (2006). Phase II study of lenalidomide in patients with metastatic renal cell carcinoma. Cancer *107*, 2609-2616.

Clague, M.J., and Urbe, S. (2010). Ubiquitin: same molecule, different degradation pathways. Cell *143*, 682-685.

Cogle, C.R., Craig, B.M., Rollison, D.E., and List, A.F. (2011). Incidence of the myelodysplastic syndromes using a novel claims-based algorithm: high number of uncaptured cases by cancer registries. Blood *117*, 7121-7125.

Colla, S., Storti, P., Donofrio, G., Todoerti, K., Bolzoni, M., Lazzaretti, M., Abeltino, M., Ippolito, L., Neri, A., Ribatti, D., *et al.* (2010). Low bone marrow oxygen tension and hypoxia-inducible factor-1alpha overexpression characterize patients with multiple myeloma: role on the transcriptional and proangiogenic profiles of CD138(+) cells. Leukemia *24*, 1967-1970.

Cortes, M., and Georgopoulos, K. (2004). Aiolos is required for the generation of high affinity bone marrow plasma cells responsible for long-term immunity. J Exp Med *199*, 209-219.

Curtin, K.D., Meinertzhagen, I.A., and Wyman, R.J. (2005). Basigin (EMMPRIN/CD147) interacts with integrin to affect cellular architecture. J Cell Sci *118*, 2649-2660.

D'Amato, R.J., Lentzsch, S., and Rogers, M.S. (2013). Pomalidomide is strongly antiangiogenic and teratogenic in relevant animal models. Proc Natl Acad Sci U S A.

D'Amato, R.J., Loughnan, M.S., Flynn, E., and Folkman, J. (1994). Thalidomide is an inhibitor of angiogenesis. Proc Natl Acad Sci U S A *91*, 4082-4085.

Dai, J.Y., Dou, K.F., Wang, C.H., Zhao, P., Lau, W.B., Tao, L., Wu, Y.M., Tang, J., Jiang, J.L., and Chen, Z.N. (2009). The interaction of HAb18G/CD147 with integrin alpha6beta1 and its implications for the invasion potential of human hepatoma cells. BMC cancer *9*, 337.

Davis, H.E., Morgan, J.R., and Yarmush, M.L. (2002). Polybrene increases retrovirus gene transfer efficiency by enhancing receptor-independent virus adsorption on target cell membranes. Biophysical chemistry *97*, 159-172.

de Vries, J.F., Te Marvelde, J.G., Wind, H.K., van Dongen, J.J., and van der Velden, V.H. (2010). The potential use of basigin (CD147) as a prognostic marker in B-cell precursor acute lymphoblastic leukaemia. Br J Haematol *150*, 624-626.

Delyon, J., Khayati, F., Djaafri, I., Podgorniak, M.P., Sadoux, A., Setterblad, N., Boutalbi, Z., Maouche, K., Maskos, U., Menashi, S.*, et al.* (2015). EMMPRIN regulates beta1 integrin-mediated adhesion through Kindlin-3 in human melanoma cells. Experimental dermatology *24*, 443-448.

Deora, A.A., Philp, N., Hu, J., Bok, D., and Rodriguez-Boulan, E. (2005). Mechanisms regulating tissue-specific polarity of monocarboxylate transporters and their chaperone CD147 in kidney and retinal epithelia. Proc Natl Acad Sci U S A *102*, 16245-16250.

Dimopoulos, M., Spencer, A., Attal, M., Prince, H.M., Harousseau, J.L., Dmoszynska, A., San Miguel, J., Hellmann, A., Facon, T., Foa, R.*, et al.* (2007). Lenalidomide plus dexamethasone for relapsed or refractory multiple myeloma. N Engl J Med *357*, 2123-2132.

Dimopoulos, M.A., Kastritis, E., Rosinol, L., Blade, J., and Ludwig, H. (2008). Pathogenesis and treatment of renal failure in multiple myeloma. Leukemia *22*, 1485-1493.

Doherty, J.R., Yang, C., Scott, K.E., Cameron, M.D., Fallahi, M., Li, W., Hall, M.A., Amelio, A.L., Mishra, J.K., Li, F.*, et al.* (2014). Blocking lactate export by inhibiting the Myc target MCT1 Disables glycolysis and glutathione synthesis. Cancer Res *74*, 908-920.

Durie, B.G., Harousseau, J.L., Miguel, J.S., Blade, J., Barlogie, B., Anderson, K., Gertz, M., Dimopoulos, M., Westin, J., Sonneveld, P.*, et al.* (2006). International uniform response criteria for multiple myeloma. Leukemia *20*, 1467-1473.

Durie, B.G., and Salmon, S.E. (1975). A clinical staging system for multiple myeloma. Correlation of measured myeloma cell mass with presenting clinical features, response to treatment, and survival. Cancer *36*, 842-854.

Ebert, B.L., Galili, N., Tamayo, P., Bosco, J., Mak, R., Pretz, J., Tanguturi, S., Ladd-Acosta, C., Stone, R., Golub, T.R.*, et al.* (2008a). An erythroid differentiation signature predicts response to lenalidomide in myelodysplastic syndrome. PLoS Med *5*, e35.

Ebert, B.L., Pretz, J., Bosco, J., Chang, C.Y., Tamayo, P., Galili, N., Raza, A., Root, D.E., Attar, E., Ellis, S.R., *et al.* (2008b). Identification of RPS14 as a 5q- syndrome gene by RNA interference screen. Nature *451*, 335-339.

Egawa, N., Koshikawa, N., Tomari, T., Nabeshima, K., Isobe, T., and Seiki, M. (2006). Membrane type 1 matrix metalloproteinase (MT1-MMP/MMP-14) cleaves and releases a 22-kDa extracellular matrix metalloproteinase inducer (EMMPRIN) fragment from tumor cells. J Biol Chem *281*, 37576-37585.

Eisen, T., Boshoff, C., Mak, I., Sapunar, F., Vaughan, M.M., Pyle, L., Johnston, S.R., Ahern, R., Smith, I.E., and Gore, M.E. (2000). Continuous low dose Thalidomide: a phase II study in advanced melanoma, renal cell, ovarian and breast cancer. British journal of cancer *82*, 812-817.

Eisen, T., Trefzer, U., Hamilton, A., Hersey, P., Millward, M., Knight, R.D., Jungnelius, J.U., and Glaspy, J. (2010). Results of a multicenter, randomized, double-blind phase 2/3 study of lenalidomide in the treatment of pretreated relapsed or refractory metastatic malignant melanoma. Cancer *116*, 146-154.

Engelhardt, M., Terpos, E., Kleber, M., Gay, F., Wasch, R., Morgan, G., Cavo, M., van de Donk, N., Beilhack, A., Bruno, B., *et al.* (2014). European Myeloma Network recommendations on the evaluation and treatment of newly diagnosed patients with multiple myeloma. Haematologica *99*, 232-242.

Epling-Burnette, P.K., Painter, J.S., Rollison, D.E., Ku, E., Vendron, D., Widen, R., Boulware, D., Zou, J.X., Bai, F., and List, A.F. (2007). Prevalence and clinical association of clonal T-cell expansions in Myelodysplastic Syndrome. Leukemia *21*, 659-667.

Falco, P., Cavallo, F., Larocca, A., Rossi, D., Guglielmelli, T., Rocci, A., Grasso, M., Siez, M.L., De Paoli, L., Oliva, S., *et al.* (2013). Lenalidomide-prednisone induction followed by lenalidomide-melphalan-prednisone consolidation and lenalidomide-prednisone maintenance in newly diagnosed elderly unfit myeloma patients. Leukemia *27*, 695-701.

Fehniger, T.A., Uy, G.L., Trinkaus, K., Nelson, A.D., Demland, J., Abboud, C.N., Cashen, A.F., Stockerl-Goldstein, K.E., Westervelt, P., DiPersio, J.F., *et al.* (2011). A phase 2 study of high-dose lenalidomide as initial therapy for older patients with acute myeloid leukemia. Blood *117*, 1828-1833.

Felgner, P.L., Gadek, T.R., Holm, M., Roman, R., Chan, H.W., Wenz, M., Northrop, J.P., Ringold, G.M., and Danielsen, M. (1987). Lipofection: a highly efficient, lipid-mediated DNA-transfection procedure. Proc Natl Acad Sci U S A *84*, 7413-7417.

Fenaux, P., Giagounidis, A., Selleslag, D., Beyne-Rauzy, O., Mufti, G., Mittelman, M., Muus, P., Te Boekhorst, P., Sanz, G., Del Canizo, C., *et al.* (2011). A randomized phase 3 study of lenalidomide versus placebo in RBC transfusion-dependent patients with Low-/Intermediate-1-risk myelodysplastic syndromes with del5q. Blood *118*, 3765-3776.

Fenaux, P., Mufti, G.J., Hellstrom-Lindberg, E., Santini, V., Finelli, C., Giagounidis, A., Schoch, R., Gattermann, N., Sanz, G., List, A., *et al.* (2009). Efficacy of azacitidine compared with that of conventional care regimens in the treatment of higher-risk myelodysplastic syndromes: a randomised, open-label, phase III study. The Lancet Oncology *10*, 223-232.

Fernandez-Saiz, V., Targosz, B.S., Lemeer, S., Eichner, R., Langer, C., Bullinger, L., Reiter, C., Slotta-Huspenina, J., Schroeder, S., Knorn, A.M., *et al.* (2013). SCFFbxo9 and CK2 direct the cellular response to growth factor withdrawal via Tel2/Tti1 degradation and promote survival in multiple myeloma. Nat Cell Biol *15*, 72-81.

Ferrajoli, A., Lee, B.N., Schlette, E.J., O'Brien, S.M., Gao, H., Wen, S., Wierda, W.G., Estrov, Z., Faderl, S., Cohen, E.N., *et al.* (2008). Lenalidomide induces complete and partial remissions in patients with relapsed and refractory chronic lymphocytic leukemia. Blood *111*, 5291-5297.

Figg, W.D., Dahut, W., Duray, P., Hamilton, M., Tompkins, A., Steinberg, S.M., Jones, E., Premkumar, A., Linehan, W.M., Floeter, M.K., *et al.* (2001). A randomized phase II trial of thalidomide, an angiogenesis inhibitor, in patients with androgen-independent prostate cancer. Clinical cancer research : an official journal of the American Association for Cancer Research *7*, 1888-1893.

Fischer, E.S., Bohm, K., Lydeard, J.R., Yang, H., Stadler, M.B., Cavadini, S., Nagel, J., Serluca, F., Acker, V., Lingaraju, G.M., *et al.* (2014). Structure of the DDB1-CRBN E3 ubiquitin ligase in complex with thalidomide. Nature *512*, 49-53.

Folkman, J. (1971). Tumor angiogenesis: therapeutic implications. N Engl J Med *285*, 1182-1186.

Fonseca, R., Bergsagel, P.L., Drach, J., Shaughnessy, J., Gutierrez, N., Stewart, A.K., Morgan, G., Van Ness, B., Chesi, M., Minvielle, S., *et al.* (2009). International Myeloma Working Group molecular classification of multiple myeloma: spotlight review. Leukemia *23*, 2210-2221.

Fonseca, R., Blood, E.A., Oken, M.M., Kyle, R.A., Dewald, G.W., Bailey, R.J., Van Wier, S.A., Henderson, K.J., Hoyer, J.D., Harrington, D., *et al.* (2002). Myeloma and the t(11;14)(q13;q32); evidence for a biologically defined unique subset of patients. Blood *99*, 3735-3741.

Fort, D.J., Stover, E.L., Bantle, J.A., and Finch, R.A. (2000). Evaluation of the developmental toxicity of thalidomide using frog embryo teratogenesis assay-xenopus (FETAX): biotransformation and detoxification. Teratogenesis, carcinogenesis, and mutagenesis *20*, 35-47.

Fowler, N.H., Davis, R.E., Rawal, S., Nastoupil, L., Hagemeister, F.B., McLaughlin, P., Kwak, L.W., Romaguera, J.E., Fanale, M.A., Fayad, L.E., *et al.* (2014). Safety and activity of lenalidomide and rituximab in untreated indolent lymphoma: an open-label, phase 2 trial. The Lancet Oncology *15*, 1311-1318.

Frederick, J.W., Sweeny, L., Hartman, Y., Zhou, T., and Rosenthal, E.L. (2016). Epidermal growth factor receptor inhibition by anti-CD147 therapy in cutaneous squamous cell carcinoma. Head & neck *38*, 247-252.

Fu, J., Fu, J., Chen, X., Zhang, Y., Gu, H., and Bai, Y. (2010). CD147 and VEGF co-expression predicts prognosis in patients with acute myeloid leukemia. Japanese journal of clinical oncology *40*, 1046-1052.

Fu, Z.G., Wang, L., Cui, H.Y., Peng, J.L., Wang, S.J., Geng, J.J., Liu, J.D., Feng, F., Song, F., Li, L., *et al.* (2016). A novel small-molecule compound targeting CD147 inhibits the motility and invasion of hepatocellular carcinoma cells. Oncotarget *7*, 9429-9447.

Futamura, N., Nishida, Y., Urakawa, H., Kozawa, E., Ikuta, K., Hamada, S., and Ishiguro, N. (2014). EMMPRIN co-expressed with matrix metalloproteinases predicts poor prognosis in patients with osteosarcoma. Tumour biology : the journal of the International Society for Oncodevelopmental Biology and Medicine *35*, 5159-5165.

Gandhi, A.K., Kang, J., Havens, C.G., Conklin, T., Ning, Y., Wu, L., Ito, T., Ando, H., Waldman, M.F., Thakurta, A., *et al.* (2014a). Immunomodulatory agents lenalidomide and pomalidomide co-stimulate T cells by inducing degradation of T cell repressors Ikaros and Aiolos via modulation of the E3 ubiquitin ligase complex CRL4(CRBN.). Br J Haematol *164*, 811-821.

Gandhi, A.K., Mendy, D., Waldman, M., Chen, G., Rychak, E., Miller, K., Gaidarova, S., Ren, Y., Wang, M., Breider, M., *et al.* (2014b). Measuring cereblon as a biomarker of response or resistance to lenalidomide and pomalidomide requires use of standardized reagents and understanding of gene complexity. Br J Haematol *164*, 233-244.

Gao, H., Jiang, Q., Han, Y., Peng, J., and Wang, C. (2015). shRNA-mediated EMMPRIN silencing inhibits human leukemic monocyte lymphoma U937 cell proliferation and increases chemosensitivity to adriamycin. Cell biochemistry and biophysics *71*, 827-835.

Garcia-Sanz, R., Gonzalez-Porras, J.R., Hernandez, J.M., Polo-Zarzuela, M., Sureda, A., Barrenetxea, C., Palomera, L., Lopez, R., Grande-Garcia, C., Alegre, A.*, et al.* (2004). The oral combination of thalidomide, cyclophosphamide and dexamethasone (ThaCyDex) is effective in relapsed/refractory multiple myeloma. Leukemia *18*, 856-863.

Georgopoulos, K., Bigby, M., Wang, J.H., Molnar, A., Wu, P., Winandy, S., and Sharpe, A. (1994). The Ikaros gene is required for the development of all lymphoid lineages. Cell *79*, 143-156.

Germing, U., Hildebrandt, B., Pfeilstocker, M., Nosslinger, T., Valent, P., Fonatsch, C., Lubbert, M., Haase, D., Steidl, C., Krieger, O.*, et al.* (2005). Refinement of the international prognostic scoring system (IPSS) by including LDH as an additional prognostic variable to improve risk assessment in patients with primary myelodysplastic syndromes (MDS). Leukemia *19*, 2223-2231.

Giagounidis, A., Mufti, G.J., Fenaux, P., Germing, U., List, A., and MacBeth, K.J. (2014). Lenalidomide as a disease-modifying agent in patients with del(5q) myelodysplastic syndromes: linking mechanism of action to clinical outcomes. Annals of hematology *93*, 1-11.

Gloeckner, C.J., Boldt, K., Schumacher, A., Roepman, R., and Ueffing, M. (2007). A novel tandem affinity purification strategy for the efficient isolation and characterisation of native protein complexes. Proteomics *7*, 4228-4234.

Graham, F.L., and van der Eb, A.J. (1973). A new technique for the assay of infectivity of human adenovirus 5 DNA. Virology *52*, 456-467.

Graubert, T.A., Payton, M.A., Shao, J., Walgren, R.A., Monahan, R.S., Frater, J.L., Walshauser, M.A., Martin, M.G., Kasai, Y., and Walter, M.J. (2009). Integrated genomic analysis implicates haploinsufficiency of multiple chromosome 5q31.2 genes in de novo myelodysplastic syndromes pathogenesis. PLoS One *4*, e4583.

Greenberg, A.J., Walters, D.K., Kumar, S.K., Vincent Rajkumar, S., and Jelinek, D.F. (2013). Responsiveness of cytogenetically discrete human myeloma cell lines to lenalidomide: lack of correlation with cereblon and interferon regulatory factor 4 expression levels. Eur J Haematol.

Greenberg, P., Cox, C., LeBeau, M.M., Fenaux, P., Morel, P., Sanz, G., Sanz, M., Vallespi, T., Hamblin, T., Oscier, D.*, et al.* (1997). International scoring system for evaluating prognosis in myelodysplastic syndromes. Blood *89*, 2079-2088.

Greenberg, P.L., Sun, Z., Miller, K.B., Bennett, J.M., Tallman, M.S., Dewald, G., Paietta, E., van der Jagt, R., Houston, J., Thomas, M.L.*, et al.* (2009). Treatment of myelodysplastic syndrome patients with erythropoietin with or without granulocyte colony-stimulating factor: results of a prospective randomized phase 3 trial by the Eastern Cooperative Oncology Group (E1996). Blood *114*, 2393-2400.

Greipp, P.R., San Miguel, J., Durie, B.G., Crowley, J.J., Barlogie, B., Blade, J., Boccadoro, M., Child, J.A., Avet-Loiseau, H., Kyle, R.A.*, et al.* (2005). International staging system for multiple myeloma. J Clin Oncol *23*, 3412-3420.

Guo, H., Zucker, S., Gordon, M.K., Toole, B.P., and Biswas, C. (1997). Stimulation of matrix metalloproteinase production by recombinant extracellular matrix metalloproteinase inducer from transfected Chinese hamster ovary cells. J Biol Chem *272*, 24-27.

Gupta, D., Treon, S.P., Shima, Y., Hideshima, T., Podar, K., Tai, Y.T., Lin, B., Lentzsch, S., Davies, F.E., Chauhan, D.*, et al.* (2001). Adherence of multiple myeloma cells to bone marrow stromal cells upregulates vascular endothelial growth factor secretion: therapeutic applications. Leukemia *15*, 1950-1961.

Gutierrez-Rodriguez, O. (1984). Thalidomide. A promising new treatment for rheumatoid arthritis. Arthritis and rheumatism *27*, 1118-1121.

Habermann, T.M., Lossos, I.S., Justice, G., Vose, J.M., Wiernik, P.H., McBride, K., Wride, K., Ervin-Haynes, A., Takeshita, K., Pietronigro, D.*, et al.* (2009). Lenalidomide oral monotherapy produces a high response rate in patients with relapsed or refractory mantle cell lymphoma. Br J Haematol *145*, 344-349.

Halestrap, A.P. (2013). Monocarboxylic acid transport. Comprehensive Physiology *3*, 1611-1643.

Halestrap, A.P., and Price, N.T. (1999). The proton-linked monocarboxylate transporter (MCT) family: structure, function and regulation. Biochem J *343 Pt 2*, 281-299.

Halestrap, A.P., and Wilson, M.C. (2012). The monocarboxylate transporter family--role and regulation. IUBMB life *64*, 109-119.

Hanson, D.J., Nakamura, S., Amachi, R., Hiasa, M., Oda, A., Tsuji, D., Itoh, K., Harada, T., Horikawa, K., Teramachi, J.*, et al.* (2015). Effective impairment of myeloma cells and their progenitors by blockade of monocarboxylate transportation. Oncotarget *6*, 33568-33586.

Hartl, F.U. (1996). Molecular chaperones in cellular protein folding. Nature *381*, 571-579.

Haslett, P.A., Corral, L.G., Albert, M., and Kaplan, G. (1998). Thalidomide costimulates primary human T lymphocytes, preferentially inducing proliferation, cytokine production, and cytotoxic responses in the CD8+ subset. J Exp Med *187*, 1885-1892.

He, Y.J., McCall, C.M., Hu, J., Zeng, Y., and Xiong, Y. (2006). DDB1 functions as a linker to recruit receptor WD40 proteins to CUL4-ROC1 ubiquitin ligases. Genes & development *20*, 2949-2954.

Heintel, D., Rocci, A., Ludwig, H., Bolomsky, A., Caltagirone, S., Schreder, M., Pfeifer, S., Gisslinger, H., Zojer, N., Jager, U.*, et al.* (2013). High expression of cereblon (CRBN) is associated with improved clinical response in patients with multiple myeloma treated with lenalidomide and dexamethasone. Br J Haematol.

Hendrickx, A.G., and Sawyer, R.H. (1978). Developmental staging and thalidomide teratogenicity in the green monkey (Cercopithecus aethiops). Teratology *18*, 393-404.

Hershko, A., and Ciechanover, A. (1998). The ubiquitin system. Annual review of biochemistry *67*, 425-479.

Hicke, L. (2001). Protein regulation by monoubiquitin. Nature reviews Molecular cell biology *2*, 195-201.

Hideshima, T., and Anderson, K.C. (2002). Molecular mechanisms of novel therapeutic approaches for multiple myeloma. Nat Rev Cancer *2*, 927-937.

Hideshima, T., Chauhan, D., Shima, Y., Raje, N., Davies, F.E., Tai, Y.T., Treon, S.P., Lin, B., Schlossman, R.L., Richardson, P.*, et al.* (2000). Thalidomide and its analogs overcome drug resistance of human multiple myeloma cells to conventional therapy. Blood *96*, 2943-2950.

Hideshima, T., Mitsiades, C., Tonon, G., Richardson, P.G., and Anderson, K.C. (2007). Understanding multiple myeloma pathogenesis in the bone marrow to identify new therapeutic targets. Nat Rev Cancer *7*, 585-598.

Higgins, J.J., Hao, J., Kosofsky, B.E., and Rajadhyaksha, A.M. (2008). Dysregulation of large-conductance Ca2+-activated K+ channel expression in nonsyndromal mental retardation due to a cereblon p.R419X mutation. Neurogenetics *9*, 219-223.

Higgins, J.J., Pucilowska, J., Lombardi, R.Q., and Rooney, J.P. (2004). A mutation in a novel ATP-dependent Lon protease gene in a kindred with mild mental retardation. Neurology *63*, 1927-1931.

Higgins, J.J., Rosen, D.R., Loveless, J.M., Clyman, J.C., and Grau, M.J. (2000). A gene for nonsyndromic mental retardation maps to chromosome 3p25-pter. Neurology *55*, 335-340.

Hohberger, B., and Enz, R. (2009). Cereblon is expressed in the retina and binds to voltage-gated chloride channels. FEBS Lett *583*, 633-637.

Horger, M., Kanz, L., Denecke, B., Vonthein, R., Pereira, P., Claussen, C.D., and Driessen, C. (2007). The benefit of using whole-body, low-dose, nonenhanced, multidetector computed tomography for follow-up and therapy response monitoring in patients with multiple myeloma. Cancer *109*, 1617-1626.

Hu, J., Dang, N., Yao, H., Li, Y., Zhang, H., Yang, X., Xu, J., Bian, H., Xing, J., Zhu, P.*, et al.* (2010). Involvement of HAb18G/CD147 in T cell activation and immunological synapse formation. J Cell Mol Med *14*, 2132-2143.

Huang, S.Y., Lin, C.W., Lin, H.H., Yao, M., Tang, J.L., Wu, S.J., Chen, Y.C., Lu, H.Y., Hou, H.A., Chen, C.Y.*, et al.* (2014). Expression of cereblon protein assessed by immunohistochemicalstaining in myeloma cells is associated with superior response of thalidomide- and lenalidomide-based treatment, but not bortezomib-based treatment, in patients with multiple myeloma. Annals of hematology *93*, 1371-1380.

Huang, W., Luo, W.J., Zhu, P., Tang, J., Yu, X.L., Cui, H.Y., Wang, B., Zhang, Y., Jiang, J.L., and Chen, Z.N. (2013a). Modulation of CD147-induced matrix metalloproteinase activity: role of CD147 N-glycosylation. Biochem J *449*, 437-448.

Huang, Z., Wang, L., Wang, Y., Zhuo, Y., Li, H., Chen, J., and Chen, W. (2013b). Overexpression of CD147 contributes to the chemoresistance of head and neck squamous cell carcinoma cells. J Oral Pathol Med.

Hung, K.H., Su, S.T., Chen, C.Y., Hsu, P.H., Huang, S.Y., Wu, W.J., Chen, M.M., Chen, H.Y., Wu, P.C., Lin, F.R.*, et al.* (2016). Aiolos collaborates with Blimp-1 to regulate the survival of multiple myeloma cells. Cell death and differentiation.

Iacono, K.T., Brown, A.L., Greene, M.I., and Saouaf, S.J. (2007). CD147 immunoglobulin superfamily receptor function and role in pathology. Exp Mol Pathol *83*, 283-295.

Ito, T., Ando, H., and Handa, H. (2011). Teratogenic effects of thalidomide: molecular mechanisms. Cell Mol Life Sci *68*, 1569-1579.

Ito, T., Ando, H., Suzuki, T., Ogura, T., Hotta, K., Imamura, Y., Yamaguchi, Y., and Handa, H. (2010). Identification of a primary target of thalidomide teratogenicity. Science *327*, 1345-1350.

Iyer, C.G., Languillon, J., Ramanujam, K., Tarabini-Castellani, G., De las Aguas, J.T., Bechelli, L.M., Uemura, K., Martinez Dominguez, V., and Sundaresan, T. (1971). WHO co-ordinated short-term double-blind trial with thalidomide in the treatment of acute lepra reactions in male lepromatous patients. Bulletin of the World Health Organization *45*, 719-732.

Jaras, M., Miller, P.G., Chu, L.P., Puram, R.V., Fink, E.C., Schneider, R.K., Al-Shahrour, F., Pena, P., Breyfogle, L.J., Hartwell, K.A.*, et al.* (2014). Csnk1a1 inhibition has p53-dependent therapeutic efficacy in acute myeloid leukemia. J Exp Med *211*, 605-612.

Jiang, Y., Dunbar, A., Gondek, L.P., Mohan, S., Rataul, M., O'Keefe, C., Sekeres, M., Saunthararajah, Y., and Maciejewski, J.P. (2009). Aberrant DNA methylation is a dominant mechanism in MDS progression to AML. Blood *113*, 1315-1325.

Jo, S., Lee, K.H., Song, S., Jung, Y.K., and Park, C.S. (2005). Identification and functional characterization of cereblon as a binding protein for large-conductance calcium-activated potassium channel in rat brain. J Neurochem *94*, 1212-1224.

Jonasova, A., Bokorova, R., Polak, J., Vostry, M., Kostecka, A., Hajkova, H., Neuwirtova, R., Siskova, M., Sponerova, D., Cermak, J.*, et al.* (2015). High level of full-length cereblon mRNA in lower risk

myelodysplastic syndrome with isolated 5q deletion is implicated in the efficacy of lenalidomide. Eur J Haematol *95*, 27-34.

Juliusson, G., Celsing, F., Turesson, I., Lenhoff, S., Adriansson, M., and Malm, C. (2000). Frequent good partial remissions from thalidomide including best response ever in patients with advanced refractory and relapsed myeloma. Br J Haematol *109*, 89-96.

Kantarjian, H., Issa, J.P., Rosenfeld, C.S., Bennett, J.M., Albitar, M., DiPersio, J., Klimek, V., Slack, J., de Castro, C., Ravandi, F.*, et al.* (2006). Decitabine improves patient outcomes in myelodysplastic syndromes: results of a phase III randomized study. Cancer *106*, 1794-1803.

Kao, T.Y., Chiu, Y.C., Fang, W.C., Cheng, C.W., Kuo, C.Y., Juan, H.F., Wu, S.H., and Lee, A.Y. (2015). Mitochondrial Lon regulates apoptosis through the association with Hsp60-mtHsp70 complex. Cell death & disease *6*, e1642.

Kasinrerk, W., Fiebiger, E., Stefanova, I., Baumruker, T., Knapp, W., and Stockinger, H. (1992). Human leukocyte activation antigen M6, a member of the Ig superfamily, is the species homologue of rat OX-47, mouse basigin, and chicken HT7 molecule. J Immunol *149*, 847-854.

Keith, T., Araki, Y., Ohyagi, M., Hasegawa, M., Yamamoto, K., Kurata, M., Nakagawa, Y., Suzuki, K., and Kitagawa, M. (2007). Regulation of angiogenesis in the bone marrow of myelodysplastic syndromes transforming to overt leukaemia. Br J Haematol *137*, 206-215.

Keizman, D., Zahurak, M., Sinibaldi, V., Carducci, M., Denmeade, S., Drake, C., Pili, R., Antonarakis, E.S., Hudock, S., and Eisenberger, M. (2010). Lenalidomide in nonmetastatic biochemically relapsed prostate cancer: results of a phase I/II double-blinded, randomized study. Clinical cancer research : an official journal of the American Association for Cancer Research *16*, 5269-5276.

Kelaidi, C., Park, S., Brechignac, S., Mannone, L., Vey, N., Dombret, H., Aljassem, L., Stamatoullas, A., Ades, L., Giraudier, S.*, et al.* (2008). Treatment of myelodysplastic syndromes with 5q deletion before the lenalidomide era; the GFM experience with EPO and thalidomide. Leuk Res *32*, 1049-1053.

Kennedy, K.M., and Dewhirst, M.W. (2010). Tumor metabolism of lactate: the influence and therapeutic potential for MCT and CD147 regulation. Future Oncol *6*, 127-148.

Kirk, P., Wilson, M.C., Heddle, C., Brown, M.H., Barclay, A.N., and Halestrap, A.P. (2000). CD147 is tightly associated with lactate transporters MCT1 and MCT4 and facilitates their cell surface expression. EMBO J *19*, 3896-3904.

Knop, S., Gerecke, C., Liebisch, P., Topp, M.S., Platzbecker, U., Sezer, O., Vollmuth, C., Falk, K., Glasmacher, A., Maeder, U.*, et al.* (2009). Lenalidomide, adriamycin, and dexamethasone (RAD) in patients with relapsed and refractory multiple myeloma: a report from the German Myeloma Study Group DSMM (Deutsche Studiengruppe Multiples Myelom). Blood *113*, 4137-4143.

Koehne, G., and Giralt, S. (2012). Allogeneic hematopoietic stem cell transplantation for multiple myeloma: curative but not the standard of care. Curr Opin Oncol *24*, 720-726.

Kordasti, S.Y., Afzali, B., Lim, Z., Ingram, W., Hayden, J., Barber, L., Matthews, K., Chelliah, R., Guinn, B., Lombardi, G.*, et al.* (2009). IL-17-producing CD4(+) T cells, pro-inflammatory cytokines and apoptosis are increased in low risk myelodysplastic syndrome. Br J Haematol *145*, 64-72.

Kroger, N., Badbaran, A., Zabelina, T., Ayuk, F., Wolschke, C., Alchalby, H., Klyuchnikov, E., Atanackovic, D., Schilling, G., Hansen, T.*, et al.* (2013). Impact of high-risk cytogenetics and achievement of molecular remission on long-term freedom from disease after autologous-allogeneic tandem transplantation in patients with multiple myeloma. Biology of blood and marrow transplantation : journal of the American Society for Blood and Marrow Transplantation *19*, 398-404.

Kronke, J., Fink, E.C., Hollenbach, P.W., MacBeth, K.J., Hurst, S.N., Udeshi, N.D., Chamberlain, P.P., Mani, D.R., Man, H.W., Gandhi, A.K., *et al.* (2015). Lenalidomide induces ubiquitination and degradation of CK1alpha in del(5q) MDS. Nature *523*, 183-188.

Kronke, J., Udeshi, N.D., Narla, A., Grauman, P., Hurst, S.N., McConkey, M., Svinkina, T., Heckl, D., Comer, E., Li, X., *et al.* (2014). Lenalidomide causes selective degradation of IKZF1 and IKZF3 in multiple myeloma cells. Science *343*, 301-305.

Kruse, F.E., Joussen, A.M., Rohrschneider, K., Becker, M.D., and Volcker, H.E. (1998). Thalidomide inhibits corneal angiogenesis induced by vascular endothelial growth factor. Graefe's archive for clinical and experimental ophthalmology = Albrecht von Graefes Archiv fur klinische und experimentelle Ophthalmologie *236*, 461-466.

Kuehl, W.M., and Bergsagel, P.L. (2002). Multiple myeloma: evolving genetic events and host interactions. Nat Rev Cancer *2*, 175-187.

Kumar, S., Witzig, T.E., Dispenzieri, A., Lacy, M.Q., Wellik, L.E., Fonseca, R., Lust, J.A., Gertz, M.A., Kyle, R.A., Greipp, P.R., *et al.* (2004). Effect of thalidomide therapy on bone marrow angiogenesis in multiple myeloma. Leukemia *18*, 624-627.

Kumar, S.K., Rajkumar, S.V., Dispenzieri, A., Lacy, M.Q., Hayman, S.R., Buadi, F.K., Zeldenrust, S.R., Dingli, D., Russell, S.J., Lust, J.A., *et al.* (2008). Improved survival in multiple myeloma and the impact of novel therapies. Blood *111*, 2516-2520.

Kyle, R.A., Gertz, M.A., Witzig, T.E., Lust, J.A., Lacy, M.Q., Dispenzieri, A., Fonseca, R., Rajkumar, S.V., Offord, J.R., Larson, D.R., *et al.* (2003). Review of 1027 patients with newly diagnosed multiple myeloma. Mayo Clin Proc *78*, 21-33.

Kyle, R.A., and Rajkumar, S.V. (2009). Criteria for diagnosis, staging, risk stratification and response assessment of multiple myeloma. Leukemia *23*, 3-9.

Lacy, M.Q., Hayman, S.R., Gertz, M.A., Dispenzieri, A., Buadi, F., Kumar, S., Greipp, P.R., Lust, J.A., Russell, S.J., Dingli, D., *et al.* (2009). Pomalidomide (CC4047) plus low-dose dexamethasone as therapy for relapsed multiple myeloma. J Clin Oncol *27*, 5008-5014.

Le Floch, R., Chiche, J., Marchiq, I., Naiken, T., Ilc, K., Murray, C.M., Critchlow, S.E., Roux, D., Simon, M.P., and Pouyssegur, J. (2011). CD147 subunit of lactate/H+ symporters MCT1 and hypoxia-inducible MCT4 is critical for energetics and growth of glycolytic tumors. Proc Natl Acad Sci U S A *108*, 16663-16668.

Lee, A., Rode, A., Nicoll, A., Maczurek, A.E., Lim, L., Lim, S., Angus, P., Kronborg, I., Arachchi, N., Gorelik, A., *et al.* (2016). Circulating CD147 predicts mortality in advanced hepatocellular carcinoma. Journal of gastroenterology and hepatology *31*, 459-466.

Lee, J., and Zhou, P. (2007). DCAFs, the missing link of the CUL4-DDB1 ubiquitin ligase. Molecular cell *26*, 775-780.

Lee, K.M., Jo, S., Kim, H., Lee, J., and Park, C.S. (2011). Functional modulation of AMP-activated protein kinase by cereblon. Biochim Biophys Acta *1813*, 448-455.

Lee, K.M., Lee, J., and Park, C.S. (2012). Cereblon inhibits proteasome activity by binding to the 20S core proteasome subunit beta type 4. Biochem Biophys Res Commun *427*, 618-622.

Lee, K.M., Yang, S.J., Kim, Y.D., Choi, Y.D., Nam, J.H., Choi, C.S., Choi, H.S., and Park, C.S. (2013). Disruption of the cereblon gene enhances hepatic AMPK activity and prevents high-fat diet-induced obesity and insulin resistance in mice. Diabetes *62*, 1855-1864.

Lee, K.M., Yang, S.J., Park, S., Choi, Y.D., Shin, H.K., Pak, J.H., Park, C.S., and Kim, I. (2015). Depletion of the cereblon gene activates the unfolded protein response and protects cells from ER stress-induced cell death. Biochem Biophys Res Commun *458*, 34-39.

Lentzsch, S., Rogers, M.S., LeBlanc, R., Birsner, A.E., Shah, J.H., Treston, A.M., Anderson, K.C., and D'Amato, R.J. (2002). S-3-Amino-phthalimido-glutarimide inhibits angiogenesis and growth of B-cell neoplasias in mice. Cancer Res *62*, 2300-2305.

Li, J.K., Liao, J.H., Li, H., Kuo, C.I., Huang, K.F., Yang, L.W., Wu, S.H., and Chang, C.I. (2013). The N-terminal substrate-recognition domain of a LonC protease exhibits structural and functional similarity to cytosolic chaperones. Acta crystallographica Section D, Biological crystallography *69*, 1789-1797.

Li, R., Huang, L., Guo, H., and Toole, B.P. (2001). Basigin (murine EMMPRIN) stimulates matrix metalloproteinase production by fibroblasts. J Cell Physiol *186*, 371-379.

Li, Y., Wu, J., Song, F., Tang, J., Wang, S.J., Yu, X.L., Chen, Z.N., and Jiang, J.L. (2012). Extracellular membrane-proximal domain of HAb18G/CD147 binds to metal ion-dependent adhesion site (MIDAS) motif of integrin beta1 to modulate malignant properties of hepatoma cells. J Biol Chem *287*, 4759-4772.

Liberti, M.V., and Locasale, J.W. (2016). The Warburg Effect: How Does it Benefit Cancer Cells? Trends Biochem Sci *41*, 211-218.

List, A., Dewald, G., Bennett, J., Giagounidis, A., Raza, A., Feldman, E., Powell, B., Greenberg, P., Thomas, D., Stone, R.*, et al.* (2006). Lenalidomide in the myelodysplastic syndrome with chromosome 5q deletion. N Engl J Med *355*, 1456-1465.

List, A., Kurtin, S., Roe, D.J., Buresh, A., Mahadevan, D., Fuchs, D., Rimsza, L., Heaton, R., Knight, R., and Zeldis, J.B. (2005). Efficacy of lenalidomide in myelodysplastic syndromes. N Engl J Med *352*, 549-557.

Lo, Y.H., Ho, P.C., and Wang, S.C. (2012). Epidermal growth factor receptor protects proliferating cell nuclear antigen from cullin 4A protein-mediated proteolysis. J Biol Chem *287*, 27148-27157.

Lode, L., Amiot, M., Maiga, S., Touzeau, C., Menard, A., Magrangeas, F., Minvielle, S., Pellat-Deceunynck, C., Bene, M.C., and Moreau, P. (2013). Cereblon expression in multiple myeloma: not ready for prime time. Br J Haematol.

Loo, M.A., Jensen, T.J., Cui, L., Hou, Y., Chang, X.B., and Riordan, J.R. (1998). Perturbation of Hsp90 interaction with nascent CFTR prevents its maturation and accelerates its degradation by the proteasome. EMBO J *17*, 6879-6887.

Lopez-Girona, A., Heintel, D., Zhang, L.H., Mendy, D., Gaidarova, S., Brady, H., Bartlett, J.B., Schafer, P.H., Schreder, M., Bolomsky, A.*, et al.* (2011). Lenalidomide downregulates the cell survival factor, interferon regulatory factor-4, providing a potential mechanistic link for predicting response. Br J Haematol *154*, 325-336.

Lopez-Girona, A., Mendy, D., Ito, T., Miller, K., Gandhi, A.K., Kang, J., Karasawa, S., Carmel, G., Jackson, P., Abbasian, M.*, et al.* (2012). Cereblon is a direct protein target for immunomodulatory and antiproliferative activities of lenalidomide and pomalidomide. Leukemia *26*, 2445.

Lowry, O.H., Rosebrough, N.J., Farr, A.L., and Randall, R.J. (1951). Protein measurement with the Folin phenol reagent. J Biol Chem *193*, 265-275.

Lu, G., Middleton, R.E., Sun, H., Naniong, M., Ott, C.J., Mitsiades, C.S., Wong, K.K., Bradner, J.E., and Kaelin, W.G., Jr. (2014). The myeloma drug lenalidomide promotes the cereblon-dependent destruction of Ikaros proteins. Science *343*, 305-309.

Lupas, A.N., Zhu, H., and Korycinski, M. (2015). The thalidomide-binding domain of cereblon defines the CULT domain family and is a new member of the beta-tent fold. PLoS computational biology *11*, e1004023.

Mahony, C., Erskine, L., Niven, J., Greig, N.H., Figg, W.D., and Vargesson, N. (2013). Pomalidomide is nonteratogenic in chicken and zebrafish embryos and nonneurotoxic in vitro. Proc Natl Acad Sci U S A *110*, 12703-12708.

Majumdar, S., Lamothe, B., and Aggarwal, B.B. (2002). Thalidomide suppresses NF-kappa B activation induced by TNF and H2O2, but not that activated by ceramide, lipopolysaccharides, or phorbol ester. J Immunol *168*, 2644-2651.

Malcovati, L., Germing, U., Kuendgen, A., Della Porta, M.G., Pascutto, C., Invernizzi, R., Giagounidis, A., Hildebrandt, B., Bernasconi, P., Knipp, S.*, et al.* (2007). Time-dependent prognostic scoring system for predicting survival and leukemic evolution in myelodysplastic syndromes. J Clin Oncol *25*, 3503-3510.

Manoharan, C., Wilson, M.C., Sessions, R.B., and Halestrap, A.P. (2006). The role of charged residues in the transmembrane helices of monocarboxylate transporter 1 and its ancillary protein basigin in determining plasma membrane expression and catalytic activity. Molecular membrane biology *23*, 486-498.

Marriott, J.B., Clarke, I.A., Dredge, K., Muller, G., Stirling, D., and Dalgleish, A.G. (2002). Thalidomide and its analogues have distinct and opposing effects on TNF-alpha and TNFR2 during co-stimulation of both CD4(+) and CD8(+) T cells. Clin Exp Immunol *130*, 75-84.

Matsuoka, A., Tochigi, A., Kishimoto, M., Nakahara, T., Kondo, T., Tsujioka, T., Tasaka, T., Tohyama, Y., and Tohyama, K. (2010). Lenalidomide induces cell death in an MDS-derived cell line with deletion of chromosome 5q by inhibition of cytokinesis. Leukemia *24*, 748-755.

McCarthy, P.L., Owzar, K., Hofmeister, C.C., Hurd, D.D., Hassoun, H., Richardson, P.G., Giralt, S., Stadtmauer, E.A., Weisdorf, D.J., Vij, R.*, et al.* (2012). Lenalidomide after stem-cell transplantation for multiple myeloma. N Engl J Med *366*, 1770-1781.

McCarty, M.F. (1997). Thalidomide may impede cell migration in primates by down-regulating integrin beta-chains: potential therapeutic utility in solid malignancies, proliferative retinopathy, inflammatory disorders, neointimal hyperplasia, and osteoporosis. Medical hypotheses *49*, 123-131.

Mellin, G.W., and Katzenstein, M. (1962). The saga of thalidomide. Neuropathy to embryopathy, with case reports of congenital anomalies. N Engl J Med *267*, 1238-1244 concl.

Mesa, R.A., Yao, X., Cripe, L.D., Li, C.Y., Litzow, M., Paietta, E., Rowe, J.M., Tefferi, A., and Tallman, M.S. (2010). Lenalidomide and prednisone for myelofibrosis: Eastern Cooperative Oncology Group (ECOG) phase 2 trial E4903. Blood *116*, 4436-4438.

Miller, A.A., Case, D., Harmon, M., Savage, P., Lesser, G., Hurd, D., and Melin, S.A. (2007). Phase I study of lenalidomide in solid tumors. Journal of thoracic oncology : official publication of the International Association for the Study of Lung Cancer *2*, 445-449.

Miller, M.T., and Stromland, K. (1999). Teratogen update: thalidomide: a review, with a focus on ocular findings and new potential uses. Teratology *60*, 306-321.

Millimaggi, D., Mari, M., D'Ascenzo, S., Carosa, E., Jannini, E.A., Zucker, S., Carta, G., Pavan, A., and Dolo, V. (2007). Tumor vesicle-associated CD147 modulates the angiogenic capability of endothelial cells. Neoplasia *9*, 349-357.

Miyauchi, T., Masuzawa, Y., and Muramatsu, T. (1991). The basigin group of the immunoglobulin superfamily: complete conservation of a segment in and around transmembrane domains of human and mouse basigin and chicken HT7 antigen. Journal of biochemistry *110*, 770-774.

Mohamedali, A., and Mufti, G.J. (2009). Van-den Berghe's 5q- syndrome in 2008. Br J Haematol *144*, 157-168.

Moller, D.R., Wysocka, M., Greenlee, B.M., Ma, X., Wahl, L., Flockhart, D.A., Trinchieri, G., and Karp, C.L. (1997). Inhibition of IL-12 production by thalidomide. J Immunol *159*, 5157-5161.

Moreau, P., Masszi, T., Grzasko, N., Bahlis, N.J., Hansson, M., Pour, L., Sandhu, I., Ganly, P., Baker, B.W., Jackson, S.R., *et al.* (2016). Oral Ixazomib, Lenalidomide, and Dexamethasone for Multiple Myeloma. N Engl J Med *374*, 1621-1634.

Muller, G.W., Chen, R., Huang, S.Y., Corral, L.G., Wong, L.M., Patterson, R.T., Chen, Y., Kaplan, G., and Stirling, D.I. (1999). Amino-substituted thalidomide analogs: potent inhibitors of TNF-alpha production. Bioorg Med Chem Lett *9*, 1625-1630.

Mullis, K.B., and Faloona, F.A. (1987). Specific synthesis of DNA in vitro via a polymerase-catalyzed chain reaction. Methods in enzymology *155*, 335-350.

Nabhan, C., Patel, A., Villines, D., Tolzien, K., Kelby, S.K., and Lestingi, T.M. (2014). Lenalidomide monotherapy in chemotherapy-naive, castration-resistant prostate cancer patients: final results of a phase II study. Clinical genitourinary cancer *12*, 27-32.

Nagler, A., Ginzton, N., Negrin, R., Bang, D., Donlon, T., and Greenberg, P. (1990). Effects of recombinant human granulocyte colony stimulating factor and granulocyte-monocyte colony stimulating factor on in vitro hemopoiesis in the myelodysplastic syndromes. Leukemia *4*, 193-202.

Nakagawa, T., and Nakayama, K. (2015). Protein monoubiquitylation: targets and diverse functions. Genes to cells : devoted to molecular & cellular mechanisms *20*, 543-562.

Naruhashi, K., Kadomatsu, K., Igakura, T., Fan, Q.W., Kuno, N., Muramatsu, H., Miyauchi, T., Hasegawa, T., Itoh, A., Muramatsu, T., *et al.* (1997). Abnormalities of sensory and memory functions in mice lacking Bsg gene. Biochem Biophys Res Commun *236*, 733-737.

Neubert, R., Hinz, N., Thiel, R., and Neubert, D. (1996). Down-regulation of adhesion receptors on cells of primate embryos as a probable mechanism of the teratogenic action of thalidomide. Life sciences *58*, 295-316.

Nguyen, T.V., Lee, J.E., Sweredoski, M.J., Yang, S.J., Jeon, S.J., Harrison, J.S., Yim, J.H., Lee, S.G., Handa, H., Kuhlman, B., *et al.* (2016). Glutamine Triggers Acetylation-Dependent Degradation of Glutamine Synthetase via the Thalidomide Receptor Cereblon. Molecular cell *61*, 809-820.

Nikesitch, N., Tao, C., Lai, K., Killingsworth, M., Bae, S., Wang, M., Harrison, S., Roberts, T.L., and Ling, S.C. (2016). Predicting the response of multiple myeloma to the proteasome inhibitor Bortezomib by evaluation of the unfolded protein response. Blood cancer journal *6*, e432.

Nogueira, A.C., Neubert, R., Felies, A., Jacob-Muller, U., Frankus, E., and Neubert, D. (1996). Thalidomide derivatives and the immune system. 6. Effects of two derivatives with no obvious teratogenic potency on the pattern of integrins and other surface receptors on blood cells of marmosets. Life sciences *58*, 337-348.

Obeng, E.A., Carlson, L.M., Gutman, D.M., Harrington, W.J., Jr., Lee, K.P., and Boise, L.H. (2006). Proteasome inhibitors induce a terminal unfolded protein response in multiple myeloma cells. Blood *107*, 4907-4916.

Ocio, E.M., Fernandez-Lazaro, D., San-Segundo, L., Lopez-Corral, L., Corchete, L.A., Gutierrez, N.C., Garayoa, M., Paino, T., Garcia-Gomez, A., Delgado, M., *et al.* (2015). In vivo murine model of acquired resistance in myeloma reveals differential mechanisms for lenalidomide and pomalidomide in combination with dexamethasone. Leukemia *29*, 705-714.

Oranger, A., Carbone, C., Izzo, M., and Grano, M. (2013). Cellular mechanisms of multiple myeloma bone disease. Clinical & developmental immunology *2013*, 289458.

Palumbo, A., and Anderson, K. (2011). Multiple myeloma. N Engl J Med *364*, 1046-1060.

Palumbo, A., Avet-Loiseau, H., Oliva, S., Lokhorst, H.M., Goldschmidt, H., Rosinol, L., Richardson, P., Caltagirone, S., Lahuerta, J.J., Facon, T.*, et al.* (2015). Revised International Staging System for Multiple Myeloma: A Report From International Myeloma Working Group. J Clin Oncol *33*, 2863-2869.

Palumbo, A., Bringhen, S., Caravita, T., Merla, E., Capparella, V., Callea, V., Cangialosi, C., Grasso, M., Rossini, F., Galli, M.*, et al.* (2006). Oral melphalan and prednisone chemotherapy plus thalidomide compared with melphalan and prednisone alone in elderly patients with multiple myeloma: randomised controlled trial. Lancet *367*, 825-831.

Palumbo, A., Cavallo, F., Gay, F., Di Raimondo, F., Ben Yehuda, D., Petrucci, M.T., Pezzatti, S., Caravita, T., Cerrato, C., Ribakovsky, E.*, et al.* (2014). Autologous transplantation and maintenance therapy in multiple myeloma. N Engl J Med *371*, 895-905.

Palumbo, A., Falco, P., Corradini, P., Falcone, A., Di Raimondo, F., Giuliani, N., Crippa, C., Ciccone, G., Omede, P., Ambrosini, M.T.*, et al.* (2007). Melphalan, prednisone, and lenalidomide treatment for newly diagnosed myeloma: a report from the GIMEMA--Italian Multiple Myeloma Network. J Clin Oncol *25*, 4459-4465.

Palumbo, A., Giaccone, L., Bertola, A., Pregno, P., Bringhen, S., Rus, C., Triolo, S., Gallo, E., Pileri, A., and Boccadoro, M. (2001). Low-dose thalidomide plus dexamethasone is an effective salvage therapy for advanced myeloma. Haematologica *86*, 399-403.

Palumbo, A., Hajek, R., Delforge, M., Kropff, M., Petrucci, M.T., Catalano, J., Gisslinger, H., Wiktor-Jedrzejczak, W., Zodelava, M., Weisel, K.*, et al.* (2012). Continuous lenalidomide treatment for newly diagnosed multiple myeloma. N Engl J Med *366*, 1759-1769.

Parks, S.K., Chiche, J., and Pouyssegur, J. (2013). Disrupting proton dynamics and energy metabolism for cancer therapy. Nat Rev Cancer *13*, 611-623.

Pellagatti, A., Jadersten, M., Forsblom, A.M., Cattan, H., Christensson, B., Emanuelsson, E.K., Merup, M., Nilsson, L., Samuelsson, J., Sander, B.*, et al.* (2007). Lenalidomide inhibits the malignant clone and up-regulates the SPARC gene mapping to the commonly deleted region in 5q- syndrome patients. Proc Natl Acad Sci U S A *104*, 11406-11411.

Petrylak, D.P., Vogelzang, N.J., Budnik, N., Wiechno, P.J., Sternberg, C.N., Doner, K., Bellmunt, J., Burke, J.M., de Olza, M.O., Choudhury, A.*, et al.* (2015). Docetaxel and prednisone with or without lenalidomide in chemotherapy-naive patients with metastatic castration-resistant prostate cancer (MAINSAIL): a randomised, double-blind, placebo-controlled phase 3 trial. The Lancet Oncology *16*, 417-425.

Petzold, G., Fischer, E.S., and Thoma, N.H. (2016). Structural basis of lenalidomide-induced CK1alpha degradation by the CRL4(CRBN) ubiquitin ligase. Nature *532*, 127-130.

Pinheiro, C., Reis, R.M., Ricardo, S., Longatto-Filho, A., Schmitt, F., and Baltazar, F. (2010). Expression of monocarboxylate transporters 1, 2, and 4 in human tumours and their association with CD147 and CD44. Journal of biomedicine & biotechnology *2010*, 427694.

Pinti, M., Gibellini, L., Nasi, M., De Biasi, S., Bortolotti, C.A., Iannone, A., and Cossarizza, A. (2016). Emerging role of Lon protease as a master regulator of mitochondrial functions. Biochim Biophys Acta.

Podar, K., Tai, Y.T., Davies, F.E., Lentzsch, S., Sattler, M., Hideshima, T., Lin, B.K., Gupta, D., Shima, Y., Chauhan, D., *et al.* (2001). Vascular endothelial growth factor triggers signaling cascades mediating multiple myeloma cell growth and migration. Blood *98*, 428-435.

Podar, K., Tai, Y.T., Lin, B.K., Narsimhan, R.P., Sattler, M., Kijima, T., Salgia, R., Gupta, D., Chauhan, D., and Anderson, K.C. (2002). Vascular endothelial growth factor-induced migration of multiple myeloma cells is associated with beta 1 integrin- and phosphatidylinositol 3-kinase-dependent PKC alpha activation. J Biol Chem *277*, 7875-7881.

Polanski, R., Hodgkinson, C.L., Fusi, A., Nonaka, D., Priest, L., Kelly, P., Trapani, F., Bishop, P.W., White, A., Critchlow, S.E., *et al.* (2014). Activity of the monocarboxylate transporter 1 inhibitor AZD3965 in small cell lung cancer. Clinical cancer research : an official journal of the American Association for Cancer Research *20*, 926-937.

Poole, R.C., and Halestrap, A.P. (1997). Interaction of the erythrocyte lactate transporter (monocarboxylate transporter 1) with an integral 70-kDa membrane glycoprotein of the immunoglobulin superfamily. J Biol Chem *272*, 14624-14628.

Pozdnyakova, O., Miron, P.M., Tang, G., Walter, O., Raza, A., Woda, B., and Wang, S.A. (2008). Cytogenetic abnormalities in a series of 1,029 patients with primary myelodysplastic syndromes: a report from the US with a focus on some undefined single chromosomal abnormalities. Cancer *113*, 3331-3340.

Quach, H., Ritchie, D., Stewart, A.K., Neeson, P., Harrison, S., Smyth, M.J., and Prince, H.M. (2010). Mechanism of action of immunomodulatory drugs (IMiDS) in multiple myeloma. Leukemia *24*, 22-32.

Quintas-Cardama, A., Kantarjian, H.M., Manshouri, T., Thomas, D., Cortes, J., Ravandi, F., Garcia-Manero, G., Ferrajoli, A., Bueso-Ramos, C., and Verstovsek, S. (2009). Lenalidomide plus prednisone results in durable clinical, histopathologic, and molecular responses in patients with myelofibrosis. J Clin Oncol *27*, 4760-4766.

Rajadhyaksha, A.M., Ra, S., Kishinevsky, S., Lee, A.S., Romanienko, P., DuBoff, M., Yang, C., Zupan, B., Byrne, M., Daruwalla, Z.R., *et al.* (2012). Behavioral characterization of cereblon forebrain-specific conditional null mice: a model for human non-syndromic intellectual disability. Behavioural brain research *226*, 428-434.

Rajkumar, S.V. (2000). Thalidomide in multiple myeloma. Oncology *14*, 11-16.

Rajkumar, S.V., Fonseca, R., Witzig, T.E., Gertz, M.A., and Greipp, P.R. (1999). Bone marrow angiogenesis in patients achieving complete response after stem cell transplantation for multiple myeloma. Leukemia *13*, 469-472.

Rajkumar, S.V., Hayman, S.R., Lacy, M.Q., Dispenzieri, A., Geyer, S.M., Kabat, B., Zeldenrust, S.R., Kumar, S., Greipp, P.R., Fonseca, R., *et al.* (2005). Combination therapy with lenalidomide plus dexamethasone (Rev/Dex) for newly diagnosed myeloma. Blood *106*, 4050-4053.

Rajkumar, S.V., and Kumar, S. (2016). Multiple Myeloma: Diagnosis and Treatment. Mayo Clin Proc *91*, 101-119.

Rajkumar, S.V., Landgren, O., and Mateos, M.V. (2015). Smoldering multiple myeloma. Blood *125*, 3069-3075.

Raza, A., Meyer, P., Dutt, D., Zorat, F., Lisak, L., Nascimben, F., du Randt, M., Kaspar, C., Goldberg, C., Loew, J., *et al.* (2001). Thalidomide produces transfusion independence in long-standing refractory anemias of patients with myelodysplastic syndromes. Blood *98*, 958-965.

Raza, A., Reeves, J.A., Feldman, E.J., Dewald, G.W., Bennett, J.M., Deeg, H.J., Dreisbach, L., Schiffer, C.A., Stone, R.M., Greenberg, P.L., *et al.* (2008). Phase 2 study of lenalidomide in transfusion-dependent, low-risk, and intermediate-1 risk myelodysplastic syndromes with karyotypes other than deletion 5q. Blood *111*, 86-93.

Ren, Y., Wang, M., Couto, S., Hansel, D.E., Miller, K., Lopez-Girona, A., Bjorklund, C.C., Gandhi, A.K., Thakurta, A., Chopra, R., *et al.* (2015). A Dual Color Immunohistochemistry Assay for Measurement of Cereblon in Multiple Myeloma Patient Samples. Applied immunohistochemistry & molecular morphology : AIMM / official publication of the Society for Applied Immunohistochemistry.

Rep, M., van Dijl, J.M., Suda, K., Schatz, G., Grivell, L.A., and Suzuki, C.K. (1996). Promotion of mitochondrial membrane complex assembly by a proteolytically inactive yeast Lon. Science *274*, 103-106.

Richardson, P.G., Schlossman, R.L., Weller, E., Hideshima, T., Mitsiades, C., Davies, F., LeBlanc, R., Catley, L.P., Doss, D., Kelly, K., *et al.* (2002). Immunomodulatory drug CC-5013 overcomes drug resistance and is well tolerated in patients with relapsed multiple myeloma. Blood *100*, 3063-3067.

Richardson, P.G., Siegel, D.S., Vij, R., Hofmeister, C.C., Baz, R., Jagannath, S., Chen, C., Lonial, S., Jakubowiak, A., Bahlis, N., *et al.* (2014a). Pomalidomide alone or in combination with low-dose dexamethasone in relapsed and refractory multiple myeloma: a randomized phase 2 study. Blood *123*, 1826-1832.

Richardson, P.G., Sonneveld, P., Schuster, M.W., Irwin, D., Stadtmauer, E.A., Facon, T., Harousseau, J.L., Ben-Yehuda, D., Lonial, S., Goldschmidt, H., *et al.* (2005). Bortezomib or high-dose dexamethasone for relapsed multiple myeloma. N Engl J Med *352*, 2487-2498.

Richardson, P.G., Weller, E., Jagannath, S., Avigan, D.E., Alsina, M., Schlossman, R.L., Mazumder, A., Munshi, N.C., Ghobrial, I.M., Doss, D., *et al.* (2009). Multicenter, phase I, dose-escalation trial of lenalidomide plus bortezomib for relapsed and relapsed/refractory multiple myeloma. J Clin Oncol *27*, 5713-5719.

Richardson, P.G., Weller, E., Lonial, S., Jakubowiak, A.J., Jagannath, S., Raje, N.S., Avigan, D.E., Xie, W., Ghobrial, I.M., Schlossman, R.L., *et al.* (2010). Lenalidomide, bortezomib, and dexamethasone combination therapy in patients with newly diagnosed multiple myeloma. Blood *116*, 679-686.

Richardson, P.G., Xie, W., Jagannath, S., Jakubowiak, A., Lonial, S., Raje, N.S., Alsina, M., Ghobrial, I.M., Schlossman, R.L., Munshi, N.C., *et al.* (2014b). A phase 2 trial of lenalidomide, bortezomib, and dexamethasone in patients with relapsed and relapsed/refractory myeloma. Blood *123*, 1461-1469.

Riethdorf, S., Reimers, N., Assmann, V., Kornfeld, J.W., Terracciano, L., Sauter, G., and Pantel, K. (2006). High incidence of EMMPRIN expression in human tumors. International journal of cancer *119*, 1800-1810.

Roodman, G.D. (2009). Pathogenesis of myeloma bone disease. Leukemia *23*, 435-441.

Roussel, M., Lauwers-Cances, V., Robillard, N., Hulin, C., Leleu, X., Benboubker, L., Marit, G., Moreau, P., Pegourie, B., Caillot, D., *et al.* (2014). Front-line transplantation program with lenalidomide, bortezomib, and dexamethasone combination as induction and consolidation followed by lenalidomide maintenance in patients with multiple myeloma: a phase II study by the Intergroupe Francophone du Myelome. J Clin Oncol *32*, 2712-2717.

Ruan, J., Martin, P., Shah, B., Schuster, S.J., Smith, S.M., Furman, R.R., Christos, P., Rodriguez, A., Svoboda, J., Lewis, J., *et al.* (2015). Lenalidomide plus Rituximab as Initial Treatment for Mantle-Cell Lymphoma. N Engl J Med *373*, 1835-1844.

Safran, H., Charpentier, K.P., Kaubisch, A., Mantripragada, K., Dubel, G., Perez, K., Faricy-Anderson, K., Miner, T., Eng, Y., Victor, J., *et al.* (2015). Lenalidomide for second-line treatment of advanced

hepatocellular cancer: a Brown University oncology group phase II study. American journal of clinical oncology *38*, 1-4.

Sampaio, E.P., Sarno, E.N., Galilly, R., Cohn, Z.A., and Kaplan, G. (1991). Thalidomide selectively inhibits tumor necrosis factor alpha production by stimulated human monocytes. J Exp Med *173*, 699-703.

San Miguel, J., Weisel, K., Moreau, P., Lacy, M., Song, K., Delforge, M., Karlin, L., Goldschmidt, H., Banos, A., Oriol, A.*, et al.* (2013). Pomalidomide plus low-dose dexamethasone versus high-dose dexamethasone alone for patients with relapsed and refractory multiple myeloma (MM-003): a randomised, open-label, phase 3 trial. The Lancet Oncology *14*, 1055-1066.

Sawamura, N., Wakabayashi, S., Matsumoto, K., Yamada, H., and Asahi, T. (2015). Cereblon is recruited to aggresome and shows cytoprotective effect against ubiquitin-proteasome system dysfunction. Biochem Biophys Res Commun *464*, 1054-1059.

Schmid, B., Hruscha, A., Hogl, S., Banzhaf-Strathmann, J., Strecker, K., van der Zee, J., Teucke, M., Eimer, S., Hegermann, J., Kittelmann, M.*, et al.* (2013). Loss of ALS-associated TDP-43 in zebrafish causes muscle degeneration, vascular dysfunction, and reduced motor neuron axon outgrowth. Proc Natl Acad Sci U S A *110*, 4986-4991.

Schneider, R.K., Adema, V., Heckl, D., Jaras, M., Mallo, M., Lord, A.M., Chu, L.P., McConkey, M.E., Kramann, R., Mullally, A.*, et al.* (2014). Role of casein kinase 1A1 in the biology and targeted therapy of del(5q) MDS. Cancer Cell *26*, 509-520.

Schuster, S.R., Kortuem, K.M., Zhu, Y.X., Braggio, E., Shi, C.X., Bruins, L.A., Schmidt, J.E., Ahmann, G., Kumar, S., Rajkumar, S.V.*, et al.* (2013). The clinical significance of cereblon expression in multiple myeloma. Leuk Res.

Segarra, M., Lozano, E., Corbera-Bellalta, M., Vilardell, C., Cibeira, M.T., Esparza, J., Izco, N., Blade, J., and Cid, M.C. (2010). Thalidomide decreases gelatinase production by malignant B lymphoid cell lines through disruption of multiple integrin-mediated signaling pathways. Haematologica *95*, 456-463.

Segler, A., and Tsimberidou, A.M. (2012). Lenalidomide in solid tumors. Cancer chemotherapy and pharmacology *69*, 1393-1406.

Sekeres, M.A., Maciejewski, J.P., Giagounidis, A.A., Wride, K., Knight, R., Raza, A., and List, A.F. (2008). Relationship of treatment-related cytopenias and response to lenalidomide in patients with lower-risk myelodysplastic syndromes. J Clin Oncol *26*, 5943-5949.

Sheskin, J. (1965). Thalidomide in the Treatment of Lepra Reactions. Clinical pharmacology and therapeutics *6*, 303-306.

Shortt, J., Hsu, A.K., and Johnstone, R.W. (2013). Thalidomide-analogue biology: immunological, molecular and epigenetic targets in cancer therapy. Oncogene *32*, 4191-4202.

Sidhu, S.S., Mengistab, A.T., Tauscher, A.N., LaVail, J., and Basbaum, C. (2004). The microvesicle as a vehicle for EMMPRIN in tumor-stromal interactions. Oncogene *23*, 956-963.

Singhal, S., Mehta, J., Desikan, R., Ayers, D., Roberson, P., Eddlemon, P., Munshi, N., Anaissie, E., Wilson, C., Dhodapkar, M.*, et al.* (1999). Antitumor activity of thalidomide in refractory multiple myeloma. N Engl J Med *341*, 1565-1571.

Smith, C.K., Baker, T.A., and Sauer, R.T. (1999). Lon and Clp family proteases and chaperones share homologous substrate-recognition domains. Proc Natl Acad Sci U S A *96*, 6678-6682.

Smithells, R.W., and Newman, C.G. (1992). Recognition of thalidomide defects. J Med Genet *29*, 716-723.

Sole, F., Luno, E., Sanzo, C., Espinet, B., Sanz, G.F., Cervera, J., Calasanz, M.J., Cigudosa, J.C., Milla, F., Ribera, J.M., *et al.* (2005). Identification of novel cytogenetic markers with prognostic significance in a series of 968 patients with primary myelodysplastic syndromes. Haematologica *90*, 1168-1178.

Solstad, T., Bains, S.J., Landskron, J., Aandahl, E.M., Thiede, B., Tasken, K., and Torgersen, K.M. (2011). CD147 (Basigin/Emmprin) identifies FoxP3+CD45RO+CTLA4+-activated human regulatory T cells. Blood *118*, 5141-5151.

Speirs, A.L. (1962). Thalidomide and congenital abnormalities. Lancet *1*, 303-305.

Stebbing, J., Benson, C., Eisen, T., Pyle, L., Smalley, K., Bridle, H., Mak, I., Sapunar, F., Ahern, R., and Gore, M.E. (2001). The treatment of advanced renal cell cancer with high-dose oral thalidomide. British journal of cancer *85*, 953-958.

Stenzinger, A., Wittschieber, D., von Winterfeld, M., Goeppert, B., Kamphues, C., Weichert, W., Dietel, M., Rabien, A., and Klauschen, F. (2012). High extracellular matrix metalloproteinase inducer/CD147 expression is strongly and independently associated with poor prognosis in colorectal cancer. Human pathology *43*, 1471-1481.

Stewart, A.K., Rajkumar, S.V., Dimopoulos, M.A., Masszi, T., Spicka, I., Oriol, A., Hajek, R., Rosinol, L., Siegel, D.S., Mihaylov, G.G., *et al.* (2015). Carfilzomib, lenalidomide, and dexamethasone for relapsed multiple myeloma. N Engl J Med *372*, 142-152.

Strati, P., Keating, M.J., Wierda, W.G., Badoux, X.C., Calin, S., Reuben, J.M., O'Brien, S., Kornblau, S.M., Kantarjian, H.M., Gao, H., *et al.* (2013). Lenalidomide induces long-lasting responses in elderly patients with chronic lymphocytic leukemia. Blood *122*, 734-737.

Strupp, C., Hildebrandt, B., Germing, U., Haas, R., and Gattermann, N. (2003). Cytogenetic response to thalidomide treatment in three patients with myelodysplastic syndrome. Leukemia *17*, 1200-1202.

Su, J., Chen, X., and Kanekura, T. (2009). A CD147-targeting siRNA inhibits the proliferation, invasiveness, and VEGF production of human malignant melanoma cells by down-regulating glycolysis. Cancer letters *273*, 140-147.

Summerton, J. (1999). Morpholino antisense oligomers: the case for an RNase H-independent structural type. Biochim Biophys Acta *1489*, 141-158.

Summerton, J., and Weller, D. (1997). Morpholino antisense oligomers: design, preparation, and properties. Antisense & nucleic acid drug development *7*, 187-195.

Sun, J., and Hemler, M.E. (2001). Regulation of MMP-1 and MMP-2 production through CD147/extracellular matrix metalloproteinase inducer interactions. Cancer Res *61*, 2276-2281.

Szlosarek, P.W., and Balkwill, F.R. (2003). Tumour necrosis factor alpha: a potential target for the therapy of solid tumours. The Lancet Oncology *4*, 565-573.

Tang, W., Chang, S.B., and Hemler, M.E. (2004a). Links between CD147 function, glycosylation, and caveolin-1. Mol Biol Cell *15*, 4043-4050.

Tang, Y., Kesavan, P., Nakada, M.T., and Yan, L. (2004b). Tumor-stroma interaction: positive feedback regulation of extracellular matrix metalloproteinase inducer (EMMPRIN) expression and matrix metalloproteinase-dependent generation of soluble EMMPRIN. Mol Cancer Res *2*, 73-80.

Tang, Y., Nakada, M.T., Kesavan, P., McCabe, F., Millar, H., Rafferty, P., Bugelski, P., and Yan, L. (2005). Extracellular matrix metalloproteinase inducer stimulates tumor angiogenesis by elevating vascular endothelial cell growth factor and matrix metalloproteinases. Cancer Res *65*, 3193-3199.

Tefferi, A., and Vardiman, J.W. (2009). Myelodysplastic syndromes. N Engl J Med *361*, 1872-1885.

Tehranchi, R., Fadeel, B., Forsblom, A.M., Christensson, B., Samuelsson, J., Zhivotovsky, B., and Hellstrom-Lindberg, E. (2003). Granulocyte colony-stimulating factor inhibits spontaneous cytochrome c release and mitochondria-dependent apoptosis of myelodysplastic syndrome hematopoietic progenitors. Blood *101*, 1080-1086.

Thakurta, A., Gandhi, A.K., Waldman, M.F., Bjorklund, C., Ning, Y., Mendy, D., Schafer, P., Lopez-Girona, A., Lentzsch, S., Schey, S.A.*, et al.* (2013). Absence of mutations in cereblon (CRBN) and DNA damage-binding protein 1 (DDB1) genes and significance for IMiD(R) therapy. Leukemia.

Thorns, C., Feller, A.C., and Merz, H. (2002). EMMPRIN (CD 147) is expressed in Hodgkin's lymphoma and anaplastic large cell lymphoma. An immunohistochemical study of 60 cases. Anticancer research *22*, 1983-1986.

Toma, A., Kosmider, O., Chevret, S., Delaunay, J., Stamatoullas, A., Rose, C., Beyne-Rauzy, O., Banos, A., Guerci-Bresler, A., Wickenhauser, S.*, et al.* (2016). Lenalidomide with or without erythropoietin in transfusion-dependent erythropoiesis-stimulating agent-refractory lower-risk MDS without 5q deletion. Leukemia *30*, 897-905.

Toole, B.P., and Slomiany, M.G. (2008). Hyaluronan, CD44 and Emmprin: partners in cancer cell chemoresistance. Drug resistance updates : reviews and commentaries in antimicrobial and anticancer chemotherapy *11*, 110-121.

Urbaniak-Kujda, D., Kapelko-Slowik, K., Prajs, I., Dybko, J., Wolowiec, D., Biernat, M., Slowik, M., and Kuliczkowski, K. (2016). Increased expression of metalloproteinase-2 and -9 (MMP-2, MMP-9), tissue inhibitor of metalloproteinase-1 and -2 (TIMP-1, TIMP-2), and EMMPRIN (CD147) in multiple myeloma. Hematology *21*, 26-33.

Vacca, A., Ribatti, D., Presta, M., Minischetti, M., Iurlaro, M., Ria, R., Albini, A., Bussolino, F., and Dammacco, F. (1999). Bone marrow neovascularization, plasma cell angiogenic potential, and matrix metalloproteinase-2 secretion parallel progression of human multiple myeloma. Blood *93*, 3064-3073.

Vardiman, J.W., Thiele, J., Arber, D.A., Brunning, R.D., Borowitz, M.J., Porwit, A., Harris, N.L., Le Beau, M.M., Hellstrom-Lindberg, E., Tefferi, A.*, et al.* (2009). The 2008 revision of the World Health Organization (WHO) classification of myeloid neoplasms and acute leukemia: rationale and important changes. Blood *114*, 937-951.

Vogelsang, G.B., Farmer, E.R., Hess, A.D., Altamonte, V., Beschorner, W.E., Jabs, D.A., Corio, R.L., Levin, L.S., Colvin, O.M., Wingard, J.R.*, et al.* (1992). Thalidomide for the treatment of chronic graft-versus-host disease. N Engl J Med *326*, 1055-1058.

Voigt, H., Vetter-Kauczok, C.S., Schrama, D., Hofmann, U.B., Becker, J.C., and Houben, R. (2009). CD147 impacts angiogenesis and metastasis formation. Cancer investigation *27*, 329-333.

Walter, M., Simanovich, E., Brod, V., Lahat, N., Bitterman, H., and Rahat, M.A. (2016). An epitope-specific novel anti-EMMPRIN polyclonal antibody inhibits tumor progression. Oncoimmunology *5*, e1078056.

Walters, D.K., Arendt, B.K., and Jelinek, D.F. (2013). CD147 regulates the expression of MCT1 and lactate export in multiple myeloma cells. Cell Cycle *12*, 3175-3183.

Wang, J.H., Avitahl, N., Cariappa, A., Friedrich, C., Ikeda, T., Renold, A., Andrikopoulos, K., Liang, L., Pillai, S., Morgan, B.A.*, et al.* (1998). Aiolos regulates B cell activation and maturation to effector state. Immunity *9*, 543-553.

Wang, M., Fayad, L., Wagner-Bartak, N., Zhang, L., Hagemeister, F., Neelapu, S.S., Samaniego, F., McLaughlin, P., Fanale, M., Younes, A., *et al.* (2012). Lenalidomide in combination with rituximab for patients with relapsed or refractory mantle-cell lymphoma: a phase 1/2 clinical trial. The Lancet Oncology *13*, 716-723.

Wang, M., Martin, T., Bensinger, W., Alsina, M., Siegel, D.S., Kavalerchik, E., Huang, M., Orlowski, R.Z., and Niesvizky, R. (2013). Phase 2 dose-expansion study (PX-171-006) of carfilzomib, lenalidomide, and low-dose dexamethasone in relapsed or progressive multiple myeloma. Blood *122*, 3122-3128.

Wang, X., Venable, J., LaPointe, P., Hutt, D.M., Koulov, A.V., Coppinger, J., Gurkan, C., Kellner, W., Matteson, J., Plutner, H., *et al.* (2006). Hsp90 cochaperone Aha1 downregulation rescues misfolding of CFTR in cystic fibrosis. Cell *127*, 803-815.

Warlick, E.D., Cioc, A., Defor, T., Dolan, M., and Weisdorf, D. (2009). Allogeneic stem cell transplantation for adults with myelodysplastic syndromes: importance of pretransplant disease burden. Biology of blood and marrow transplantation : journal of the American Society for Blood and Marrow Transplantation *15*, 30-38.

Weber, D.M., Chen, C., Niesvizky, R., Wang, M., Belch, A., Stadtmauer, E.A., Siegel, D., Borrello, I., Rajkumar, S.V., Chanan-Khan, A.A., *et al.* (2007). Lenalidomide plus dexamethasone for relapsed multiple myeloma in North America. N Engl J Med *357*, 2133-2142.

Weidenbach, A. (1959). [Total phocomelia]. Zentralblatt fur Gynakologie *81*, 2048-2052.

Weidle, U.H., Scheuer, W., Eggle, D., Klostermann, S., and Stockinger, H. (2010). Cancer-related issues of CD147. Cancer Genomics Proteomics *7*, 157-169.

Wiernik, P.H., Lossos, I.S., Tuscano, J.M., Justice, G., Vose, J.M., Cole, C.E., Lam, W., McBride, K., Wride, K., Pietronigro, D., *et al.* (2008). Lenalidomide monotherapy in relapsed or refractory aggressive non-Hodgkin's lymphoma. J Clin Oncol *26*, 4952-4957.

Wilson, M.C., Meredith, D., Fox, J.E., Manoharan, C., Davies, A.J., and Halestrap, A.P. (2005). Basigin (CD147) is the target for organomercurial inhibition of monocarboxylate transporter isoforms 1 and 4: the ancillary protein for the insensitive MCT2 is EMBIGIN (gp70). J Biol Chem *280*, 27213-27221.

Wilson, M.C., Meredith, D., and Halestrap, A.P. (2002). Fluorescence resonance energy transfer studies on the interaction between the lactate transporter MCT1 and CD147 provide information on the topology and stoichiometry of the complex in situ. J Biol Chem *277*, 3666-3672.

Winter, G.E., Buckley, D.L., Paulk, J., Roberts, J.M., Souza, A., Dhe-Paganon, S., and Bradner, J.E. (2015). DRUG DEVELOPMENT. Phthalimide conjugation as a strategy for in vivo target protein degradation. Science *348*, 1376-1381.

Witzig, T.E., Wiernik, P.H., Moore, T., Reeder, C., Cole, C., Justice, G., Kaplan, H., Voralia, M., Pietronigro, D., Takeshita, K., *et al.* (2009). Lenalidomide oral monotherapy produces durable responses in relapsed or refractory indolent non-Hodgkin's Lymphoma. J Clin Oncol *27*, 5404-5409.

Xin, W., Xiaohua, N., Peilin, C., Xin, C., Yaqiong, S., and Qihan, W. (2008). Primary function analysis of human mental retardation related gene CRBN. Molecular biology reports *35*, 251-256.

Xu, G., Jiang, X., and Jaffrey, S.R. (2013). A mental retardation-linked nonsense mutation in cereblon is rescued by proteasome inhibition. J Biol Chem *288*, 29573-29585.

Xu, J., Shen, Z.Y., Chen, X.G., Zhang, Q., Bian, H.J., Zhu, P., Xu, H.Y., Song, F., Yang, X.M., Mi, L., *et al.* (2007a). A randomized controlled trial of Licartin for preventing hepatoma recurrence after liver transplantation. Hepatology *45*, 269-276.

Xu, J., Xu, H.Y., Zhang, Q., Song, F., Jiang, J.L., Yang, X.M., Mi, L., Wen, N., Tian, R., Wang, L.*, et al.* (2007b). HAb18G/CD147 functions in invasion and metastasis of hepatocellular carcinoma. Mol Cancer Res *5*, 605-614.

Yanaba, K., Asano, Y., Tada, Y., Sugaya, M., Kadono, T., Hamaguchi, Y., and Sato, S. (2012). Increased serum soluble CD147 levels in patients with systemic sclerosis: association with scleroderma renal crisis. Clinical rheumatology *31*, 835-839.

Yoshida, S., Shibata, M., Yamamoto, S., Hagihara, M., Asai, N., Takahashi, M., Mizutani, S., Muramatsu, T., and Kadomatsu, K. (2000). Homo-oligomer formation by basigin, an immunoglobulin superfamily member, via its N-terminal immunoglobulin domain. Eur J Biochem *267*, 4372-4380.

Zhu, D., Wang, Z., Zhao, J.J., Calimeri, T., Meng, J., Hideshima, T., Fulciniti, M., Kang, Y., Ficarro, S.B., Tai, Y.T.*, et al.* (2015). The Cyclophilin A-CD147 complex promotes the proliferation and homing of multiple myeloma cells. Nature medicine *21*, 572-580.

Zhu, Y.X., Braggio, E., Shi, C.X., Bruins, L.A., Schmidt, J.E., Van Wier, S., Chang, X.B., Bjorklund, C.C., Fonseca, R., Bergsagel, P.L.*, et al.* (2011). Cereblon expression is required for the antimyeloma activity of lenalidomide and pomalidomide. Blood *118*, 4771-4779.

Zhu, Y.X., Braggio, E., Shi, C.X., Kortuem, K.M., Bruins, L.A., Schmidt, J.E., Chang, X.B., Langlais, P., Luo, M., Jedlowski, P.*, et al.* (2014). Identification of cereblon-binding proteins and relationship with response and survival after IMiDs in multiple myeloma. Blood *124*, 536-545.

Zonder, J.A., Crowley, J., Hussein, M.A., Bolejack, V., Moore, D.F., Sr., Whittenberger, B.F., Abidi, M.H., Durie, B.G., and Barlogie, B. (2010). Lenalidomide and high-dose dexamethasone compared with dexamethasone as initial therapy for multiple myeloma: a randomized Southwest Oncology Group trial (S0232). Blood *116*, 5838-5841.

8 Publications

8.1 Articles in peer-reviewed journals

Eichner R., Heider M., Fernández-Sáiz V., van Bebber F., Garz A.K., Lemeer S., Rudelius M., Targosz B.S., Jacobs L., Knorn A.M., Slawska J., Platzbecker U., Germing U., Langer C., Knop S., Einsele H., Peschel C., Haass C., Keller U. Schmid B., Götze K.S., Kuster B., Bassermann F. Immunomodulatory drugs disrupt the cereblon–CD147–MCT1 axis to exert antitumor activity and teratogenicity. **Nature Medicine (2016)**

Bassermann F., **Eichner R.**, Pagano M. The ubiquitin proteasome system - implications for cell cycle control and the targeted treatment of cancer. **Biochimica et Biophysica Acta (2014)**

Fernández-Sáiz V., Targosz B.S., Lemeer S., **Eichner R**., Langer C., Bullinger L, Reiter C, Slotta-Huspenina J., Schroeder S., Knorn A.M., Kurutz J., Peschel C., Pagano M., Kuster B., Bassermann F. SCF-Fbxo9 and CK2 direct the cellular response to growth factor withdrawal via Tel2 and Tti1 degradation and promote survival in multiple myeloma. **Nature Cell Biology (2013)**

8.2 Conference contributions

Eichner R., Heider M., Fernández-Sáiz V., van Bebber F., Garz A.K., Lemeer S., Rudelius M., Targosz B.S., Jacobs L., Knorn A.M., Slawska J., Platzbecker U., Germing U., Langer C., Knop S., Einsele H., Peschel C., Haass C., Keller U. Schmid B., Götze K.S., Kuster B., Bassermann F. Immunomodulatory drugs disrupt the cereblon–CD147–MCT1 axis to exert antitumor activity and teratogenicity.

European Mantle Cell Lymphoma Network Annual Meeting, Vicenza, 2015. Talk.

Eichner R., Heider M., Fernández-Sáiz V., van Bebber F., Garz A.K., Lemeer S., Targosz B.S., Knorn A.M., Platzbecker U., Germing U., Peschel C., Haass C., Keller U. Schmid B., Götze K.S., Kuster B., Bassermann F. Immunomodulatory drugs restrain the CD147/MCT1 complex to exert antitumor activity and teratogenicity.

DKTK 2nd Munich Cancer Retreat, Herrsching, 2015. Poster.

Eichner R., Fernández-Sáiz V., Heider M., Lemeer S., van Bebber F., Targosz B.S., Peschel C., Schmid B., Kuster B., Bassermann F. Immunomodulatory drugs attenuate CRBN-dependent activation of the CD147-MCT1 complex to promote anti-myeloma activity and teratogenicity.

EMBO Meeting Ubiquitin and UBLs - from Chromatin to Protein, Buenos Aires, 2014. Poster.

9 Acknowledgements

The current study is the result of more than four years of work in the lab of Prof. Dr. Florian Bassermann. Thanks to many people, these years were filled with enthusiasm, curiosity, learning, discussions, crazy ideas and concepts, lots fun, valuable experiences and new precious friends. I am very grateful for this time and wish to thank everyone who has contributed to the success of this work and who made these years special!

My biggest thanks go to Prof. Dr. Florian Bassermann, whose enthusiasm inspired me right at the first interview and made me join his lab. Thank you for giving me the opportunity to work in your lab and for suggesting the exciting topic to decipher the molecular mechanism of IMiDs. Thank you for all your input, for being so direct and uncomplicated, for being demanding but understanding at the same time, and for constantly supporting me and this project!

Special thanks go Michael Heider, who I had the pleasure to supervise for his medical dissertation. Very soon, you evolved from being a student “who needs supervision” to a veritable partner on the project with own ideas and suggestions and moreover, to a great friend! Thank you for all your motivation and constant commitment throughout the years and for significantly contributing to the success of this work (including all the significance analyses!).

A big thank you also goes to Dr. Vanesa Fernández-Sáiz, who initially helped me finding my way in the new lab, together with Dr. Bianca Targosz and Ursula Baumann, and later supported this project with her valuable experience in protein biochemistry and particularly with innumerable ideas and hypotheses ranging from crazy to genius. Thank you for always being the creative one thinking outside the box and for continuously making this lab a fun place!

I would also like to thank all other members of the Bassermann Lab, for being such an open and helpful crowd! Thank you for constructive comments, input, support and the good times! Special thanks go to Anna Knorn and Petra Schenk, the technicians who helped with the experiments and provided crucial support particularly during my time in the clinic.

Moreover, I would like to thank Prof. Dr. Katharina Götze for suggesting evaluation of MDS in the CD147 context and for the successful and uncomplicated collaboration. Likewise, I want to thank Dr. Frauke van Bebber and Dr. Bettina Schmid for continuously and diligently working on the zebrafish part of this project! Thank you also to Dr. Simone Lemeer and Prof. Bernhard Küster for the fruitful and uncomplicated collaboration! Further thanks go to PD Dr. Martina Rudelius and all other collaborators!

Special thanks go to Prof. Dr. Christian Peschel, the head of the III. Medical Department, for encouraging medical doctors to pursue basic research besides the clinical work and for actually giving me the opportunity to repeatedly focus on research full-time.

Next, I would like to thank both the PhD Program Medical Life Science and Technology as well as the Kommission für Klinische Forschung (KKF) at the Medical Faculty at Klinikum rechts der Isar for supporting this project with a stipends and a research grant for one year each!

Last but not least, I would also like to thank my family, my friends and particularly my boyfriend Olli for constant support, encouragement and understanding when I was again spending the night or the weekend in the lab instead of spending time with them. Thank you for your patience and for believing in me!